THE BIOLOGY OF CD4^{+} T CELLS IN THE BLOOD AND CENTRAL NERVOUS SYSTEM

BY

MARIE ANN VOICE

A thesis submitted to
The University of Birmingham
for the degree of
DOCTOR OF PHILOSOPHY

School of Immunity and Infection
College of Medical and Dental Sciences
University of Birmingham
June 2015

ABSTRACT

Marie Ann Voice, School of Immunity and Infection, College of Medical and Dental Sciences, University of Birmingham.

A thesis submitted to the University of Birmingham for the degree of

DOCTOR OF PHILOSOPHY

$CD4^+$ T cells modulate an immune response through the production of effector cytokines. In some circumstances the effector function of $CD4^+$ T cells is diminished, which may have beneficial (peripheral tolerance) or detrimental (exhaustion, senescence) consequences. Here I characterise a population of $CD4^+$ cells in human peripheral blood which exhibit complete hyporesponsiveness to *in vitro* stimulation, as indicated by an absence of CD69 upregulation and the failure to secrete any of thirteen candidate cytokines. These T cells had an effector memory phenotype ($CD45RA^-CCR7^{-/+}CD62L^{lo}CD27^{lo}$), but their intermediate expression of PD-1 did not suggest a state of exhaustion. Although regulatory T cells ($CD25^{hi}CD127^{lo}$) contributed to the hyporesponsive population it was not predominated by this phenotype. However, the possibility that these hyporesponsive cells represent a non-classical regulatory subset could not be excluded.

$CD4^+$ T cells can enter the central nervous system (CNS) via the blood cerebrospinal fluid barrier, but their biological activity and recruitment pathways are under-defined. Preliminary studies had suggested that hyporesponsive $CD4^+$ T cells were enriched in uninflamed human cerebrospinal fluid (CSF). However, this investigation found that CSF and brain-derived $CD4^+$ T cells readily upregulate CD69 upon activation (mouse, human) and have robust IFNγ responses (rat). This evidence supports a role for $CD4^+$ T cells in CNS immune surveillance and immunity.

This investigation also showed that the proportion of $CCR7^+$ and $CCR7^-$ memory $CD4^+$ T cells in the CSF was a direct reflection of the distribution in the peripheral blood in both mouse and man. This suggests that CSF recruitment is not CCR7-dependent as is previously described, and shows effector memory cells enter the CSF space in the absence of neuropathology. Such findings have implications for the understanding of normal immune function in the CNS, and the protective or pathogenic contribution of $CD4^+$ T cells to neuroinflammatory disorders such as multiple sclerosis.

DEDICATION

"Success isn't how far you got, but the distance

you've travelled from where you started..."

~ Steve Prefontaine

For Mum, Dad, and Pete.

ACKNOWLEDGEMENTS

I would like to thank my supervisor Dr John Curnow for his intellectual input, guidance and mentorship throughout this process. I truly appreciate the amazing support I have received from John and the Curnow group throughout my PhD and give particular thanks to Miss Lindsay Durant for her technical support and friendship over the years. I'd also like to thank Dr Graham Wallace for his guidance during my time at Birmingham; Graham your knowledge and passion for immunology is truly inspirational.

Large parts of my animal work would not have been possible without the technical training I have received from the Molecular Neuroscience Group. A huge thank you goes to Dr Ana-Maria Gonzalez for her help with neural tissue dissection and sectioning, and to Lisa Hill and Adam Thompson for their assistance with rodent CSF collections.

I must also thank Dr Robert Shaw for my microscopy training, Roger Bird for his assistance with FACS and the staff at BMSU for facilitating my mouse work.

My time at the University of Birmingham has been an amazing journey on an intellectual, professional and personal level. Lastly, I would like to acknowledge the Wellcome Trust for funding my research and making this experience possible.

TABLE OF CONTENTS

LIST OF FIGURES

LIST OF TABLES

ABBREVIATIONS

AICD	Activation induced cell death
AMPK	5' AMP-activated protein kinase
AP-1	Activator protein 1
APC	Antigen presenting cell
BBB	Blood-brain-barrier
BCR	B cell receptor
BCSFB	Blood-cerebrospinal fluid-barrier
BLMB	Blood-leptomeningeal-barrier
CCL	Chemokine receptor ligand
CCR	Chemokine receptor
CD	Cluster of differentiation
CDK	Cyclin dependent kinase
CIS	Clinically isolated syndrome
CLN	Cervical lymph nodes
CLP	Common lymphoid progenitor
CLR	C-type lectin receptor
CMP	Common myeloid progenitor
CMV	Cytomegalovirus
CNS	Central nervous system
CP	Choroid plexus
CSF	Cerebrospinal fluid
Ct	Cycle threshold
CTLA-4	Cytotoxic T-lymphocyte-associated protein 4
DC	Dendritic cell
EAE	Experimental autoimmune encephalomyelitis
EBV	Epstein Barr virus
ELP	Early lymphoid progenitors
FACS	Fluorescence-activated cell sorting
FOXP3	Forkhead box P3
HCV	Hepatitis C virus
HIV	Human immunodeficiency virus
HSC	Haematopoietic stem cell
ICAM-1	Intracellular adhesion molecule 1
IFNγ	Interferon gamma

IL-	Interleukin
IS	Immunological synapse
ISF	Interstitial fluid
ITAM	Immuoreceptor tyrosine-based activation motifs
iT_{reg}	Inducible regulatory T cell
JAM	Junctional adhesion molecule
LCK ($p56^{lck}$)	lymphocyte-specific protein tyrosine kinase
LCMV	lymphocytic choriomeningitis virus
LFA-1	Lymphocyte function-associated antigen 1
LM	*listeria monocytogenes*
mAb	Monoclonal antibody
MACS	Magnetic-activated cell sorting
MAdCAM-1	Mucosal vascular cell adhesion molecule 1
MHC	Major histocompatibility complex
MMP	Matrix metalloproteinase enzyme
MS	Multiple sclerosis
NFAT	Nuclear factor of activated T-cells
NK	Natural killer (cell)
NLR	Nod-like receptor
nT_{reg}	Natural regulatory T cell
OND	Other neurological disease
ONID	Other neurological inflammatory disease
PAMP	Pathogen-associated molecular pattern
PBMC	Peripheral blood mononuclear cell
PD-1	Programmed cell death receptor 1
PD-L1	Programmed cell death ligand 1
PKCϴ	Protein kinase C theta
PMA	Phorbol myristate acetate
PP-MS	Relapsing remitting multiple sclerosis
PRR	Pathogen recognition receptor
PVS	Perivascular space
qPCR	Quantitative real time polymerase chain reaction
RR-MS	Relapsing remitting multiple sclerosis
S1P	Sphingosine-1 phosphate
$S1P_1$	Sphingosine-1 phosphate receptor 1
SEB	Staphylococcal enterotoxin B

STAT	Signal transducer and activator of transcription
T_{cm}	Central memory T cell
TCR	T cell receptor
T_{eff}	Effector memory T cell
TEM	Transendothelial migration
TGFβ	Transforming growth factor beta
T_{helper}	T helper cells
TLR	Toll-like receptor
TNF	Tumour necrosis factor
T_{reg}	Regulatory T cell
T_{RM}	Resident memory T cell
T_{SCM}	Stem cell-like memory T cells
UoB	University of Birmingham
VIP	Vasoactive intestinal peptide
VLA-4	Very late antigen 4

CHAPTER 1

GENERAL INTRODUCTION

1 GENERAL INTRODUCTION

1.1 The foundations of human immunity.

1.1.1 The innate immune system.

The ability of an organism to protect itself against pathogenic invasion is an evolutionary conserved feature that likely predates the emergence of multicellular organisms over 600 million years ago[1]. Mechanisms of host defence in humans have evolved to protect against a plethora of pathogens (e.g. bacterium, viruses, fungi, helminth) and are therefore multi-layered and complex. The first line of protection against such organisms is the physical barriers that must be breached in order to access the body. In humans, potentially vulnerable sites for pathogen entry include the skin, gut and respiratory mucosa. Consequentially the evolution of immune modifications at these sites is heavily favoured[2]. Taking the skin as an example site, such mechanisms include keratinisation and desquamation of the tissue surface[3], production of sweat and anti-microbial organic acids[4], and commensal skin flora which inhibits the colonisation of pathogenic microbes[5].

Once a pathogen has breached these physical barriers, the second line of immune defence is a collection of fast-acting cellular and humoral responses that fall under the definition of 'innate immunity'. With consideration to the cellular component, all innate immune cell lineages are derived from haematopoietic stem cells (HSC) in the bone marrow[6]. These pluripotent cells differentiate into multi-potent common myeloid progenitors (CMP) which can then differentiate into granulocytes (neutrophils, eosinophils, basophils) or monocytes[7]. A summary of some important features of these cells is shown in Table 1.1.

Origin	Lineage Precursor	Niche signals	Lineage Precursor	Niche signals	Cell Type	Summary of function
Haematopoietic stem cell	Common myeloid progenitor	GM-CSF	Myloblast	G-CSF GM-CSF IL-3 IL-4	Neutrophil	Rapid response to bacterial infection. Phagocytosis and microbe killing though hydrolytic enzyme and superoxide production (ROS). Degranulation and release of NET's to trap and kill microbes.
				GM-CSF IL-3 IL-4	Basophil	Protection from ectoparasites through degranulation; release of histamine, proteoglycans, proteolytic enzymes. Source of IL-4 cytokine.
				GM-CSF IL-3 IL-5	Eosinophil	Protection from parasites and multi-cellular pathogens. Degranulation to release cytotoxic inflammatory mediators including; cationic proteins, cytokines, leukotrienes, ROS.
		GM-CSF M-CSF	Monocyte	GM-CSF M-CSF	macrophage	Phagocytosis of apoptotic cells, cellular debris, microbes. Production of monokines (CSF, IL-1, IFNα, IFNβ, TNFα). Support of adaptive immunity (antigen presentation)
				GM-CSF IL-4	Dendritic cell	Antigen processing and presentation. Support of adaptive immunity.

Table 1.1 Summary of the lineage and function of notable innate immune cells. Table includes an overview of some important cytokines and growth factors involved in the differentiation of each lineage. The summary of function includes some of the most significant roles of each cell type. **G-CSF;** granulocyte colony stimulating factor, **GM-CSF;** granulocyte macrophage-colony stimulating factor, **M-CSF;** macrophage-colony stimulating factor, **SCF;** stem cell factor, **IL-1, IL-3, IL-4, IL-5, IL-6;** Interleukin family members, **TNFα;** Tumour necrosis factor alpha, **IFNα** and **IFNβ;** Interferon alpha and beta, **ROS;** Reactive oxygen species, **NET;** Neutrophil extracellular trap.

A conserved feature of innate immune cells is the ability to recognise molecular motifs on potential invaders and mount an appropriate molecular response. This is achieved through a series of pathogen recognition receptors (PRR's) which recognise a variety of pathogen-associated molecular patterns (PAMP's) that are specific to non-host cellular structures. Examples of PAMP's include; 1) double stranded RNA and unmethylated CpG DNA motifs (viral), 2) lipopolysaccharide and lipoteichoic acid (bacterial) and 3) β-glycan and mannan (fungal)[8]. Once PRR signalling is triggered, an intracellular signalling cascade is initiated that results in the release of numerous inflammatory mediators. These mediators are recognised by receptors expressed by multiple immune cell types, and thus the clearing of the pathogen is orchestrated. The recognition and clearance of pathogens is enhanced by serum proteins that form components of the complement system[9]. Two pathways of the complement system are triggered by the binding of acute phase response proteins (C-reactive protein or mannose-binding lectin) directly to the bacterial surfaces. These proteins are elevated in inflammation and the resulting proteolytic cascade of complement products can; 1) enhance phagocytosis (C3b protein), 2) act as a chemoattractant for other innate immune cells (C5a proteins), 3) activate eosinophils and basophil degranulation (C3A and C5A), 4) form a membrane attack complex that results in the osmotic lysis of bacterial cells (C5b, C6, C7, C8, C9 association)[10].

1.1.2 Adaptive immunity.

Innate immune function provides generalised protection against classes of pathogens that is largely non-specific, but such function is rapid and essential for survival. In complex organisms an additional arm of defence is provided through 'adaptive' immune function. Early adaptive immune cells acquired the expression of recombinase enzymes to rearrange gene segments in their pathogen recognition receptors[1,11]. This generation of receptor diversity permitted the recognition of an almost infinite number of antigens and thus broadened both the specificity and range of the immune response. However, an inherent

danger of such a mechanism is the risk of generating reactivity against self-antigen. Therefore, protective molecular processes that prevent self-reactivity have co-evolved, although are not always fail-safe.

Through the ability to maintain expanded clonal populations of pathogen specific cells following an infection the basis of immunological memory is formed[12,13]. Immune memory is a key feature of adaptive immunity and is defined by rapid recall responses upon re-exposure to an infectious agent, coupled with enhanced immune protection against a secondary reinfection. B cell and T cells are two predominant cell types which form the basis of adaptive immunity in vertebrates, and are described in the following chapters with an emphasis upon human T cell biology.

1.2 Overview of B cell biology.

B cells undergo development in the bone marrow and recognise antigen through expression of their B cell receptor (BCR). Systematic gene rearrangement (somatic recombination) of the BCR immunoglobulin genes generates receptor diversity[14]. Mature B cells migrate to the lymph nodes, and may become short lived plasma cells if their BCR recognises cognate antigen in the medullary region[15]. These produce large quantities of moderate affinity immunoglobulin (soluble BCR) of an IgM isoform and are important in the immediate immune response[16]. Production of immunoglobulin with high affinity requires B cell – T cell interaction[17]. If a BCR recognises an antigen it can internalise this complex and process the antigen into peptides. These peptides can be presented to T cells via major histocompatibility complex (MHC). If the peptide antigen is recognised by T cells, the T cell interaction induces B cell proliferation and migration to the dark zone of germinal centres within the lymph nodes[18]. These ‘centroblasts’ undergo somatic hypermutation of their BCR through expression of activation induced deaminase enzyme, which introduces point mutations into the BCR’s antigen recognition sequence[19]. Centroblasts migrate to the light zone of the

germinal centre and become centrocytes. Through their interaction with follicular dendritic cells and T cells, centrocytes with an increased affinity for antigen are maintained whilst those with decreased affinity die by apoptosis[18]. High affinity B cells undergo class switching of their immunoglobulin heavy chain and differentiate into long lived plasma cells or memory B cells[20]. Long lived plasma cells produce large quantities of high affinity soluble immunoglobulin which may; 1) Neutralise soluble antigens, 2) Increase phagocytosis through pathogen opsonisation, 3) Activate the complement cascade via an immunoglobulin mediated pathway (the classical pathway). Memory B cells are maintained in the periphery and have the potential to differentiate rapidly into plasma cells upon re-exposure to antigen[21].

1.3 T cell biology.

1.3.1 T cell development.

In addition to supporting B cell function T cells have an integral role in multiple aspects of the immune response. The development of pre-T cells begins in the bone marrow through differentiation of HSC into common lymphoid progenitor (CLP) cells. CLP then differentiate into early T lineage progenitors (ETP) under the influence of cytokine mediators such as the interleukin family (IL) members IL-2, IL-4, IL-7, IL-9 and IL-10[22,23]. ETP lack their antigen recognition receptor (T cell receptor) but maintain the stem cell marker CD34[24]. ETP migrate from the bone marrow to the thymus to undergo maturation. In around 95% of T cells their T cell receptor (TCR) is an α/β protein heterodimer joined by disulphide bonds, whereas the remaining 5% have an alternative γ/δ chain arrangement[25]. Variation of TCR antigen specificity is a result of genetic recombination events where combinatorial splicing of receptor genes results in variation in the proteins amino acid sequence. In the subscapular region of the thymus cells with pre-TCR complexes are formed as rearrangement of the β-chain genes precedes complete α-chain development[26,27]. Rearrangement of the α-chain coincides with the acquisition of both CD4 and CD8 TCR co-receptors[28]. With expression of functional TCR complete, positive selection of double positive thymocytes occurs through

interaction with MHC receptor presented by cortical thymic epithelial cells. Cells that do not recognise peptides presented via MHC die by neglect, whereas cells that moderately bind MHC receive survival signals and migrate through the corticomedullary region via acquisition of the chemokine receptor CCR7[29].

In the medulla thymocytes interact with dendritic cells (DC) and medullary epithelial cells, the latter of which expresses a repertoire of tissue specific antigens under the control of transcription factors such as the AIRE gene promotor[30,31]. Double positive thymocytes which bind strongly to self-antigen MHC complex are deleted by apoptosis through negative selection. Thymocytes which remain lose expression of either CD4 or CD8 depending on their MHC isoform recognition and become mature single positive cells. Although only 1-3% of progenitors which enter the thymus survive[32,33], these mechanisms ensure highly self-reactive mature T cells are not released into the periphery whilst maintaining a repertoire of cells that can bind antigen-MHC complex.

1.3.2 Naïve T cell activation and intracellular signalling.

Following maturation in the thymus T cells circulate in the blood in a 'naïve' antigen-inexperienced state (T_{naive}). In order to encounter antigen and activate these cells must home to secondary lymphoid organs[34]. This is achieved through surface expression of the adhesion molecule CD62L (L-selectin) and the chemokine receptor CCR7. CD62L and CCR7 interact with glycosylated peripheral node addressins[35] and CCL21[36] respectively. These ligands are expressed on high endothelial venules and facilitate T cell migration into lymph nodes. Peripheral DC loaded with tissue-derived antigens also migrate to the secondary lymphoid organs via afferent lymphatic vessels in a CCR7-dependent manner[37,38]. DC present processed peptide antigen to the naïve T cells via MHC complex in the T cell zones of the lymph nodes. $CD8^+$ T cells typically bind antigen presented by MHC I receptors whereas $CD4^+$ T cells bind antigen-MHC II complex. Intracellular antigens are presented by MHC I

whereas MHC II presents extracellular antigens that have been endocytosed by the APC. However, this is not a stringent characterisation as presentation of intracellular antigen by MHC II is also documented[39].

The αβ heterodimer that forms the TCR is part of a larger TCR complex which includes the transmembrane protein CD3 (ε,δ,γ,ζ chains) (Figure 1.1). CD3 transduces the signal from the TCR and other co-receptor input through the phosphorylation of ITAM sequences (immuoreceptor tyrosine-based activation motifs) in its cytoplasmic tail. ITAM phosphorylation induces membrane translocation and clustering of signalling mediators leading to a cascade of intracellular events. These result in the nuclear translocation of transcription factors which interact with gene promotors to initiate T cell gene expression. Fig 1.1 depicts some important molecules and signalling pathways associated with $CD4^+$ T cell activation. Co-stimulatory signals from receptors such as CD28, ICOS and CD40L are essential for complete T cell activation[40]. Primed APC upregulate ligands for these receptors in response to danger signals in the local environment. These signals provides a check point for the initiation of T cell responses, whilst engagement of inhibitory receptors such as CTLA-4 (cytotoxic T-lymphocyte-associated protein 4) which shares ligands with CD28 can attenuate an activation event[41].

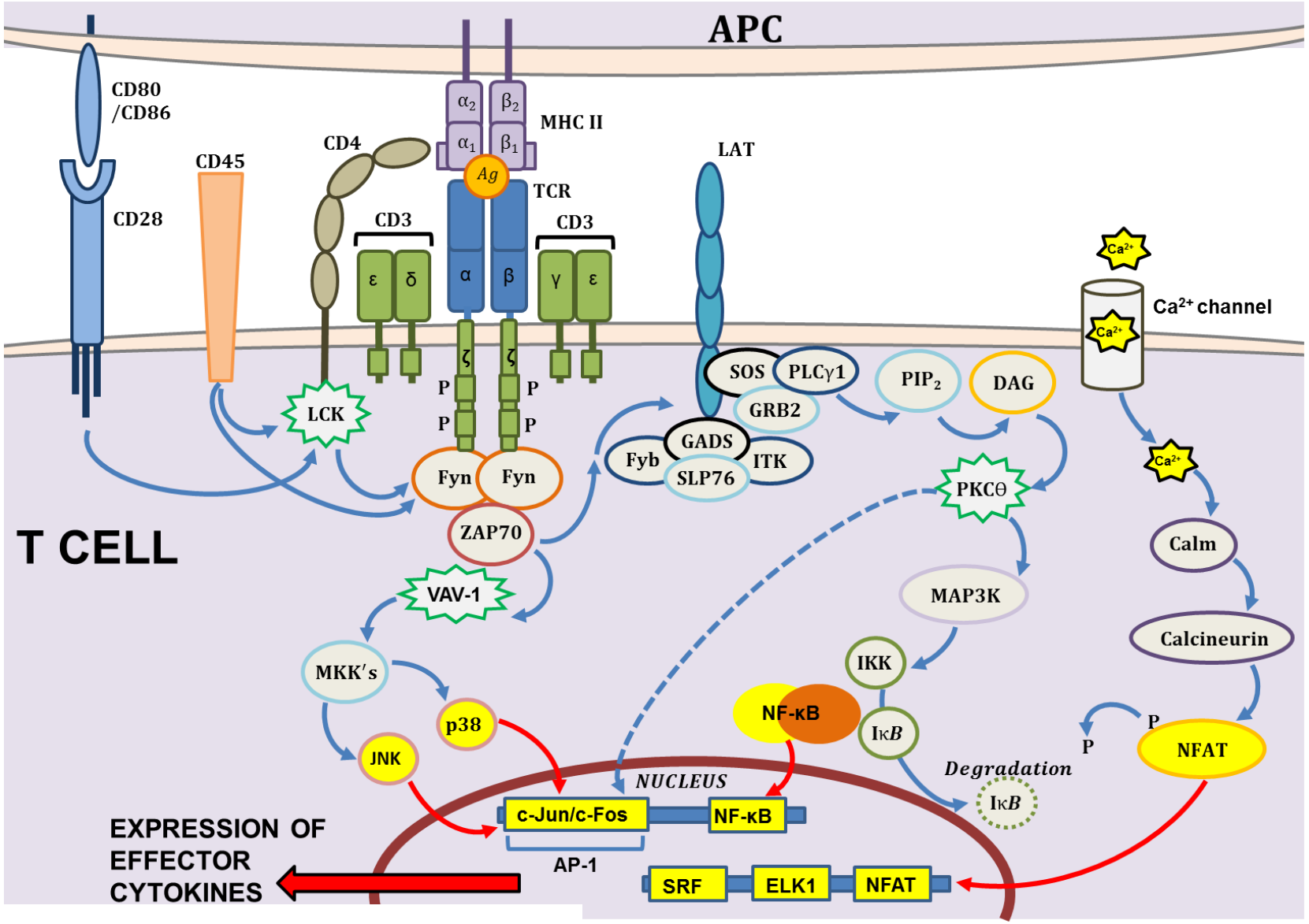

*For figure legend see next page

Figure 1.1 Simplified schematic diagram of some important molecular pathways in $CD4^+$ T cell activation. Antigen-MHC II complex recognition by the T cell receptor (TCR) leads to phosphorylation of ITAM motifs on the CD3 zeta chains. This signal is amplified through activation of Src-family kinases Lck, Fyn and ZAP70. Lck is associated with CD4 and is also activated through signalling via CD28 co-stimulation and its dephosphorylation by CD45. ZAP70 activates LAT (linker of activated T cells) which induces the phospholipase-C-gamma-1 pathway (PLCγ1) via SOS (son of sevenless) and GRB2 (growth factor receptor bound protein 2). Production of the secondary messenger DAG then interacts with PKCϴ (protein kinase C theta) and initiates a mitogen-activated protein kinase pathway (MAP3K). This results in the activation of IKK (IκB kinase) which phosphorylates inhibitory IκB molecules. This releases the inflammatory transcription factor NF- κB for nuclear translocation. PKCϴ is also shown to influence AP-1 transcription activity independent of JNK-dependent activation, and thus links NF- κB to AP-1 activity.

ZAP70- and LAT-associated mediators also phosphorylate the guanine nucleotide exchange factor VAV-1. VAV-1 activates a cascade of mitogen-activated protein kinase kinase (MKK) activity which results in the activation of MAPK family members p38 and JNK. These directly phosphorylate components of the AP-1 transcription factor complex, which itself modulates inflammatory gene activation.

An increase in intracellular calcium (Ca^{2+}) is initially induced through PLCγ1 mediated inositol triphosphate action on endoplasmic reticulum receptors (pathway not shown). This initial rise causes an influx of extracellular $Ca2^+$ through membrane calcium release activated calcium channels (CaCn). Increased Ca^{2+} prevents the inhibitory effects of calmodulin (calm) upon calcineurin. Calcineurin dephosphorylates the transcription factor NFAT, which is released into the nucleus and activates gene transcription.

This diagram is modified from QIAGEN's original image which can be found at [508].

Modifications include adaptations from Figure 1. *N.R.J Gascoigne (2008)*[509].

1.3.3 Phenotypic markers of T cell activation.

T cell activation can be identified by changes in surface receptors expressed at the cell membrane. The type II c-lectin superfamily member CD69 is a highly glycosylated transmembrane protein that is detectable within 1h of TCR-induced T cell activation[42]. CD69 is also rapidly upregulated by phorbol esters such as PMA (phorbol myristate acetate)[43], which by-passes TCR signalling by passing through the T cell membrane and directly activating protein kinase C Θ (PKCΘ). CD69 expression is maintained for up to 72h post activation in T cell cultures[42], yet its true role in the T cell response is under defined. The cytoplasmic domain of CD69 is stunted and the accessory signalling components required for signal transduction are not fully established. In addition, no definitive ligand for CD69 has been identified although in studies of recombinant protein interaction the extracellular domain of CD69 has shown binding to galectin which is expressed by DC[44]. Despite its strong association with activation there is significant evidence that CD69 negatively regulates T cell function. Studies have identified a paradoxical re-upregulation of CD69 on terminally differentiation cells that progressively lose their functionality (see section 1.6.2), suggesting its involvement in inhibiting T cell responses[45,46]. In mouse models, when TCR-transgenic mice are injected with TCR-specific antigen the activation and proliferation of T cells is unaffected by a $CD69^{-/-}$ background[47]. Conversely, in a model of inflammatory arthritis CD69 deficient mice show an exaggerated disease phenotype[48]. There is also evidence that CD69 negatively regulates the induction of pro-inflammatory $CD4^+$ T cell subsets such as Th_{17} cells via inhibition of subset associated transcription factors[49].

CD25 is also upregulated upon T cell activation and correlates with an increased sensitivity of activated T cells to IL-2. CD25 is upregulated via *de novo* transcription and is detectable at 6h post activation with PMA or anti-CD3 stimulation[50]. Therefore, CD25 protein upregulation is typically first observed from 6-12h and therefore lags behind CD69, but is maintained for a

longer duration[51]. Other markers of T cell activation that upregulate later than CD25 include the transferrin receptor (CD71) and the MHC II variant HLA-DR[51].

1.3.4 Memory and antigen recall in the T cell compartment.

During the resolution of an immune response, populations of clonally expanded effector T cells contract in a process that facilitates the maintenance of immunological 'space' and permits diversity within the T cell repertoire. >90% of activated effector T cells die by activation induced cell death (AICD) and studies in CD95 deficient mice have indicated that this is mediated by FAS/FAS ligand induced apoptosis[52,53]. Mechanisms which govern this contraction phase are still incompletely defined, although mouse models of lymphocytic choriomeningitis virus (LCMV) and *listeria monocytogenes* (LM) infection have indicated that the contraction of $CD8^+$ effector T cells is independent of the antigen load, pathogen clearance and the magnitude of the expansion phase[54]. In mouse studies it is found that a population of 2-10% of effector cells persist to become memory T cells irrespective of the pathogen type. The ability to survive the contraction phase may be a characteristic that is pre-programmed early in the inflammatory response[55] and involve the persistent expression of the IL-7 receptor α-subunit (CD127). IL-7 receptor signalling is essential for the homeostatic maintenance of memory T cell populations[56]. The mechanisms governing the generation of long lived memory T cells are controversial and inconsistent between mice and men. Three models by which memory T cells are generated are described below. A consistent feature between these models is that the T cell memory pool can be divided into two distinct populations of central memory (T_{cm}) and effector memory (T_{eff}) cells based on their expression of homing receptors and migratory behaviour. This classic paradigm was first proposed by *F. Sallusto et al* in 1999 and demonstrates that T_{cm} maintain expression of CD62L and CCR7 like T_{naive} cells, whereas T_{eff} lose expression of both these markers[57]. Therefore, although both T_{cm} and T_{eff} are found in the blood T_{cm} typically circulate between the blood and lymphatics system whereas T_{eff} home to peripheral tissues.

- **Model 1 – Linear differentiation model**

Early studies of $CD8^+$ T cell differentiation in mice indicated that the generation of memory was a linear progression from T_{naive} to T_{memory} via short lived effector cells[58,59]. Following LCMV infection effector $CD8^+$ T cell populations gave rise to memory T_{eff} which then differentiated into lymphoid homing T_{cm} (Figure 1.2A). Therefore, homeostatic turnover of terminally differentiated T_{cm} populations provide the maintenance of memory. This is in keeping with findings showing T_{cm} have a greater proliferative capacity than T_{eff}[60]. However, this is inconsistent with other areas of biology where progressive differentiation is usually accompanied by a decrease in replicative potential.

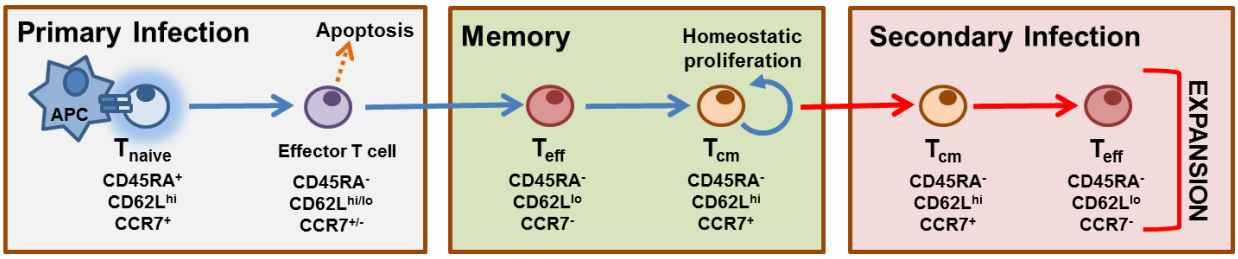

Figure 1.2A Diagram shows a linear differentiation model of memory T cell formation and antigen recall response. Figure adapted from [63].

- **Model 2 – Asymmetric division model**

This model proposes that activated T_{naive} cells divide asymmetrically to generate populations of short lived effector cells, memory T_{cm} and memory T_{eff} populations. This is achieved through reorganisation of the mitotic spindles to disproportionally segregate signalling proteins and transcriptional regulators amongst T_{naive} cell progeny[61]. It is proposed that asymmetric division is an early event in T_{naive} cell activation and is irreversible beyond a very few cellular divisions. This model is consistent with early findings by *N. Manjunath et al (2001)*. Here a fluorescent GFP reporter which is lost during differentiation showed that long lived T_{naive} progeny ($CCR7^+$ T_{cm}) differentiate independently from short lived effector cells[62].

In addition, the balance between the lineages could be influenced *in vitro* by exogenous IL-2 and IL-15 [62].

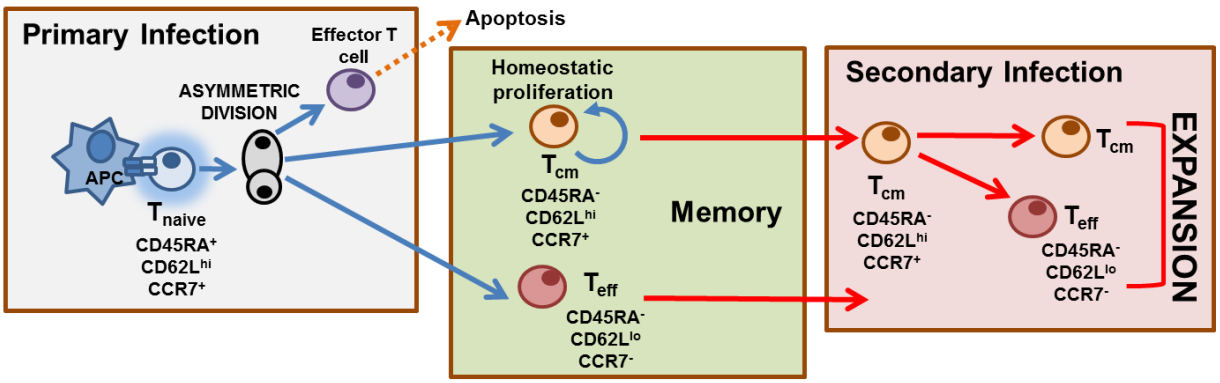

Figure 1.2B An asymmetric differentiation model of memory T cell formation and antigen recall response. Figure adapted from [63].

- **Model 3 – Stem cell-like memory maintenance.**

Memory T cells have historically been compared to stem cells given their ability to self-renew to maintain their frequency in the periphery. Recently, a population stem cell like memory cells (T_{SCM}) has been defined[64]. These represent 2-3% of both the $CD8^+$ and $CD4^+$ T cell populations and maintain T_{naive} characteristics ($CD45RA^+$) in addition to stem cell properties (c-Kit expression, elevated wnt signalling)[65]. However, these T_{SCM} have undergone antigen-driven clonal expansion, have robust cytokine responses *ex vivo* and proliferate in response to IL-7 and IL-15[64]. As these cells are shown to be highly proliferative, multipotent and persistent in lymphoid organs it is proposed that they represent the precursors of all effector T cells. Therefore, T_{SCM} are pivotal in this latest model of differentiation and as asymmetric division is a feature strongly associated with stem cell biology there is some overlap between the asymmetric and T_{SCM} models (Figure 1.2C). Although this differentiation model has been applied to $CD4^+$ T cell biology the majority of understanding comes from work in $CD8^+$ T cells. There is little work which temporally relates the complex lineage differentiation of $CD4^+$ T helper subsets (section 1.5.1) to this model of memory formation.

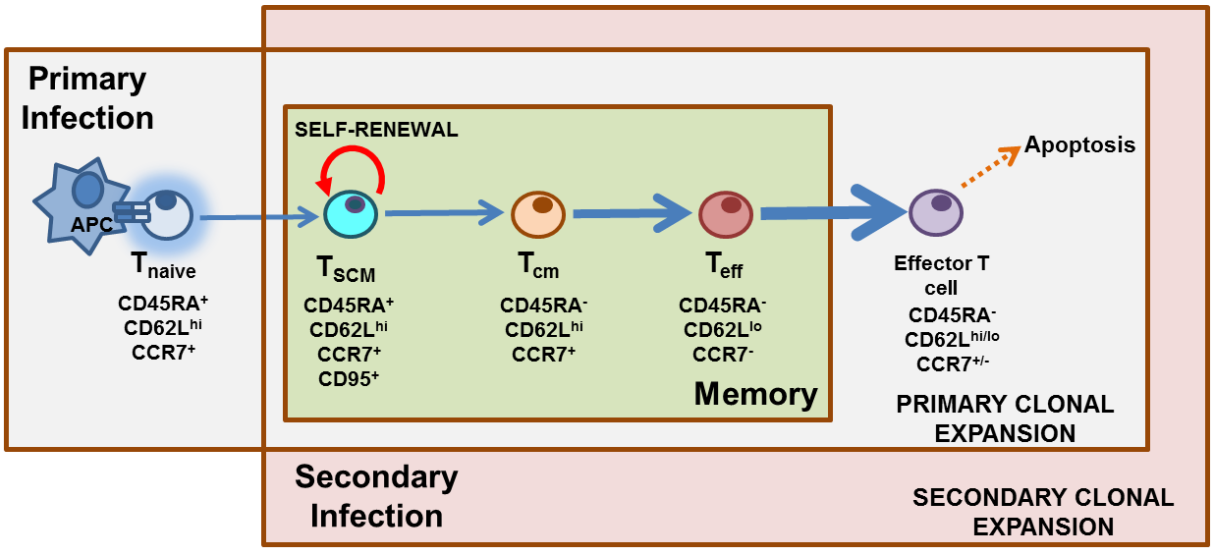

Figure 1.2C An 'self-renewal' model of memory T cell differentiation via a common stem-cell like central memory progenitor (T_{SCM}). Adapted from [510].

1.3.5 Tissue specific homing of effector memory T cells.

The primary role of T_{eff} is to elicit rapid effector function at the site of infection (or reinfection). In contrast, T_{cm} populations have a greater proliferative capacity and greater resistance to apoptosis, so are more accredited with the maintenance of immune memory[66]. However, following reactivation the cytokine responses of T_{cm} populations are shown to be almost as robust as their T_{eff} counterparts[67,68]. Therefore, the definition of T_{cm} and T_{eff} is largely based on the anatomical location of each population (lymph node versus peripheral tissue) as opposed to their functional capacity.

To provide the most effective immune surveillance effector memory T cells preferentially migrate to the tissue where the inflammatory response was initiated. Therefore, a notable proportion of these populations are sequestered in the tissues and their representation in the blood is an underestimation of their frequency[69,70]. Peripheral tissue migration occurs at post-capillary venules which have endothelial expression of chemokine receptor ligands and adhesion molecules. The pattern of adhesion receptors which may recognise these ligands is imprinted by activating DC at the time of T cell differentiation[71]. The processes that

underpin T cell recruitment to peripheral tissue can be summarised in the following four stages;

1. **Capture –** T_{eff} cells are captured onto the luminal surface of the endothelium and are slowed against the blood flow. This involves the interaction of endothelial selectin molecules with highly glycosylated protein ligands on the T cell surface. These ligands can have specific carbohydrate modifications at particular residues that increase their specificity. For example, skin homing T_{eff} express a CLA (cutaneous lymphocyte antigen) which is a modified form of the more ubiquitous PSGL-1 (P-selectin glycoprotein ligand-1). This binds P-selectin that is constitutively expressed in the vascular beds of the skin[72].
2. **Activation** - Selectin-mediated capture causes the T cells to roll along the endothelium and permits more firm binding of chemokine receptors. Chemokine receptors are transmembrane G protein coupled receptors which transduce an intracellular signal upon binding their chemokine ligands[73]. These ligands can be expressed by vascular endothelium constitutively and/or upregulated in inflammation. Chemokine receptor binding activates the cell by elevating intracellular cyclic AMP and initiating RHO GTPase and phospholipase C mediated signalling pathways[73]. Through these pathways integrin receptors are activated via the intracellular protein talin and firm adhesion is achieved[74]. Chemokine receptor expression is strongly associated with tissue specific homing of T_{eff} subsets. For example, CCR4 and CCR10 expression are associated with skin homing signals via their respective interactions with CCL17 and CCL27[75,76]. Conversely, CCR9/CCL25 interaction is association with intestinal tropism[77,78].
3. **Adhesion –** Integrins are heterodimeric transmembrane proteins that become activated through chemokine receptor signalling. Conformational changes within integrins increase the receptors affinity for immunoglobulin superfamily members expressed by

vascular endothelium[79]. The integrin heterodimer $\alpha_4\beta_7$ binds MAdCAM-1 (mucosal vascular cell adhesion molecule 1)[80,81]. $\alpha_4\beta_1$ (VLA-4) and $\alpha_L\beta_2$ (LFA-1) preferentially bind VCAM-1 (vascular cell adhesion protein 1) and ICAM-1 (Intracellular adhesion molecule 1) respectively[82]. Integrin binding mediates the firm arrest of T cells on the endothelial surface, cytoskeletal rearrangements involved in lymphocyte 'crawling', and early transendothelial migration events[83].

4. **Transendothelial migration** – Two defined modes of transendothelial migration (TEM) are the paracellular and transcellular routes[84]. Paracellular migration requires the crawling of lymphocytes to an endothelial cell-cell interface and remodelling of tight junctions to allow passage through the barrier. This is facilitated by ICAM-1-induced cytoskeletal contraction to pull apart and weaken endothelial tight junctions[84,85]. In studies of leukocyte extravasation, junctional adhesion molecules (JAMs) (which normally dimerise at cell junctions) are shown to interact with LFA-1 (JAM-A) and VLA-4 (JAM-B/C) to facilitate lymphocyte passage[86,87]. Homophilic interactions between PECAM-1 molecules (platelet endothelial cell adhesion molecule-1) that are expressed by leukocytes and endothelial cells are also a significant step in paracellular TEM[88]. In contrast, transcellular migration involves the passage of immune cells through the middle of endothelial cells, typically where the endothelial layer is thin or weakened. ICAM-1 is enriched around the leukocyte interface and this induces cytoskeletal remodelling of the endothelial cell[85] which is also facilitated by JAM-A and PECAM-1[89]. Such interactions form a channel through the endothelial cell via the linking of ICAM-1 rich caveolae forming vesiculo-vacuolar organelles[90]. Therefore, a pore is formed directly through the endothelial cell to facilitate diapedesis.

Once beyond the endothelial barrier the migration of T cells away from the vasculature is mediated by tissue-specific stromal factors and chemokine gradients. Interestingly, the

persistence of memory T cells within peripheral compartments is not uniform within the population. Work examining $CD8^+$ memory subsets in organs including the skin, gut, lungs and reproductive tracts has identified populations of 'tissue resident' memory (T_{RM}) cells that are distinct from those which continuously circulated between blood and tissue[70,91,92]. Parabiosis experiments in mice demonstrate that traceable antigen-specific $CD8^+$ T cells from each mouse do not readily equilibrate in certain tissues such as the gut mucosa[93,94]. This implies that these cells do not recirculate between animals and are maintained within the donor tissues. T_{RM} are distinctive from T_{eff} as they constitutively express α_E integrin (CD103) and CD69[70,95]. T_{RM} are also characterised in the $CD4^+$ T cell compartments, although the expression of CD103 in these subsets is not as elevated as in their $CD8^+$ counterparts. It is proposed that T_{RM} are derived from circulating T_{eff} but the signals that regulate this conversion are incompletely defined. As CD69 is more classically associated with T cell activation it is possible that the presence of persistent antigen may promote the T_{RM} phenotype. However, in a mouse model of lung infection influenza-specific $CD4^+$ T_{RM} persist in the lungs long after antigen clearance indicating the stability of the T_{RM} population irrespective of persistent antigen and inflammation[96].

Another characterised role of CD69 expression in regulating migration is exemplified in the lymph nodes, where activated $CD69^{hi}$ T cells are retained through the inhibition of sphingosine-1 phosphate receptor 1 ($S1P_1$) expression[97]. $S1P_1$ is required for lymph node egress via chemotactic attraction to its ligand (S1P) which is at a higher concentration in the circulation than in the lymph. This process is modulated by the drug FTY720 (Fingolimod) which blocks S1P/ $S1P_1$ binding and prevents self-reactive T cells leaving the lymph nodes[98]. However, the reciprocal expression of CD69 and $S1P_1$ or other mediators is not currently described in studies of T_{RM}. Alternatively, as CD103 is an integrin subunit it is suggested that its adhesion properties may be involved in T_{RM} tissue retention[99].

In non-inflamed peripheral tissues the egress of circulating T_{eff} is dependent on their upregulation of the chemokine receptor CCR7 which binds CCL21 ligand on the afferent tissue lymphatics[100]. In human skin up to 50% of skin-derived memory $CD4^+$ T cells express CCR7[69]. Such a finding is difficult to reconcile with the original definition of T_{eff} cells which are distinguishable from T_{cm} by their lack of CCR7 expression. Interestingly, *in vivo* studies tracing the origins and fate of cutaneous $CD4^+$ memory T cells have suggested that a population of $CCR7^+CD62L^{int}$ T_{eff} can recirculate between both the peripheral tissue and the lymphatics via the blood[101]. These recirculating cells may be distinct from classical T_{eff} that lack CCR7 expression and whose fate on tissue entry remains undefined. It is clear that the definition of memory can be considered more complex than the T_{cm}/T_{eff} paradigm[57]. Processes that drive the generation and migration patterns of memory $CD4^+$ T cell subsets are essential for the maintenance of long-lasting peripheral immu**n**ity. A deeper understanding of these mechanisms is essential for the recognition and prevention of aberrant T cell responses in inflammatory pathologies.

1.4 $CD8^+$ T cells and other killer cell subsets.

$CD8^+$ T cells are characterised by their ability to recognise antigens presented by MHC I. Expression of the CD8 glycoprotein facilitates this interaction through binding to the non-polymorphic MHC I α3 domain[102]. As MHC I is associated with the presentation of intracellular antigens, $CD8^+$ T cells are most recognised for their cytotoxic response against virally infected and transformed tumour cells. Once activated, cytotoxic T cell subsets begin producing effector cytokines such as interferon gamma (IFNγ). IFNγ has pleotropic autocrine and paracrine functions including; 1) the enhancement of natural killer cell (NK cell) activity[103], 2) activation of granulocytes and monocytes[104], 3) T cell subset differentiation[105], and 4) the upregulation of adhesion molecules on endothelium to promote the trafficking of immune cells to inflamed tissues[106]. $CD8^+$ cells produce cytokine and proliferate rapidly, initiating target cell killing through release of perforin and granzyme

proteins. Perforin punctuates the target cell membrane to allow granzyme entry. This triggers a cascade of serine proteases resulting in caspase mediate apoptosis and lethal mitochondrial ROS production[107]. Alternatively, $CD8^+$ T cells can induce caspase-dependent apoptosis via upregulation of FAS ligand, which binds to target cells expressing the FAS death receptor (CD95)[108].

NK cell subsets share cytolytic killing features with the $CD8^+$ T cell lineage and can eliminate infected, stressed and transformed cells. NK cells are part of the innate lymphoid cell family, which are derived from lymphoid progenitors but lack a TCR receptor so do not recognise antigen specifically. These cells are shown to develop in multiple sites (e.g. bone marrow, thymus, lungs and uterus[109]) and distinguish stressed from unaffected cells by integrating changes in cellular motifs on cell surfaces. These changes are recognised through a multitude of self-recognition receptors, for example the KIR family (killer cell immunoglobulin-like receptor) which can detect downregulation of MHC I on virally infected cells[110]. NK cells are often identified by varying surface expression of CD56 and CD161. These markers can also identify other innate lymphoid subsets such as natural killer T cells and natural killer-like T cells[111]. The existence of such populations demonstrates the overlap between innate and adaptive immune function.

1.5 $CD4^+$ T cells.

1.5.1 $CD4^+$ T cell differentiation.

By modulating the function of other innate and adaptive immune cells $CD4^+$ T cells (T_{helper} cells) are considered master orchestrators of complete immune responses. Upon activation T_{naive} cells proliferate rapidly forming a pool of multipotent progenitors termed Th_0 cells[112]. This expansion is driven by autocrine and paracrine IL-2 signalling through the IL-2 receptor complex. At this phase the IL-2 receptor is converted into its highest affinity state via expression of the IL-2Rα subunit (CD25)[113]. During the expansion phase T_{naive} differentiate into a number of T_{helper} subsets with specific effector functions. The antigen avidity, duration

and input from co-receptors are determinants of this differentiation phase and prime T_{helper} responses to be most appropriate for optimal pathogen clearance. The cytokine milieu provided by local APC and other resident cells is dependent on the nature of initial pathogenic insult, which in turn polarises the differentiation of T_{helper} cells[114].

Cytokines are small soluble proteins that bind to their corresponding cell surface receptors. There are many subtypes of cytokine receptors with numerous structural conformations. For example, the common gamma chain cytokine family are composed of various combinations of heterodimeric or heterotrimeric transmembrane subunits which determine their specificity for IL-2, IL-4 IL-7, IL-9, IL-15 and IL-21[115]. A common mechanism of cytokine receptor signal transduction is via receptor association with Janus kinase (JAK) molecules that phosphorylate STAT family members (signal transducer and activator of transcription). Nuclear translocation of STATs initiates the transcription of key regulators that determine the differentiation pathway of effector T_{helper} cells (Figure 1.3). However, not all cytokine receptors signal via the JAK/STAT pathway. For example, the tumour necrosis factor alpha (TNFα) receptors TNFR1 and TNFR2 signal via various adaptor proteins including TRADD (TNFR1-associated death domain protein), TRAF2 (TNF receptor-associated factor 2) and RIP (receptor-interacting protein). Together with other mediators these activate proinflammatory pathways via NF-κB and AP-1 transcription factors and can also mediate caspase-dependent apoptotic pathways[116].

Historically, two 'flavours' of T helper cell were described by Mosmann and Coffman which were defined as Th_1 and Th_2 subsets[117]. Th_1 genes are expressed through Tbet transcription factor activity[118] which promotes IFNγ production. In contrast, GATA3 induced IL-4, IL-5 and IL13 secretion and is characteristic of Th_2 subsets[119]. These Th_2 cytokines promote B cell activation, proliferation and class switching. Cytokine-induced polarisation towards a particular phenotype is enhanced by inhibiting genes that promote alternative lineage differentiation. For example, IL-4 induced GATA3 expression transiently inhibits IFNγ

production and thus limits Th_1 differentiation[120]. Many additional T_{helper} subsets have been defined in subsequent decades (Figure 1.3). A degree of plasticity between T_{helper} lineages is also documented, where a particular subtype can acquire phenotypic traits of another under strong polarising conditions[121]. For example, fate mapping experiments in mice have demonstrated that under chronic neuroinflammatory conditions (experimental autoimmune encephalomyelitis (EAE)), differentiated Th_{17} cells switch on IFNγ production which is an atypical cytokine for this lineage[122]. A detailed synopsis of every characterised T_{helper} subtype is beyond the reach of this introduction. However, what is important to note is that differentiated $CD4^+$ T_{helper} cells are defined by their ability to make cytokine and this is the mechanism by which they elicit their various effector functions.

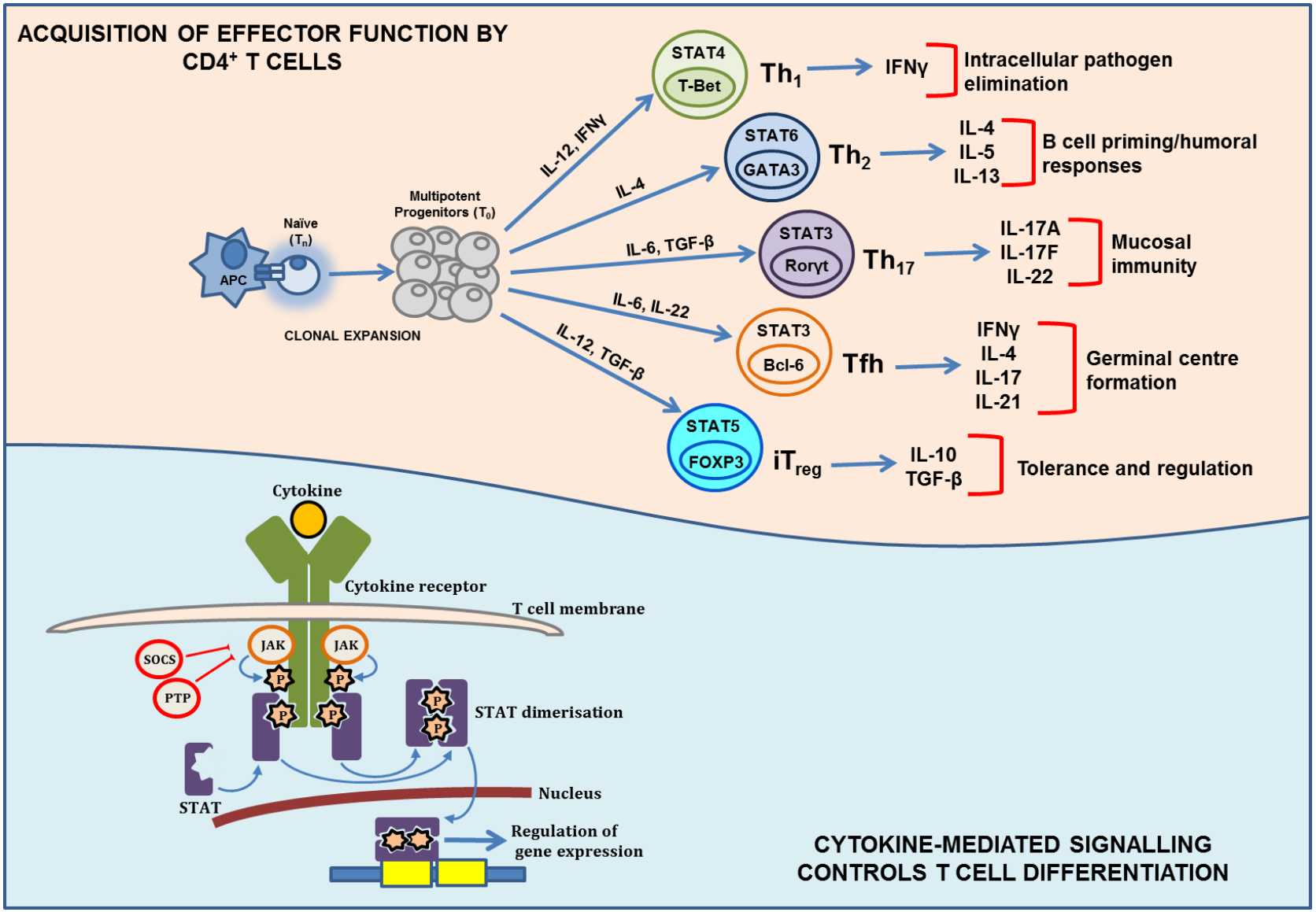

*For figure legend see next page

Figure 1.3 Cytokine signalling and $CD4^+$ T cell differentiation. Top panel; On interaction with cognate antigen–MHC II complex presented by antigen presenting cells (APC), naïve $CD4^+$ T cells proliferate to produce a pool of multi-potent progenitor cells (T_0). These differentiate to form various effector Thelper subsets, which is driven by the presence of cytokines in the surrounding milieu. Bottom panel; Extracellular cytokines regulate gene expression through interaction with their relevant receptors at the T cell membrane. Receptor activation induces the activation of associated JAKs (janus-activated kinases), which phosphorylate the cytokine receptors cytoplasmic tail. JAK activation can be inhibited through the activity of SOCS (suppressor or cytokine signalling) and other PTPs (protein tyrosine phosphatases). Receptor phosphorylation triggers the recruitment and phosphorylation of STATs (signal transducer and activator of transcription). STATs dimerise and are translocated to the nucleus where they promote the expression of their associated master regulators of T cell programming (top panel). The various transcriptional programs of the Thelper lineages are associated with specific patterns of cytokine secretion. These modulate the behaviour of other immune cells and introduce diversity into the way specific pathogens are controlled.

This diagram is an adapted representation of figures presented in [511] (top panel) and [512] (bottom panel).

1.5.2 Regulatory $CD4^+$ T cell subsets.

$CD4^+$ T cells have the potential to elicit profound damage to the hosts if their activation is not strictly regulated. Therefore, if mechanisms assigned to prevent the generation of dangerous and self-reactive T cells in the thymus should fail there are additional processes in the periphery to protect against aberrant T cell activation. One such mechanism is the presence of regulatory T cell subsets (T_{reg}) which are transcriptionally programmed to modulate the activity of other immune cells. Some molecular processes through which regulatory subsets suppress inflammatory and autoimmune responses are summarised in Table 1.2.

T_{reg} either develop naturally during thymic maturation (nT_{reg}) or differentiate in the periphery following conventional T_{naive} activation (iTreg) (Figure 1.3). Expression of the transcription factor FOXP3 is essential for nT_{reg} development in mice and humans. Mice with loss-of-function mutations in FOXP3 develop fatal multi-organ inflammatory pathologies attributed to loss of T_{reg} induced tolerance[123]. nT_{reg} gain FOXP3 expression in the medullary region of the thymus as indicated by experiments using FOXP3 reporter gene constructs[124]. pre-T_{reg} programming may occur before the SP thymocyte stage through undefined mechanisms, but strong recognition of self-peptide MHC II complex presented by medullary APC is essential for nT_{reg} maturation[125]. Adequate co-stimulation is important for this process as CD28 deficiency significantly reduces the frequency of peripheral nT_{reg}[126]. Intensive signalling to nT_{reg} induces the upregulation of CD25, which rescues the population from negative selection through an increased responsiveness to IL-2. Both IL-2 and IL-7 are shown to be important in T_{reg} development in mice in conjunction with other stromal factors such as glucocorticoid-induced TNFR-related protein (GITR) and lymphopoietin[124]. nT_{reg} thymic emigrants are phenotypically naïve and are recognised by $CD45RA^+CD25^{hi}CD127^{lo}FOXP3^{lo}$ expression in humans[127]. When activated naïve nT_{reg} differentiate into effector T_{reg} ($CD45RA^-$) they upregulate FOXP3 and co-inhibitory mediators. These can limit proinflammatory responses in the local environment (Table 1.2).

T_{reg} marker/ molecular signature	Mechanism	Target	Outcome	Ref
CTLA-4	Competitive inhibition of CD28 mediated co-stimulation. Reduced presentation of CD80/CD86 by APC	T cells	↓ TCR costimulation	[128,129]
	IDO production by DC - altered tryptophan metabolism	T cells	↑ anergy, ↑ apoptosis	[130,131]
		T_{reg}	↑ T_{reg} activity	
CD73-CD39	Sequential extracellular metabolism of adenosine. Binds A_{2A} receptors on both conventional T cells and Treg.	$CD4^+$ T cell	↓ TCR signalling ↓ IL-2 signalling	[132]
			↑ CTLA-4 expression	[133]
			↑ PD-1 expression	
		T_{reg}	↑ FOXP3 expression	[134]
CD25	Sequestration/consumption of IL-2	T cells	↓ IL-2 signalling and effector cell proliferation	[135]
Granzyme/perforin	Cytolysis of target cell - cell death	T cells	↓ Effector cell availability	[136,137]
FASL	FAS/FAS ligand induced apoptosis - cell death	$CD8^+$ T cells		[138]
TCR-peptide MHC binding	Bystander effect	DC	Prevents DC interaction with effector T cells	[139]
Cytokines				
IL-10	Modulation of DC function, polarisation of effector T cell differentiation	DC	↓CD40, ↓IL-12, ↑ IL-10, ↓CD80/CD86,	Reviewed in [140]
TGF-β		$CD4^+$ T cell	↑ Treg differentiation	[141,142]
IL-35*	Enhances T_{reg} survival and IL-10 production (*is not expressed by human T_{reg})	$CD4^+$ T cell	↓ Th_1, Th_{17}, ↑ Treg differentiation	[143]

Table 1.2 Summary of some notable molecular mechanisms associated with regulatory T cell function.

Like conventional $CD4^+$ T cells the differentiation of nT_{reg} can be polarised by the local cytokine milieu to optimise their suppressive function. For example, co-expression of FOXP3 and GATA3 by effector T_{reg} is important in suppressing Th_{17}-mediated inflammation[144]. Selective deletion of STAT3 in intestinal $FOXP3^+$ T_{reg}, which increases susceptibility to Th_{17} driven inflammation in a model of colitis[145]. The effector T_{reg} pool can also be divided into circulating and tissue resident subpopulations and $CD103^+$ subsets are enriched in the skin and lungs[146,147]. Whereas naïve T_{reg} can represent around 10% of circulating $CD4^+$ T cells in adults, effector T_{reg} represent only 1-4%. Similar to T_{helper} cells the naïve T_{reg} population decreases with age in line with thymic involution whereas the effector pool is expanded. In contrast to nT_{reg}, the iT_{reg} population are derived from conventional naive $CD4^+$ T cells in the periphery and only contribute to the effector T_{reg} pool[148]. The nT_{reg} and iT_{reg} populations are phenotypically similar, making it challenging to distinguish between the populations in the periphery. Conventional $CD4^+$ T cells also transiently upregulate CD25 and FOXP3 during activation which adds further to the complexity of separating these populations[51,149]. Interestingly, $CD25^{hi}FOXP3^+$ T_{helper} cells share features with T_{reg} which is informative about their biology. Mouse T_{reg} can be hyporesponsive to *in vitro* stimulation so historically the population was synonymous with an anergic T cell phenotype[150] (see section 1.6.1). Subsequent studies have demonstrated that conventional $CD25^{hi}FOXP3^+$ T_{helper} cells also show abrogated cytokine secretion and proliferation *in vitro*, indicating that FOXP3 upregulation may negatively regulate T cell activation[151]. FOXP3 also influences the expression of NFAT family member NFATc2. TCR-induced upregulation of NFAT drives FOXP3-dependent inhibition of cytokine production (IL-2) and forms a negative-feedback loop further suppressing NFAT activity[152,153].

FOXP3 expression has a significant role in T_{reg} homeostasis and T_{reg} have a higher proliferative capacity than conventional $CD4^+$ T cells *in vivo*. In mice $CD25^{hi}$ T_{reg} incorporate more BrdU dye into their replicating DNA than non-T_{reg} subsets which indicates that they

undergo more mitotic divisions[154]. Analysis of human blood populations shows that a greater percentage of T_{reg} express the proliferation marker Ki-67 than non-T_{reg}[155]. This higher proliferative capacity is offset by an accelerated rate of apoptosis which maintains T_{reg} homeostasis, particularly following clonal expansion[156]. T_{reg} have an intrinsic propensity to undergo apoptosis through their expression of FOXP3, which promotes the expression of pro-apoptotic BCL-2 family members Bim and PUMA[157]. Bim and PUMA antagonise the effects of anti-apoptotic Mcl-1 which releases Mcl-1-dependent inhibition of apoptosis initiators BAX and BAK[158]. This intrinsic apoptosis pathway is counterbalanced by IL-2 availability and production by other local effector T cells. IL-2 signalling via CD25 overrides the activity of Bim and PUMA by promoting Mcl-1 activity, thus inhibiting the apoptosis pathway. The T_{reg} population then expands until the local IL-2 is depleted through the suppression of effector cells. FOXP3 pathway again predominates and thus a feedback mechanism is provided by which T_{reg} homeostasis is maintained[156].

Although FOXP3 is important in maintaining some T_{reg} populations the suppressive function of T_{reg} cannot be wholly attributed to FOXP3 expression. Conventional $CD4^+$ T cells which upregulate $FOXP3^+$ do not actively suppress other non-T_{reg} cells *in vitro*[151]. Other regulatory populations have also been described that lack expression of FOXP3 or CD25. For example, Tr_1 regulatory cells are characterised by their expression of anti-inflammatory IL-10 cytokine[159]. Tr_1 cells may also be derived from Th_{17}/Th_1 lineages in chronic inflammatory conditions and their suppressive function may have a role in inhibiting autoimmune responses[160,161]. In contrast, a characterised Th_3 regulatory subset is predominantly defined by TGF-β-mediated suppression[162].

1.6 T cell hyporesponsiveness and its implications for T cell-mediated immunity.

1.6.1 T cell anergy as a form of peripheral tolerance.

T cell intrinsic mechanisms have been characterised which limit T cell activation and promote tolerance. The concept of 'anergy' describes how $CD4^+$ T cells become hyporesponsive to TCR stimulation in the absence of sufficient co-stimulation[163,164]. This is a protective mechanism by which TCR recognition of self or non-pathogenic peptides will not trigger an immune response without additional 'danger signals' from mediators upregulated in inflammation. Some *in vitro* models of anergy induction include; 1) TCR stimulation with anti-CD3 coated beads in the absence of anti-CD28[165], 2) low affinity peptide presentation by APC[166], 3) peptide presentation by quiescent APC (e.g. resting B cells)[167], 4) induction of calcium dependent pathways by the calcium ionophore ionomycin[168]. A unifying mechanism behind the hyporesponsiveness in these models is an imbalance of signalling, leading to a combination of exacerbated NFAT transcription factor activity and diminished contribution of AP-1[169]. AP-1 assembly and translocation is required for IL-2 production which is abrogated through deficiencies in upstream MAPK activity.

As NFAT signalling is Ca^{2+} dependent, its role in the anergic pathway is demonstrated through the hyporesponsive state induced by ionomycin. Conversely, anergy is reversed by the calcineurin inhibitor cyclosporine A which blocks NFAT activity[170,171]. Over activity of NFAT promotes the expression of E3 ubiquitin ligases Cbl-b, GRAIL and ITCH[172]. Gene knock out mice for these ubiquitin ligases have anergy-resistant T cells which are hyper-responsive to TCR [173–175]. Ultimately these mice develop severe early onset multi-system autoimmunity, thus exemplifying the importance of anergising processes in the maintenance of self-tolerance. E3 ligases function by tagging ubiquitin motifs on to signalling components involved in TCR transduction[164]. Ubiquitination targets these proteins for proteasome degradation thus preventing TCR signalling. Cbl-b is shown to dephosphorylate and

ubiquitinylate PLC-γ and so inhibits Ca^{2+} signalling in the anergised state[176]. Both ITCH and another related E3-ligase NEDD4 monoubiquitinylate PKCϴ and PLC-γ, with the latter disrupting LAT-associated signalling[177]. LAT then cannot translocate to the 'immunological synapse' (IS) which represents the foci of signalling molecules clustered around the TCR complex upon antigen recognition. In anergic cells LAT is excluded from the lipid raft membrane formations required for its recruitment to the IS[178]. Cbl-b also inhibits IS recruitment through the ubiquitination of PI3K (phosphoinositide 3-kinase) which prevents the interaction of CD28 with the TCRζ chains[179]. In addition, Cbl-b negatively regulates VAV-1 which prevents the cytoskeletal rearrangements required for trafficking of TCR signalling component[180,181]. The function of Cbl-b overlaps with GRAIL with both reducing JNK transcription factor activity. GRAIL also inhibits actin cytoskeletal remodelling by inhibiting RHO GTPase, which itself is essential for actin polymerisation[182].

The physiological translation of the anergic T cell phenotype is controversial. *In vivo* mouse models of anergy include; 1) injection of superantigen SEB (staphylococcal enterotoxin B), which binds the TCR Vβ8 repertoire to MHC II with high affinity in an antigen independent manner[183] leading to prolonged overstimulation of Vβ8 T cells. 2) the adoptive transfer of transgenic T cells into a host that expresses the cognate antigen endogenously (e.g. tumour antigens)[184], and 3) immunisation with soluble peptide in the absence of adjuvant into transgenic animal which recognise that peptide[185]. It is speculated that the hyporesponsive T cell phenotype is governed by variable molecular mechanisms in these different models[186]. Biochemical inconsistencies between the *in vivo* versus *in vitro* anergic state are also described[187]. Firstly, *in vivo* anergy can be induced in naïve T cell subsets whereas the nature of *in vitro* anergy describes hyporesponsiveness in effector subsets that don't respond to a restimulation event. Secondly, *in vivo* hyporesponsive T cells require chronic persistence of cognate antigen in the periphery to remain 'tolerised' but reverse their anergic-like state following antigen clearance[188]. In contrast, reversal of *in vitro* anergy is unrelated to antigen

removal but requires the presence of IL-2[189]. Addition of IL-2 restores AP-1 related pathways and inhibits the expression of anergy-related genes. Lastly, in *in vivo* anergy TCR signalling defects are further upstream than in cell culture systems and include diminished phosphorylation of ZAP70 as opposed to defects further down in the MAPK chain[190]. In light of these differences *R.H Schwartz et al* have redefined *in vivo* anergy as 'adaptive tolerance'[187,188,190]. However, the phenomenon of adaptive tolerance in human physiology is under defined and no true 'tolerised' $CD4^+$ T cells have been identified *ex vivo*. Further understanding hyporesponsiveness in T cell populations has implications for peripheral tolerance, mechanisms underpinning autoimmunity and initiating factors that drive the failure of anti-tumour responses.

1.6.2 T cell exhaustion.

In addition to the mechanisms of T cell suppression required for the maintenance of self-tolerance 'exhausted' T cells also demonstrate a hyporesponsive phenotype with distinctive characteristics. T cell 'exhaustion' describes a progressive decline in functionality in response to chronic antigen stimulation such as persistent viral load or in a tumour microenvironment. Processes which underpin T cell exhaustion are best defined in the $CD8^+$ T cell subset, with chronic LCMV infection in mice commonly used as a model for inducing the exhausted state[191]. In humans an analogous phenotype is also recapitulated in Hepatitis C (HCV) or human immunodeficiency virus (HIV) infection. In contrast to T cell anergy or tolerance, exhaustion is characterised by a progressive step-wise cessation of functionality, beginning with reduced proliferation and IL-2 production, followed by loss of TNFα and IFNγ secretion[46]. In infection, high antigen load and excessive co-stimulation promote the exhausted phenotype and so different exhaustion models show variable outcomes depending on the severity of infection. For example, IFNγ production in HIV is maintained but accompanied by a loss of cytotoxic function whereas HCV infection is associated with diminished IFNγ expression[192–194].

Exhausted $CD8^+$ T cells express a host of inhibitory receptors including PD-1 (programmed cell death receptor 1), TIM-3 (T cell immunoglobulin mucin-3), LAG-3 (lymphocyte-activation gene 3) and CTLA-4[195]. Of these PD-1 is the most extensively studied and has a significant role in dampening anti-tumour responses[196]. PD-1 interacts with the ligands PD-L1 or PD-L2 which are highly represented in some tumour microenvironments[197]. The binding of PD-1 to its ligands induces phosphorylation of its cytoplasmic tail which recruits tyrosine phosphatases such as SHP-1 and SHP-2[198]. The localisation of these phosphatases to TCR microdomains results in dephosphorylation of important proximal signalling components such as ZAP70, which then prevents T cell activation[199]. PD-1 activation also induces cell cycle arrest in G_1-S phase though AKT inhibition and induction of the cyclin-dependent kinase (CDK) inhibitor p27[200,201]. Attenuation of AKT signalling also inhibits the anti-apoptotic Bcl family member Bcl-xL, which increases a cells propensity to undergo apoptosis.

PD-1 is an associative but not definite marker of exhaustion as it is also upregulated on functional T cells where it may serve to attenuate T cell activation[202,203]. Consistent with its association with activation $CD8^+$ T cells acquire PD-1 expression in the early stages of chronic infection and PD-1 or PD-L1 antibody blockade rescues the exhaustive phenotype at this point[204]. Additionally, transfer of murine $PD\text{-}1^{hi}$ $CD8^+$ cells from a $LCMV^+$ host to a pathogen free donor reverses the exhausted phenotype if sufficiently early in the immune response[205]. However, in chronic infection these $PD\text{-}1^{hi}$ cells further differentiate and alter their transcriptional profile through upregulation of the transcription factor eomesodermin and downregulation of Tbet[206]. At this stage cells fail to proliferate without persistent antigen presentation and cannot be maintained homeostatically by IL-7 and IL-15. These cells do not survive on adoptive transfer and are beyond the point of rescue by PD-1 intervention.

The physiological rationale behind the persistence of exhausted T cells in the periphery is unknown. The fact that exhausted cells accumulate and are not cleared from the body suggests that they have some immunological relevance. The progression to 'exhaustion' may serve to prevent excessive collateral inflammatory damage in response to viral infection by self-limiting the anti-viral response. Therefore, although the ability to clear virus declines, filling of the $CD8^+$ T cell niche with exhausted cells may represent a trade-off to minimise damage and prevent autoimmunity [207]. However, in the context of anti-tumour immunity the accumulation of exhausted T cells is considered to be deleterious with their inhibitory receptors presenting an attractive target for anti-cancer therapies[208,209].

Although exhaustion is classically associated with $CD8^+$ T cells an exhausted $CD4^+$ T cell phenotype is described. Shared features between the $CD4^+$ and $CD8^+$ subsets include high PD-1 and inhibitory receptor expression, but transcriptional profiling studies have demonstrated notable differences in their transcription factor activity and the nature of their loss-of-function[210]. The importance of the relationship between the $CD4^+$ and $CD8^+$ compartments in exhaustion is also documented. Robust $CD4^+$ T cell responses are essential for providing sufficient help to the $CD8^+$ compartment[211] and virus-specific $CD4^+$ T cells restore the function of exhausted $CD8^+$ T cells in murine LCMV infection[212]. Conversely, T_{reg} activity enhances $CD8^+$ T cell exhaustion and hampers viral clearance[213]. T_{reg} cytokines such as IL-10 and TGFβ also have a role in promoting exhaustion in chronic viral infection[214,215]. As the understanding of $CD4^+$ T cells in exhaustion lags behind that of their $CD8^+$ counterparts, further examining their behaviour is essential and has implications for anti-viral vaccine development and cancer therapeutics.

1.6.3 T cell senescence.

Senescence describes dysregulated cellular responses caused by environmental stressors which inhibit normal growth and differentiation. Ageing and senescence are inextricably

linked due to cumulative cellular stresses that occur over time. However, by limiting the replication of aged cells that are exposed to repeated DNA damaging events senescence ultimately serves to prevent oncogenesis[216,217]. T cell dysfunction in senescence significantly contributes to diminished immunity and vaccine responses in elderly populations. In addition, chronic infection, cancer and other immunological stressors which drive differentiation accelerate senescence in T cell subsets. For example, the age-associated senescent T cell phenotype is reproducible in young individuals with chronic HIV and CMV infections[218,219]. CMV seropositivity also correlates with increased comorbidity and mortality in ageing[220]. Modelling of senescence in mice is limited by their shortened life span, replicative differences in T cell turnover and the lack of pathogen-driven T cell proliferation in sterile housing facilities. Therefore, studies which contribute to the current understanding of T cell senescence are often modelled on a background of chronic infection in humans.

Senescence is classically attributed to the shortening of telomeres, which are repeated hexameric sequences at the end of chromosomes that protect DNA integrity. T cells upregulate telomerase activity following activation which preserves telomere length during clonal expansion and homeostatic cell division[221]. However, replicative T cell senescence is associated with diminished telomerase activity and DNA damage[222]. Together this causes cell cycle arrest at G_1 phase through an elevation in CDK inhibitor activity, including p16, p21, p38 and p53 proteins[217,223]. Senescent T cells are commonly characterised by loss of CD28 and CD27 expression. In long term cell culture experiments most senescent $CD8^+$ T cells are $CD28^-$ and $CD27^-CD28^-$ cells are more frequent in elderly individuals[224,225]. Although diminished CD28 signalling itself inhibits telomerase activity this alone is insufficient to define where their terminal differentiation ends and senescence begins[226]. $CD27^-CD28^-$ $CD4^+$ and $CD8^+$ T cells can elicit robust IFNγ responses despite a reduced replicative capacity[227,228]. Therefore additional distinguishing features of senescent T cells include; 1) gain of CD57 expression, which is inversely associated with the loss of CD28 on

HIV-specific senescent T cells[229], 2) the inability to facilitate B-cell responses through loss of CD40L expression[230], and 3) expression of killer cell lectin-like receptors, which promote NK cell-like cytolytic activity that is independent of TCR activation[231].

As exhaustion and senescence are modelled in the same systems it is questioned whether they are interrelated[232]. Despite an apparent connection between exhaustion and senescence there is evidence that biochemically these represent independent cellular states. Firstly, effector cytokine expression is systematically lost in exhaustion but senescent T cells maintain dysregulated cytokine profiles. The latter is partially attributed to a lineage skewing towards a Th_1 phenotype[227,233]. Secondly, there is evidence that senescent T cells are resistant to apoptosis *in vitro* whereas exhausted cells are highly prone to cell death[234]. This is consistent with the accumulation of $CD27^-CD28^-$ T cells in ageing, but the anti-apoptotic signals that maintain the population are not fully elucidated *in vivo*. Lastly, PD-1 signalling has a significant role in T-cell exhaustion but is not classically associated with senescence. Although PD-1 activity leads to inhibition of CDK activity via p27, senescence blocks cell cycle processes via alternative CDK inhibitors[200,232,235]. Despite this distinction, functional block of PD-1 is shown to inhibit telomere shortening and increases telomerase activity in HIV-specific $CD8^+$ T cells, thus supporting a connection between exhaustion and senescence[236].

Whether induced through senescence, exhaustion, or anergy-related processes there are circumstances where hyporesponsiveness in the T cell compartment may be considered beneficial or detrimental to the immune response. There is evidence that common modalities contribute to diminished T cell activity and mechanisms of hyporesponsiveness may synergise, thus exacerbating a cells deactivated phenotype[232]. This has contributed to discontinuity in the literature regarding the classification of each state, particularly regarding the $CD4^+$ T cell subset. Additionally, there is little insight into the frequency or characteristics

of hyporesponsive T cells in normal adults in the absence of ageing or chronic infection. In my investigation $CD4^+$ T cells that fail to produce cytokine responses *in vitro* are examined for features that may account for their altered behaviour, including those related to anergy, exhaustion and senescence.

1.7 Immune Privilege – Tissue-mediated T cell suppression.

Tissues described as 'immune privileged' have an intrinsic inability to regenerate and have multiple tolerogenic mechanisms protecting them from immune-mediated inflammatory damage. The ovaries, testis, placenta, eye and central nervous system (CNS) are traditionally considered to be immune privileged sites, where tissue explants are less readily rejected than in other non-privileged sites[237,238]. In the context of supressing T cell responses in the ocular compartment some notable mechanisms associated with immune privilege include;

- **Physical barriers (e.g. the blood-retinal barrier) -** Endothelial and basement membrane modifications such as tight junctions and the impermeable 'Bruch's membrane' prevent immune cell access and prevent dissemination of tissue specific antigens[239]. The absence of lymphatics network prevents antigen drainage into nearby lymph nodes.
- **Constitutive expression of inhibitory T cell ligands** – Ocular tissue presents PD-L1 and FASL which promotes apoptosis of infiltrating $PD\text{-}1^+$ and FAS^+ T cells[240,241].
- **Production of soluble T cell mediators** – Secretion of anti-inflammatory TGFβ into the ocular fluid compartments suppresses T cell activation whilst promoting T_{reg} induction. Production of VIP (vasoactive intestinal peptide) and IDO also promotes T_{reg} activity whilst inhibiting inflammatory pathways[242–244].
- **Downregulation of antigen presentation** – MHC I expression is restricted in ocular tissues[245]. Cytotoxic T cells are ignorant to the presence of their antigen which prevents cytolytic damage of ocular tissue.

Whilst upholding evidence supporting the aforementioned adaptations, immune 'privilege' may now be considered inappropriate phraseology to describe some tissue sites included in the original definition. Dynamic interaction between immune privileged tissues and resident or infiltrating immune cells is now described. This is well described in the CNS which may be considered more immune 'modified' than immune 'privileged' *per se*[246]. Evidence that T cells are recruited to the CNS in both health and disease has significant implications for the understanding of CNS immunity.

1.8 T cell migration into the central nervous system.

The CNS was historically regarded as 'immune privileged' and disconnected from peripheral immune processes in the absence of pathology. It is now established that the CNS has an absolute requirement for immune surveillance and that resident and infiltrating immune cells contribute to immune homeostasis and support neuronal function. There are approximately 1000 leukocytes per ml of cerebrospinal fluid (CSF) and 60% of these are lymphocytes[247]. $CD4^+$ T cells strongly predominate this lymphocyte compartment and are over represented in the CSF comparative to the blood[247,248]. Naïve $CD4^+$ T cells are largely excluded from the CSF compartment with the population mostly composed of a T_{cm} phenotype as defined by expression of $CD45RO^+$ with $CCR7^+$ or $CD27^{hi}$[247,249]. It is proposed that the homogeneity of this population is achieved through selective recruitment of T cells from the blood to CSF[250]. However, endothelial modifications associated with CNS vasculature (collectively referred to as the blood brain barrier; BBB) were once thought to inhibit T cell migration completely. Although the fundamental concepts of this model hold true this ideology is now considered over simplistic as the CNS vasculature is not uniform. Therefore, the BBB properties (as they are classically defined) are only applicable to distinct areas of the CNS and spinal cord microvasculature[251]. By studying the migration of encephalitogenic T cells across cerebral microvessels investigators have identified sites where CNS T cell migration can occur[252]. These sites include the blood-leptomeningeal barrier (BLMB) and blood-cerebrospinal fluid

barrier (BCSFB) which are well characterised in the context of T cell migration by *B. Engelhardt and R.M Ransohoff (2012)*[253]. The structure and molecular motifs associated with CNS barriers are described below in line with current understanding of homeostatic T cell migration.

1. The blood brain-barrier (BBB).

The BBB represents a collection of structural adaptations associated with the CNS parenchymal spinal cord microvasculature[254]. Tight and adherins junctions between endothelial cells and a dense basement membrane (basal lamina) are the initials barriers to migrating T cells. Embedded within the basal lamina are pericytes, which contribute to tight junction formation, extracellular matrix secretion, vascular flow control and can phagocytose cellular debris and pathogens[255,256]. The inner most barrier is the *glia limitans perivascularis*, which is compose of astrocyte cell formations in the outermost parenchymal layers[257]. Astrocyte 'foot end' cellular projections associate with the basal lamina ensheathing the vasculature. At the level of capillaries these structures are tightly fused together to form the 'neurovascular unit'[258]. However, arteriolar branches penetrating the brain parenchyma may have perivascular spaces (PVS) between the endothelial layer and *glia limitans perivascularis*[259]. PVS are also seen in the post-capillary venules, which are the primary site of T cell migration in the periphery. PVS are continuous with the subarachnoid space and are filled with cerebrospinal fluid (CSF) which allows molecular exchange between the CSF and interstitial fluids[260,261]. Within the PVS there are $CD11c^+$ dendritic cells and perivascular macrophages which can process CNS antigen[262,263]. These PVS cells are continuously replenished by recruitment from the circulation whereas parenchymal microglia are embryonically-derived and self-maintained.

Perivascular macrophages are phenotypically similar to microglia and both cell types express the markers F4/80, MHC II and CD11b[264]. CD45 can be used to distinguish between these

populations as elevated expression is observed upon peripherally-derived perivascular populations[265,266].

In the absence of endothelial activation only pre-activated T cells can cross the BBB, as demonstrated by live intravital imaging of BBB migration across spinal cord microvessels. When encephalitogenic Th_1 cells are traced this way the migration rate is extremely inefficient and dependent on VLA-4/VCAM-1 interaction with subsequent LFA-1/ICAM-1 signalling[252]. The latter may have a role in extravasation by facilitating T cell 'crawling' to BBB regions that are permissive for TEM[267]. Breach of the BBB is strongly associated with neuroinflammatory diseases such as multiple sclerosis (Section 1.11).

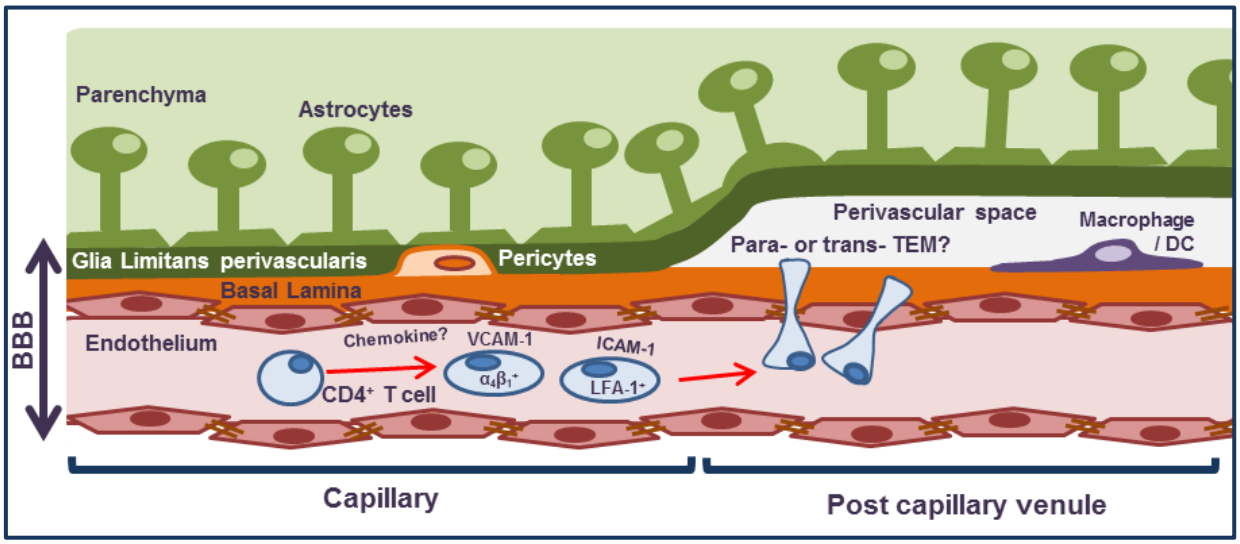

Figure 1.4A CD4$^+$ T cell migration across the blood brain barrier (BBB). Figure represents an adaptation from [253].

2. The blood-leptomeningeal barrier (BLMB).

The BLMB describes the vasculature associated with the meningeal vessels. Here vessels traverse the subarachnoid space between the arachnoid mater (dura and skull side) and the *glia limitans superficialis* (parenchymal side). The *glia limitans superficialis* and *perivascularis* represent analogous structures at distinct anatomical locations, although the former has an additional '*pia mater*' membrane[268]. *Pia mater* is fluid-impermeable and retains the CSF within the subarachnoid cavities. The subarachnoid space is densely

populated with MHC II^+ APC suggesting antigen presentation is highly significant here[269,270]. Murine intravital microscopy studies show activated T cells accumulate within the leptomeningeal compartments rapidly after adoptive transfer irrespective of their antigen-specificity[252]. This mode of migration is inefficient without prior endothelial activation, but such work suggests that T cell migration across the BLMB is more permissive than the BBB. This is consistent with differential patterns of endothelial adhesion molecule expression between the vasculatures. P-selectin is constitutively expressed by the BLMB endothelium and is upregulated in inflammation, which facilitates the 'capture' phase of T cell migration[252,271]. BLMB and BBB endothelium are also exposed to differential rates of blood flow. Vascular flow is shown to alter endothelial permeability, tight junction formation and adhesion molecule expression which may influence migration kinetics[272,273]. Despite these observations other studies have found a complete absence of T cell adhesion to resting BLMB vasculature in mice[274]. Therefore, the BLMB is unlikely to be the primary route of T cell migration into CNS without underlying inflammatory processes.

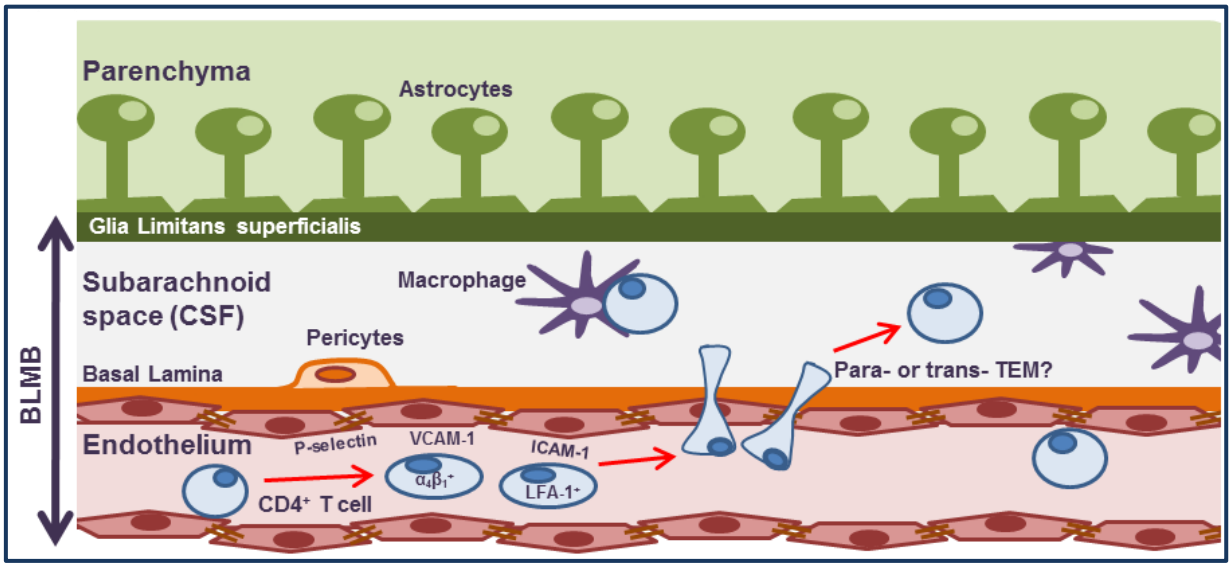

Figure 1.4B $CD4^+$ T cell migration across the blood leptomeningeal barrier (BLMB). Figure represents an adaptation from [253].

3. The blood-cerebrospinal fluid barrier (BCSFB).

The BCSFB typically refers to the barrier between the blood and CSF at the anatomical level of the choroid plexus (CP). The CP is a highly villous ependymal epithelial structure that encloses a dense network of fenestrated capillaries. The CP forms out pouches of the ventricular lining and hangs into the lateral, 3rd and 4th ventricles[275]. The CP produces CSF through diffusion, selective transport and secretion of plasma molecules across the epithelial surface into the ventricular space. For migrating T cells to pass from blood to ventricles they must firstly cross the CP microvasculature. CP capillaries are fenestrated so migration here is more permissive than at the BBB and BLMB[276,277]. Secondly, an extravasation step across the epithelium (basolateral to apical side) is required. This is rate limiting due to a network of inter-epithelial tight junctions[278,279]. Dendritic cells and macrophages are also found within the CP stroma and at the apical surface of CP epithelium[280,281]. The association of APC with the CP again demonstrates the importance of CNS antigen presentation in the CSF compartment.

CD4$^+$ T cells are associated with the CP stroma in both unchallenged mice and normal post-mortem human CP tissue[271,282]. As there is continuous flow of CSF from the ventricles throughout the subarachnoid and perivascular cavities the CP is considered as the primary source of CSF T cells in healthy individuals. The cellular composition of CSF is consistent when sampling from the ventricles or the lumbar spine region which supports this theory[283]. Despite these observations the molecular mechanisms behind CD4$^+$ T cells recruitment via the BCSFB are not fully elucidated. Most candidate chemokine and adhesion molecules linked to BCSFB migration are associated with the epithelial barrier and stroma but not the endothelial layer. These include VCAM-1 and ICAM-1 which are restricted to the apical surface of the CP epithelium in normal mice[284]. Therefore, these are more likely to have a role in late diapedesis or tethering T cells to the ventricular walls than early stage TEM *per se*. The majority of CSF CD4$^+$ T cells express CCR7 so a role for this receptor in BCSFB

migration has been proposed[247,271]. However, reports investigating the localisation of CCR7 ligands CCL19 and CCL21 in CNS are conflicting. In mice, constitutive expression of CCL19 but not CCL21 is shown in brain and spinal cord post capillary venules whereas both CCL19 and CCL21 upregulate in EAE[285]. Similarly, CCL19 mRNA has been detected in non-diseased human brain homogenates and is upregulated in neuroinflammation, but here there was no involvement of CCL21 irrespective of disease status[286]. This is in contrast to a study by *P. Kivisakk et al (2004)* where a positive immunofluorescence signal for CCL21 is reported at the CP epithelium in normal human post-mortem brain tissue[249]. Specific CCL21 expression at the CP suggests that if BCSFB migration is CCR7-dependent this ligand has a more dominant role than CCL19.

P-selectin is one of few ligands that are definitively associated with uninflamed CP endothelium[271]. This is localised to larger stromal venules of the CP but not the microvessels as identified by immunohistochemistry performed on post-mortem human tissue[271]. Studies of P-selectin$^{-/-}$ mice show that the accumulation of CD4^{+} T cells observed within the CP is P-selectin dependent[252]. Human CSF T cells are also shown to express higher levels of the P-selectin ligand PSGL-1 than T cells in the blood which supports P-selectin/PSGL-1 involvement in BCSFB recruitment [271,287].

Chemokine receptors are fundamentally important for T cell transmigration (section 1.5.5). However, although CXCR3^{+} CD4^{+} T cells are enriched in uninflamed CSF the receptor requirements for homeostatic BCSFB migration are not defined[288]. In contrast, a plethora of chemokine receptor interactions are associated with pathogenic T cell infiltrates in multiple sclerosis and are discussed in Section 1.11.

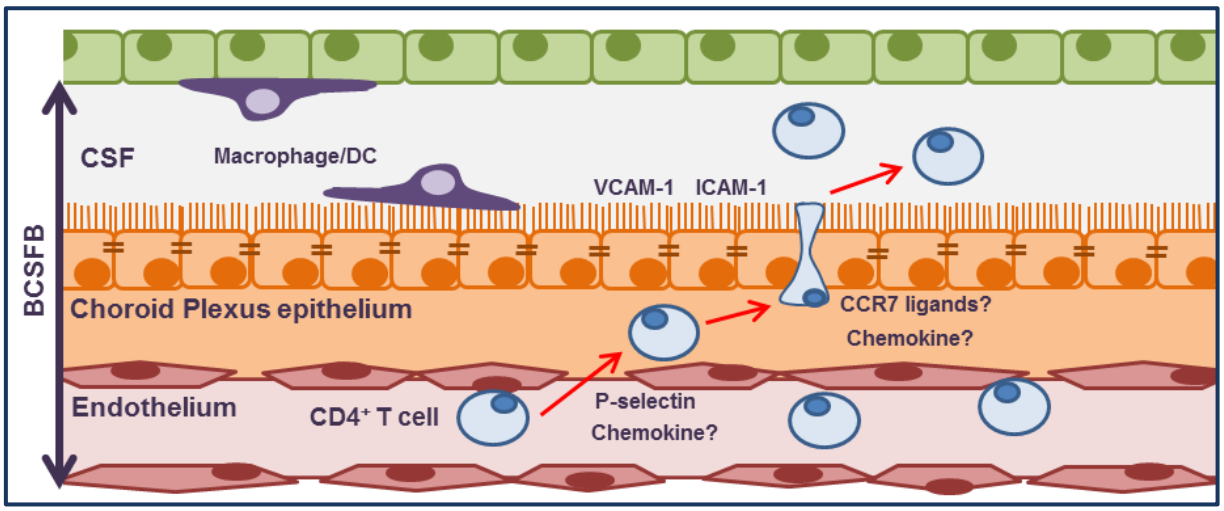

Figure 1.4C CD4$^+$ T cell migration across the blood cerebrospinal fluid barrier (BCSFB) at the choroid plexus. Figure represents an adaptation from [253].

1.9 The role of T cells in CNS immune surveillance.

The primary function of CSF T cells is to perform immune surveillance and this proposal is supported by numerous findings. Firstly, the presence of MHC II$^+$ APC in the CSF space suggests these cells interact and activate CD4$^+$ T cells *in situ*[289]. Secondly, immunocompromised individuals are predisposed to CNS infection and tumours[290]. Lastly, pharmacological block of T cell migration into CNS can result in reactivation of latent endemic viruses. Treatment of MS patients with the α4-integrin inhibitor Natalizumab can result in loss of John Cunningham virus (JC virus) control in the brain leading to oligodendrocyte death and fatal demyelination[291].

In order to appreciate how CSF CD4$^+$ T cells can perform immune surveillance their access to parenchymal antigens (via APC), residency within the CNS compartment and their recirculation back to the periphery require consideration. Parenchymal protein antigens in the associated interstitial fluid (ISF) are largely separated from the CSF compartment. However, injection of fluorescence tracers into the CSF can be tracked to the parenchymal interstitium[292]. This shows that the ISF and CSF interconnect in the perivascular spaces providing access for perivascular APC to uptake and present soluble CNS antigens to T cells. An elegant analogy by *B. Engelhardt et al (2011)* describes the processes required for

immune surveillance as the workings of a medieval castle[257]. Activated T cells cross the outer walls of the castle, which represents normal homeostatic routes of migration (BCSF, BLMB). In the CSF space (castle moat) macrophages and DC (castle guards) may present CNS antigens to the patrolling T cells to inform them of any dangers to the castle inhabitants (neurons). If their specific antigen is presented by the guards the patrolling T cells become activated and open the outer walls (BBB endothelial activation) to let in more troops. Cytokines released by the T cells further activate myeloid cells which secrete factors such as matrix metalloproteinase enzymes (MMP) that facilitate the breach of the inner castle wall (the *glia limitans*). The patrolling T cells can then access the castle and protect the inhabitants from infectious invaders and damage[257].

Although the CNS lacks a true lymphatics network it is proposed that the circulation of CSF may substitute for its absence. Anecdotally this analogy is consistent with the predominating CSF T cell subset which expresses the lymph node homing chemokine CCR7[247,248]. The CSF turns over 4 times daily[293] and is resorbed by either; 1) direct reabsorption into the circulation via arachnoid granulations which drain into the venous sinuses embedded in the *dura mater*, 2) drainage via the olfactory lymphatics through connections with the subarachnoid space (<50% of CSF outflow in animals), 3) drainage via lymphatics associated with other cranial or spinal nerves[294,295]. CSF reuptake via arachnoid granulations permits the transport of soluble CNS antigens into the circulation but is not a described mode of APC and T cell efflux. However, lymphatic vessels draining into the cervical lymph nodes in the neck (CLN) do provide trafficking route for both antigen and cells[295]. The appearance of particulate tracer and proteins in the CLN following their injection into the CNS parenchyma and subarachnoid space demonstrates the viability of this route for antigen drainage[296,297]. In addition, APC loaded with EAE-associated myelin antigens are found in the CLN of mice, primates and human MS patients[298,299]. Although recirculating APC are thought to be excluded from the CNS parenchyma a study by *M.G. Mohammad et al (2014)* has shown that

$CD11c^+$ and $CD11b^+CD11c^+$ DC migrate to the CLN via a parenchymal route in normal and EAE mice. These blood derived-DC follow the path of olfactory neural outgrowths from the lateral ventricles to the olfactory bulb (the rostral migratory stream) and here cross into the olfactory lymphatics and CLN[300]. Together these studies suggest the importance of such lymphatic drainage routes for APC recirculation, but there are fewer reports demonstrating that CSF T cells egress via the CLN. When stimulated transgenic T cells expressing green fluorescent protein are injected into the lateral ventricles they do accumulate in the CLN via the nasal mucosa[301]. However, in the study by *M.G. Mohammad et al (2014)* $CD3^+$ T cells did not share the migratory pathways described for DC[300]. Lack of evidence supporting the efferent pathways of unmanipulated CSF T cells leaves open questions regarding their function and fate once within the CSF spaces. Defining the functionality and migratory behaviour of these cells is pivotal for further understanding their role in CNS immunity.

1.10 The CNS microenvironment promotes immune suppression.

In the absence of pathology the CNS microenvironment is considered to be highly anti-inflammatory. Tolerogenic DC which drain from the CNS are important for the induction of T_{reg} in the CLN and peripheral tolerance to CNS antigen[300]. This is demonstrated by pharmacological block of this pathway with Fingolimod which increases disease prevalence in a spontaneous mouse model of EAE. Furthermore, the nasal lymphatics that drain into the CLN have a significant role in tolerance induction as is demonstrated by a delayed type hypersensitivity model when peptides are introduced intranasally[302]. However, despite the proposed role of the CLN in tolerance induction, disease severity in EAE is reduced when the CLN are surgically removed prior to disease onset[303]. The lack of disease exacerbation here suggests that any tolerogenic role of the CLN is overridden in this neuroinflammatory disease model

Most work related to T cell suppression in the CNS refers to interactions occurring within the CNS parenchyma for the purpose of dampening inflammation. Within the parenchyma features of immune privilege are highly applicable such as constitutive FASL and an absence of MHC expression[304,305]. The default setting for astrocytes and microglia is anti-inflammatory and serves to promote neural protection. However, as under normal conditions T cells rarely penetrate the parenchyma any cell-cell contact mediated suppression is likely restricted to astrocyte feet at the *glia limitans*[257]. However, soluble factors secreted by astrocytes are important for modulating CSF T cell responses and maintaining the barrier integrity. These include cytokines and effector molecules such as TGFβ, IL-10, IL-27 and retinoic acid[306].

Early studies of immune privilege showed that *in vitro* culture of activated T cells in CSF reduces their IFNγ responses[307]. Such suppression is attributed to a plethora of soluble anti-inflammatory cytokines in the CSF such as TGFβ, VIP, prostaglandin D2 and some neuropeptides[308–311]. With reference to outer CSF barriers adaptations the CP epithelium is shown to be highly dynamic and immune modulatory. CP epithelium constitutively expresses IDO and CD73 along with the anti-inflammatory cytokines TGFβ, IL-10 and IL-13[312]. In addition, work which demonstrates constitutive PD-L1 expression on brain endothelium compliments studies documenting a high level of PD-1 expression by CSF T cells[313–315]. Here PD-1 interaction may suppress activated T cells upon CSF entry as opposed to being indicative of T cell exhaustion[313]. Interestingly, PD-L1 is expressed by both microglia and perivascular macrophages and negatively regulates T cell activation in both *in vitro* culture and EAE[316,317]. CP-associated perivascular macrophages are also skewed towards an M2 anti-inflammatory phenotype and local DC may also provide an important source of anti-inflammatory IL-10[318,319]. Such findings suggest that the passage of $CD4^+$ T cells across the CP into the CSF may modulate their phenotype and function. The ability of CSF T cells to

make cytokine having undergone such a migration process is examined as part of my investigation.

1.11 Changes in CD4$^+$ T cell CNS recruitment and the pathogenesis of multiple sclerosis.

Multiple sclerosis (MS) is an autoimmune neuroinflammatory disease characterised by lesion sites in the brain and spinal cord which are detectable by magnetic resonance imaging[320]. Disability in MS is caused by demyelination and axonal loss at lesion sites resulting in loss of conductivity and neuronal function. A single neurological episode is defined as clinically isolated syndrome (CIS) and presents with MS symptoms. However, 60-80% of CIS patients experience further episodes and subsequently develop MS[321]. The majority of MS patients experience recurrent inflammatory flares with intermittent periods of remission that are accompanied by some neurological recovery (relapsing remitting MS; RR-MS). In around 80% of individuals recovery periods are eventually accompanied by progressive disability caused by repetitive neuronal damage (secondary progressive MS)[322]. Around 10-15% of MS patients have progressive disease from the outset with no apparent inflammatory flares (primary progressive MS; PP-MS)[323]. PP-MS and RR-MS have their own distinctive pathophysiology with the former representative of more chronic inflammatory processes whilst latter are more acute[324]. Risk factors associated with the development of MS are well defined and include; 1) an aberrant response to infection (namely Epstein Barr virus)[325], 2) HLA polymorphisms that are associated with loss of tolerance to CNS antigens[326], and 3) environmental factors including vitamin D deficiency, as vitamin D is important for maintaining central tolerance and can skew CD4$^+$ T cell responses away from a pro-inflammatory phenotype[327,328].

The pathogenesis of MS is multi-factorial and not yet fully understood. However, on a cellular level autoreactive T cells which recognise myelin antigen-specific antigens (e.g. myelin basic protein and myelin oligodendrocyte glycoprotein) are strongly implicated in the

immune-mediated damage[329,330]. Interestingly, myelin-specific T cells can be identified in healthy individuals and these may become suppressive iT_{reg} when exposed to cognate antigen[331–333]. Therefore, loss of peripheral tolerance is implicated in MS pathogenesis and may involve the inability of DC to tolerise T cells in a potent inflammatory environment as is seen in particular infections[334]. Such processes may involve CNS antigen presentation in the CLN as demonstrated in a mouse model of EAE[300].

With consideration to $CD4^+$ T cell function in MS two main contenders that are implicated in MS inflammation are effector Th_1 and Th_{17} populations but there is much debate regarding their relative contribution to disease. Mice deficient in the IL-12 p40 subunit are resistant to EAE which initially suggested a dominant role for a Th_1 phenotype. However, mice deficient in the alternative IL-12 subunit p35 remain susceptible to EAE[335]. p40 is also part of the IL-23 heterodimer p19/p40 which is required for the maintenance and expansion of Th_{17}.This suggests a more dominant role of IL-23 dependent Th_{17} mediated inflammation in MS pathogenesis[336]. In addition, when myelin-specific $CD4^+$ T cells are polarised to Th_{17} by IL-23 and transferred into a naïve host they induce EAE that is symptomatically consistent with transfer of IL-12 polarised Th_1 cells[337]. The chemokine CCR6 is classically expressed by Th_{17} and $CCR6^{-/-}$ mice do not develop EAE[338] . This is attributed to an inability to home to the CNS in the early stages of EAE as the ligand for CCR6 (CCL20) is constitutively expressed on CP epithelium in both mice and humans[338,339]. Observations that show Th_1 are numerically dominant in MS relapse may suggest a greater contribution in established disease. In addition, IFNβ is an effective therapy preventing MS relapse and IFNβ inhibition of Th_1 function is well characterised. However, its effects on the Th_{17} population are conflicting with murine Th17-mediated EAE proving unresponsive to IFNβ treatment[340,341]. A degree of plasticity between Th_1 and Th_{17} lineages adds further complexity to their relative contribution in MS. Th_{17} cells can acquire Th_1 characteristics such as Tbet mediated IFNγ expression[342,343]. These cells are found in MS lesions, are highly pro-inflammatory and can

penetrate the BBB more efficiently than either Th_1 or Th_{17} cells[344]. Findings that show $Tbet^{-/-}$ Th_{17} cells are not encephalitogenic upon adoptive transfer into naïve mice supports a role of these $IFN\gamma^{+}IL\text{-}17^{+}$ $CD4^{+}$ T cells in MS pathogenesis[122].

Immunohistochemisty analysis of parenchymal MS lesions reveals an infiltration of T cells alongside inflammatory macrophages[345,346]. Local resident microglia and astrocytes are also shown to be highly activated and secrete neurotoxic factors such as TNFα, IL-1β and nitric oxide[347]. In the absence of inflammation T cells are restricted to the CSF spaces at the brains borders and do not penetrate the *glia limitans*. Such perivascular retention is logical from a surveillance perspective, as it keeps potentially dangerous lymphocytes out of the brain and in close proximity to the CNS drainage routes[348]. In support of this, evidence suggests that the chemokine CXCL12, which is expressed on the basolateral side of the vascular endothelium facilitates the retention of $CXCR4^{+}$ $CD4^{+}$ T cells in the PVS and that its upregulation in EAE serves as an anti-inflammatory mechanism to limit parenchymal infiltration[349,350]. It is proposed that an increased permeability of the *glia limitans* accompanied by a loss of signals which retain T cells within the CSF space is significant in MS pathogenesis. In EAE models the onset of neurological symptoms is temporally associated with a breach of the *glia limitans* by myelin specific $CD4^{+}$ cells and their reactivation by APC within the PVS is requirement for this step[351–353]. Although both $CD4^{+}$ and $CD8^{+}$ T cells are found at MS lesion sites it appears that $CD8^{+}$ T cells preferentially move into the parenchyma whilst $CD4^{+}$ T cells are more readily retained and accumulate in perivascular 'cuffs'[354,355]. Increased MMP-2 and MMP-9 enzyme activity by activated myeloid cells is reported to promote T cell migration from PVS across *the glia limitans*[351].

In many respects the concepts of immune surveillance and the pathogenesis of MS are inextricably related. CNS T cell infiltration in MS is commonly described as a two-step process that is comparable to the medieval castle analogy described by *Engelhardt et al*

(2011)[257,356]. Switching pathogen-specific for autoreactive $CD4^+$ T cells that have broken self-tolerance mechanisms, 'pioneer' T cells enter the CSF spaces and open the BBB flood gates for further inflammatory infiltrates. This is achieved directly through BBB endothelial activation by T cell cytokines (IFNγ, IL-1β, TNFα) or indirectly through activation of local macrophages[289]. Chemokines implicated in this critical stage of inflammatory recruitment include the CCR2 ligand (CCL2)[357–359], CCR5 ligands (CCL3/CCL4/CCL5)[288,360], and CXCR3 ligands (CXCL9/CXCL10)[360,361]. From here the *glia limitans* is breached and as autoimmune inflammation is not resolved like an infectious insult, these processes set up a perpetuating cycle of T cell-mediated damage. This is maintained by subsequent BBB breakdown and by ectopic tertiary lymphoid organs that are formed in the meninges which promotes the reactivation of T and B cells within the CNS[362–364]. As homeostatic T cell recruitment pathways are both important for CNS immunity and may be implicated in the very early stages of MS pathogenesis, it is important to further understand the characteristics of T cells in the CSF space in the absence of disease. This is particularly important given that pathogenic Th_{17} share the same CP entry route as those cells that may protect the CNS from infection[338]. In addition, the study of non-pathogenic CSF T cells may shed light upon either peripheral or CSF-restricted tolerogenic mechanisms which are lost in the onset of neuroinflammatory disease.

1.12 Thesis aims.

Preliminary studies have examined the cytokine secreting potential of $CD4^+$ T cells from the blood and CSF of patients with and without neuroinflammatory diseases including multiple sclerosis (unpublished data from the Curnow group, University of Birmingham). In these investigations, a population of $CD4^+$ cells was identified in the peripheral blood and CSF that did not make any of seven tested cytokines (IFNγ, TNFα IL-17, IL-21, IL-22, IL-10, IL-5) in all patient cohorts. It was then considered whether these cells expressed alternative cytokines or whether the absence of a cytokine profile was reflective of a truly hyporesponsive

phenotype. It was considered whether the complete absence of a cytokine response in this T cell population was an indication of an altered cellular state and may be representative of anergy, senescence or exhaustion. As such states are incompletely defined in an *ex vivo* setting this led to the formation of the first two aims of this investigation;

1) **Establish a complete definition of 'cytokine^{-ve}' CD4^{+} T cells in the peripheral blood of healthy humans.**
2) **Interrogate the phenotype of cytokine^{-ve} CD4^{+} for features associated with regulatory or hyporesponsive T cell biology.**

The next intention of this investigation was to model normal CSF in a cohort of patients without inflammatory disease to provide insight into CD4^{+} T cell recruitment from blood to CSF. To complement this work, modelling healthy CSF, CP and brain in rodents would permit a comparative phenotypic analysis of the T cells in each associated compartment. Based on findings in current literature the hypothesis drawn for this work is that recruitment of CD4^{+} T cells from blood to CSF will be T_{cm} specific in both human and rodent systems[247,249]. The main aims of this line of investigation were to;

3) **Examine the frequency and phenotype of CD4^{+} T cells in rodent CNS compartments.**
4) **Investigate the relationship between the phenotype of CD4^{+} T cells in the blood and CSF of patients without inflammatory disease.**

As part of preliminary investigations the cytokine expression of CD4^{+} T cells from cerebrospinal fluid samples was examined. In individuals without inflammatory disease the cytokine responses of the memory CD4^{+} T cell population were diminished comparative to the blood (Figure 1.5). This led to many questions regarding their ability of homeostatically recruited CD4^{+} T cells to perform immune surveillance; 1) were the cytokine^{-ve} cells observed in the peripheral blood enriched in the CSF through direct recruitment? 2) alternatively, was the cytokine secreting potential of CSF CD4^{+} T cells switched off as part of their recruitment process to prevent inflammatory responses in the CSF space? or 3) were active mechanisms of immune suppression operating in the CSF space to dampen the cytokine responses of these

cells once within the CNS? The following aims were formulated to begin to address these questions;

5) **Confirm that the cytokine responses of $CD4^+$ T cells in 'normal' human CSF are truly diminished comparative to the blood.**
6) **Examine the activation status and cytokine production of $CD4^+$ T cells in rodent CNS compartments.**

The overall hypothesis for this investigation is that CSF $CD4^+$ T cells have diminished cytokine responses through specific recruitment of a hyporesponsive central memory population from the blood. The rationale behind the proposed hypothesis is that the lack of cytokine production by CSF $CD4^+$ T cells protects the CNS tissue from inflammatory damage and is in keeping with the tissues status as an 'immune privileged' site.

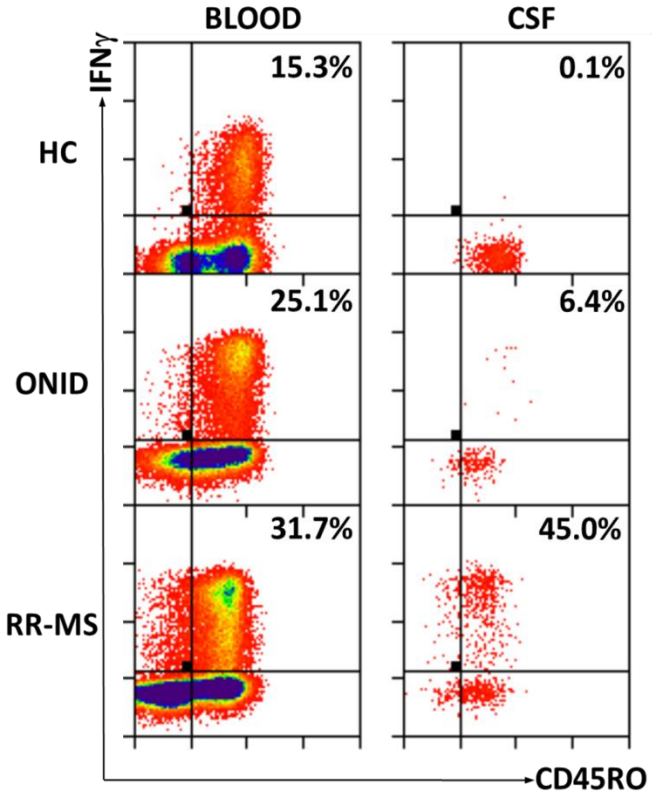

Figure 1.5 Pilot data showing an absence of IFNγ expression by CSF CD4$^+$ T cells in patients without inflammatory disease. Peripheral blood mononuclear cells and cellular isolates from CSF were sampled from patients with relapsing remitting multiple sclerosis (RR-MS), non-inflammatory neurological disease (ONID) and healthy controls (HC). Cells were stimulated for 3h with PMA/ionomycin and percentage of memory CD4$^+$ T cells (CD3$^+$CD4$^+$CD45RO$^+$) that expressed the cytokine IFNγ was measured by flow cytometry. Representative flow cytometry plots show the percentage of IFNγ$^+$ CD4$^+$ T cells in the memory compartment. Data indicates that IFNγ$^+$ cells are under-represented in the CSF of individuals without inflammatory disease (HC and ONID group), but elevated in the CSF of RR-MS patients.

CHAPTER 2

MATERIALS AND METHODS

2 MATERIALS AND METHODS

2.1 Reagents

2.1.1 Culture medium and solutions

RPMI medium: RPMI (Roswell Park Memorial Institute) 1640 [Sigma-Aldrich Irvine, UK] supplemented with 1% GPS (2mM l-glutamine, 100U/ml penicillin, 100ug/ml streptomycin) [HyClone, Northumberland, UK] and 1% HEPES (4-(2-hydroxyethyl)-1-piperazineethanesulfonic acid) [Sigma-Aldrich]

RPMI 10% HIFCS: RPMI 1640 medium supplemented with 10% Heat Inactivated Fetal Calf Serum (HIFCS) [Biosera, Ringmer, UK]

PBS: Phosphate Buffered Saline (8g/l NaCl, 0.26/l KCl, 1.15g/l NA_2HPO_4, 0.2g/ml KH_2PO_4); 1 PBS tablet added per 100ml distilled H_20 [Oxoid, Basinstoke,UK]

PBS 2% BSA: PBS, 2% Bovine Serum Albumin (BSA) [Sigma-Aldrich].

MACS buffer: PBS, 0.5% BSA, 2mM Ethylenediaminetetraacetic acid (EDTA) [Sigma-Aldrich].

ACK buffer: 0.15M Ammonium Chloride (NH_4Cl), 10mM potassium hydrocarbonate ($KHCO_3$), 0.1mM Ethylenediaminetetraacetic acid (EDTA) [all Sigma-Aldrich] in dH_20.

4% PFA: 37% Formaldehyde solution [252549, Sigma-Aldrich] diluted to 4% in PBS.

Cryopreservation Solution: Tissue freezing medium containing 50% 0.05M Sodium Phosphate Buffer (pH 7.3), 30% Ethylene Glycol (Sigma-Aldrich E9129), 20% Glycerol (Sigma-Aldrich G15516) in dH20.

2.1.2 Additional Reagents

Reagent	Product number	Company	Additional Information
Nuclease free water	AM9932	Ambion® (Life Technologies)	
Cell Permeabilization Kit	GAS001S-100 GAS002S-100	Caltag-Medsystems Limited, UK	
Compensation beads	01-1111	eBioscience	One Comp eBeads
Tissue-Tek™ Cryo-OCT	14-373-65	Fisher Scientific	
Ficoll-Paque Plus	17-1440-03	GE Healthcare, Bioscience, Amersham, UK	
Recombinant human cytokines	11340025 11340073 11340153	Immunotools, Germany	rhIL-2, rhIL-7, rhIL-15
Dynabeads Human T-activator CD3/CD28	1131D	Invitrogen	
Hoechst 33258	H21491	Invitrogen	Stock of10mg/ml in DMSO
Sytox Blue	s34857	Invitrogen	
Heparin Sodium	HeparinLEO®	Leo Laboratories LTD, UK	
CD4 microbeads	130-097-048	Miltenyi Biotech	lyophilized anti-human CD4 microbeads
CD45 Microbeads	130-097-153	Miltenyi Biotech	Anti-mouse (lyophilized)
Memory CD4+ T cell Isolation Kit (human)	130-091-893	Miltenyi Biotech	
Pan T cell microbeads	130-090-320	Miltenyi Biotech	Anti-rat OX52
T_{reg} isolation kit	130-091-301	Miltenyi Biotech	Anti-human
µMACS one-step cDNA kit	130-091-902	Miltenyi Biotech	
µMACS mRNA isolation kit	130-075-201	Miltenyi Biotech	
Annexin Buffer (X10)	N/A	N/A	0.1M Hepes pH7.4, 1.4M NaCl, 25mM CaCl2 in dH20
DNAse I enzyme	10104159001	Roche Applied Science, UK	
Fast start universal probe master	4913957001	Roche Applied Science, UK	
Velcade (Bortezomib)	sc-217785	Santa Cruz Biotech Inc.	
Brefeldin A	B5936	Sigma-Aldrich, UK	
Evans Blue	E2129	Sigma-Aldrich, UK	
Formaldehyde solution	F15587	Sigma-Aldrich, UK	
Ionomycin	I9657-1mg	Sigma-Aldrich, UK	
PMA	P8139-1mg	Sigma-Aldrich, UK	Phorbol 12-myristate 13-acetate
Sucrose	s0389	Sigma-Aldrich, UK	
DMSO	D4540-100ml	Sigma-Aldrich, UK	Dimethyl Sulphoxide
Collagenase CLSPA	LS005275	Worthington Biochemical Corporation UK	

Table 2.1Table of additional reagents,

2.2 Participants and ethical approval (human studies).

Venous blood was taken from healthy participants recruited into the studies 'T cell differentiation and function' (ERN_10-0728) and 'Immune mechanisms in the ocular microenvironment' (06/Q2702/63). These studies were approved by the life and health science ethical review committee, University of Birmingham (UoB). All participants were UoB staff or students and sampling was performed in a designated phlebotomy room within the University research laboratories.

Age Group (yrs)	Gender ♂	Gender ♀	Total (n)
19-21	0	2	**2**
21-30	5	10	**15**
31-40	7	2	**9**
Total (n)	**12**	**14**	**26**

Table 2.2 Age and gender of healthy blood donors recruited from the University of Birmingham.

Cerebrospinal fluid (CSF) samples obtained via lumbar puncture and matched peripheral blood samples were taken from patients consented into the study 'Pathogenic and regulatory T cells in relapsing-remitting multiple sclerosis' (ERN_10-0762). All samples were pre-diagnostic and representative of patients attending neurology clinics at the Queen Elizabeth Hospital Birmingham. Samples were sourced via the Human Biomaterials Resource Centre, UoB. In some experimental objectives, patients with a multiple sclerosis (MS) diagnosis were further categorized according to the clinical course of the disease (Table 2.4). However, for others this was not possible due to insufficient sampling and all MS patients were assigned to one cohort (Table 2.3). Healthy control blood samples for these experiments were representative of staff and students at UoB. A description of these controls is included in table (Table 2.3) alongside the patient demographic.

Group (n)	Sample (B/CSF)	Age (median and range)	Diagnosis
HC (9)	B	27 (22-36)	Healthy control (no diagnosis)
MS (8)	B/CSF	44.5 (24-63)	Clinically isolated syndrome (1), relapsing remitting multiple sclerosis (3), primary progressive multiple sclerosis (4)
OND (18)	B/CSF	47.5 (21-74)	Primary headache disorder (5), idiopathic intracranial hypertension (2), normal pressure hydrocephalus (2), anxiety (1), chronic pain syndrome (1), Meniere's disease (1), motor axonal polyneuropathy (1), post-concussion syndrome (1), sensory neuropathy (1), sensory symptoms (1), undetermined (1)

Table 2.3 Demographic of patients and healthy controls in the study of CD69 expression by CD4 T cells. All diagnoses were assigned to patient samples post analysis. HC; healthy control, MS; multiple sclerosis, OND; other neurological disease, B; blood, CSF; cerebrospinal fluid.

Group (n)	Sample (B/CSF)	Age (median and range)	Diagnosis
CIS (12)	B/CSF	34.5 (22-50)	Clinically isolated syndrome
PP-MS (9)	B/CSF	56 (48-62)	Primary progressive multiple sclerosis
RR-MS (20)	B/CSF	39.5 (19-72)	Relapsing remitting multiple sclerosis
OND (51)	B/CSF	43 (21-87)	Anxiety (6), idiopathic intracranial hypertension (5), migraines (5), tension headaches (4), leukodystrophy (3), neuropathy (3), degenerative ataxia (2), non-epileptic attack (2), normal pressure hydrocephalus (2), post chemotherapy neuropathy (2), carpal tunnel syndrome (1), cervical spondylosis (1), chronic fatigue syndrome (1), convergence spasm (1), facial pain (1), fibromyalgia (1), gastrointestinal disturbances (1), hereditary spastic paralysis (1), inclusion body myositis (1), muscle tension headache (1),multi-systems atrophy (1), previous TB meningitis (1), previous viral encephalitis (1), stroke (1), hydromyelia (1), vascular MRI changes (1), non-inflammatory visual disturbances (1).
ONID (12)	B/CSF	48.5 (24-83)	Sarcoidosis (2), antiphospholipid syndrome (1), aseptic meningitis (1), asymmetric axonal neuropathy (1), autoimmune neuropathy (1), Bechet's syndrome (1), chronic inflammatory demyelinating polyneuropathy (1), compressive myelopathy (1), neurosarcoidosis (1), inactive neuromyelitis optica (1), viral neuroretinitis (1)

Table 2.4 Demographic of patients in the study of the memory status of CD4 T cells in the blood and CSF. All diagnoses were assigned to patient samples post analyses. OND; other neurological disease, ONID; other inflammatory neurological disease, B; blood, CSF; cerebrospinal fluid.

2.3 Isolation of human peripheral blood mononuclear cells (PBMC).

Blood was extracted from the median cubital vein of healthy donors. This was transferred into a 50ml falcon tube containing heparin sodium at 5IU/ml blood. Blood from diagnostic patient samples (both inflammatory and non-inflammatory) was collected directly into BD Vacutainer® K_2EDTA Tubes (containing 1.8mg EDTA/ml blood). All subsequent cell culture work with blood products was performed in a class II safety cabinet under sterile conditions. Blood was diluted at a 1:1 ratio with RPMI culture medium and layered over 7ml of Ficoll-Paque Plus gradient into a 25ml universal tube. Tubes were centrifuged at 400g with brake 0 for 30min. The PBMC buffy coat was extracted and transferred to a tube containing RPMI supplemented with 10% heat inactivated fetal calf serum (HIFCS). Cells were washed twice in RPMI 10% HIFCS at 300g/21°C/10min and counted using a haemocytometer. After a final wash cells were resuspended at $1x10^6$ cells per 50µl of RPMI 10% HIFCS for cell culture or in a volume appropriate for subsequent cell separation techniques.

2.4 Preparation of human CSF-derived cellular material.

Human CSF fluid was centrifuged at 300g/4°C/4min in 1.5ml Eppendorf tubes. The supernatant was aspirated and the cell pellets resuspended in RPMI 10% HIFCS for cell culture or PBS 2% BSA for flow cytometry. Where multiple Eppendorf's were required the cells were pooled and centrifuged again before being resuspended in an appropriate volume.

2.5 Separation of human T cell subsets by magnetic-activated cell sorting (MACS).

Where human PBMC-derived populations were separated by MACS the volumes indicated are appropriate for 10^7 starting cells. For experiments where higher cell counts were required reagent volumes were scaled up accordingly. In all MACS experiments the MACS buffer was degassed through storage at 2-4ºC for 12h and kept ice cold throughout the procedure.

2.5.1 Positive selection of $CD4^+$ T cells from PBMC (MACS).

For the isolation of $CD4^+$ T cells freshly isolated PBMC were counted and washed at 300g/4°C/10min in cold PBS. The cell pellet was resuspended in 80µl of MACS buffer. 20µl of anti-human CD4 microbeads were added and the suspension thoroughly agitated. Cells were refrigerated for 15min at 2-8 ºC to allow $CD4^+$ cell binding to the anti-CD4 antibody conjugated magnetic beads. The cell suspension was washed in 2ml of MACS buffer at 300g/4°C/10min to remove unbound microbeads. Up to 10^8 cells were resuspended in 500µl of buffer and applied to a MS separation column [130-042-201, Miltenyi Biotech], which was positioned on a MiniMACS™ Separator in a magnetic field. Bead-bound $CD4^+$ cells were magnetically retained on the column whilst the unlabelled $CD4^-$ fraction passed through and was collected for later purity analysis. The column was washed three times with 500µl of MACS buffer to remove unbound cells. It was then removed from the MiniMACS™ separator and the labelled $CD4^+$ cell fraction flushed off the column into a fresh tube using a plunger. $CD4^+$ and $CD4^-$ cell fractions were washed in MACS buffer at 300g/4°C/10min and again in RPMI 10% HIFCS. The purity of the cell fractions was analysed by flow cytometry following surface staining for CD4. $CD4^+$ cell populations with a purity >95% were counted and used in subsequent cell culture and cDNA preparations (for purities see Chapter 3 Figure 3.26).

2.5.2 Negative selection of CD4 memory T cells from PBMC by MACS.

A memory $CD4^+$ T cell isolation kit was used to purify $CD4^+CD45RA^-$ T cells from PBMC for gene expression analysis. PBMC were counted, washed in cold PBS at 300g/4°C/10min and resuspended in 40µl of MACS buffer/10^7 cells. Non-CD4 memory T cells were labelled with a cocktail of biotin conjugated antibodies against CD8/CD14/CD16/CD19/CD36/CD56/CD45RA/CD123/TCRγδ/glycophorin A for 10min at 2-8ºC. After a washing step, 30µl of buffer and 20µl of magnetic anti-biotin microbeads (per 10^7 cells) were added to the cell suspension and refrigerated for an additional 15min at 2-8 ºC.

Excess antibody and microbeads were removed by washing the cells in 2ml MACS buffer at 300g for 10min. Labelled PBMC were resuspended in 500µl of MACS buffer and applied to an LS separation column [130-042-401, Miltenyi Biotech] on a MiniMACS™ Separator in a magnetic field. Unlabelled $CD4^+CD45RA^-$ cells were collected in the column effluent. These cells were passed through the column for a second time to increase their purity and were collected into a fresh tube. The mixed non-T cell and naïve T cell fraction was collected by removing the column and flushing the cells out in 1ml MACS buffer using a plunger. Cell fraction were washed in MACS buffer 300g/4°C/10min, followed by a second wash in RPMI 10% HIFCS. Analysis of purity was assessed by flow cytometry following surface staining for CD4 and CD45RA (shown in results chapter 3 Figure 3.27). $CD4^+CD45RA^-$ memory cells were then counted and held on ice prior to cDNA preparation.

2.5.3 The separation of regulatory and helper $CD4^+$ T cell subsets by MACS.

$CD4^+$ T_{reg} ($CD25^{hi}$) were separated from non-T_{reg} $CD4^+$ T cells in a two-step MACS isolation process. Firstly $CD4^+$ T cells were enriched from PBMC by depleting non-$CD4^+$ T cells. PBMC were prepared by washing the cells in cold PBS at 300g/21°C/10min. Cells were resuspended in 90µl of MACS buffer (per 10^7 cells) and non-$CD4^+$ T cells were labelled with 10µl of biotin conjugated antibody cocktail against CD8/CD14/CD15/CD16/CD19/CD36/CD56/CD123/TCRγδ/glycophorin A. Following 5min of refrigeration at 2-8 ºC 20µl of anti-biotin microbeads were added and cells refrigerated for a further 10min. Excess antibody and microbeads were removed by washing the cells in 2ml MACS buffer at 300g/4°C/10min. PBMC were resuspended in 500µl of MACS buffer and applied to a buffer rinsed LS separation column [130-042-401, Miltenyi Biotech] on a magnetic MidiMACS™ Separator. Unlabelled $CD4^+$ cells were collected in the column effluent and washed at 300g/4°C/10min in MACS buffer. Enriched $CD4^+$ cells were resuspended in 90µl of MACS buffer and labelled with 10µl of anti-CD25 magnetic microbeads.

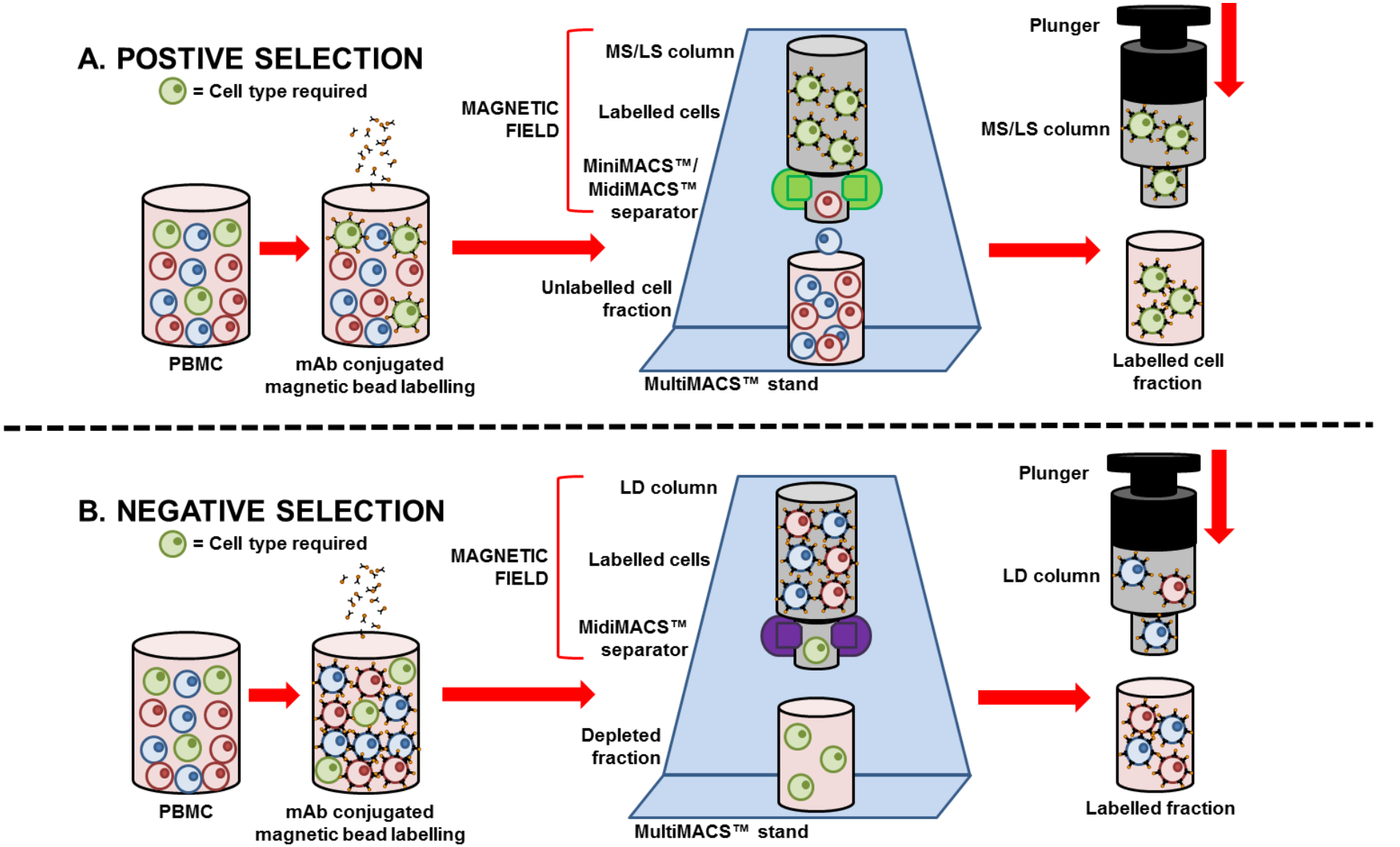

Figure 2.1 Diagram demonstrating the principles of positive and negative selection of T cell subsets from peripheral blood mononuclear cell cultures by magnetic activated cell sorting (MACS).

Cells were refrigerated for 15min at 2-8 ºC to label the $CD25^{hi}$ $CD4^{+}$ T_{reg} population. After a washing step, cells were resuspended in 500µl of MACs buffer and applied to a MS column on a magnetic MiniMACS™ Separator. Labelled $CD25^{hi}$ T_{reg} were retained on the column whereas the $CD25^{int}$ non-T_{reg} fraction was collected in the column effluent. The non-T_{reg} fraction was passed over the column again to remove contaminating T_{reg} and the column washed 3 times with 500µl of MACS buffer. The T_{reg} fraction was eluted by removing the column and flushing 1ml of buffer through with a plunger. The T_{reg} and non-T_{reg} cell fractions were washed in MACS buffer (300g/4°C/10min) and again in RPMI 10% HIFCS. Cells were counted and resuspended in RPMI 10% HIFCS for subsequent cell culture. The purity of the cell fractions was analysed by flow cytometry following surface staining for CD3, CD4, CD8, CD25 and CD127 (for purities see Chapter 3, Figure 3.20A, Figure 3.20B).

2.6 Fluorescence activated cell sorting (FACS) of human peripheral blood mononuclear cells.

Multiple T cell populations were purified from freshly isolated human PBMC by FACS (see Table 2.5). PBMC were washed in PBS 2% BSA at 300g/4°C/4min and resuspended 1ml. The wash step was repeated and the cell pellet resuspended in a cocktail of fluorescently conjugated anti-T cell monoclonal antibodies (mAb) diluted in PBS 2% BSA (250µl mAb/$25x10^6$ PBMC). The cells were refrigerated at 2-8°C for 15min to allow mAb binding. This step was performed under constant rotation to prevent cell clumping. 1ml of PBS 2% BSA was added to dilute unbound mAb and the cells washed at 300g/4°C/4min. Labelled PBMC were resuspended in <500µl RPMI 10% HIFCS and held in sealed polystyrene tubes on ice. FACS was performed by a MoFlo high speed cell sorter [Beckman Coulter] using Summit® v4.3 software. Hoechst 33258 nuclear stain was added so dead cells could be gated out of the FACS process. The dye was diluted in RPMI 10% HIFCS to a working concentration of 0.5µg/ml and added to the cell suspensions 10min prior to sorting. T cell populations were sorted directly into FACS tubes or Eppendorf's rinsed in RPMI 10% HIFCS

with a residual volume of ~200µl. The purities of sorted populations were verified by flow cytometry on a Dako-Cyan flow cytometer [Beckman Coulter].

No. FACS steps required	Figure*	T cell markers	FACS sorted T cell subsets
1	**3.13**	CD4,CD8, CD45RA,CCR7	T_{naive} T_{cm} T_{eff}
	3.14 **3.15**	CD4,CD8, CD45RA, CCR7, CD62L	T_{cm} $CD62L^{hi}$ T_{cm} $CD62L^{lo}$ T_{eff} $CD62L^{hi}$ T_{eff} $CD62L^{lo}$
	3.16	CD4,CD8, CD69	CD4 $CD69^{hi}$ CD4 $CD69^{lo}$
	3.19	CD4,CD8, CD45RA, CCR7, CD56, TCRγδ	T_{cm} T_{eff} CD4 Lin^{+} ($CD8^{+}$/$CD56^{+}$/$TCR\gamma\delta^{+}$)
	3.21	CD4, CD45RA, CCR7, CD25, CD127	T_{cm} T_{helper} T_{cm} T_{reg} T_{eff} T_{helper} T_{eff} T_{reg}
	3.23	CD4,CD8, CD45RA, CCR7, PD-1	T_{cm} $PD\text{-}1^{hi}$ T_{cm} $PD\text{-}1^{lo}$ T_{eff} $PD\text{-}1^{hi}$ T_{eff} $PD\text{-}1^{lo}$
2	**3.27** **3.29** **3.31**	**Pre cell culture**	
		CD4, CD45RA, CCR7	T_{eff}
		Post cell culture	
		CD4, CD69	T_{eff} $CD4^{int}CD69^{lo}$ T_{eff} $CD4^{lo}CD69^{hi}$

Table 2.5 List of T cell subsets purified by FACS. The corresponding surface receptors used to identify each phenotype are listed. The table is indicative of experiments where both a single FACS procedure was required (white), and where cells were sorted and then resorted following cell culture (grey). *FACS was associated with experiments shown in the figures indicated (Chapter 3 of this investigation).

2.7 Human cell culture.

All *in vitro* assays were performed in 96-well culture plates in a total volume of 200µl RPMI 10% HIFCS. When freshly isolated PBMC were cultured $1x10^6$ cells were applied to each well. Where T cell populations were separated by MACS or FACS prior to culture the cell number was dependent on the cell recovery. In such instances a minimum of $1x10^5$ and a maximum of $1x10^6$ purified T cells were cultured per well. Cultures in RPMI 10% HIFCS alone acted as a negative control for stimulation assays (see below) and were also used for independent T cell phenotyping experiments.

2.7.1 *In vitro* stimulation assays.

To induce T cell activation PMA and ionomycin was added to PBMC or T cell cultures at a final concentration of 50ng/ml and 750ng/ml respectively (unless otherwise indicated). Alternatively, T cell activator Dynabeads® were added to cultures for direct engagement of CD3 and CD28. Prior to culture, Dynabeads® were washed by adding an appropriate volume of beads to an Eppendorf containing 1ml of PBS and placing it next to a magnet. The magnetic Dynabeads® were retained by the magnetic field whilst the supernatant was removed and the beads were resuspended in RPMI 10% HIFCS. The washed Dynabeads® were added to cell cultures in a 1:1 bead to cell ratio.

In both PMA/ionomycin and Dynabeads® stimulation assays cells were cultured at 5% CO_2/37ºC/6 hours (unless otherwise indicated). For experiments where cytokine expression was to be subsequently analysed exocytosis was blocked with Brefeldin A [Sigma-Aldrich, UK]. This was added 3 hours prior to the end of the culture at a final concentration of 2µg/ml.

2.7.2 Addition of recombinant cytokines to *in vitro* stimulation assays.

Where indicated the recombinant human cytokines rhIL-2, rhIL-7 and rhIL-15 [Immunotools] were added for the duration of some PMA/ionomycin stimulation assays. Cytokines were diluted in RPMI 10% HIFCS to a concentration of 50IU/ml (IL-2), 20IU/ml (IL-7), 80IU/ml

(IL-15) and were applied alone or in combination. Unstimulated cultures (-PMA/ionomycin) and cytokine free cultures were included to control for the effect of both the stimulation and cytokine.

2.7.3 Proteasome inhibition in *in vitro* stimulation assays.

The proteasome inhibitor Velcade® (Bortezomib) was added to PMA/ionomycin stimulated cultures to inhibit proteolytic degradation. The inhibitor was added for the complete 6 hour culture duration and was titrated at a concentration between 1-1000ng/ml. A vehicle control (DMSO) was used to control for the effect of the inhibitor.

2.8 Analysis of gene expression in human CD4 T cell subsets.

2.8.1 Isolation of mRNA from CD4 T cell subsets.

mRNA was isolated from human CD4 T cell subsets that had undergone prior enrichment by MACS (section 2.5) or FACS (section 2.6). A μMACS mRNA isolation kit [130-075-201, Miltenyi Biotech] was used to purify the mRNA from these T cell populations. All buffers, microbead reagents and separation columns referred to in this section are included as part of this kit.

Cells were counted and washed in cold PBS at 300g/4ºC/8min. The supernatant was completely aspirated and cell pellets resuspended in 1ml of lysis/binding buffer. Cells were vortexed for 5min to ensure complete cell lysis. The lysate was transferred to a fresh Eppendorf and the DNA content sheered by repeatedly passing the material through a 21G needle into a 1ml syringe. Foaming of the lysate was eliminated by centrifugation at 13,000g/4ºC/1min. To remove cell debris the lysate was applied to a lysate clear column which was inserted over a collection tube and centrifuged at 13,000g/4ºC/3min. mRNA was labelled by dispersing 50μl of Oligo(dT) Microbeads into the clear lysate by repeatedly pipetting the liquid up and down. A μMACS column was prepared by placement onto a thermoMACS™ separator on a MACS multistand [Miltenyi Biotech]. The column was rinsed

with 100ml of lysis/binding buffer and the bead-labelled lysate applied, thus allowing labelled mRNA to be magnetically retained whilst non-mRNA material passed through. The column was washed twice with lysis/binding buffer and four times with wash buffer to remove contaminating rRNA and DNA. From here the purified mRNA retained on the column was converted to cDNA using a μMACS one-step cDNA kit [130-091-902, Miltenyi Biotech] as described in section 2.8.2.

2.8.2 cDNA synthesis from purified mRNA.

Purified mRNA held on a μMACS column was converted into cDNA using a μMACS one-step cDNA kit [130-091-902, Miltenyi Biotech]. All buffers and reagents described in this section were supplied in this kit and were used at the volumes indicated below.

The μMACS column held on the thermoMACS separator™ was washed twice with equilibration/wash buffer to rinse the bound mRNA. 20μl of resuspension buffer was added to preformed aliquots of lyophilized enzyme and the solution added to the column. The thermoMACS separator™ was set to 42ºC and the column incubated for 1h to allow the reverse transcription of mRNA to cDNA. 1μl of sealing solution was applied to the top of the column matrix to prevent evaporation. Following incubation the column was rinsed twice with 100μl of equilibration/wash buffer. 20μl of cDNA release solution was then added to the column and incubated for a further 10min at 42ºC. Newly transcribed cDNA was then eluted from the column into an Eppendorf in 50μl of cDNA elution buffer. cDNA was stored at -80ºC in preparation for gene expression analysis.

2.8.3 Quantitative real time polymerase chain reaction (qPCR).

qPCR was performed on cDNA samples prepared in section 2.8.2 for relative analysis of gene expression. All assays were performed in triplicate in a 384 well plate, with a total reaction volume of 5μl per well. Taqman® gene expression assays [Life Technologies] were used to

measure amplification of both a target gene and control gene in the same reaction (all measured genes are listed in Table 2.6).

Target gene	Primer/probe set	Conjugate	Associated Function
CD69	Hs00934033_m1	FAM	Activation/Immune response
IFNγ	Hs00989291_m1	FAM	
LCK	Hs00178427_m1	FAM	
PRKCQ	Hs00989970_m1	FAM	TCR Signalling
VAV1	Hs01041613_m1	FAM	
PRKAA1	Hs01562315_m1	FAM	Metabolism
Control gene	**Primer/probe set**	**Conjugate**	**Associated pathways**
GAPDH	Hs99999905_m1	VIC	Metabolism

Table 2.6 Taqman gene expression assays from Life Technologies. Table shows the target and control genes examined in this investigation.

In each well 0.35µl of target gene primer/probe and 0.35µl of control gene primer/probe were added to 2.5µl of fast start universal probe master (X2) [Roche] and 1.8µl of cDNA. Where required the concentration of cDNA was diluted with RNAse free water [Ambion®] prior to its addition to the reaction mix. Plates were centrifuged briefly and sealed with plastic film before performing the qPCR reaction. cDNA amplification was performed by a Lightcycler®480 II instrument [Roche] with parameter for thermal cycling as indicated in Table 2.7.

Stage	Cycles	Temp (°C)	Time (h:min:sec)	Ramp (°C/sec)
Preincubation	1	95	00:10:00	4.4
Amplification	50	95	00:00:15	4.4
		60	00:01:00	2.2
		72	00:00:01	4.4
Melt curve	1	95	00:00:10	4.4
		40	00:00:30	2.5
		80	Hold	0.06
Cooling	1	40	00:00:10	2

Table 2.7 Thermal cycling conditions for the amplification of cDNA. Table indicates the cycling program of a Lightcycler®480 II instrument.

2.8.4 Relative gene expression analysis.

Amplification curves resulting from qPCR reactions were analysed using Lightcycler®480 SW1.5 software. For each qPCR reaction an amplification cycle threshold (Ct) was measured for the target and control gene. The difference in cycle threshold between the Ct_{target} and the $Ct_{control}$ was measured and the mean value attained from the technical triplicates. The fold change (*fc*) in expression between the target and control gene for each sample was then calculated using the equation below.

$$fc = 2^{\wedge -(Ct_{target} - Ct_{control})}$$

Variation in fold change between cell populations of interest was then analysed as a function of relative gene expression.

2.9 Animals.

All animal procedures were performed at the biomedical services unit, University of Birmingham in accordance with the Animals (Scientific Procedures) Act 1986. The housing and use of animals in this study was licenced by the UK Home Office (project licence 30/2720) and was approved by the university ethics committee. All procedures in this investigation were performed on tissue harvested *post mortem*. Schedule One culling of rats and mice through exposure to increasing concentrations of CO_2 gas was performed by the investigator (personal licence No. PIL 70/25469). Adult male Sprague Dawley rats (150-200g weight) [Harlan Laboratories, UK] were housed in the biomedical services unit for a maximum of 3 weeks prior to culling. Male and female C57BL/6 mice (8-16 weeks) were sourced from in house stock colonies, and were kindly provided by Dr Robert Barry. All animals were monitored daily by staff at the biomedical services unit.

2.10 Post mortem tissue preparation (mouse and rat).

2.10.1 Collection of cerebrospinal fluid (CSF).

For CSF collection the rat or mouse was laid prone with the head secured in a stereotactic frame post mortem. The head was then lifted and stabilised with the nose pointing down leaving the body suspended at a ~135° angle. An incision was made at the base of the cranium down the midline and the muscle tissue and fascia teased apart with forceps. This exposed the atlanto-occipital membrane through which a glass micropipette was inserted avoiding the arteris dorsalis spinalis vessels. For mouse experiments this process was performed under a dissection microscope. CSF was drawn through the micropipette from the underlying cistern magna by gently pulling on an attached 1ml syringe. Approximately 50-150µl of CSF per rat and 10-20µl per mouse was placed in an Eppendorf containing 100µl RPMI 10% HIFCS. CSF from 3-4 rats or 4-6 mice was pooled into the same tube and held on ice for subsequent analysis.

2.10.2 Cardiac puncture and vascular perfusion.

Blood was collected from both mice and rats via cardiac puncture. An incision was made down the midline of the animal and the thoracic cavity opened by piercing the diaphragm and then cutting upwards through the ribcage with scissors. The ribs were opened to expose the heart and it was freed from its surrounding fascia. For blood collection a 25mm gauge needle was inserted into the right atrium and blood drawn into a 1ml or 5ml syringe for mouse and rat respectively. Blood was transferred into a heparinised Eppendorf and held at 2-8°C.

In all animal experiments it was important that dissected tissue was free of blood contamination. Therefore a whole body vascular perfusion was performed to flush blood out of the circulation. A pipette tip attached to a saline drip line was inserted into the left ventricle and the right atrium punctured with scissors. PBS was allowed to flow from the drip into the left ventricle and circulate throughout vasculature, with the effluent leaving the animal via the punctured atrium. The flow of PBS was controlled via the drip line and the animal perfused until the atrial effluent was free of blood and ran clear. In some instances a solution of 0.5% w/v of Evans blue dye in PBS was perfused. This solution was made by dissolving powdered dye in PBS prior to the perfusion process.

In instances where fixation of tissue was required following PBS perfusion the animal was also perfused with 4% PFA solution. This was continued until the limbs and neck of the animal became rigid and stiff indicating successful fixation.

2.10.3 Preparation of rodent peripheral blood leukocyte and splenocyte cultures.

Peripheral blood collected via cardiac puncture (section 2.10.2) was treated with a red cell lysis buffer (ACK lysis buffer). 10ml of ACK lysis buffer was added per 1ml of whole blood and held for 3min at room temperature. The lysis buffer was diluted in 40ml PBS and the remaining leukocyte cells washed at 300g/21°C/8min.

Preparation of splenocyte cultures also required red blood cell lysis. Rodent spleen was harvested and transferred to a culture dish (3.5cm diameter) in 1ml RPMI 10% HIFCS. The spleen was cut into small pieces with a scalpel and transferred to a 70µm cell strainer held over a 50ml falcon tube. The pieces were crushed through the strainer using the plunger end of a syringe. The tissue was washed through the strainer with 20ml of RPMI 10% HIFCS and centrifuged at 300g/21°C/8min. The cell pellet was resuspended in 10ml of ACK lysis buffer for 3min to haemolyse the red blood cells. The lysis buffer was diluted in 40ml PBS and the cells washed at 300g/21°C/8min. Following red cell lysis both splenocyte and peripheral blood leukocytes were resuspended in RPMI 10% HIFCS for subsequent cell culture or PBS 2% BSA for flow cytometry.

2.10.4 Neural tissue dissection.

Rodent brain was dissected following the vascular perfusion process (section 2.10.2). The head was decapitated and the craniofacial tissues removed with scissors and serrated forceps. The skull was peeled back in pieces with bone cutting implements [Fine Science Tools Inc.] to expose the brain. The whole brain was detached from the facial and optic nerves and separated from the head by snipping the olfactory bulb. A spatula was used to scoop the brain into a 50ml falcon tube containing RPMI 10% HIFCS or 4% PFA and stored on ice.

Choroid plexus (CP) was dissected from rat and mouse brain (Figure 2.2) under a dissection microscope (Nikon SMZ1270). During the process the brain was bathed in ice cold PBS to keep the tissue hydrated. CP was dissected from the lateral and fourth ventricles and transferred to wells of a 24-well plate containing 100µl cold RPMI 10% HIFCS. Non-CP debris was removed from the preparations prior to tissue digestion (see section 2.10.4).

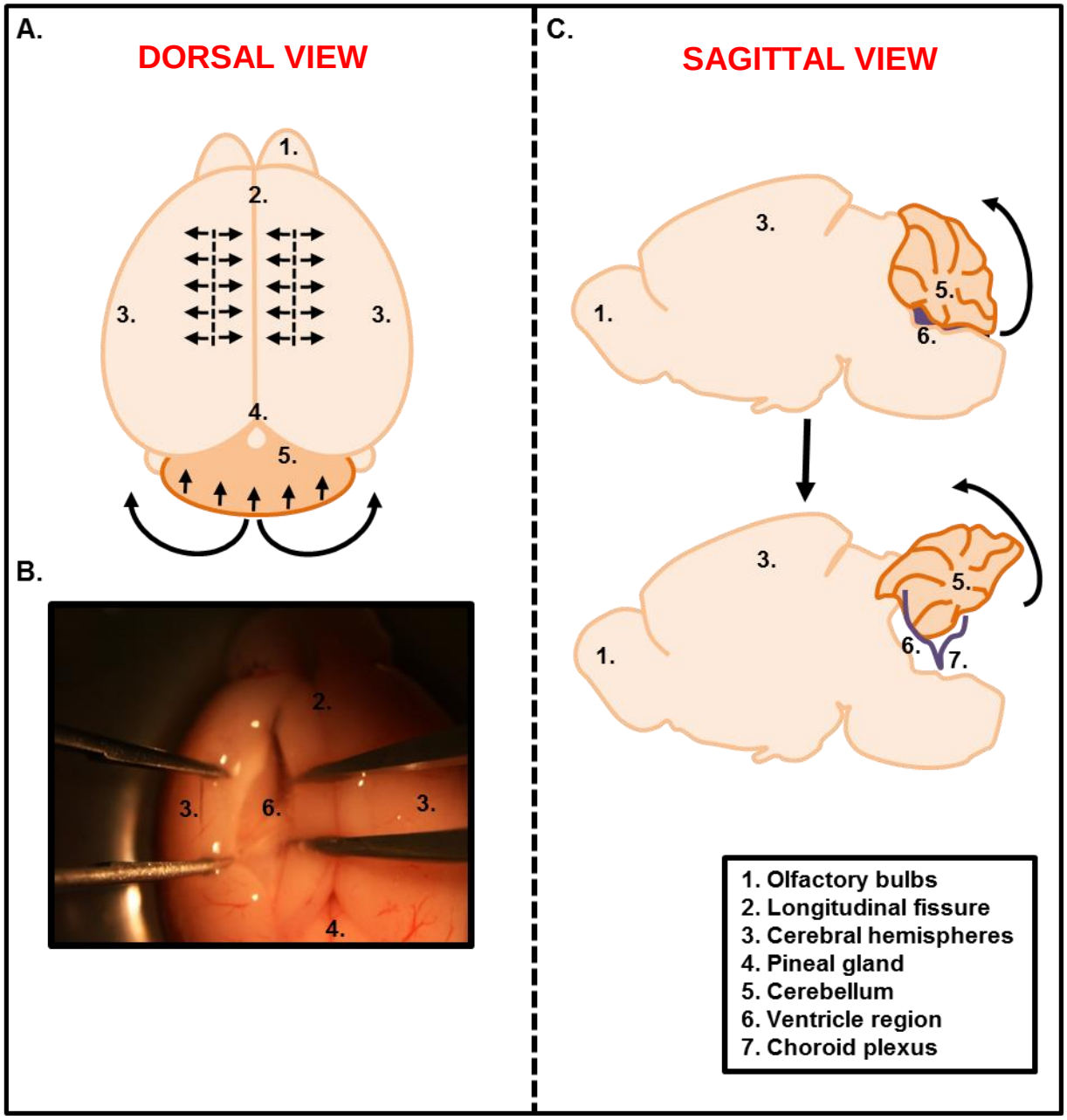

Figure 2.2 Dissection of rodent choroid plexus tissue. Choroid plexus (CP) was dissected from the lateral and fourth ventricles of freshly harvested rat and mouse brain. **A.** Diagram shows a dorsal view of mouse brain indicating the two incision points to gain entry into the lateral ventricles. Incisions were made in both cerebral hemispheres approximately 1mm parallel to the longitudinal fissure. CP was located suspended within the ventricular cavity. The cerebellum was also peeled upwards to reveal the 4th ventricle CP. **B.** Image captured from a dissection microscope view showing the use of forceps to open the incision point above the left lateral ventricle. The ventricle was located approximately 1mm deep into the cerebral hemisphere. **C.** Diagram shows a sagittal view of a mouse brain and shows the 4th ventricle located beneath the cerebellum (top panel). The cerebellum was lifted with forceps to reveal the CP suspended from the roof of the ventricle (bottom panel). The CP was extracted by gripping one end with forceps and gently pulling toward the contra lateral side cerebellum until it became fully detached.

2.11 Enzymatic digestion of rodent brain and choroid plexus tissue.

This section describes the enzymatic digestion of murine brain tissue prior to the extraction of associated lymphocytes. Where rat whole brain tissue was used, the same concentration of enzyme was applied to the tissue but the reagent volume was increased threefold.

Whole mouse brain was transferred into a 5cm petri-dish containing 2ml of fresh RPMI medium without serum. The brain was teased apart into small pieces using a sterile scalpel and tweezers. The tissue and liquid was transferred into a gentleMACS™ C tube [130-09-237, Miltenyi Biotech] and made up to 5ml with RPMI medium. A gentleMACS™ dissociator machine [130-093-235, Miltenyi Biotech] was used to mechanically disrupt the tissue structure in three stages. Firstly, the C tube was attached to the gentleMACS™ dissociator and the program **m_brain_01** applied to begin tissue homogenisation. The C tube was removed and 20IU/ml of collagenase CLSPA enzyme [Worthington Biochemical Corporation, UK] applied to the tissue. The tissue was incubated at 37°C/5% CO_2/15min on an angled rotator [MACSmix™ tube rotator, Miltenyi Biotech]. The tissue was dissociated for a second time by running the **m_brain_02** program on the gentleMACS™ machine. 0.5mg/ml of DNAse I enzyme [Roche, UK] was added to the tissue followed by a further 37°C/5% CO_2/15min incubation under continuous rotation. This incubation step was repeated following a final tissue dissociation process by running program **m_brain_03** on the gentleMACS™. The collagenase and DNAse I enzymes were then diluted by transferring the cell suspension to a new 50ml falcon and filling the tube with RPMI 10% HIFCS. The cells were washed at 300g/21°C/10min and resuspended in 20ml of RPMI 10% HIFCS. To remove cellular debris the suspension was passed through a 70µm cell strainer into a fresh tube using the plunger end of a 5ml syringe. The resulting cell suspension was then washed in RPMI 10% HIFCS at 300g/21°C/10min in preparation for the extraction of associated leukocytes (section 2.12).

CP was also digested enzymatically with 20IU/ml of collagenase CLSPA and 0.5mg/ml of DNAse I enzyme. However due to the size of the tissue it was not possible to perform

mechanical digestion using the gentleMACS™ system. Therefore, freshly isolated CP from multiple animals was pooled into a 3.5cm culture dish containing 1ml RPMI medium. The tissue was gently teased apart with forceps under a dissection microscope to dislodge the cells from the associated membranes. The remaining CP tissue and free cells were transferred to an Eppendorf in a 1ml volume and incubated with enzyme as described above.

2.12 Magnetic-activated cell sorting (MACS) of rodent brain cell suspensions.

Antibody conjugated microbeads [Miltenyi Biotech] were used to purify leukocyte subsets from the enzymatically digested rodent brain suspensions described in chapter 2.11 (the principles of MACS are shown in Figure 2.1). Due to the very high starting cell numbers for these experiments the reagent volumes were scaled up to be appropriate for starting cell equivalent of 10^8 cells.

2.12.1 Isolation of $CD45^+$ cells from murine brain by MACS.

Microbeads targeting the murine CD45 receptor were used to enrich $CD45^+$ leukocytes from murine brain. The brain cell suspension was washed in PBS at 300g/21°C/10min and resuspended in 900µl of MACS buffer. 100µl of anti-CD45 microbeads [130-097-153, Miltenyi Biotech] were thoroughly mixed into the suspension and the cells refrigerated for 15min at 2-8°C. Excess microbeads were removed by washing the cells in 10ml of MACS buffer at 300g/21°C/10min. The cell pellet was resuspended in 1ml of MACS buffer and applied to a LS column [130-042-401, Miltenyi Biotech] on a MidiMACS™ Separator in a magnetic field. $CD45^+$ cells were retained on the column whilst unlabelled cells were washed through with 3x1ml of MACS buffer. The $CD45^+$ cells were eluted in 1ml MACS buffer by forcing the liquid through with a column plunger. This process was then repeated by passing the eluted fraction over a second MS column [130-042-201, Miltenyi Biotech] to further purify the $CD45^+$ cells. Once eluted from the second column the cells were washed MACS

buffer at 300g/21°C/10min and resuspended in RPMI 10% HIFCS for cell culture or PBS 2% BSA for flow cytometry.

2.12.2 Isolation of T cells from rat brain by MACS.

Pan T cell microbeads targeting the rat OX-52 antigen (CD6) were used to purify T cells from rat brain cell suspensions. The brain cell suspension was washed in PBS at 300g/21°C/10min and resuspended in 800µl of MACS buffer. 200µl of pan T cell microbeads [130-090-320, Miltenyi Biotech] were added and the cells refrigerated for 15min at 2-8°C. The cells were then washed in MACS buffer at 300g/21°C/10min in preparation for magnetic separation. The magnetic separation process was analogous to that used to purify mouse brain cell suspensions as described in section 2.12.1.

2.12.3 Rodent cell culture.

Rodent splenocyte, peripheral blood, CSF and brain derived cells were resuspended in RPMI 10% HIFCS and stimulated for 3 hours with 50ng/ml PMA and 750ng/ml ionomycin as described in section 2.7.1. Unstimulated (RPMI 10% HIFCS only) controls were performed for all samples except CSF-derived cultures due to their low cellularity. Following stimulation, cultures were washed in PBS 2% BSA and analysed by flow cytometry (section 2.14).

2.13 Immunofluorescence imaging

2.13.1 Fixation and cryopreservation of murine tissue.

Murine brain and spleen were fixed in situ by cardiac perfusion of 4% PFA solution. The organs were then harvested and immersed in 4% PFA for 3 hours. The fixed tissues were rinsed in PBS and dehydrated through immersion in 10% sucrose solution. Following 12h of refrigeration the sucrose concentration was increased to 20% then 30% for two additional 12h periods. The tissue was then thoroughly dried and embedded in Tissue Tek™ Cryo-OCT freezing medium (OCT). For this procedure a plastic Cryomold™ was placed on crushed dry

ice and filled with OCT. The tissue was immersed in the freezing medium before it froze and hardened. The frozen blocks of tissue were stored at -80°C prior to sectioning.

Serial sections of brain and spleen tissue were cut from frozen OCT blocks by a cryostat [OFT5000, Bright Instruments] at 20µm thickness. Sections were not mounted on to slides immediately, but were floated in wells of a 24-well plate filled with cryopreservation medium (see section 2.1 for cryopreservative composition). Approximately 150 sections were taken per mouse brain (predominantly from the midbrain region) and stored at -20°C. To mount the sections onto microscope slides they were individually extracted from the cryopreservation plate with a 'hooked' spatula instrument and washed through floatation in a 5cm culture dish filled with ice cold PBS. Microscope slides were partially immersed in the PBS and the sections carefully guided in to position with a paint brush. Slides were laid flat and air dried at room temperature for a minimum of 3 hours prior to immunofluorescence staining.

2.13.2 Immunofluoresence staining of murine brain and spleen sections.

All buffers described in the immunofluorescence staining procedure are listed in table 2.8. Rinsing and wash steps were performed by immersing the slides in glass coplin jars filled with the appropriate buffer, then gently shaking the jar on a plate shaker for 3min. This was repeated three times by tipping out the buffer with the slides held in place and refilling the jar with buffer. Monoclonal antibodies used for staining are described in Figure 2.3 alongside a schematic diagram of the immunostaining procedure.

Reagent	Composition
Rinsing buffer	PBS, 0.05% Tween 20
Blocking buffer 1	PBS, 0.05% Tween 20,10% donkey serum
Primary mAb buffer	PBS, 0.05% Tween 20, 0.5% BSA
Blocking buffer 2	PBS, 0.05% Tween 20, 10% rabbit serum
Secondary mAb buffer	PBS, 0.05% Tween 20, 0.5% BSA, 1.5% rabbit serum
Blocking buffer 3	PBS, 0.05% Tween 20, 10% donkey serum
Tertiary mAb buffer	PBS, 0.05% Tween 20, 0.5% BSA, 1.5% donkey serum

Table 2.8 Buffers required for the immunofluorescence staining of murine brain sections.

Firstly, each section on the slides was circled with a hydrophobic pen [S2002, Dako] and the ink allowed to dry. The slides were rinsed 3 times in rinsing buffer and the excess fluid removed. 100µl of blocking buffer 1 was added to the centre of each hydrophobic ring thus immersing encircled section. The slides were incubated at room temperature for 30min in a darkened humidified chamber. The blocking buffer was then tapped off and the slides dried before adding 100µl of primary mAb cocktail (pre-diluted in primary mAb buffer). The sections were refrigerated in a slide box overnight at 4°C. The slides were then washed 3 times in rinsing buffer and blotted dry. 100µl of blocking buffer 2 was added to each spot and incubated for 30min at room temperature in the dark. The excess blocking buffer was removed and 100µl of secondary antibody (prediluted in secondary mAb buffer) added to each section. Slides were incubated for 1 hour in a dark humidified chamber at room temperature, and then washed with rinsing buffer. This procedure was repeated for tertiary mAb staining, with a pre-block step using blocking buffer 3 and antibodies diluted in tertiary mAb diluting buffer. After the final staining step slides were washed 3 times in PBS and dried at room temperature. Slides were mounted by adding one drop of Prolong® Gold anti-fade reagent with DAPI to the centre of each section and placing a coverslip over the top. The mounting medium was allowed to dry for a minimum of 12 hours at room temperature. The slides were then sealed with nail varnish and stored at 2-8°C.

A.

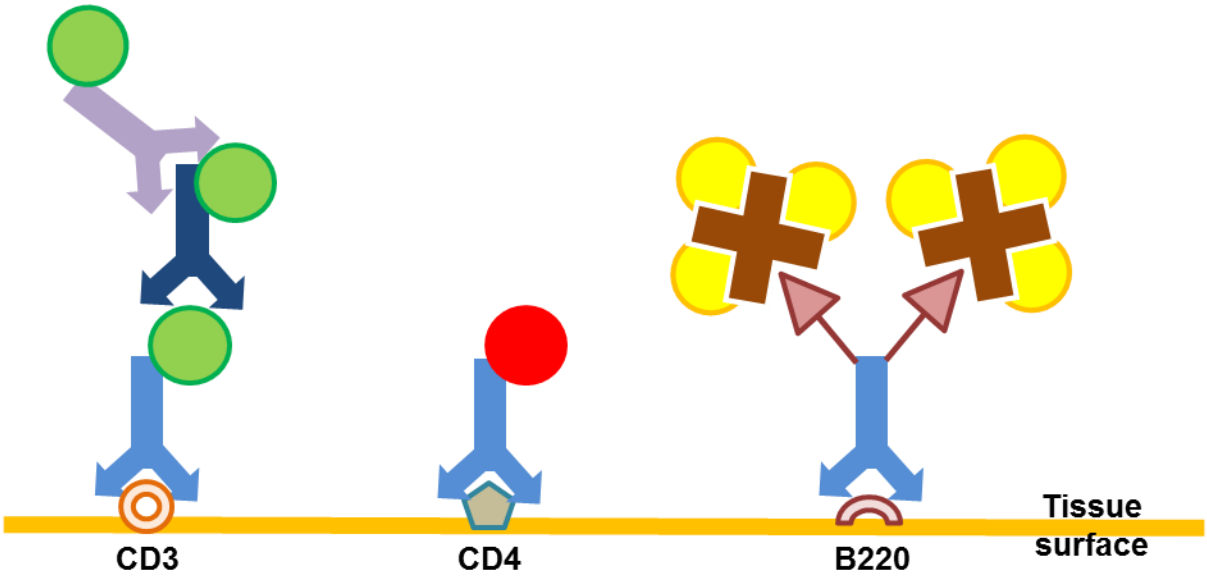

B.

Stage	Symbol	Antibody	Product Code	Source	Dilution
		Block - 10% Donkey Serum			
Primary		Hamster-anti-mouse CD3 FITC	11-0033-82	eBioscience, Hatfield, UK	1/200
		Rat anti-mouse CD4 Alexa Fluor® 647*	14-0041-81	eBioscience, Hatfield, UK	1/100
		Rat anti-mouse B220 biotin	13-0452-82	eBioscience, Hatfield, UK	1/200
		Block - 10% Rabbit Serum			
Secondary		Rabbit anti-FITC Alexa Fluor® 488	A11090	Invitrogen, Paisley, UK	1/200
		Block - 10% Donkey Serum			
Tertiary		Donkey anti-rabbit Alexa Fluor® 488	A-21206	Invitrogen, Paisley, UK	1/200
		Streptavidin (Alexa Fluor® 555 Conjugate)	S-32355	Invitrogen, Paisley, UK	1/500

C.

Stage	Symbol	Antibody	Product Code	Source	Dilution
		Block - 10% Donkey Serum			
Primary	-	Irrelevant hamster IgG FITC	11-4914	eBioscience, Hatfield, UK	1/200
	-	Irrelevant rat IgG2b Alexa Fluor® 647*	14-4031	eBioscience, Hatfield, UK	1/100
	-	Irrelevant rat IgG2a biotin	400503	Cambridge bioscience, UK	1/200

Figure 2.3 Immunofluorescence staining of murine tissue sections. A. Schematic diagram summarising the staining procedure. B. Table of monoclonal antibodies indicating the steps in the staining procedure and associated blocking stages. **C.** Table of isotype controls for primary antibodies. *Antibody conjugated with Alexa Fluor® 647 in house.

2.13.3 Image analysis

Epifluoresence microscopy was performed on a Leica DM6000780 widefield microscope using Leica Application Suite Advanced Fluorescence (LAS AF) software. This software allowed for the tiling of images, where multiple fields were electronically stitched together to represent a larger field of view.

Confocal imaging was performed using a Zeiss LSM780 microscope with Zen 2010 software. Image analysis was performed offline using Zeiss LSM software. Isotype control staining was performed for each brain region independently, with a staining intensity above the isotype threshold used to indicate positive staining for $CD3^+$, $CD4^+$ and $CD3^+CD4^+$ subsets.

For comparative analysis of T cell subset frequencies in various regions of murine brain, 5-12 images were captured in the meninges, cerebral cortex, periventricular and choroid plexus regions. The number of $CD3^+$, $CD4^+$ and $CD3^+CD4^+$ cells were counted in each field of view, and average cell count per field of view ($133475\mu m^2$) was calculated for each region. This value was multiplied to give a representative cell count per mm^2 of brain tissue (see equation below).

$$1mm^2 = 1000000\mu m^2$$

Field of view = 365µm x 365µm = 133475 μm^2 Conversion factor = 1000000/133475 = 7.492

Average cells per field of view x 7.492 = Cells per mm^2

2.14 FLOW CYTOMETRY (rodent and human)

2.14.1 Surface receptor immunofluorescence staining of T cell subsets for flow cytometry.

With the exception of staining prior to fluorescence activated cells sorting (FACS) experiments (see section 2.6) staining of all freshly isolated and cultured cells was performed in 96-well plates. The cells were centrifuged at 300g/4ºC/4min and the culture supernatant flicked away. The cell pellets were briefly vortexed and resuspended in 50µl of a mAb cocktail diluted in PBS 2% BSA (see table 2.9 and 2.12 for list of mAb). Cells were stained on ice in the dark for 15min to allow the antibodies to bind to their respective surface receptors. Excess antibody was removed by washing cells twice at 300g/4ºC/4min in 150µl PBS 2% BSA. For immediate analysis by flow cytometry cells were transferred to an appropriate polystyrene tube in PBS 2% BSA (300µl final volume) and held at 2-8ºC. Alternatively, cells were fixed prior to intracellular staining (see next section 2.14.2).

2.14.2 Cell permeabilisation and intracellular cytokine staining.

In instances where intracellular staining of cytokine was required, cells were fixed with 50µl of Reagent A from the Catlag cell permeablisation kit. Following a 15min fixation in the dark at room temperature (~21°C) cells were washed with 150µl PBS 2%BSA (300g/4ºC/4min). Cell pellets were resuspended in a cocktail of mAb diluted in 50µl of permeabilisation Reagent B (see table 2.11 and 2.12). The plates were incubated for 15min in the dark at room temperature to allow mAb to bind intracellular epitopes. Cells were washed twice in 150µl PBS 2%BSA (300g/4ºC/4min) to remove excess antibody. For immediate analysis cells were resuspended in total volume of 300µl PBS 2%BSA. Alternatively cells were stored in 100µl of PBS 2%BSA at 2-8ºC.

2.14.3 Anti-human monoclonal antibodies for flow cytometry.

Surface Markers	Fluorochrome	Company	Product No.	Dilution
Annexin V*	FITC	eBioscience	BMS147F1	1/20
CCR7	Alexa Fluor® 488	Biolegend	353206	1/20
CD3	APC-eFluor® 780	eBioscience	47-0038-42	1/100
	V500	BD Bioscience	561417	1/20
CD4	PE-Cy7	Biolegend	317414	1/160
CD8	Viogreen	Miltenyi Biotech	130-096-902	1/20
	APC	eBioscience	17-0086-42	1/20
CD25	PerCP-Cy5.5	Biolegend	302026	1/20
CD27	APC-Cy7	Biolegend	302816	1/20
CD45RA	PE-TR	BD Bioscience	562298	1/400
CD45RO	PE-TR	BD Bioscience	562299	1/40
CD56	APC	eBioscience	17-0567-42	1/40
CD62L	PECY5	Biolegend	304808	1/20
CD69	APC-Cy7	Biolegend	310914	1/40
	PE	Biolegend	310906	1/40
CD127	FITC	eBioscience	11-1278-42	1/20
PD-1	PE	Biolegend	329906	1/20
TCRγδ	APC	Biolegend	331212	1/20

Table 2.9 Monoclonal antibodies against human T cell surface receptors.

*phosphatidylserine is the cell surface target for Annexin V.

Isotype control	Fluorochrome	Company	Product No.	Dilution
Irrelevant IgG1κ	PE	Biolegend	400111	1/320
Irrelevant IgG2a	PE	Biolegend	400311	Variable
Irrelevant IgG1	PE	ebioscience	12-4301-82	Variable

Table 2.10 Isotype control reagents for the staining of human T cells.

Intracellular Markers	Fluorochrome	Company	Product No.	Dilution
CD69	APC-Cy7	Biolegend	310914	1/20
IL-2	PE	eBioscience	12-7029-82	1/4000
IL-4	PE	eBioscience	12-7049-42	1/80
IL-5	PE	eBioscience	500904	1/80
IL-9	PE	eBioscience	12-7098-71	1/40
IL-10	PE	eBioscience	12-7108-82	1/160
IL-13	PE	BD Bioscience	559328	1/40
IL-17A	PE	eBioscience	12-7179-42	1/160
IL-17F	PE	eBioscience	12-7169-41	1/160
IL-21	PE	eBioscience	12-7219-42	1/400
IL-22	PE	eBioscience	12-7229-42	1/400
GM-CSF	PE	eBioscience	12-7319-42	1/80
IFNɣ	PE	eBioscience	12-7349-82	1/200
TNFα	PE	BD Bioscience	554507	1/160

Table 2.11 Monoclonal antibodies against human markers tested by intracellular staining.

2.14.4 Anti-rodent monoclonal antibodies for flow cytometry.

Mouse Surface Markers	Fluorochrome	Company	Product No.	Dilution
CD3	PE-Cy7	eBioscience	25-0031-82	1/20
CD4	PerCP-Cy5.5	eBioscience	45-0042-82	1/80
CD8	V500	BDBiosciences	560776	1/40
CD44	APC-eFluor780	eBioscience	47-0441-82	1/160
CD45.2	FITC	eBioscience	11-0454-82	1/40
CD62L	PE	eBioscience	12-0621-82	1/160
CD69	APC	Biolegend	104517	1/20

Rat Surface Markers	Fluorochrome	Company	Product No.	Dilution
CD3	Alexa Fluor® 488	Biolegend	201405	1/20
CD4	Alexa Fluor® 647	Biolegend	201513	1/20
CD45RC	PE	Biolegend	204007	1/40

Rat Intracellular Markers	Fluorochrome	Company	Product No.	Dilution
IFNɣ	V450	BDBiosciences	559498	1/20

Table 2.12 All anti-mouse and anti-rat monoclonal antibodies for flow cytometry

2.14.5 Simultaneous staining of a receptors surface and intracellular pool (human only).

In some experiments the surface and intracellular pools of the CD69 receptor were examined in the same CD4 T cell population. This was achieved by staining with two anti-CD69 mAb of the same clone each conjugated to different fluorochromes. One anti-CD69 conjugate was included in the surface mAb staining protocol (as described in section 2.14.1), whilst the other was included in an intracellular staining panel (section 2.14.2). Surface staining was performed on ice and all reagents were kept cold to limit endocytosis of the surface receptor

pool. In these experiments the cytokine IFNγ was used as a control for cell stimulation and the intracellular expression of CD69.

2.14.6 Indicators of cell death and apoptosis.

For flow cytometry experiments where no fixation step for intracellular staining was required, dead cells were excluded from the analysis by addition of a Sytox® nuclear stain. Sytox® blue was diluted from reconstituted stock PBS 2%BSA. The diluted Sytox® blue was added to flow cytometry tubes containing stained cells at a final dilution of 1/800 in PBS 2%BSA. The tubes were vortexed and held in the dark on ice for a maximum of 10min prior to the running of samples on the flow cytometer. Dead cells were indicated by a strong positive signal in the appropriate violet laser channel (maximum excitation and emission spectra at 444nm and 480nm).

For studies specifically measuring the degree of apoptosis in cell cultures, following surface staining (see chapter 2.14.1) cells were resuspended in 300ul of 1X Annexin binding buffer and stained for 10min with AnnexinV at room temperature. Cells were then washed (300g/4ºC/4min) and resuspended in 300ul Annexin binding buffer, and analysed by flow cytometry within 1 hour. Sytox® blue dye was added 10min prior to the running of samples on the flow cytometer.

2.14.7 Flow cytometry analysis.

Multi-colour flow cytometry for both human and rodent samples was performed on a Dako-Cyan flow cytometer (Beckman Coulter). Digital and manual correction for spectral overlap was performed using Summit® v4.3 software. Single colour staining of onecomp ebeads were used to set the fluorescence parameters of each mAb to be compensated. All flow cytometry and FACS data was analysed using the Summit v4.3 program.

2.15 Statistics

Statistical analysis was performed using GraphPad Prism® 6 software. Non-parametric statistical testing was applied to human datasets, whereas parametric tests were appropriate for comparative analysis of rodent samples. There were not enough data points to test for normal distribution in most rodent experiments. Parametric testing was justified as the median and mean values were found to be numerically similar in these cases. In all tests statistical inferences were considered significant at the level $p<0.05$ (confidence interval 95%) and below.

CHAPTER 3

RESULTS

INVESTIGATION OF HUMAN PERIPHERAL BLOOD $CD4^+$ T CELLS THAT FAIL TO PRODUCE EFFECTOR CYTOKINE.

3 INVESTIGATION OF HUMAN PERIPHERAL BLOOD CD4$^+$ T CELLS THAT FAIL TO PRODUCE EFFECTOR CYTOKINE.

3.1 Rationale.

A characteristic function of CD4$^+$ T helper cells is the ability to produce cytokine in response to a cellular or molecular change in the local environment. The cytokine secreting potential of a cell population can be revealed through *ex vivo* stimulation which triggers relevant signalling pathways that drive cytokine-related gene expression. A combination of the protein kinase C activating phorbol myristate acetate (PMA) and ionomycin (to elevate intracellular calcium) is a common non-physiological stimulus notable for its potency and polyclonal properties[365,366]. During stimulation the expression of cytokine on an individual cell basis is detectable by preventing protein secretion during cell culture with an endocytic block[367]. Monoclonal antibodies are used to label T cell surface markers and intracellular cytokine (the latter following cell membrane permeabilisation)[368] and subsequent analysis by flow cytometry is a powerful tool for measuring the number of cytokine-producing cells and the relative amount of cytokine expressed per cell.

Preliminary studies have used such techniques to investigate cytokine secretion by CD4$^+$ T cells in the peripheral blood and CSF of healthy volunteers. In these studies a variable proportion of memory CD4$^+$ T cells (CD3$^+$CD4$^+$CD45RA$^-$) expressed one of seven common effector cytokines (IFNγ, TNFα IL-17, IL-21, IL-22, IL-10, IL-5) following PMA/ionomycin stimulation. In addition to analysing patterns of cytokine expression it was noted that a large proportion of CD4$^+$ T cells did not express any of the cytokines measured and thus their effector function was unaccounted for. It was considered whether the cytokine secreting potential of all peripheral CD4$^+$ T cells could be revealed by extending the panel to include additional markers or whether a population of cytokine^{-ve} cells would persist. The aim of this

work is to characterise a population of $CD4^+$ T cells with no apparent cytokine function, beginning with an extensive analysis of cytokine expression by $CD4^+$ T cells in the blood.

I subsequently identified a population of memory $CD4^+$ T cells that showed true hyporesponsiveness to PMA/ionomycin stimulation (as defined by atypical activation marker expression and absent cytokine production). The inability of such cells to activate *ex vivo* may be indicative of either; 1) previous activation events *in vivo*, 2) a modulated differentiation pathway resulting in deactivation of inflammatory response genes, or 3) an atypical response to PMA/ionomycin stimulation (e.g. defective PKCθ signalling). In this investigation flow cytometry and gene expression analysis are used to examine these potential scenarios. As T cell hyporesponsiveness can be indicative of anergy, senescence or exhaustion the $CD4^+$ T cell population identified in this chapter is also examined for characteristics associated with these distinctive cellular states.

Further understanding the cellular processes that underpin the T cell hyporesponsiveness has significant implications related to multiple areas of T cell biology, including mechanisms underpinning the maintenance of self-tolerance, understanding the impairment of adaptive immune responses in senescence and the ability to produce robust anti-vaccine or anti-tumour T cell responses.

3.2 Strategy for detecting $CD4^+$ T cells that don't make cytokine by flow cytometry.

3.2.1 Stimulation assay optimisation for the maximum detection of cytokine.

Preliminary studies had defined a $cytokine^{-ve}$ $CD4^+$ T cells as those that did not make any IFNγ, TNFα IL-17, IL-21, IL-22, IL-10 or IL-5. As it was possible that this defined $cytokine^{-ve}$ population expressed cytokines not included in this list this was tested by extending the panel to include other notable T cell effector cytokines. Thirteen T cell cytokines in total were chosen (IL-2, IL-4, IL-5, IL-9, IL-10, IL-13, IL-17A, IL-17F, IL-21, IL-22, GM-CSF, IFNγ, TNFα) to give a more robust definition of '$cytokine^{-ve}$'. However, the secretion kinetics of all

these cytokines are not identical and so the point where maximal expression is detectable by flow cytometry is variable. Therefore, to begin the investigation a stimulation assay time course was performed. This could ascertain an optimal stimulation time point where the expression of the most cytokines would be maximal but they all could be detected (Figure 3.1).

Peripheral blood mononuclear cells (PBMC) were stimulated for 2-24 hours with PMA/ionomycin and the percentage of cytokine^{+ve} cells within the CD4^{+} T cells compartment (CD3^{+}CD4^{+} lymphocytes) was measured at five time points by flow cytometry. As unstimulated CD4^{+} T cells do not produce cytokine the threshold for a cytokine^{+ve} signal was set at a fluorescence intensity above level observed in unstimulated cultures. As anticipated the cytokine producing T cells were predominantly in the memory CD45RA^{-} compartment with the exception of IL-2. Figure 3.1 shows five representative examples where the percentage of cytokine producing memory cells was recorded over time. Cytokine expression was detectable within 2h from all cytokines tested with maximum expression peaking between 6-8h with the exception of TNFα where expression peaked at 4h (data not shown). Based on this finding it was decided to test for true cytokine^{-ve} cells following a 6h PMA/ionomycin stimulation in subsequent experiments.

3.2.2 Single fluorochrome intracellular staining strategy for detection of multiple cytokines.

At the time of these experiments it was not possible to test one cytokine per fluorochrome using the flow cytometry machines available due to an insufficient number of fluorescence channels. As an alternative strategy all thirteen cytokines were stained simultaneously using specific anti-cytokine antibodies conjugated to the same fluorochrome. This approach could clearly distinguish between cytokine^{+ve} and cytokine^{-ve} cells without being concerned with what cells expressed what cytokine in the positive fraction.

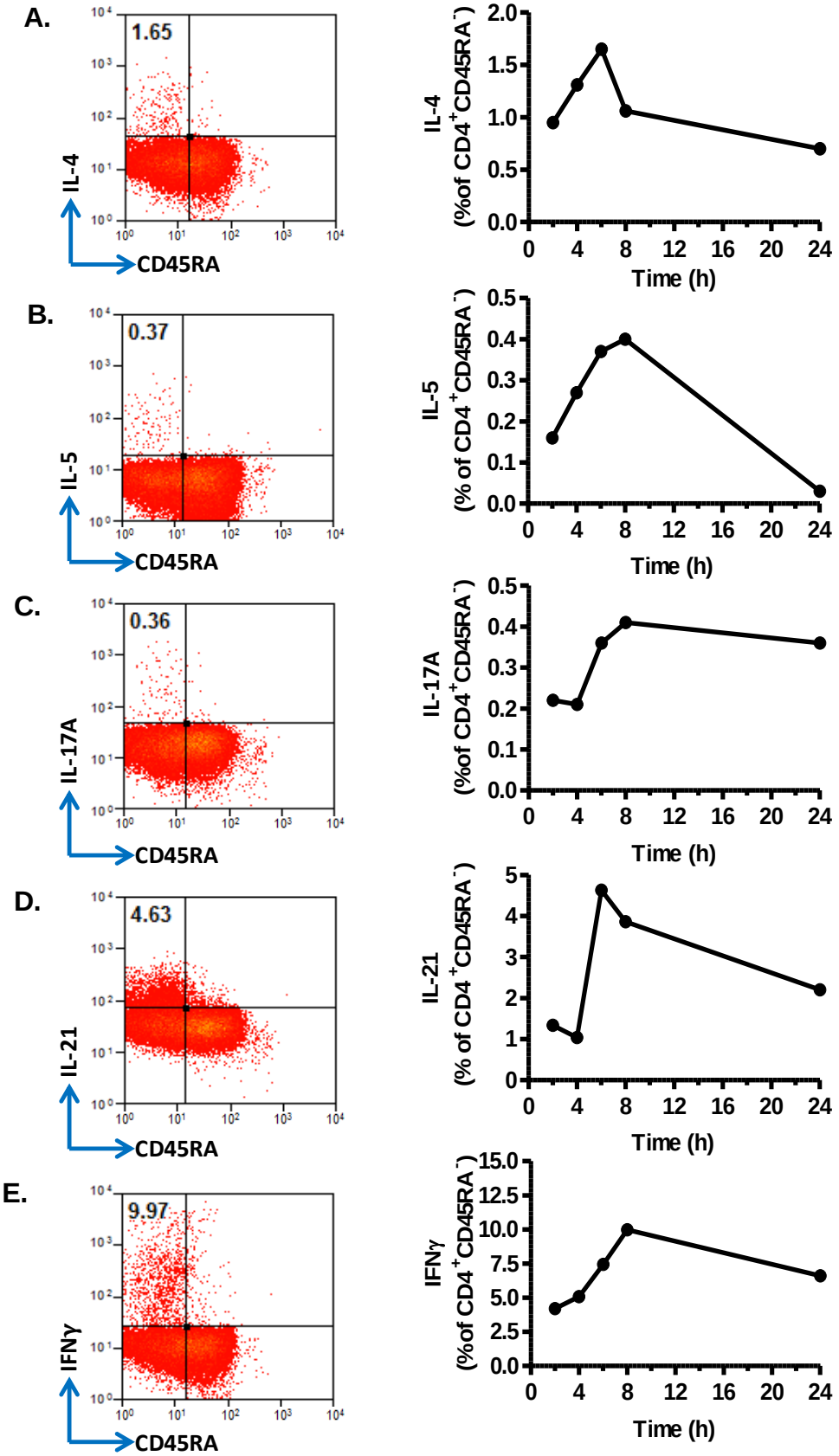

Figure 3.1 Cytokine secretion kinetics in the CD4$^+$ memory T cell compartment. Peripheral blood mononuclear cells were stimulated for 2-24 hours with PMA/ionomycin. Cultures were surface stained for CD3,CD4,CD45RA, stained intracellularly for expression of IL-4, IL-5, IL17A, IL-21 and IFNγ, then analysed by flow cytometry. **A-E.** The percentage of CD3$^+$CD4$^+$CD45RA$^-$ T cells that express each cytokine (right hand panel). Adjacent plots represent expression at the 6h time point (left hand panel). Each cytokine was measured once using PBMC from 1 healthy donor.

Pooling multiple anti-cytokine antibodies required optimisation to minimise the background staining whilst retaining a detectable positive signal for all cytokines. This optimisation reduced the risk of background signals from one antibody overlapping the signal for another, thus avoiding contamination of the cytokine^{-ve} population. Each anti-cytokine antibody was titrated individually to identify a dilution giving the maximum signal to noise ratio (Figure 3.2A-N). This was measured quantitatively by dividing the median fluorescence intensity (MFI) of cytokine^{+ve} cells by the MFI of the cytokine^{-ve} cells in the memory CD4^{+} T cell fraction (Figure 3.2A-N right hand panel). However, the dilution with the most favourable MFI cytokine^{+ve}/MFI cytokine^{-ve} ratio was not always taken forward. In some cases where the absolute background was considered too high (such as with IL-2 (Figure 3.2B) and IFNγ (Figure 3.2M)) the dilution factor was increased to further reduce the non-specific signal. This ensured that cytokines expressed at a very low level (for example IL-9 and IL-21 (Figure 3.2E and 3.2J respectively)) were not obscured by the background noise. Once the most favourable dilution for each antibody was established all cytokine antibodies were pooled together in subsequent experiments.

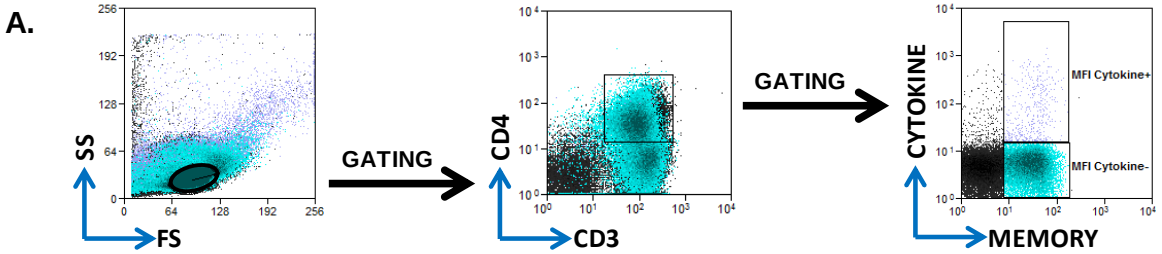
A.
SS
FS
GATING
CD4
CD3
GATING
CYTOKINE
MEMORY
MFI Cytokine+
MFI Cytokine-

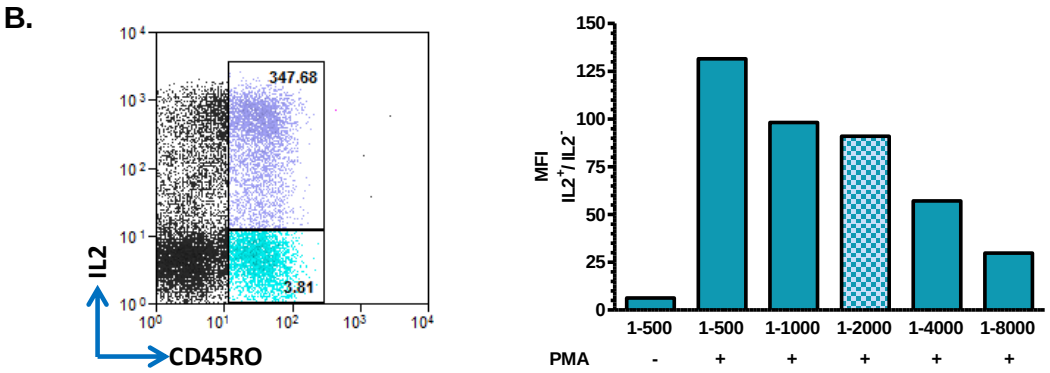
B.
347.68
3.81
IL2
CD45RO
MFI IL2+/IL2-
1-500 1-500 1-1000 1-2000 1-4000 1-8000
PMA - + + + + +

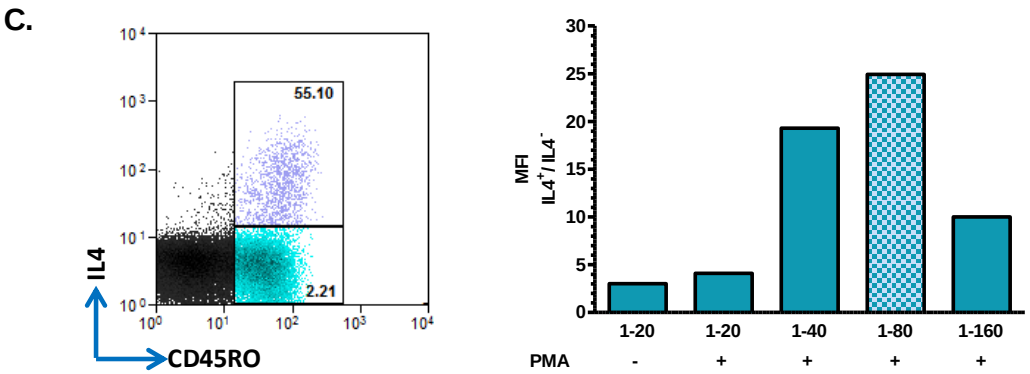
C.
55.10
2.21
IL4
CD45RO
MFI IL4+/IL4-
1-20 1-20 1-40 1-80 1-160
PMA - + + + +

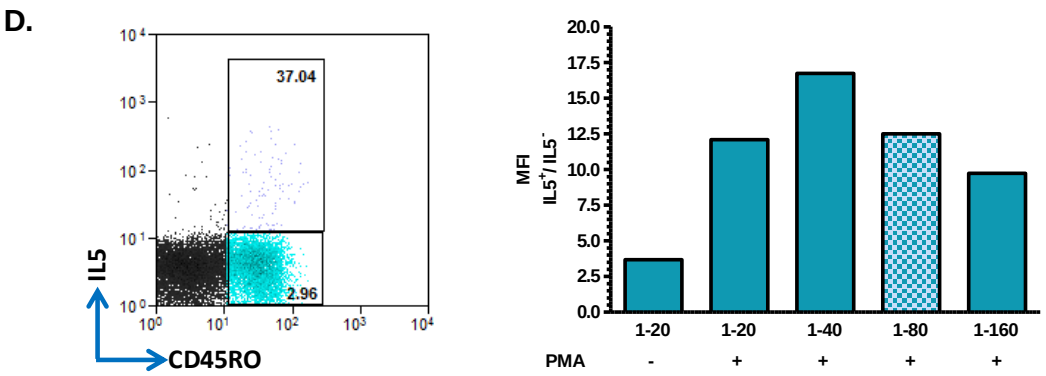
D.
37.04
2.96
IL5
CD45RO
MFI IL5+/IL5-
1-20 1-20 1-40 1-80 1-160
PMA - + + + +

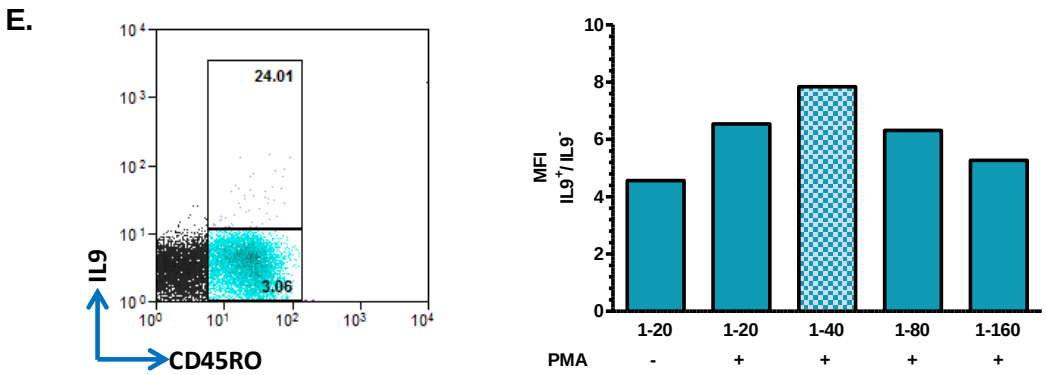
E.
24.01
3.06
IL9
CD45RO
MFI IL9+/IL9-
1-20 1-20 1-40 1-80 1-160
PMA - + + + +

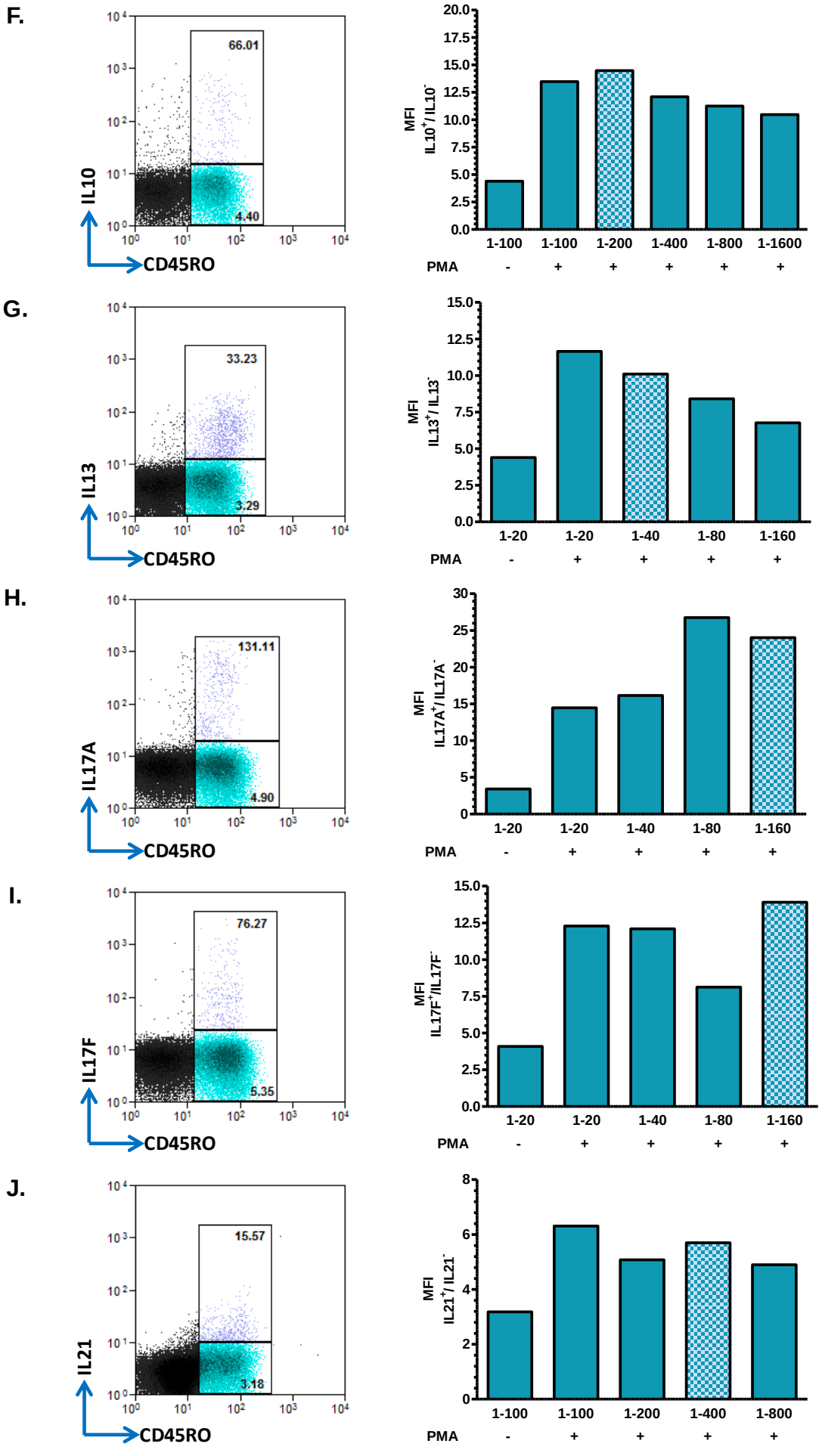
F.
66.01
4.40
IL10
CD45RO
MFI IL10+/IL10-
1-100 1-100 1-200 1-400 1-800 1-1600
PMA - + + + + +
G.
33.23
3.29
IL13
CD45RO
MFI IL13+/IL13-
1-20 1-20 1-40 1-80 1-160
PMA - + + + +
H.
131.11
4.90
IL17A
CD45RO
MFI IL17A+/IL17A-
1-20 1-20 1-40 1-80 1-160
PMA - + + + +
I.
76.27
5.35
IL17F
CD45RO
MFI IL17F+/IL17F-
1-20 1-20 1-40 1-80 1-160
PMA - + + + +
J.
15.57
3.18
IL21
CD45RO
MFI IL21+/IL21-
1-100 1-100 1-200 1-400 1-800
PMA - + + + +

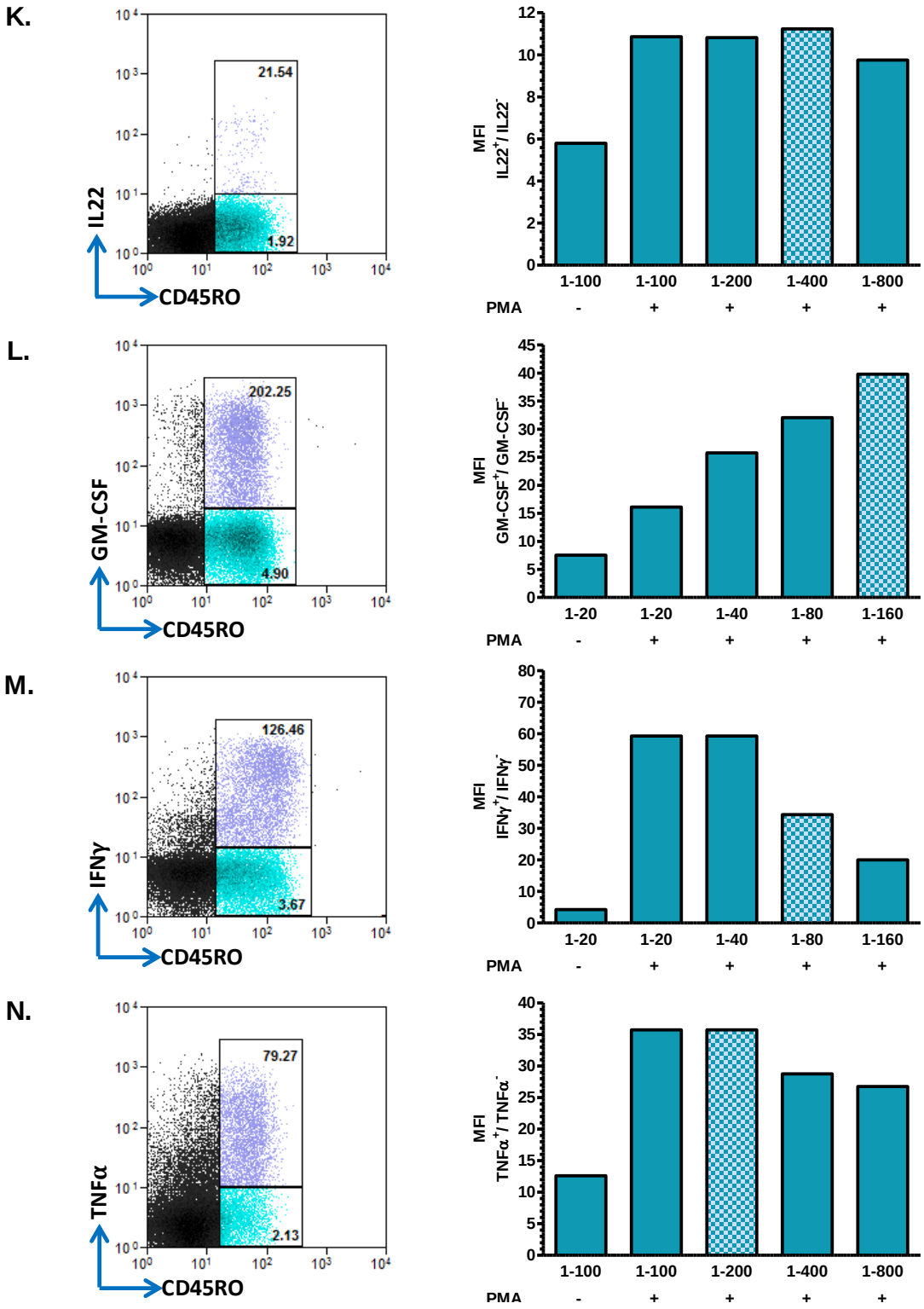

Figure 3.2 Optimisation of intracellular cytokine staining protocol. PBMC were stimulated for 6h with PMA/ionomycin. Cells were stained for T cell surface markers and intracellularly for the expression of thirteen cytokines, then analysed by flow cytometry. **A.** Gating strategy for analysis of cytokine expression by $CD3^+CD4^+CD45RO^+$ memory T cells. **B-N (left).** The median fluorescence intensity (MFI) of $cytokine^+$ (purple) and $cytokine^-$ (cyan) CD4 memory T cells for each cytokine tested (shown numerically on representative flow cytometry plots). **B-N (right).** Graphs show the MFI $cytokine^+$/MFI $cytokine^-$ ratio at increasing dilution of anti-cytokine monoclonal antibody. Chequered bars indicate the final dilution selected for subsequent experiments (corresponding plots are shown left). Each cytokine was tested once using PBMC from 1 healthy donor.

3.3 Phenotypic analysis of cytokine negative $CD4^+$ T cell in human peripheral blood.

Experiments were performed to quantify the percentage of cells that were 'cytokine^{-ve}'. PBMC cultures were stimulated for 6 hours with PMA/Ionomycin, stained intracellularly for cytokine and analysed by flow cytometry. The gating threshold for cytokine^{-ve} cells was set at the background level in unstimulated cultures where cytokine was not expressed (Figure 3.3A). Although background staining was high when all thirteen antibodies were pooled a distinct cytokine^{-ve} population in both the naïve ($CD45RO^-$) and memory ($CD45RO^+$) $CD4^+$ T cell subsets were detected. In five independent experiments the median percentage of cytokine^{-ve} cells in the total population was 36.1% (27.7-41.2 IQR) (Figure 3.3C). However, this was heavily biased by a high frequency of naïve cytokine^{-ve} cells which appeared as a double peak in the negative population. This double peak may be explained by contamination of the cytokine^{-ve} population with cells expressing a low level of IL-2. When naïve (T_{naive} ($CD45RO^-CCR7^+$)), central memory (T_{cm} ($CD45RO^+CCR7^+$)) and effector memory (T_{eff} ($CD45RO^+CCR7^-$)) $CD4^+$ T cells were analysed independently the median percentage of the T_{cm} and T_{eff} populations that failed to secrete cytokine were similar (18.0% (12.2-22.3) and 14.5% (12.2-17.5) respectively (Figure 3.3B, Figure 3.3D)). It was also noted that the cytokine expression by those cells that did secrete cytokine was higher in the T_{eff} population than in the T_{cm} subset as indicated by an elevated MFI (Figure 3.3B). Together these findings indicate that; 1) a significant percentage of memory $CD4^+$ T cells lack a cytokine secretion profile even when tested for thirteen T cell cytokines, 2) the frequency of these cytokine^{-ve} cells is similar between the T_{cm} and T_{eff} populations, 3) on an individual cell basis T_{eff} cell cytokine expression is more potent than their T_{cm} counterparts.

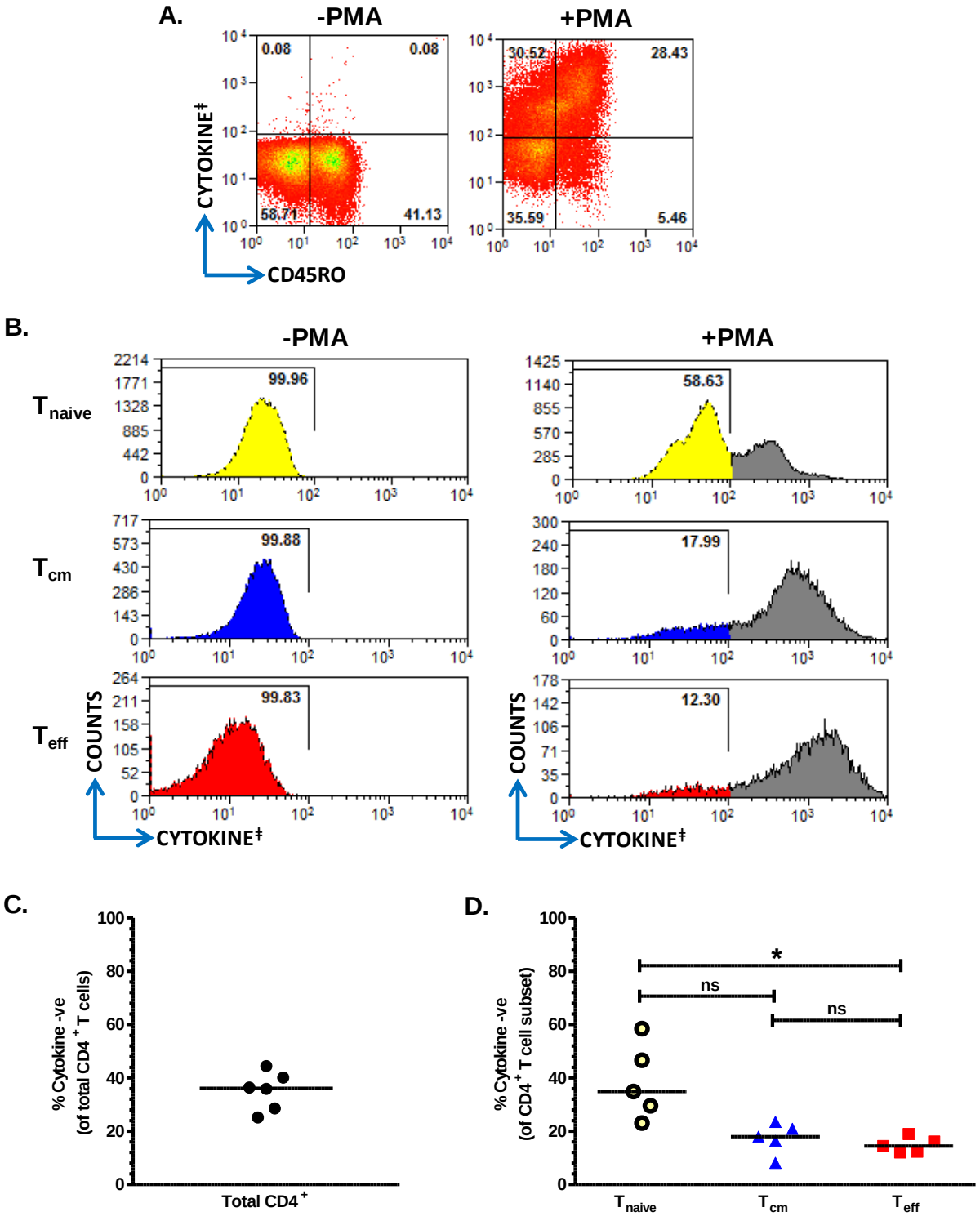

Figure 3.3 Analysis of CD4 T cells that do not produce cytokine following *in vitro* stimulation. $CD3^{+}CD4^{+}$ T cells from PBMC cultures were stained intracellularly for 13 combined cytokines$^{\pm}$. The absence of cytokine expression was analysed by flow cytometry. **A.** Representative plots showing cytokine expression by $CD4^{+}$ T cells with and without stimulation. **B.** Histograms show the percentage of cytokine negative cells in the naïve ($CD45RO^{-}CCR7^{+}$), central memory ($CD45RO^{+}CCR7^{+}$) and effector memory subsets ($CD45RO^{+}CCR7^{-}$). **C-D.** Graphs show the median percentage of cytokine negative cells in the total CD4 population (**C**) and in individual subsets (**D**). *$p<0.05$ depicts statistical significance, ns=no significance at $p<0.05$ (Friedman's statistical test followed by Dunn's multiple comparisons analysis). Data is representative of measurements from n=5 healthy donors. Cytokine‡**;** IL-2, IL-4, IL-5, IL-9, IL-10, IL-13, IL-17A, IL-17F, IL-21, IL-22, GM-CSF, IFNγ, TNFα.

3.4 Do cytokine^{-ve} CD4^{+} T cells activate in response to PMA/ionomyin stimulation?

It was then questioned whether cytokine^{-ve} cells were completely ignorant to stimulation or were readily activated but devoid of any cytokine gene expression. CD69 is a transmembrane glycoprotein that is rapidly upregulated in response to T cell activation (reportedly within 1h in *in vitro* assays[42]). In the peripheral blood the majority of CD4^{+} T cells do not express CD69 at the surface (less than 10% of circulating CD4^{+} T cells[369,370]). Therefore, CD69 upregulation was measured to determine whether cytokine^{-ve} cells were activated by PMA/ionomycin stimulation.

3.4.1 Isotype control testing for CD69 staining protocols.

Matched isotype control staining for a specific CD69 antibody was performed following 6h culture of PBMC with and without PMA/ionomycin (Figure 3.4). Although the MFI of CD69 staining in unstimulated cultures was not perfectly matched to the corresponding isotype control the values were very similar in measuring at 3.6±0.4 and 3.1±0.4 respectively (mean±SEM) (Figure 3.4A, Figure 3.4B). It was decided that the threshold for CD69 upregulation could be gated as expression greater than the gate set upon the unstimulated control cultures. This would ensure consistency between experiments and allow permissive internal control for subtle changes in staining intensity between different days. However, the isotype control staining did increase marginally (5.2±1.4 mean±SEM) in stimulated cultures which was perhaps due to a slight elevation in cell autofluorescence induced by cell stimulation. In contrast, the specific CD69 staining reflected the significant upregulation of CD69 by CD4^{+} T cells in the stimulated cultures (629.7±228.0 mean±SEM).

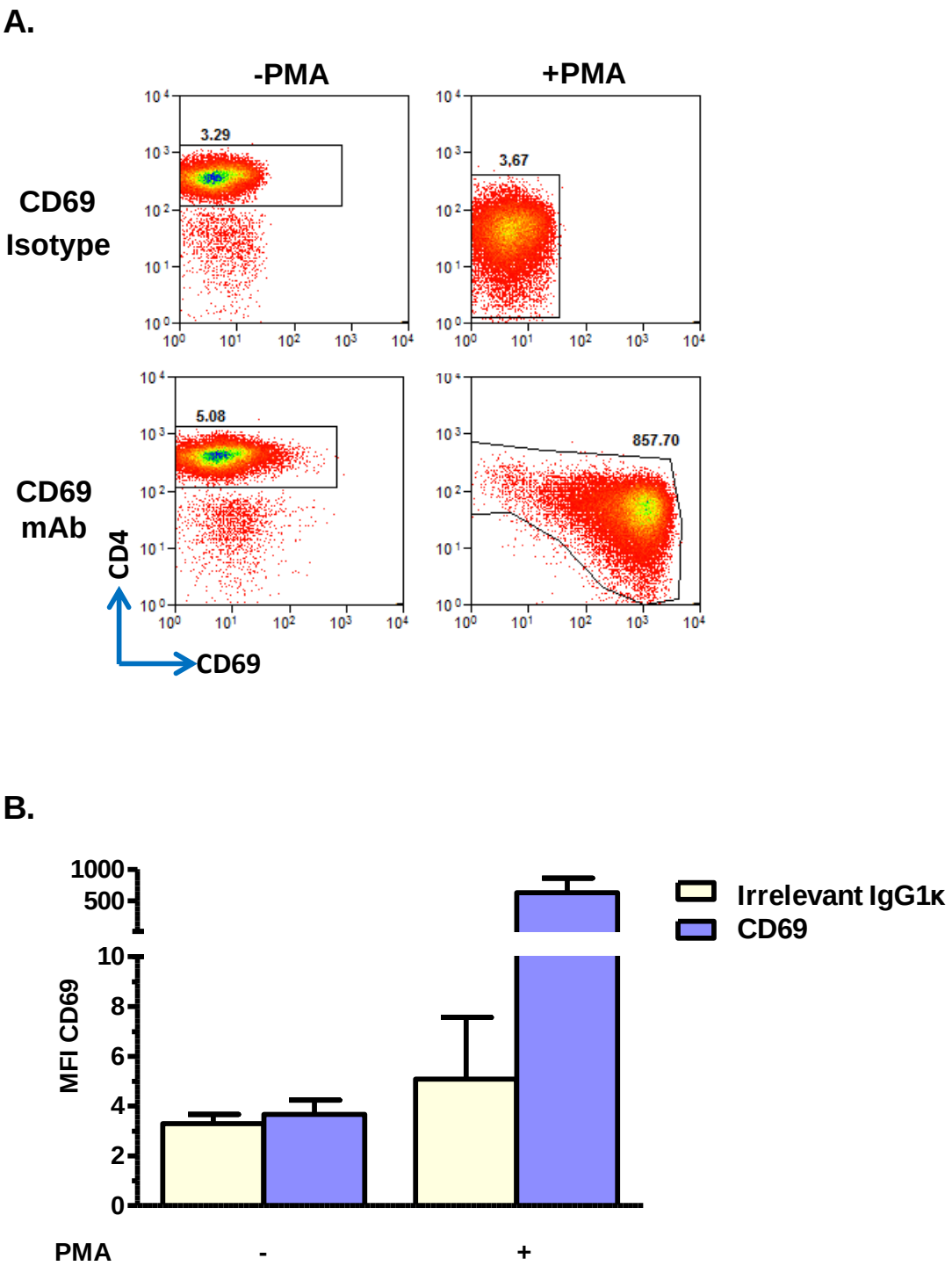

Figure 3.4 Isotype control staining for CD69 expression by CD4 T cells. Peripheral blood mononuclear cells were cultured with and without PMA/Ionomycin for 6h. The $CD3^{+}CD8^{-}CD4^{+}$ T cell fraction was analysed by flow cytometry for expression of CD69. **A.** Representative flow cytometry plots with numbers indicating the median fluorescence intensity (MFI) of specific CD69 staining (bottom panel) and matched isotype control staining (top panel) in unstimulated and stimulated $CD4^{+}$ T cells. **B.** Graph shows the mean±SEM MFI of CD69 staining for the specific antibody and the isotype control (irrelevant IgG1κ) group. Data is representative of n=3 healthy donors measured across 3 independent experiments.

3.4.2 Expression of CD69 by $CD4^+$ T cells that do not produce cytokine.

The $CD4^+$ T cell population was identified by flow cytometry as $CD4^+CD8^-$ cells within the lymphocyte forward and side scatter gate. Due to variation in the frequency of $cytokine^{-ve}$ cells in different T cell subsets $T_{naïve}$ ($CD45RO^-$) and T_{memory} ($CD45RO^+$) populations were analysed independently (gating strategy is shown in Figure 3.5A). The expression of CD69 by $CD4^+$ T_{naive} and T_{memory} was similar in unstimulated cultures (Figure 3.5B) but this was not so in cultures stimulated with PMA/ionomycin. In the T_{naive} subsets both the $cytokine^{-ve}$ and $cytokine^{+ve}$ populations readily upregulated CD69 with only 0.6% and 0.02% of cells left in the unstimulated control gate respectively (Figure 3.5C). In contrast, whereas $cytokine^{+ve}$ T_{memory} cells also readily upregulated CD69 23.3% of the $cytokine^{-ve}$ population did not. Not only did this T_{memory} subpopulation not upregulate CD69 but these cells also failed to completely downregulate $CD4^+$ to the level of $CD69^{hi}$ cells (Figure 3.5C), despite this being a well-documented phenomenon associated with PMA/ionomycin induced activation[371,372]. Although there was a partial decrease in the $CD4^+$ MFI in the $CD69^{lo}$ fraction (as indicated in Figure 3.4A) this population was clearly distinguishable from its activated counterpart and appeared incompletely responsive to the stimulation.

The observation that almost a quarter of memory $cytokine^{-ve}$ $CD4^+$ T cells did not show signs of activation with PMA/ionomycin stimulation was striking. It suggested that there may be differential biological processes occurring that was reflected in their hyporesponsiveness in these *in vitro* assays. Additional questions were also raised regarding the physiological significance of this population and why it might be maintained *in vivo*. At this point, the $CD4^+$ T cell population with a $CD4^{int}CD69^{lo}$ phenotype following stimulation was given the definition of 'non-responsive', as opposed to the 'responsive' cell fraction with a $CD4^{lo}CD69^{hi}$ phenotype. These cells are investigated in depth in the remainder of this chapter.

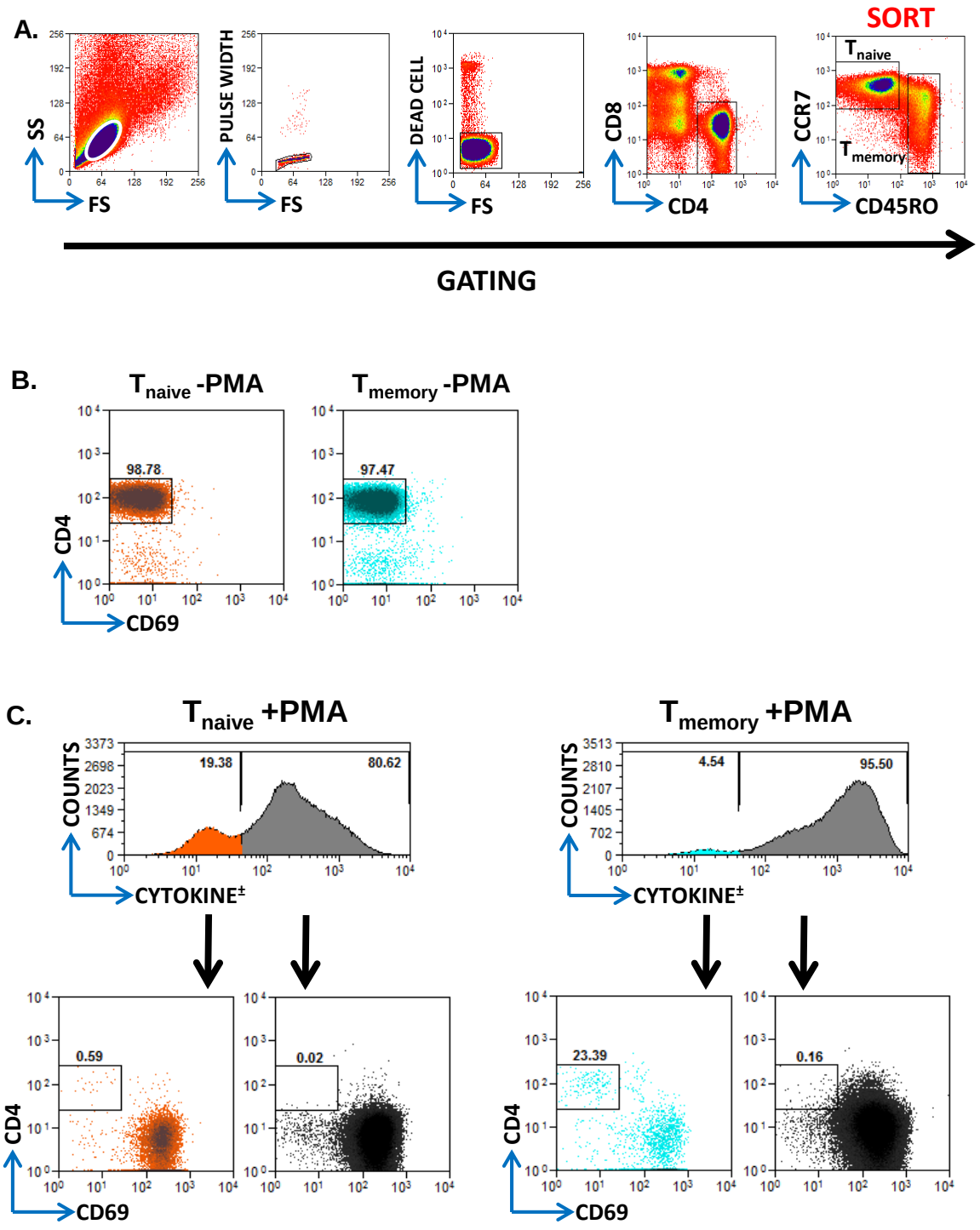

Figure 3.5 Analysis of cell populations unresponsive to stimulation in purified naive, central memory and effector memory CD4^{+} cell cultures. Peripheral blood mononuclear cells (PBMC) underwent fluorescence activated cell sorting (FACS) to purify naive (CD45RO^{-}) and memory (CD45RO^{+}) CD4^{+}CD8^{-} T cells. Purified populations were stimulated for 6h with PMA/Ionomycin. The expression of activation marker CD69 and a combined panel of 13 cytokines$^{\pm}$ were analysed by flow cytometry. **A.** Gating strategy for FACS purification of PBMC. **B.** Flow cytometry plots showing CD4 and CD69 expression by naïve (orange) and memory (cyan) sort fractions. **C. (top panel)** The percentage of cytokine^{-ve} cells by naïve and memory fractions following stimulation. **C. (bottom panel)** Expression of CD4 and C69 in the cytokine^{-ve} and cytokine^{+ve} populations in each subset. Numbers are representative of the percentage of cells failing to respond to the PMA stimulation in n=2 experiments. A membrane viability dye (Sytox) was used to exclude dead cells from the analysis. $^{\pm}$ IL-2, IL-4, IL-5, IL-9, IL-10, IL-13, IL-17A, IL-17F, IL-21, IL-22, GM-CSF, IFNɣ, TNFα.

3.5 Validation of the *in vitro* model for the analysis of 'non-responsive' $CD4^+$ T cells

3.5.1 Longitudinal analysis of CD69 upregulation in response to *in vitro* stimulation.

It was necessary to test the kinetics of CD69 upregulation to confirm that the observed non-responsive $CD4^{int}CD69^{lo}$ population was not a transient phenotype. For initial assays, purified $CD4^+$ cells were cultured for 1-6 hours with PMA/ionomyin and the percentage of non-responsive cells in the T_{naive} ($CD45RA^+$) and T_{memory} ($CD45RA^-$) populations recorded hourly (Figure 3.6B left panel, Figure 3.6C). For these experiments $CD4^+$ T cells were purified from PBMC using magnetic activated cell sorting technology (MACS system from Miltenyi Biotech). Anti-$CD4^+$ magnetic microbeads were used to separate $CD4^+$ cells onto a magnetic column which were then eluted independent of the $CD4^-$ fraction. Flow cytometry was used to measure the percentage purity of each fraction with the purity of the $CD4^+$ fraction measured at 99.1% of the recovered material (Figure 3.6A).

Between 1-3 hours of stimulation there was a rapid upregulation of CD69 by the majority of $CD4^+$ T cells in both the naïve and memory populations. By the 4h time point the frequency of the non-responsive population had begun to stabilise and there was relatively little change in the percentage of non-responsive cells between the 5-6h time points. In keeping with previous experiments, the percentage of non-responders in the T_{memory} subset was greater than in the T_{naive} population although their absolute frequency was notably diminished.

In parallel with this assay it was investigated whether the non-responsive phenotype was present using a more physiological stimulus than PMA/ionomycin. For this purpose anti-CD3/anti-CD28 monoclonal antibody coated Dynabeads® were added to the $CD4^+$ T cell cultures. Use of Dynabeads® simulates antigenic stimulation by activating signal transduction directly through the TCR and co-stimulatory CD28 molecules. This is more equivalent to what occurs physiologically than PMA/ionomycin stimulation.

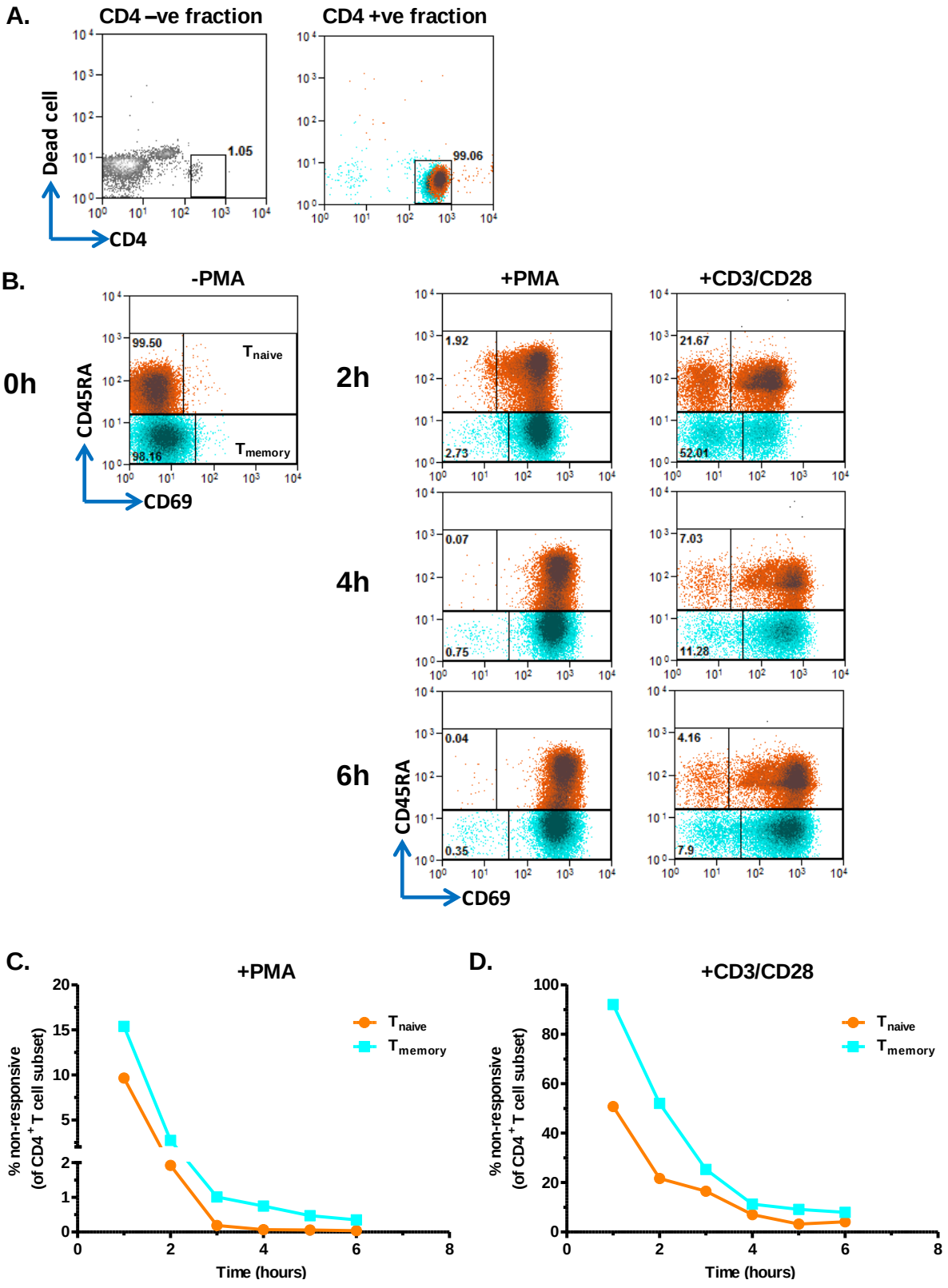

Figure 3.6 Longitudinal expression of CD69 by naïve and memory CD4$^+$ T cell subsets during polyclonal and T cell receptor stimulation. CD4$^+$ T cells were isolated from PBMC and stimulated for 1-6h with PMA/ionomycin or CD3/CD28 conjugated beads. **A.** The percentage purity of the CD4$^+$ and CD4$^-$ cell fractions (ungated). **B.** Expression of CD69 by naïve (orange) and memory (cyan) CD4$^+$ subsets was analysed by flow cytometry. Numbers represent the percentage of each subset that failed to upregulate CD69 at each time point (shown graphically for each stimulus in **C.** and **D.**). Data is representative of n=1 experiment.

Consistent with the PMA/ionomycin stimulation assay, the percentage of non-responsive cells decreased with increased CD3/CD28 incubation time (Figure 3.6B right panel, Figure 3.6D). Between 4-6h of stimulation the non-responsive population stabilised, thus indicating the reproducibility of the non-responsive phenotype with a more physiological stimulant. However, although the trend between the two stimulations was comparable the frequency of hyporesponsive cells in the CD3/CD28 assays was greater than was observed with PMA/ionomycin stimulation (Figure 3.6D). Due to this numerical disparity it could not be concluded whether the PMA/ionomycin and CD3/CD28 induced a phenotypically identical non-responsive population from this experiment alone.

In a separate experiment PBMC were cultured in PMA/ionomycin for up to 26h to examine the non-responsive population over an extended stimulation period. Here the frequency of non-responsive $CD3^{+}CD4^{+}CD8^{-}$ T cells was consistent at 6h and 12h (Figure 3.7A, Figure 3.7C). The percentage of non-responsive cells increased by approximately a third in overnight cultures (20h time point) but there was little change at 26h (Figure 3.7C). However, gating on true non-responsive cells was challenging at later time points due to considerable cell death and debris in the cultures. An altered forward and side scatter of the total lymphocyte population (indicating a decrease in cell size and granularity) was further evidence of PMA/ionomycin-induced cell death (data not shown). Therefore, cell viability of the non-responsive and responsive $CD4^{+}$ T cell fractions was measured more directly by use of a Sytox® viability dye (Figure 3.7B, Figure 3.7D). There was considerable cell death in both the non-responsive and responsive populations when exposed to PMA/ionomycin for 12h or more. However, the frequency of viable cells ($Sytox^{-ve}$) in the non-responsive population was notably diminished comparative to the responsive phenotype. This was particularly striking in cultures over 6h with a negligible frequency of viable cells following 20h of stimulation.

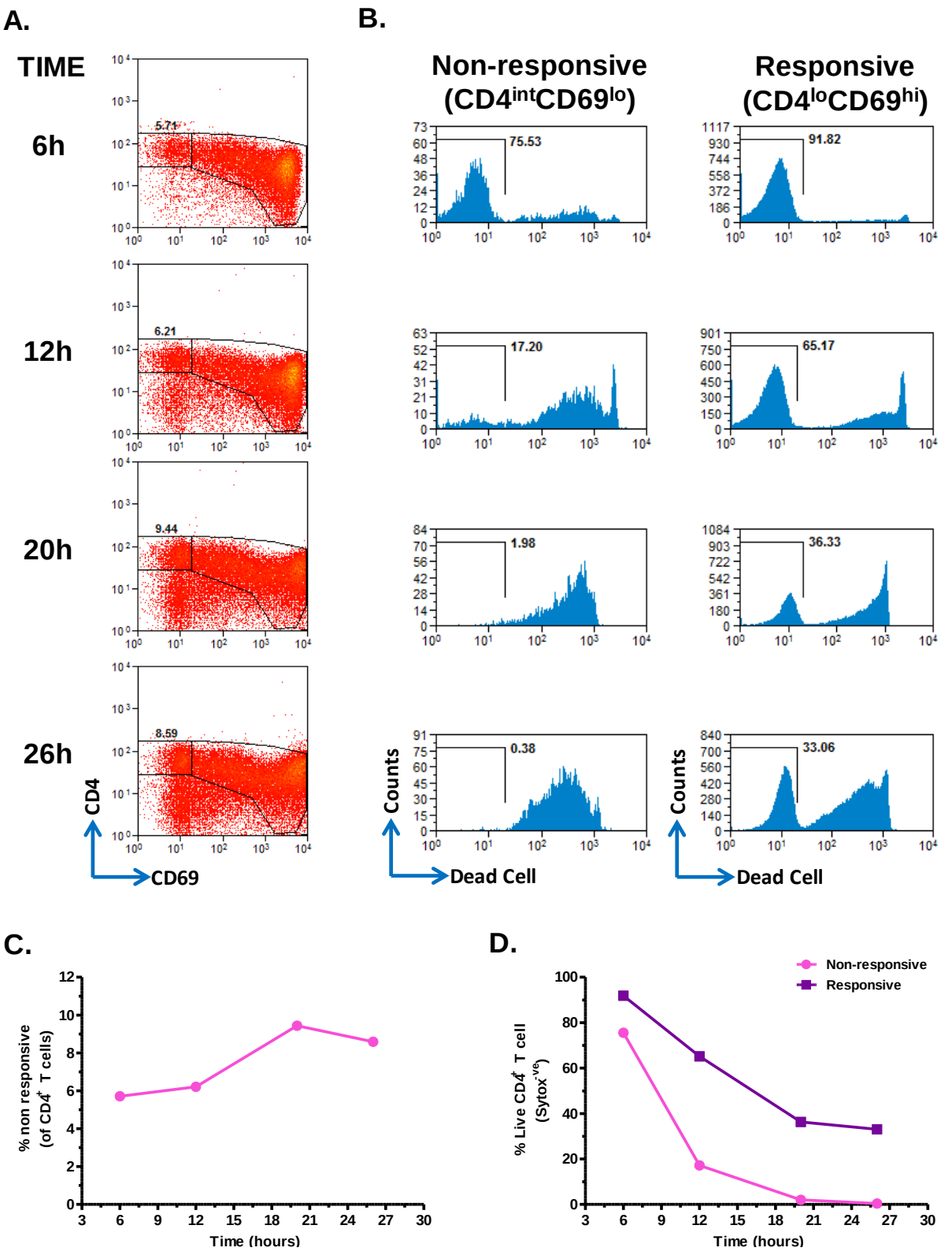

Figure 3.7 Maintenance of the CD4^{int}CD69^{lo} T cell phenotype during prolonged *ex vivo* stimulation. Peripheral blood mononuclear cells were stimulated for 6-26 hours with PMA/ionomycin. **A**,**C.** At each time point measured the CD3^{+}CD8^{-}CD4^{+} T cell fraction was analysed for the percentage of CD4^{+} T cells that did not respond to PMA ionomycin stimulation (CD4^{int}CD69^{lo}) by flow cytometry. **B,D.** The percentage of live cells (sytox^{-ve}) in the non-responsive and responsive CD4^{+} T cell populations was measured at each time point. Flow cytometry plots and graphs are representative of n=1 experiment.

Together this data indicated that although the non-responsive $CD4^+$ T cell population persists in longer term cultures cell viability is severely compromised with prolonged stimulation. With regards to studying the molecular biology of the hyporesponsive phenotype PMA/ionomycin exposure greater than 6h was shown to jeopardise the viability and retrieval of the cells for subsequent analysis. A more detailed examination of apoptosis markers in a more completely defined non-responsive phenotype is described later in this chapter (Section 3.9).

3.5.2 The effect of PMA and ionomycin dosage on the frequency of non-responsive $CD4^+$ T cells.

To assess whether the concentration of PMA/ionomycin added to the PBMC cultures was affecting CD69 upregulation by $CD4^+$ T cells PBMC were stimulated for 6 hours with PMA and ionomycin at a range of concentrations (0-1500ng/ml) (Figure 3.8). $CD4^+$ T cells were analysed by flow cytometry (gating shown in Figure 3.8A and Figure 3.8B) for the percentage of unresponsive cells under each condition. When stimulated with ionomyin alone the population of cells that did not upregulate CD69 was substantial, with over 50% of cells remaining within the gate set on unstimulated cells at concentrations below 75ng/ml (Figure 3.8B, Figure 3.8C). At a higher dosage of ionomycin the percentage of non-responsive cells did decrease but not comparative to the frequency observed in the presence of PMA. This showed that the predominant stimulatory effect in the cultures was PMA although the maximum dose (1500ng/ml) did not result in more $CD4^+$ cells responding and the non-responsive population was still present at this high concentration. Interestingly, all doses of PMA tested followed the same trend with respect to the induced frequency of non- responders with the exception of the 750ng/ml test, which may represent a technical anomaly (Figure 3.8C). It appeared that it was the combinatorial effect of PMA and ionomycin concentration that had the greatest effect on the frequency of non-responsive cell in a dose

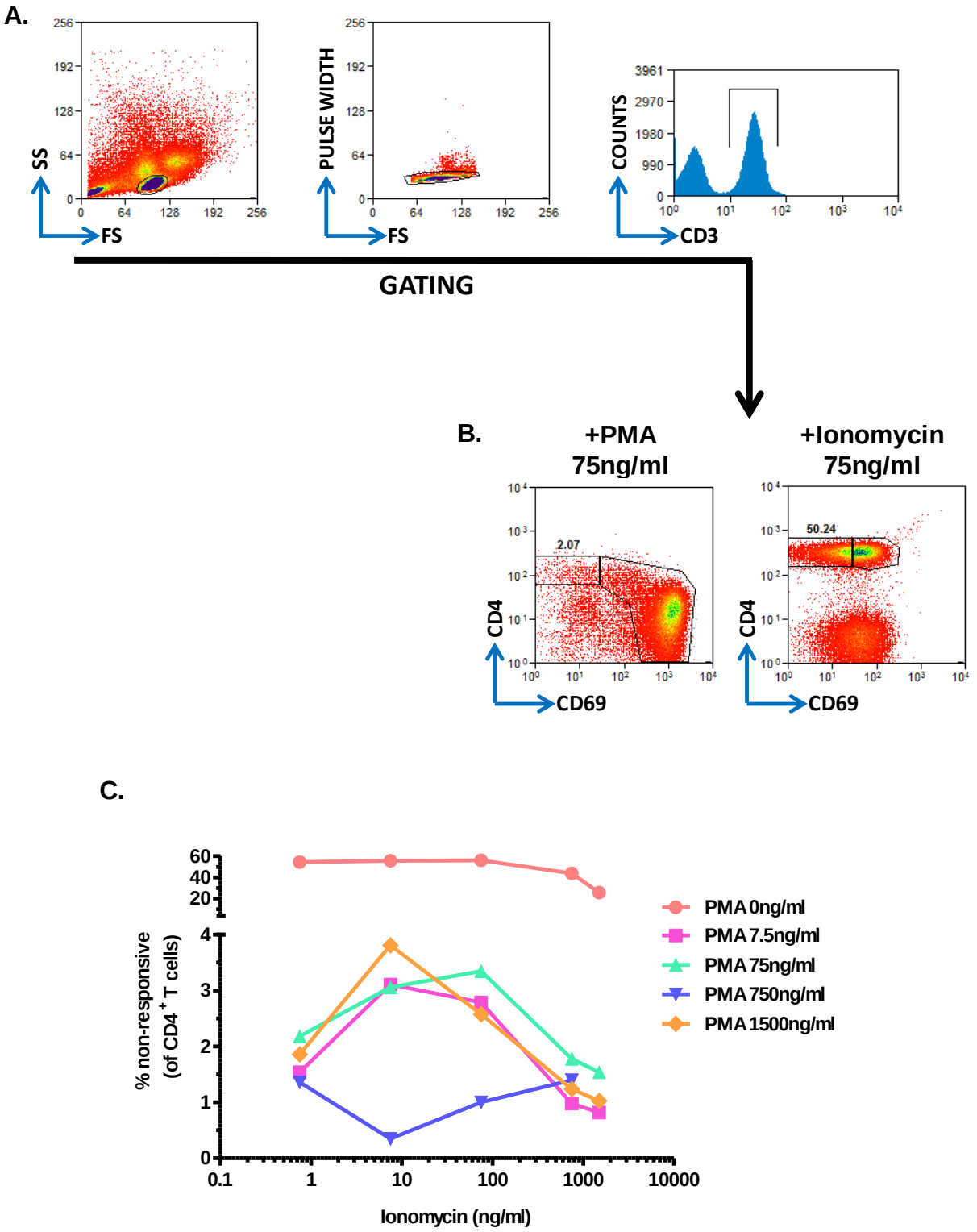

Figure 3.8 Effect of PMA and ionomycin concentration on the unresponsiveness of CD4$^+$ T cells in *in vitro* cultures. Peripheral blood mononuclear cells were stimulated for 6h with increasing concentrations of PMA and ionomycin. The CD3$^+$CD4$^+$ T lymphocyte population was analysed for the failure to upregulate CD69 when stimulated under each condition. **A.** Flow cytometry gating strategy for analysis of CD69 by CD4$^+$ T cells. **B.** Representative plots show upregulation of CD69 and downregulation of CD4$^+$ when cells are stimulated with either PMA or ionomycin alone. Numbers represent the proportion of unresponsive cells as a percentage of CD4$^+$ T cells (gated). **C.** Graph shows the percentage of CD69^{lo} (non-responsive) CD4$^+$ T cells in each culture condition. Data is representative of n=1 experiment.

dependent manner, with the highest non-responder frequency measured between 10-100ng/ml ionomycin in combination with 7.5-1500ng/ml PMA (Figure 3.8C). In order to minimise AICD and preserve maximum cell viability in the 6h cultures it was decided to proceed using a concentration of 50ng/ml of PMA, which is midrange of what is reported for intracellular cytokine staining[373–375]. This was used in conjunction with a high concentration of ionomycin (750ng/ml) to ensure all cells with the potential to respond upregulated CD69 within the culture period.

3.6 Changes in the 'non-responsive' $CD4^+$ T cell population as a consequence of inter- and intra- donor variability.

3.6.1 The effect of age and gender variation on the frequency of the non-responsive $CD4^+$ T cells.

The frequency of the non-responsive $CD4^+$ T cell population was measured in multiple healthy individuals to establish a range of inter-donor variability. 26 PBMC samples were stimulated for 6h with PMA/ionomycin (50ng/ml and 750ng/ml respectively) and the $CD4^+$ T cell population analysed for the non-responsive cell frequency by flow cytometry. For these and all subsequent flow cytometry experiments $CD4^+$ T cells were defined as $CD3^+CD8^-CD4^+$ lymphocytes (Figure 3.9A). The $CD8^-$ gate was added in conjunction with $CD3^+$ definition to minimise the percentage contamination of the non-responsive $CD4^+$ population. Results showed that the median frequency of the non-responsive population in the total cohort was 1.2% (0.65-1.9 IQR). The range of the non-responsive cell frequency was notable, with clear differences in frequency of non-responsive cells between individuals even when assays were conducted in parallel (Figure 3.9B). No significant difference in the percentage of non-responsive cells was observed when the cohort was separated into male and female groups (Figure 3.9C) with median frequencies measured at 1.5% (0.8-2.2 IQR) and 1.2% (0.5-1.6 IQR) respectively.

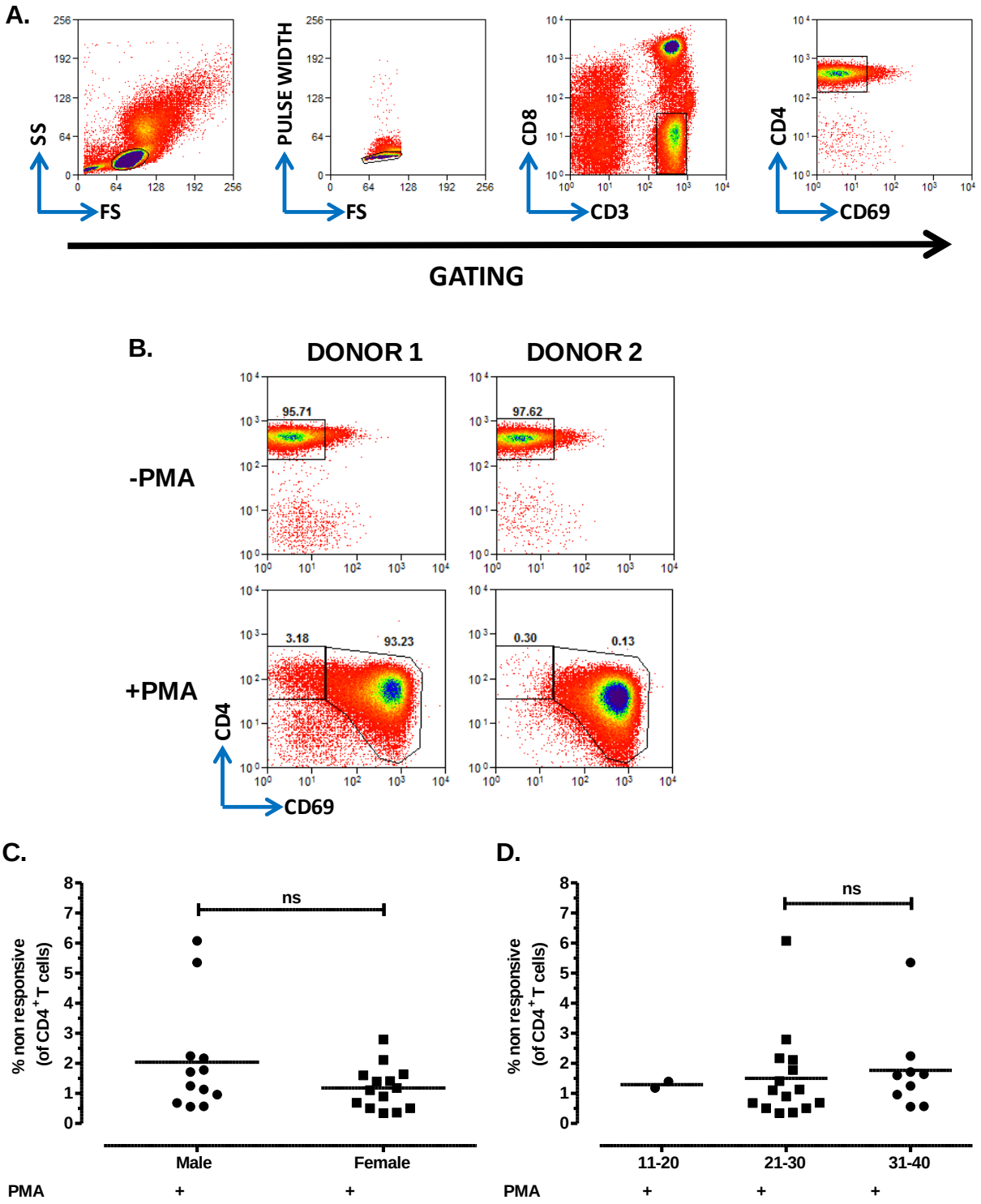

Figure 3.9 Age and sex demographic of CD4$^+$ T cells unresponsive to *in vitro* stimulation in a healthy cohort. PBMC were cultured for 6h with and without PMA/Ionomyin and the CD4$^+$ T cell population analysed for the absence of CD69 upregulation by flow cytometry. **A.** Typical gating strategy for analysis of CD69 expression by CD4$^+$ T cells. **B.** Representative flow cytometry plots showing CD69 expression in unstimulated and stimulated cultures. Data is representative of two donors from the same experiment, and demonstrates the donor variability in the population unresponsive to stimulation (CD4^{int}CD69^{lo} – with gate set at fluorescence intensity of unstimulated cells). **C.** Median percentage of unresponsive cells in male and female donors. **D.** The median percentage unresponsive grouped by age of participant. **ns** = no significance at $p<0.05$ (Mann Whitney U statistical test). Data is representative of samples taken from n=26 healthy donors.

In addition to separation by gender subjects were categorised into three age groups (18-20yrs, 21-30yrs, 31-40yrs) and their corresponding non-responsive cell frequencies were compared. There was a small increase in the median frequency of non-responsive cells between the 21-30yr and 31-40yr age categories. Regrettably the number of younger participants in the 18-20yr age group meant that this category could not be used meaningfully in the analysis.

It is also acknowledged that as all of the participants in this study were below the age of 40yrs, any age-related findings are not representative as the wider local population as a whole.

3.6.2 Longitudinal analysis of non-responsive $CD4^+$ T cell frequency in individual healthy participants.

There are numerous environmental factors that may influence the phenotype and functionality of an individual's $CD4^+$ T cells. The stability of the non-responsive $CD4^+$ T cell population was assessed by recording its frequency in four donors that were tested repeatedly over a 24 month period (Figure 3.10). It was found that the frequency of the non-responsive population in peripheral blood was not always consistent when an individual was repeatedly tested. In three of the four participants there were notable spikes where the population would increase or decrease significantly (Figure 3.10B-D). However, such changes did not correspond with those observed in other donors, and there was no discernible relationship between frequency of the non-responsive cells and seasonal timing of the measurements. It was therefore recognised that the unresponsive population is not stable and other physiological influences may play a significant role in the failure of these cells to upregulate CD69.

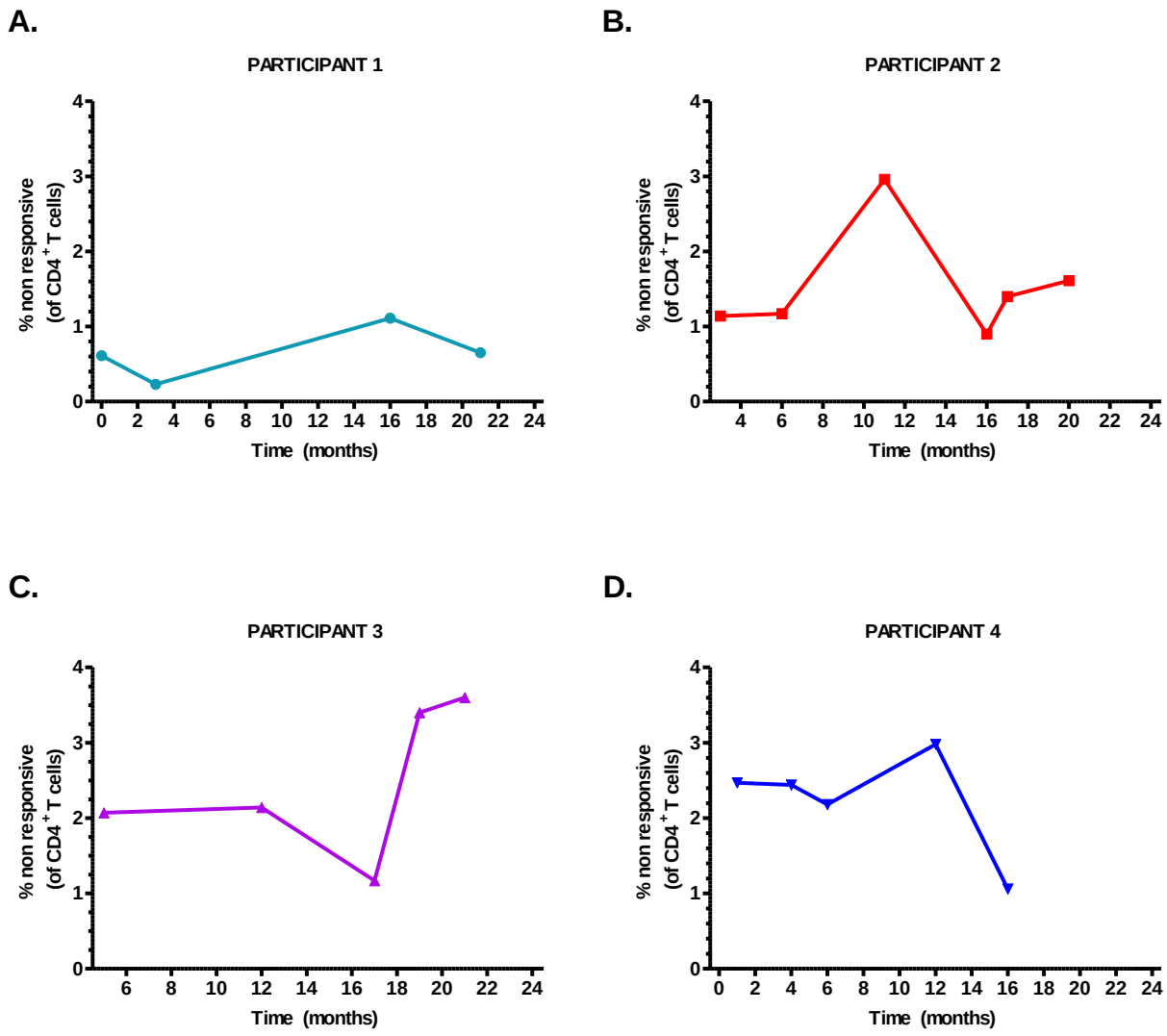

Figure 3.10 Longitudinal analysis of the unresponsive population identified in $CD4^+$ T cells in four healthy participants. Peripheral blood mononuclear cells from four healthy donor was cultured with PMA/Ionomycin for 6h. The percentage of live $CD4^+$ T cells ($CD3^+CD8^-CD4^+$) that failed to upregulated CD69 when stimulated (the non-responsive population) was analysed by flow cytometry. This analysis was performed at varying time points over a 24 month period in four healthy donors. **A-D.** Graphs show the changes in the percentage of total $CD4^+$ T cells failing to upregulate CD69 over time, and thus intra-donor variability of the non-responsive population.

3.7 Phenotypic analysis of the memory subset distribution within the non-responsive $CD4^+$ T cell population.

3.7.1 Subset analysis of the non-responsive $CD4^+$ T cell population in cultures of peripheral blood mononuclear cells.

To begin establishing a surface receptor profile of non-responsive $CD4^+$ T cells the population was induced through 6h of PMA/ionomycin stimulation and analysed for the distribution of T_{naive} ($CD45RA^+CCR7^+$), T_{cm} ($CD45RA^-CCR7^+$) and T_{eff} ($CD45RA^-CCR7^-$) subsets (Figure 3.11A) within the population. Using flow cytometry the initial approach to gating each subset could be described as a 'forward gating' strategy, with analysis based on this design revealed that the non-responsive population was predominated by a T_{cm} phenotype (65.7% 61.2-69.9 (median and IQR)) (Figure 3.11C).

Reanalysis of the same data set was performed at a later date where the T_{naive}, T_{cm}, and T_{eff} populations were independently examined for the percentage of non-responsive cells in each subset (reverse gating shown in Figure 3.11B). As with the previous analysis the T_{naive} subset had a very low frequency of non-responsive cells. In contrast to previous findings, a similar percentages of non-responsive cells were found in both the T_{cm} and T_{eff} subsets with median values of 6.3% (2.3-11.9 IQR) and 4.8% (4.0-12.5 IQR) respectively (Figure 3.11D). It was striking how alternative analyses could produce such contrasting results as this reanalysed data set was more consistent with the non-responsive population being a more heterogeneous memory phenotype as opposed to predominantly central memory. As findings from the alternative gating strategies were conflicting, it was considered whether the percentage representation of each subset within the total $CD4^+$ T cell population was influencing the analysis of the non-responsive phenotype. Therefore, the representation of T_{naive}, T_{cm} and T_{eff} subsets within the total $CD4^+$ T cell population was analysed by flow cytometry (Figure 3.12). Results showed that the T_{naive} cells were the most heavily represented subset, with a median percentage of 60.6% (45.3-65.0 IQR). 30.9% (25.9-65.0 IQR) of the $CD4^+$ population were a T_{cm} phenotype and only 7.9% (5.6-10.6 IQR) were T_{eff} cells.

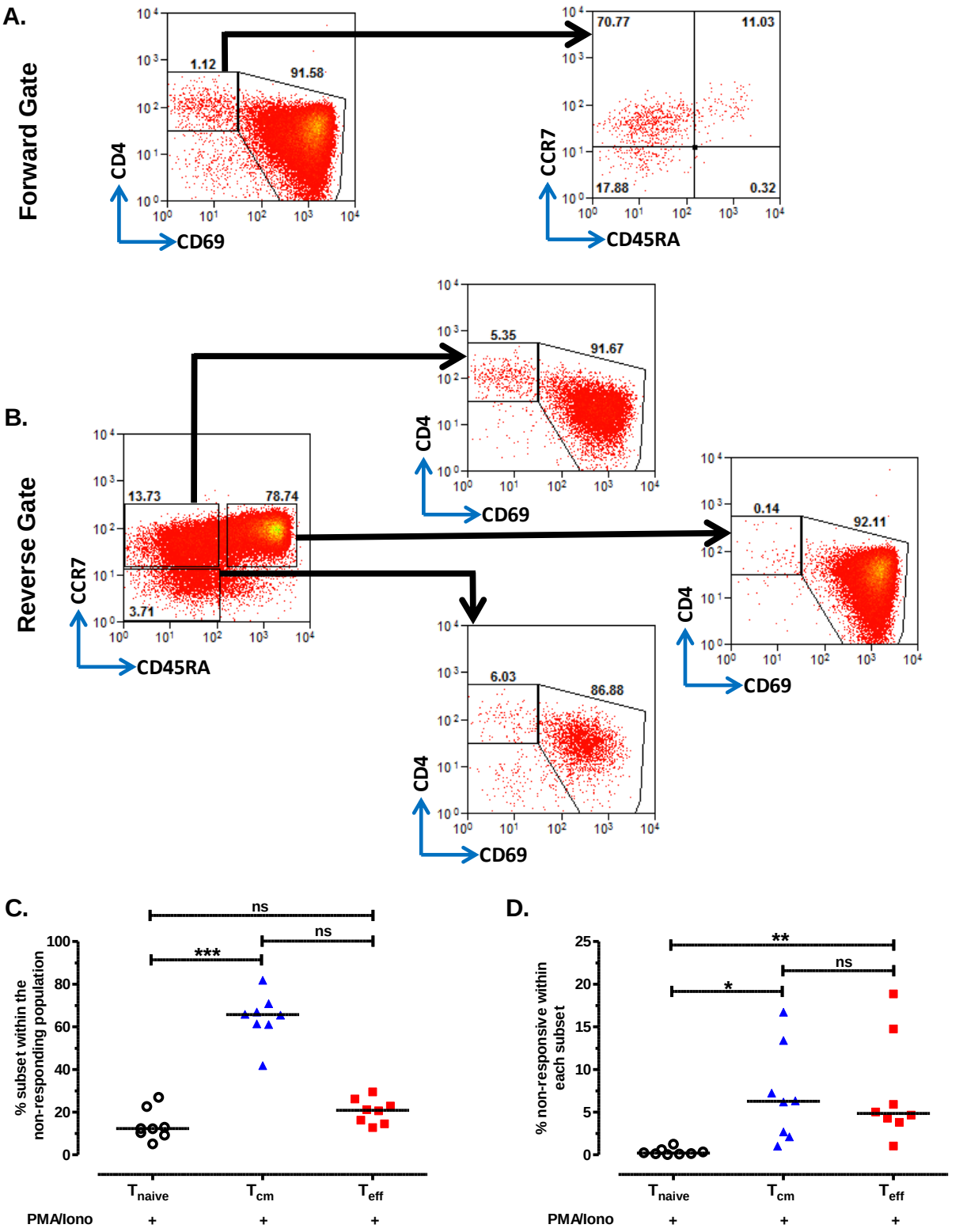

Figure 3.11 Alternative gating strategies for analysis of $CD4^+$ T cells unresponsive to *in vitro* stimulation. Peripheral blood mononuclear cells were stimulated for 6h with PMA/ionomyin and $CD3^+CD8^+CD4^+$ T cells analysed by flow cytometry for absence of CD69 upregulation. **A, C.** Forward gating strategy – analysis of the $CD4^+$ T cell subset distribution with the $CD69^{lo}$ population following stimulation. **B, D.** Reverse gating strategy – identifies the percentage of each $CD4^+$ T cell subset that is $CD69^{lo}$ following stimulation.*p<0.05 **p<0.01, ***p<0.0001, ns=no significance at p<0.05 (Friedman statistical test, followed by Dunn's multiple comparisons analysis). Data was collected from n=8 healthy donors.

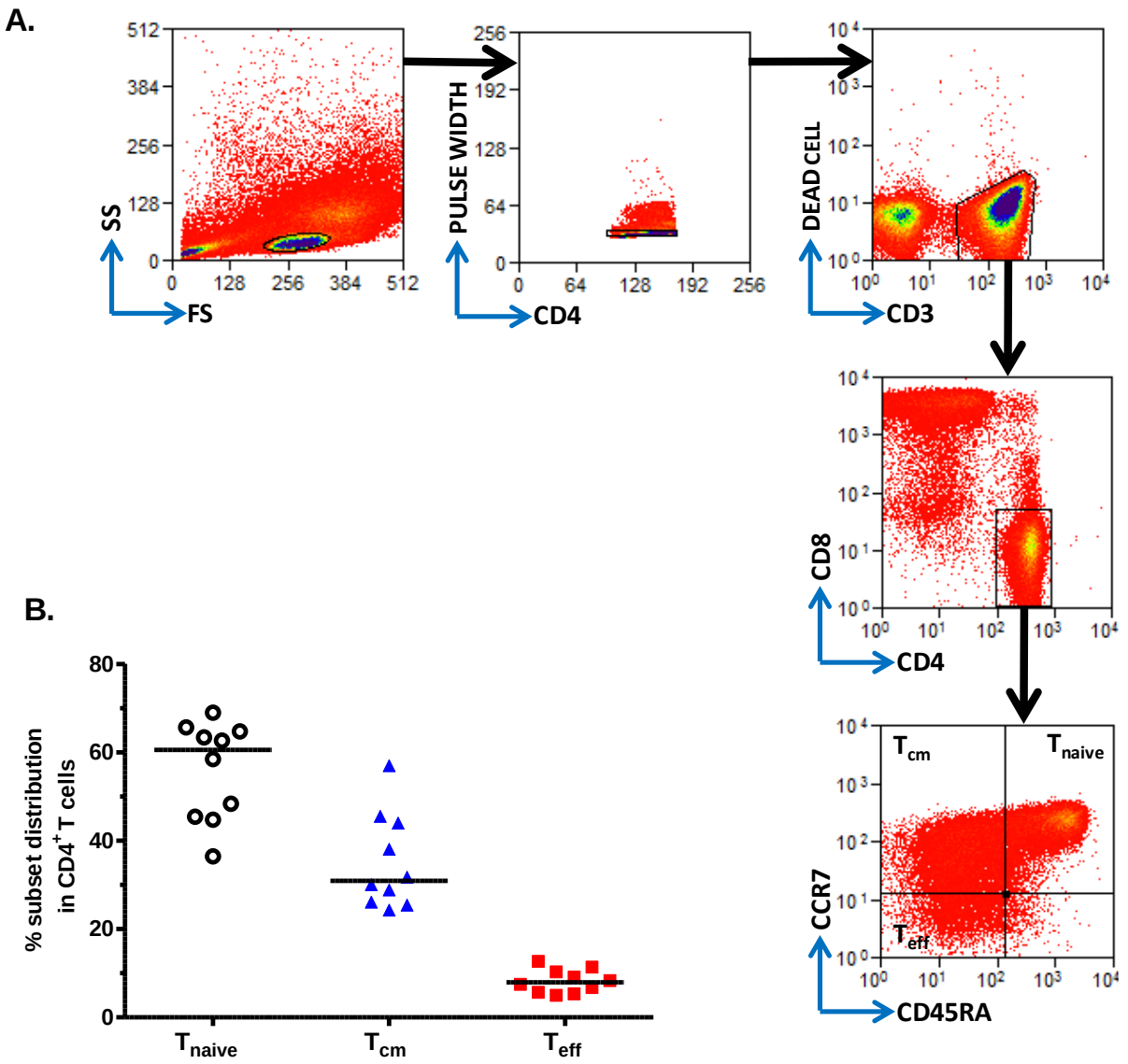

Figure 3.12 Distribution of naïve, central memory and effector memory populations in human peripheral blood CD4$^+$ T cells. Peripheral blood mononuclear cells were rested for 6h in complete medium, stained for lymphocyte cell surface markers and analysed by flow cytometry. **A.** Gating strategy for identification of CD4$^+$ T cell populations. CD4$^+$ T cells were defined by CD3$^+$CD8$^-$CD4$^+$ expression by cells within a live lymphocyte gate (doublets and dead cells were excluded from the analysis). Expression of CD45RA and CCR7 were used to determine subset distribution within the CD4 gate. **B.** Median percentage frequency of naive (T_{naive} (CCR7+CD45RA$^+$)), central memory (T_{cm} (CCR7$^+$CD45RA$^-$)), and effector memory (T_{eff} (CCR7$^-$CD45RA$^-$)) CD4 T cells in healthy blood donors. Data is representative of n=10 healthy donors measured independently.

As the non-responsive population are shown to be a memory phenotype it became clear that when applying the 'forward gating' phenotypic analysis it appeared that this population was predominated by T_{cm} cells simply because T_{cm} predominate the memory pool in the blood. Based on these findings the 'reverse gating' strategy is the more appropriate analysis, as measuring the prevalence of non-responsive cells within each subset removes any bias due to each subset's overall representation. Together these findings in PBMC cultures indicate that the non-responsive population is a memory $CD45RA^{-}CCR7^{+/-}$ phenotype, as both T_{cm} and T_{eff} subsets show similar proportions of non-responsive cells post stimulation.

3.7.2 Refinement of the phenotypic analysis of non-responsive $CD4^{+}$ T cells through pre-stimulation fluorescence activated cell sorting.

By gating on $CD4^{+}$ T cell subsets in PBMC cultures there was a possibility that the surface marker expression of the cells could change during the culture period or be influenced by the stimulation. Additionally, the non-responsive population could potentially be influenced by other non-$CD4^{+}$ T cells or any soluble mediators secreted into the culture milieu. To alleviate these factors a fluorescence activated cell sorting (FACS) approach was used to purify T_{naive}, T_{cm}, and T_{eff} populations from PBMC prior to the 6h stimulation process. For these experiments PBMC were separated by FACS according to the gating strategy shown in Figure 3.13A. Following FACS the T_{naive}, T_{cm}, and T_{eff} populations were stimulated for 6h with PMA/ionomycin and analysed for the percentage non-responsive cells (Figure 3.13B). As anticipated the proportion of the T_{naive} cultures that failed to downregulate $CD4^{+}$ and upregulate CD69 was minimal (median 0.3% 0.1-0.4 IQR) as shown in Figure 3.13C. In contrast to results produced in PBMC cultures the frequency of the sorted T_{cm} that did not respond was also low (median 2.5% 0.6-5.7 IQR). In addition, results indicated that the proportion of non-responsive T_{eff} cells was significantly higher than in the T_{cm} subset (median 34.2% 16.9-47.4 IQR). Although there was notable variability in the percentage of

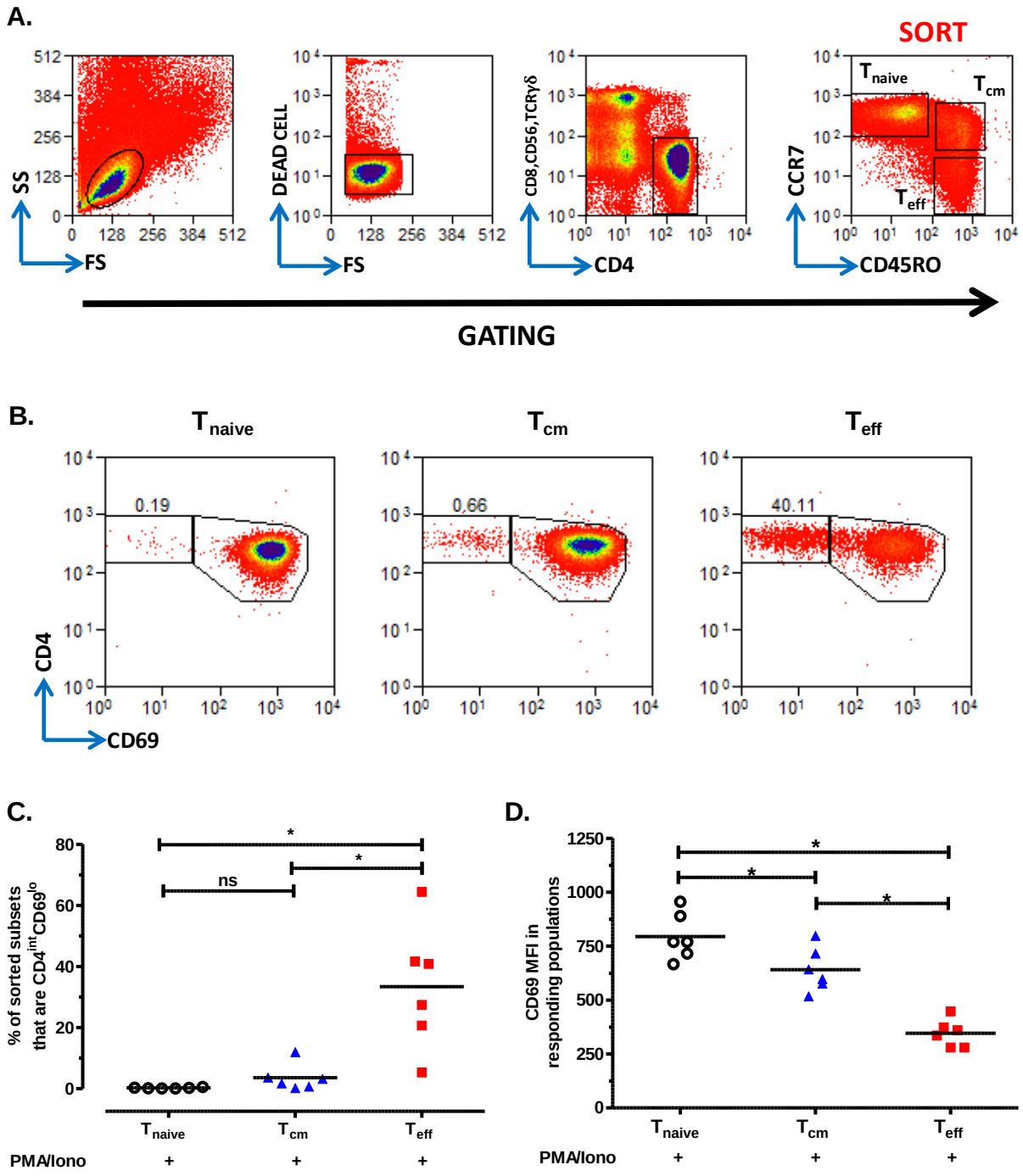

Figure 3.13 Analysis of cell populations unresponsive to stimulation in purified naive, central memory and effector memory CD4$^+$ T cell cultures. Peripheral blood mononuclear cells underwent fluorescence activated cell sorting (FACS) to purify naive (T_{naive} ($CCR7^+CD45RA^+$)), central memory (T_{cm} ($CCR7^+CD45RA^-$)), and effector memory (T_{eff} ($CCR7^-CD45RA^-$)) $CD4^+$ T cells. Purified populations were stimulated for 6h with PMA/Ionomycin and the expression of activation marker CD69.analysed by flow cytometry. **A.** Gating strategy for FACS purification of PBMC. **B.** Flow cytometry plots showing CD69 upregulation in response to PMA/ionomycin from each population. Plot numbers represent the percentage of cells failing to upregulate CD69, which is also presented graphically in **C. D.** The median fluorescence intensity of CD69 expression by those cells responsive to stimulation. **C-D.** ns; no significance at $p<0.05$, *$p<0.05$ (Wilcoxon matched-pairs sign rank test) Data is representative of n=6 healthy donors measured in 3 independent experiments.

non-responsive T_{eff} cells finding from these experiments suggest the non-responsive phenotype are more of a $CCR7^{-}$ T_{eff} phenotype than $CCR7^{+}$ T_{cm} (Figure 3.13C).

As a further analysis of CD69 expression in these sorted populations, the MFI of CD69 in the responding cell fraction was also measured (Figure 3.13B, Figure 3.13D). The responding cells from the sorted T_{naive} cultures displayed the highest CD69 MFI, showing that this population expressed the most receptor on a per cell basis. The expression of CD69 by the responding T_{eff} cells was significantly lower with the T_{cm} responder CD69 MFI measured as an intermediary (Figure 3.13D). This result indicates that upregulation of CD69 following stimulation is progressively reduced as $CD4^{+}$ T cells differentiate.

3.7.3 Analysis of CD62L expression in activated $CD4^{+}$ T cell cultures.

There was some disparity between the memory phenotype of the non-responsive population observed from PBMC cultures (both $CCR7^{+}CD45RA^{-}$ and $CCR7^{-}CD45RA^{-}$) and where subsets were sorted prior to stimulation (predominantly $CCR7^{-}CD45RA^{-}$). Therefore, alternative markers associated with T_{cm} and T_{eff} phenotypes were investigated to further characterise the memory status of non-responsive cells.

Both CCR7 and L-selectin (CD62L) are classically associated with T_{naive} and T_{cm} $CD4^{+}$ T cell populations but are not expressed by the T_{eff} subset[57]. Therefore differential CD62L expression in $CD45RA^{-}$ memory populations was used in conjunction with CCR7 to look for changes in 'responsiveness' between phenotypes. As the ectodomain of CD62L is readily shed in the presence of PMA/ionomycin this posed a problem in terms of analysing the receptor post-stimulation. CD62L ectodomain cleavage requires MMP enzyme activity[376]. Therefore, an attempt was made to prevent shedding in initial experiments through addition of an indirect MMP inhibitor [TAPI-2, Enzo Life Sciences] to PBMC cultures (as described in [377]). However, even at high concentrations of the MMP inhibitor the expression of CD62L by stimulated $CD4^{+}$ T did not match the level seen in unstimulated cultures (data not shown).

Due to the incomplete inhibition of shedding and consideration for the indirect effects of the MMP inhibitor an alternative strategy was approached where memory T cells with differential expression of CD62L were sorted by FACS prior to stimulation (Figure 3.14). $CD4^+$ T_{cm} and T_{eff} (based on a CCR7 and CD45RA definition) were separated into their $CD62L^{hi}$ and $CD62L^{lo}$ compartments (Figure 3.14A). As anticipated the T_{cm} $CD62L^{hi}$ and T_{eff} $CD62L^{lo}$ were the dominant populations in each phenotype. However, small atypical T_{cm} $CD62L^{lo}$ and T_{eff} $CD62L^{hi}$ populations were also identifiable. Interestingly, these cells with an inversed relationship of CCR7/CD62L expression had the highest frequency of non-responsive cells when stimulated with PMA/ionomycin (Figure 3.14B, Figure 3.14C). This trend was reproduced when each population was stimulated with anti-CD3/anti-CD28 Dynabeads®, although here the T_{cm} $CD62L^{lo}$ population showed the greatest percentage non-responsiveness with only a marginal proportion of these cells upregulating CD69 at all (Figure 3.14D, Figure 3.14E). These finding suggest that changes in CD62L expression within $CCR7^+$ and $CCR7^-$ memory populations can predict the absence of CD69 upregulation to an exogenous stimuli. However, this combination of markers alone is insufficient to identify a pure non-responsive population prior to stimulation.

3.7.4 Analysis of CD27 expression as a measure of differentiation status in $CD4^+$ T cell cultures.

As $CD4^+$ T cells differentiate they progressively lose expression of the surface receptor CD27[378,379]. As T_{cm} have a higher CD27 expression than T_{eff} this marker was used to investigate whether the non-responsive $CD4^+$ T cell population represented cells close to becoming terminally differentiated. For these experiments, T_{cm} ($CCR7^+CD45RA^-$) and T_{eff} ($CCR7^-CD45RA^-$) subsets with $CD62L^{hi/lo}$ expression were separated into four populations by FACS as previously described in Figure 3.14A. Each population was cultured for 6h with PMA/ionomycin and the percentage of $CD27^{lo}$ cells measured in the non-responsive and matched responsive groups by flow cytometry (Figure 3.15A, Figure 3.15B).

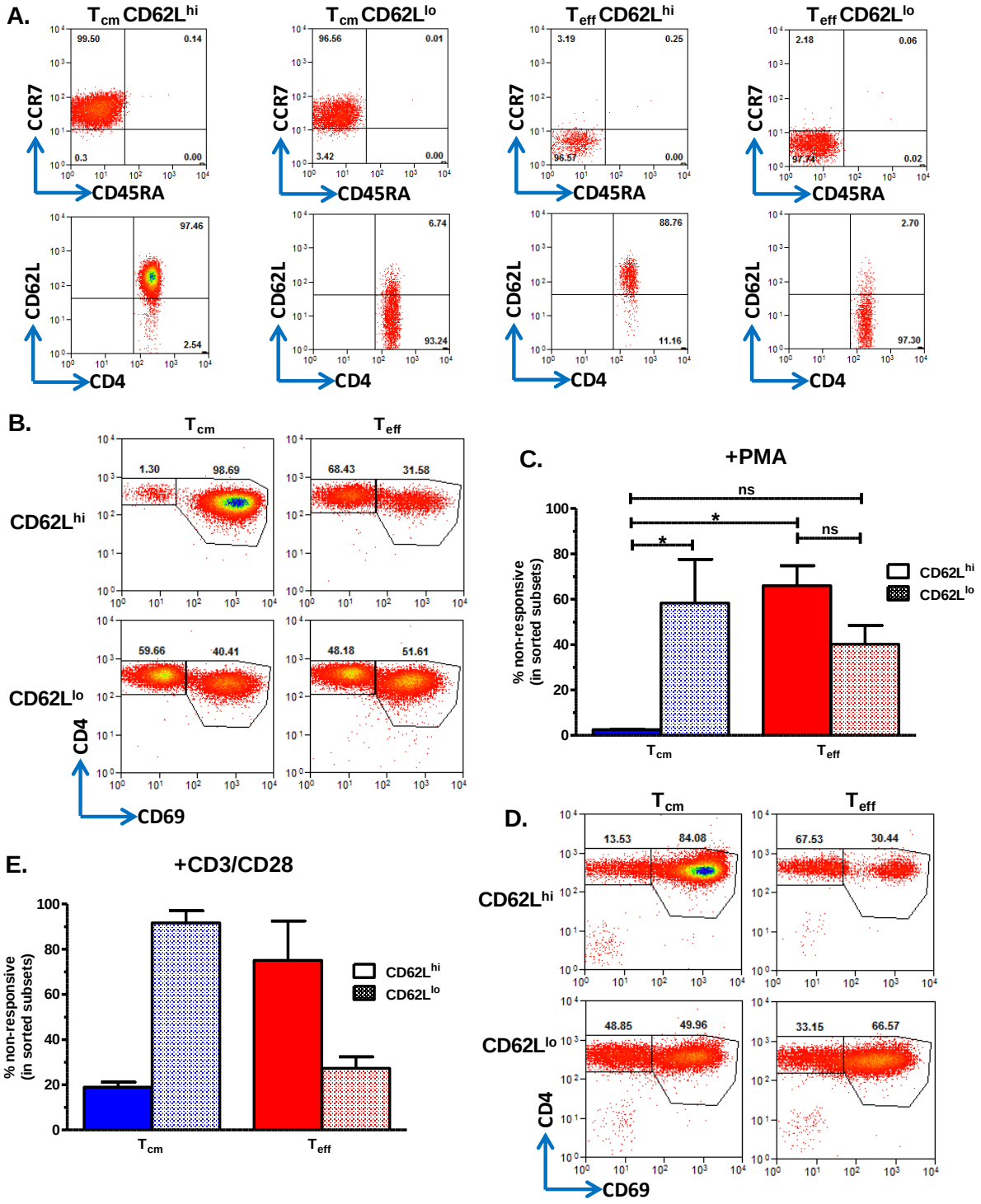

Figure 3.14 Differential CD62L expression may predict unresponsiveness in CD4$^+$ memory T cell populations. Central (CD45RA$^-$CCR7$^+$) and effector (CD45RA$^-$CCR7$^-$) memory CD4$^+$ T cells with high and low CD62L expression were separated by fluorescence activated cells sorting (fraction purities are shown in **A**). Cells were stimulated for 4h with PMA (**B,C**) or CD3/28 beads (**D,E**) and analysed for the absence of CD69 upregulation. **B,D.** Representative flow cytometry plots showing CD69 expression post stimulation. **C,E.** Graphs show the median percentage of unresponsive cells per population. *p<0.05, ns; no significance at p<0.05 (Friedman's statistical test followed by Dunn's multiple comparisons analysis). Data is representative of n=2 (**D,E**) and n=4 (**B,C**) healthy donors in 4 independent experiments.

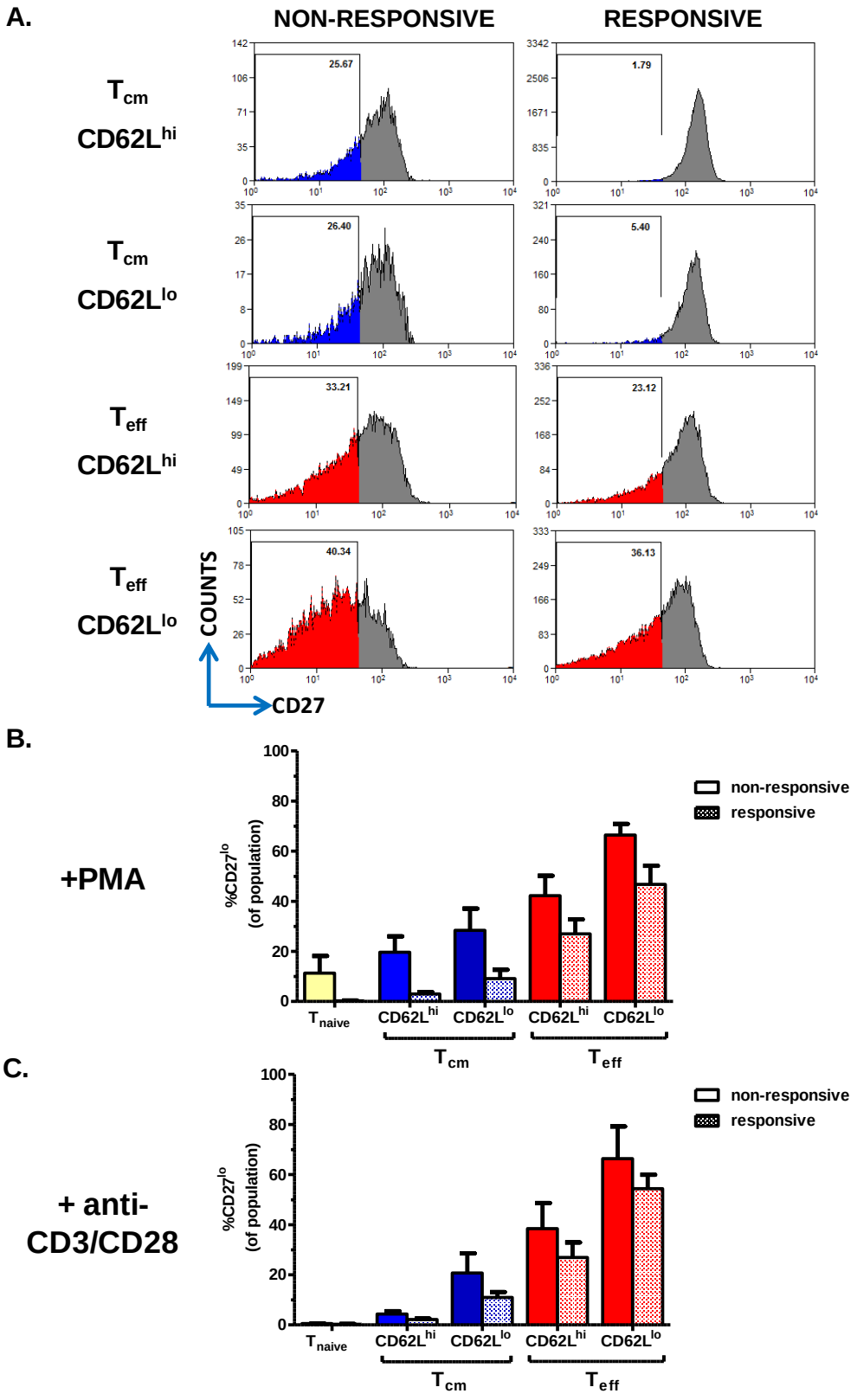

Figure 3.15 The association of CD27 expression and CD69 upregulation following *in vitro* stimulation. Central ($CD45RA^{-}CCR7^{+}$) and effector ($CD45RA^{-}CCR7^{-}$) memory $CD4^{+}$ T cells with high and low CD62L expression were separated by fluorescence activated cells sorting. Populations were stimulated with PMA/Ionomycin or CD3/CD28 beads. **A.** Representative flow cytometry plots showing the percentage of $CD27^{lo}$ cells in populations responsive ($CD4^{hi}CD69^{lo}$) and non-responsive ($CD4^{int}CD69^{hi}$) to stimulation. **B,C.** Graphs shows the median percentage $CD27^{lo}$ population in each subset following PMA **(B)** and CD3/CD28 **(C)** stimulation. Data is representative of n=2-3 healthy donors in 3 independent experiments.

In every sorted subset the percentage of $CD27^{lo}$ cells in the non-responsive fraction was greater than in the corresponding responsive fraction. However, the trend suggested that the frequency of the $CD27^{lo}$ cells correlated with the differentiation status of the population measured (i.e. increasing $CD27^{lo}$ frequency from T_{cm} $CD62L^{hi}$ through to T_{eff} $CD62L^{lo}$), as opposed to differentiating between the non-responsive versus responsive groups specifically (Figure 3.15B). These findings were recapitulated in the same system when PMA/ionomycin stimulation was substituted for anti-CD3/anti-CD28 Dynabeads® activation (Figure 3.15C). Together these findings suggest that expression of CD27 is associated with a particular state of memory and not specifically linked to the non-responsive phenotype.

3.8 The non-responsive $CD4^+$ T cell population does not represent cells recently activated *in vivo*.

It was considered whether the $CD4^{int}CD69^{lo}$ non-responsive population represented memory cells recently activated *in vivo*. PBMC were purified by FACS to separate resting $CD4^+$ T cells ($CD69^{lo}$) from those recently activated ($CD69^{hi}$) (Figure 3.16A). A small but discernible population of recently activated cells were identified but their expression of CD69 was not as high as cells artificially stimulated with PMA (Figure 3.16A, Figure 3.16B). When these cells were removed by FACS a population of non-responsive cells remained, indicating that non-responsive cells are not recently activated *in vivo*. In support of this the resting sorted population significantly upregulated CD69 when stimulated but the CD69 expression of recently activated cells did not change (Figure 3.16B). Therefore, these cells did not fall within the parameters of a $CD4^{int}CD69^{lo}$ gate following stimulation. In addition a substantial proportion of the recently activated cells died during the stimulation assay (Figure 3.13C, Figure 3.16D). The fact that recently activated cells only represent a very small fraction of total $CD4^+$ T cells (<1.2% in these experiments) and the majority of those die during culture (median death 82.0% (76.7-87.4 IQR)) is further evidence against their contribution to the non-responsive population.

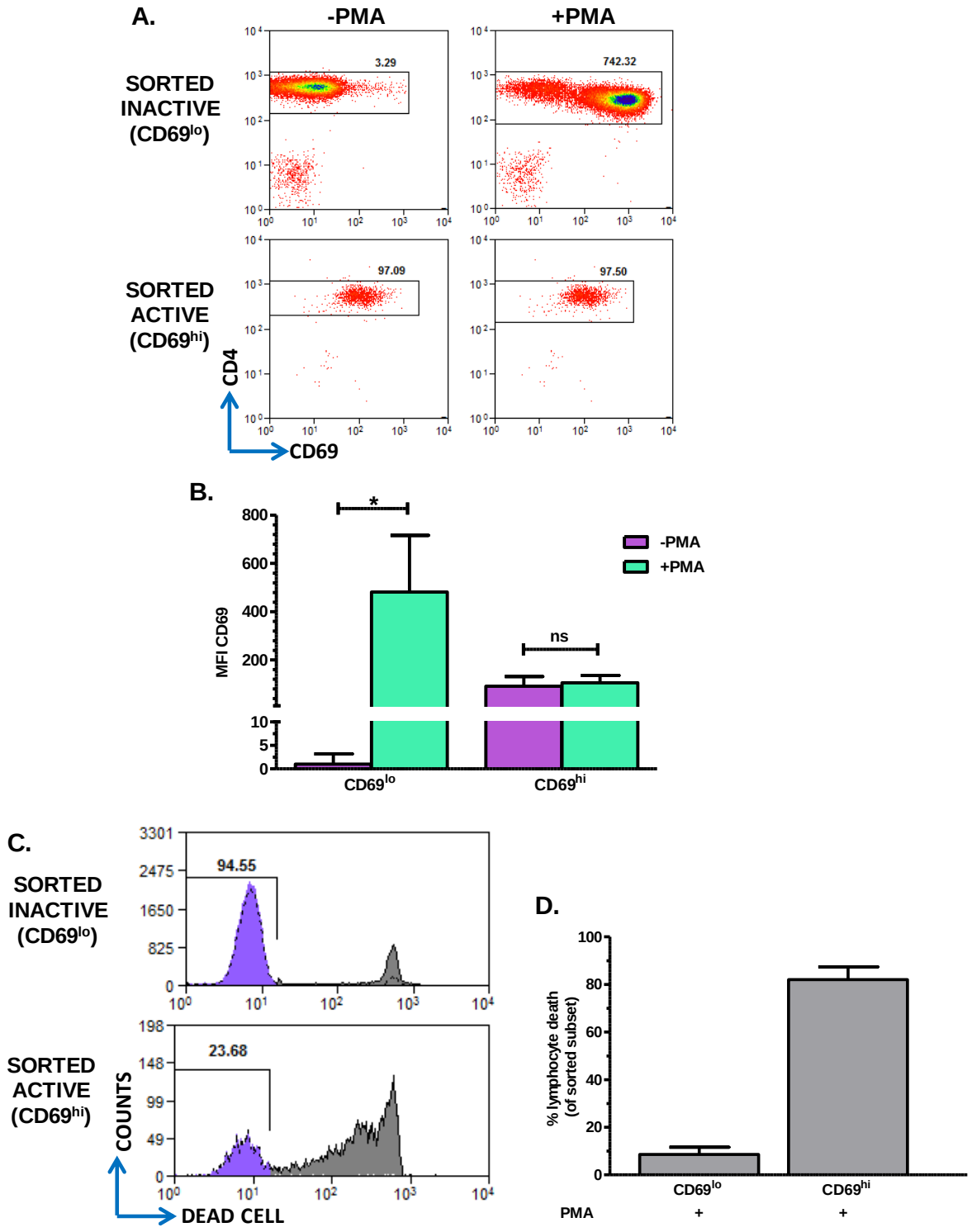

Figure 3.16 Contribution of CD4$^+$ T cells activated *in vivo* to the unresponsive population observed following *in vitro* stimulation. Fluorescence activated cell sorting was used to separate recently activated (CD69^{hi}) CD4$^+$ T cells from those at rest (CD69^{lo})**.** Populations were stimulated for 6h with PMA/Ionomycin and analysed for expression of CD69. **A** Flow cytometry plots showing the median fluorescence intensity (MFI) of sorted CD4$^+$ T cell fractions with and without PMA stimulation (also shown graphically in **B**). **C** Plots show the percentage of surviving cells (purple) in stimulated cell cultures**. D** Graph shows the mean percentage of cell death of each culture. *p<0.05, ns; no significance at p<0.05 (Mann Whitney U statistical test. Data is representative of n=2-3 healthy donors in 2 independent experiments).

Never-the-less for subsequent experiments where *in vivo* activated cells were observed in unstimulated cultures they were excluded from the $CD69^{lo}$ gate to make certain that they did not contribute to subsequent analysis.

3.9 The propensity of non-responsive and responsive $CD4^+$ T cells to undergo apoptosis

As the non-responsive $CD4^+$ T cell population could not be maintained in cultures over 12h the population's viability and resistance to apoptosis was reassessed. PBMC were cultured for 6h with PMA/ionomycin and the $CD4^+$ T cell population analysed for surface expression of phosphatidylserine residues. Annexin V binds to these residues and can be measured by flow cytometry in conjunction with a cell membrane permeability dye[380] (Sytox® blue). Therefore, combinatorial expression of Annexin V and Sytox is able to distinguish early apoptotic ($AnnexinV^+Sytox^-$) and late apoptotic/necrotic ($AnnexinV^+Sytox^+$) cells from the viable population.

As anticipated there was very little apoptosis in the 6h cultures without PMA/ionomycin (Figure 3.17A) but strong evidence of apoptosis in the simulated cultures (Figure 3.17B, Figure 3.17C). The $CD4^{int}CD69^{lo}$ non-responsive population had a greater percentage frequency in early apoptosis than their responding $CD4^{lo}CD69^{hi}$ counterparts but this was not statistically significant (Figure 3.17C). In contrast, there was significantly more late apoptosis/necrosis within the non-responsive population when compared to responsive cells as represented by median (IQR) values of 13.0% (5.8-22.9) and 3.3% (0.7-7.9) respectively (Figure 3.17B, Figure 3.17C). This trend suggests that although the majority of non-responsive cells are viable they are susceptible to apoptosis and have a lower survival rate than responsive $CD4^+$ T cells.

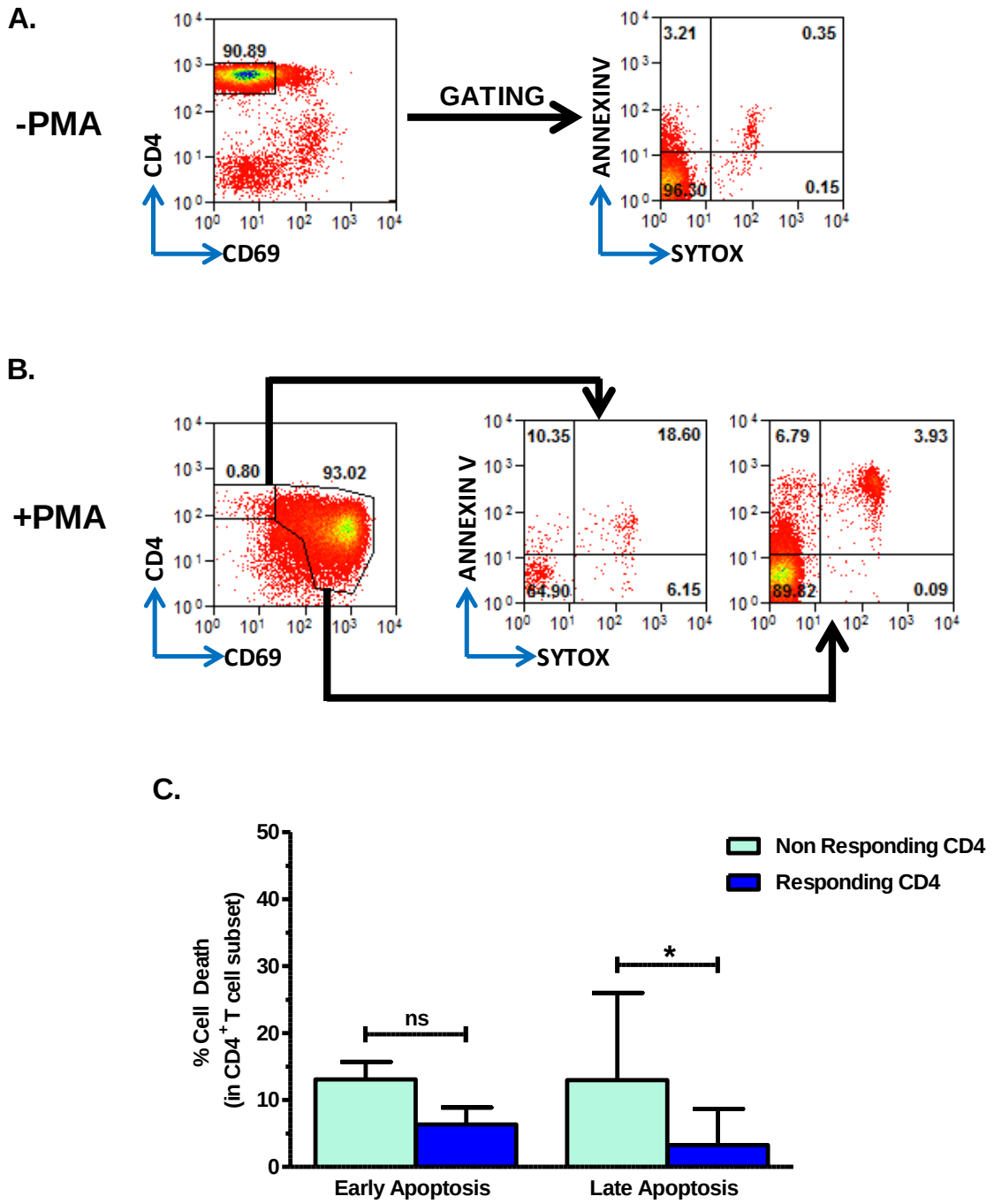

Figure 3.17 Analysis of apoptosis markers expressed by $CD4^+$ T cells following PMA/Ionomycin stimulation. PBMC were cultured for 6h ± PMA/ionomycin stimulation. $CD4^+$ T cells (defined by $CD3^+CD8^-CD4^+$ expression) activated by PMA stimulation ($CD4^{lo}CD69^{hi}$), and the population which failed to respond ($CD4^{int}CD69^{lo}$) were analysed for expression of apoptotic markers. **A.** Representative plots showing $CD4^+$ T cells in early ($AnnexinV^+Sytox^-$) and late ($AnnexinV^+Sytox^+$) apoptosis in unstimulated cultures. **B.** Evidence of early and late apoptotic marker expression by unresponsive and responsive $CD4^+$ T cells following stimulation. **C.** Graph shows the median percentage of unresponsive and responsive $CD4^+$ T cells in early and late apoptosis. *$p<0.05$ depicts statistical significance ns; no significance at $p<0.05$ (Friedman's statistical test followed by Dunn's multiple comparisons analysis). Data is representative of n=4 healthy donors measured in 2 experiments.

3.10 Investigation of the lymphocyte lineage of the non-responsive $CD4^+$ T cell population.

3.10.1 Is the non-responsive $CD4^+$ T cell population derived from a non-T helper cell lineage?

To ensure that the non-responsive population represented classical T helper cells it was assessed whether they expressed markers associated with three less prevalent cell types. The three non-classical T cell lineages chosen were gamma delta T cells, natural killer like T cells (NKT-like) and $CD4^+CD8^+$ double positive T cells that express both TCR co-receptors. To represent each of these lineages in the analysis PBMC were additionally stained for TCRγδ, CD56 and CD8. As the question was not concerned with which one of these lineages the non-responders might be TCRγδ, CD56 and CD8 were stained using the same fluorochrome. Cells with a positive signal in this channel were collectively termed Lin^{+ve} and analysis of this mixed group was performed alongside T_{cm} and T_{eff} subsets of the 'Lin^{-ve}' T_{helper} population (gating strategy is shown in Fig3.18A).

The aim of initial experiments was to calculate the maximum potential contribution of Lin^{+ve} cells to the non-responsive population based on their frequency and subset distribution in the blood. Results from flow cytometry performed on unstimulated PBMC cultures indicated that collectively Lin^{+ve} cells represented less than 2% of $CD4^+$ T cells (median 1.8% (1.1-2.2 IQR)) (Figure 3.18B). This small mixed population was distributed more evenly across the T_{naive}, T_{cm}, and T_{eff} subsets than conventional TCRαβ T_{helper} cells. However, the T_{naive}/T_{memory} ratio was inverted with the most Lin^{+ve} cells being an T_{eff} phenotype (median 39.8% (31.5-43.7 IQR)) (Figure 3.18B). Using the data on the percentage frequency and subset distribution of the Lin^{+ve} cells it was estimated what their maximum contribution to the non-responsive population would be if every cell in each subset did not respond (Figure 3.18D). This theoretical data was superimposed on matching data showing the actual percentage of each subset that did not respond in these experiments (Figure 3.18D).

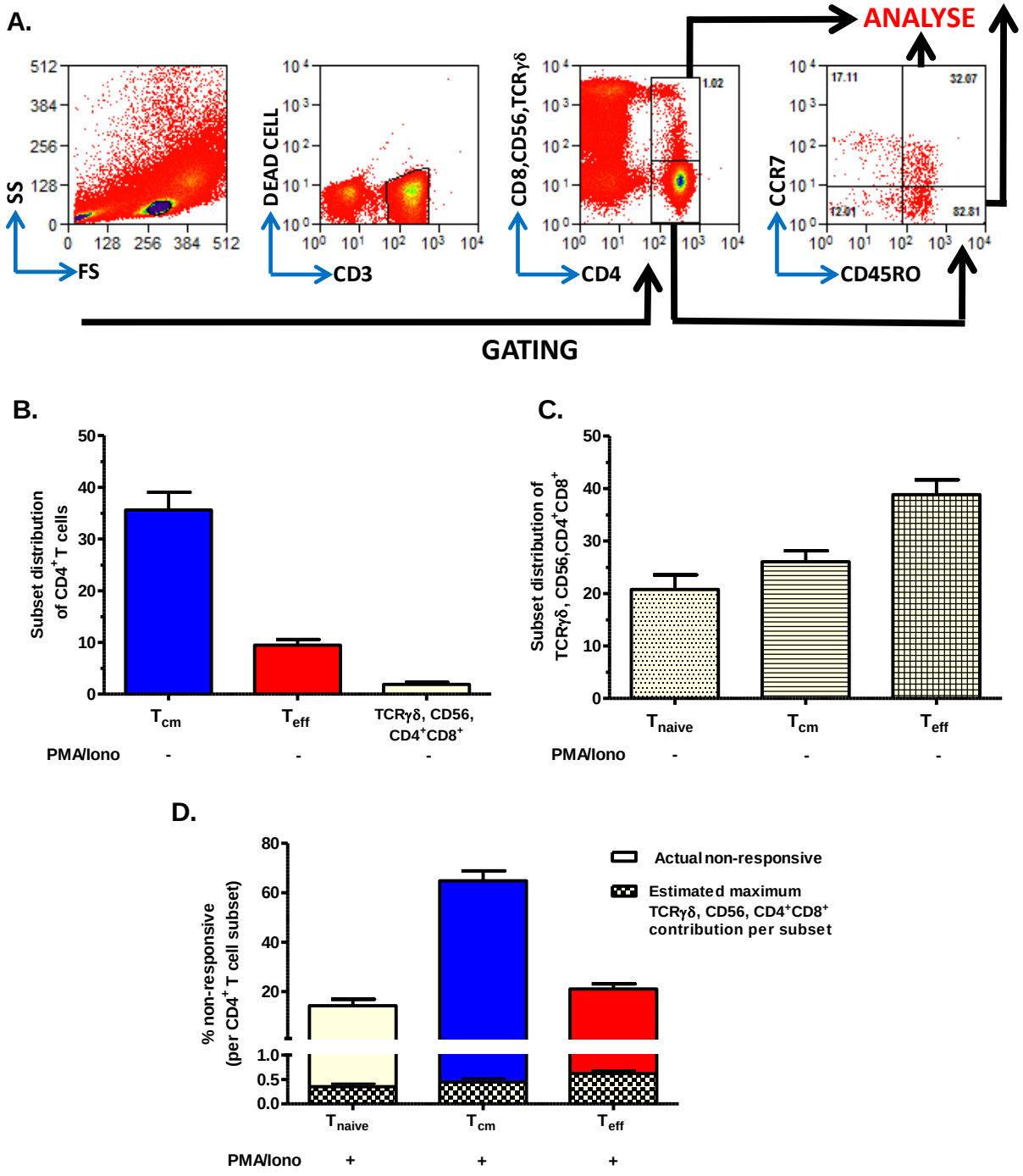

Figure 3.18 Investigation of the theoretical contribution of non-T helper CD4$^+$ lineages to the non-responsive CD4$^+$ T cell population. Flow cytometry was used to quantify the proportion of CD4$^+$ T cells in peripheral blood that collectively expressed either CD56, TCRγδ or CD8, in order to estimate their potential contribution to the previously identified non-responsive population (gating strategy is shown in **A.**). **B.** The median frequency of this mixed population was compared to the proportion of CD4$^+$ T cells with a central memory (T_{cm}; CCR7$^+$CD45RO$^+$), and effector memory (T_{eff}; CCR7$^-$CD45RO$^+$) phenotype. **C.** The percentage distribution T_{naive} (CCR7+CD45RO$^-$), central memory T_{cm} (CCR7$^+$CD45RA$^-$), and effector memory T_{eff} (CCR7$^-$CD45RA$^-$) within the mixed CD56/TCRγδ/CD8 population was also quantified. **D.** Graph represents the theoretical maximum contribution of mixed lineage cells to each non-responsive fraction if every cell failed to upregulate CD69 when stimulated. Calculation is based on data representative of n=6 healthy donors measured in 3 independent experiments.

The frequency of the mixed Lin^{+ve} population suggests that these cells would not substantially contribute to the non-responsive fraction of each memory subset even if every Lin^{+ve} cell was hyporesponsive.

To add more direct evidence to this finding Lin^{+ve} cells were purified by FACS alongside conventional T_{cm} and T_{eff} memory $CD4^+$ T cells (for gating strategy see Figure 3.19A). Each population was cultured with and without PMA/ionomycin and the percentage of non-responsive cells measured by flow cytometry (Figure 3.19B, Figure 3.19C). Stimulation caused the expression of the Lin^{+ve} markers to downregulate on some cells of the sorted fraction (Figure 3.19B middle panel) but it was impossible to identify which of the three markers was responsible. The proportion of the sorted Lin^{+ve} cells with the $CD4^{int}CD69^{lo}$ non-responsive phenotype was similar to the sorted conventional T_{eff} population, with median values measured at 26.8% (18.7-38.1 IQR) and 26.8% (5.5-69.1 IQR) respectively. Despite this the majority of the Lin^+ population did respond which implies their contribution to the non-responsive population was even lower than was initially estimated. In addition, PMA/ionomycin induced cell death was substantially greater in the Lin^+ population than other subsets, further indicating that these cells cannot substantially contribute to the non-responsive phenotype (Figure 3.19D).

3.10.2 Do non-responsive $CD4^+$ T cells display characteristics associated with a regulatory T cell phenotype?

It was investigated whether the non-responsive population had a T_{reg} phenotype by separating T_{reg} from non-T_{reg} then examining their responsiveness to PMA/ionomycin. In initial experiments, MACS technology (Miltenyi Biotech) was used to purify $CD4^+$ T cells and then separate this population into T_{reg} and non-T_{reg} components based on expression of CD25. The percentage purity of the $CD4^+$ isolation and the distribution of T_{reg} within that population was measured by flow cytometry (Figure 3.20A left panel). In the second MACS step $CD25^{int}$ cells (non-T_{reg}) were depleted of $CD25^{hi}$ (T_{reg}) cells through a negative selection process and

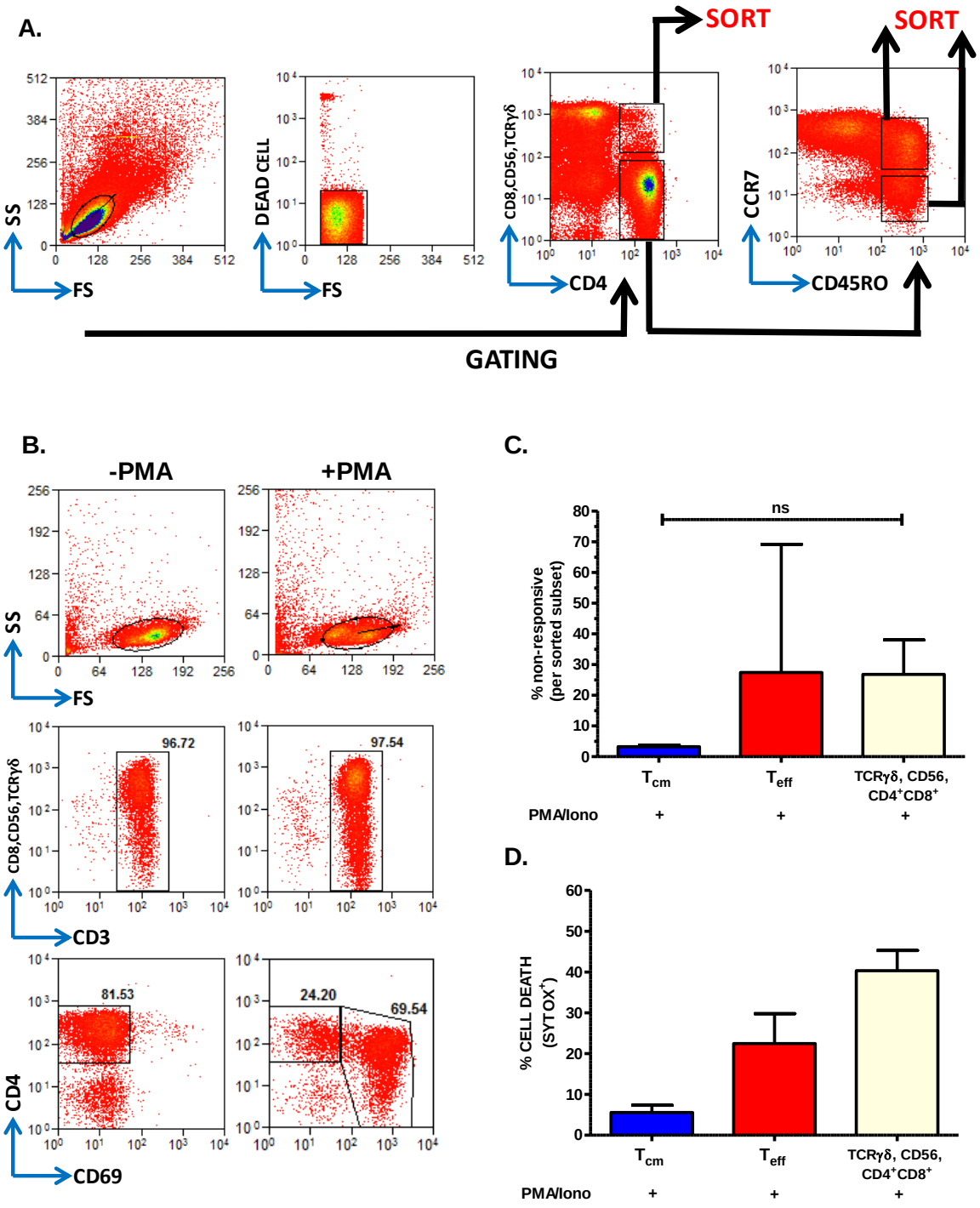

Figure 3.19 Expression of CD69 by non T helper CD4$^+$ lineages following PMA/Ionomycin stimulation. Fluorescence activated cell sorting was used to purify a mixed CD4$^+$ non-T helper cell population (CD56/TCRγδ/CD8) and two T helper memory subsets (Gating shown in **A**). **B.** The mixed lineage population was cultured for 6h ± PMA and analysed for expression of CD3, CD4 and CD69. **C.** The percentage of cells unresponsive to stimulation was compared to that observed in T helper memory subsets. **D.** The cell death in stimulated cultures was measured by the percentage of CD3$^+$ cells that were positive for the dead cell dye sytox. Data is representative of the median and IQR values from n=2-3 healthy donors measured across 2 experiments. ns = no significance (Friedman statistical test, followed by Dunn's multiple comparisons analysis).

the purity of these fractions was measured (Figure 3.20A right panel). $CD25^{hi}$ alone is an incomplete definition of a T_{reg} population and this was reflected in the poor purities achieved through the second separation. Although there was approximately a five-fold enrichment of T_{reg} in the $CD25^{hi}$ fraction based on a $CD25^{hi}CD127^{lo}$ definition there was 70% contamination with non-T_{reg} $CD4^+$ T cells. The depletion of T_{reg} from the non-T_{reg} fraction was also poor (Figure 3.20A right panel). Never-the-less, samples from the total $CD4^+$ isolation along with the T_{reg} and T_{reg}-depleted fractions were stimulated with PMA/ionomyin and analysed for the presence of the non-responsive population. The T_{reg} population was found to have more non-responsive cells than the T_{reg}-depleted fraction (Figure 3.20B, Figure 3.20C). Reciprocally, removal of T_{reg} caused a small reduction of non-responsive cells in the T_{reg}-depleted fraction when compared to total $CD4^+$ population (Figure 3.20B, Figure 3.20C). This data suggests that T_{reg} which fail to upregulate CD69 may significantly contribute to the non-responsive population. Despite such findings it was noted that the majority of T_{reg} upregulate CD69 readily. Therefore if T_{reg} do contribute to the non-responsive population it may be a distinct sub-population T_{reg} as opposed to the population as a whole.

Based on the significance of IL-2 in T_{reg} function and maintenance it was then questioned whether addition of exogenous IL-2 cytokine to T_{reg} cultures would perturb the non-responsive population. Recombinant IL-2 was added to the total $CD4^+$, T_{reg} and T_{reg}-depleted cultures at the beginning of each stimulation assay. It was found that addition of IL-2 had no effect on the non-responsive population in any of the cultures (Figure 3.20D). This finding suggests that lack of CD69 upregulation is not related to IL-2 deficiency in the culture milieu and consequential insufficient signalling through the IL-2 pathway.

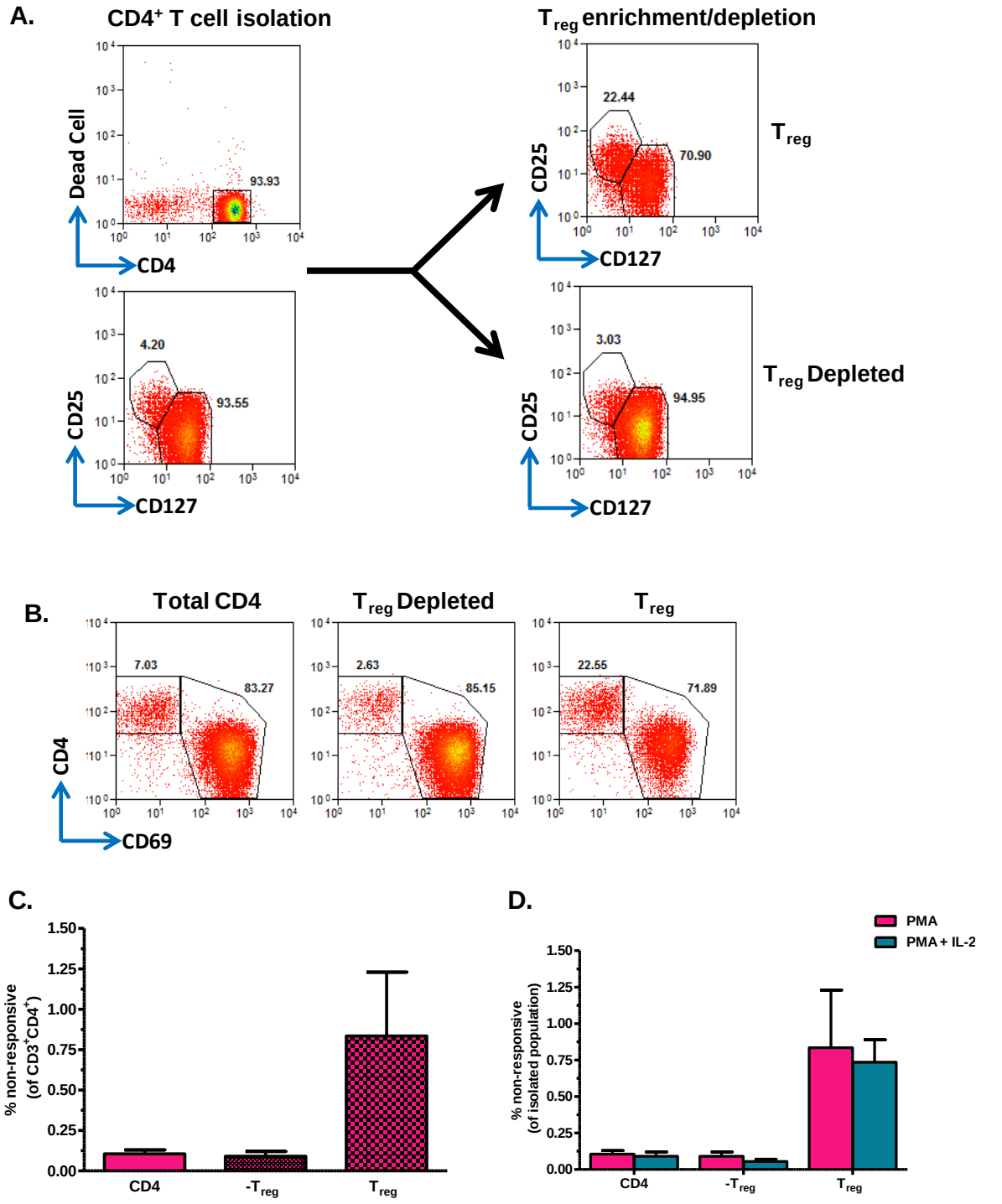

Figure 3.20 CD69 expression by Treg and non-Treg CD4$^+$ T cell populations in response to *in vitro* stimulation. CD4$^+$ T cells were isolated from PBMC and then separated into T_{reg} (CD25^{hi}) and non-T_{reg} (CD25^{int}) compartments in a two-step magnetic activated cell sorting process. Populations were stimulated for 6h with PMA/ionomycin ± the cytokine IL-2, then analysed for the absence of CD69 upregulation. **A.** Representative flow cytometry plots showing purity of the CD4$^+$ isolation and T_{reg}/non-T_{reg} separation based on a CD25 and CD127 gating definition. **B.** Example plots showing CD4^{int}CD69^{lo} and CD4^{lo}CD69^{hi} populations in each subset. **C.** The median percentage non-responsive cells (CD4^{int}CD69^{lo}) in each subset and the interquartile range. **D.** The effect of IL-2 addition on lack of CD69 upregulation in stimulated cultures. Data is representative of n=2 healthy donors measured independently.

Although informative these findings were attained on a background of poor $CD4^+$ T_{reg} and non-T_{reg} purities using MACS separation. In the following experiments this was substituted for FACS to give a more complete T_{reg} definition using both CD25 and CD127 (for gating strategy see Figure 3.21A). As mainly cells within the memory $CD4^+$ T cell compartment contributed to the non-responsive population only T_{cm} and T_{eff} populations were separated into their T_{reg} and non-T_{reg} constituents. These four FACS-separated populations were cultured for 6h with PMA/ionomycin and the percentage of non-responsive cells measured by flow cytometry (Figure 3.21B, 3.21C). Consistent with other experiments the frequency of non-responsive cells was considerably higher than when the same population was analysed by gating from a PBMC culture. Results indicated that the T_{eff} T_{reg}-depleted non-responsive population was considerably more prevalent than in corresponding T_{cm} cultures (Figure 3.21C). The T_{reg} cultures from both subsets had a comparable frequency of non-responsive cells that were more prevalent than in subset-matched non-T_{reg} assays. The MFI of CD69 in the responding population ($CD69^{hi}$) of each fraction was also measured and indicated that responding T_{reg} had lower CD69 expression than their non-T_{reg} counterparts in both the T_{cm} and T_{eff} subsets. This shows that T_{reg} do not upregulate CD69 in response to PMA/ionomycin to the same extent as non-T_{reg} cells and supports initial findings that T_{reg} contribute to the non-responsive population.

3.11 Characteristics associated with hyporesponsiveness in the non-responsive $CD4^+$ T cell population.

3.11.1 Expression of PD-1 by stimulated $CD4^+$ T cell subsets.

Up to this point no combination of T cell homing receptors, indicators of differentiation status or lineage markers measured could define the non-responsive population specifically. With reference to their lack of activation it was considered whether these cells might have characteristics consistent with T cell exhaustion. PD-1 expression is associated with T cell exhaustion in the context of chronic overstimulation, such as in the tumour microenvironment

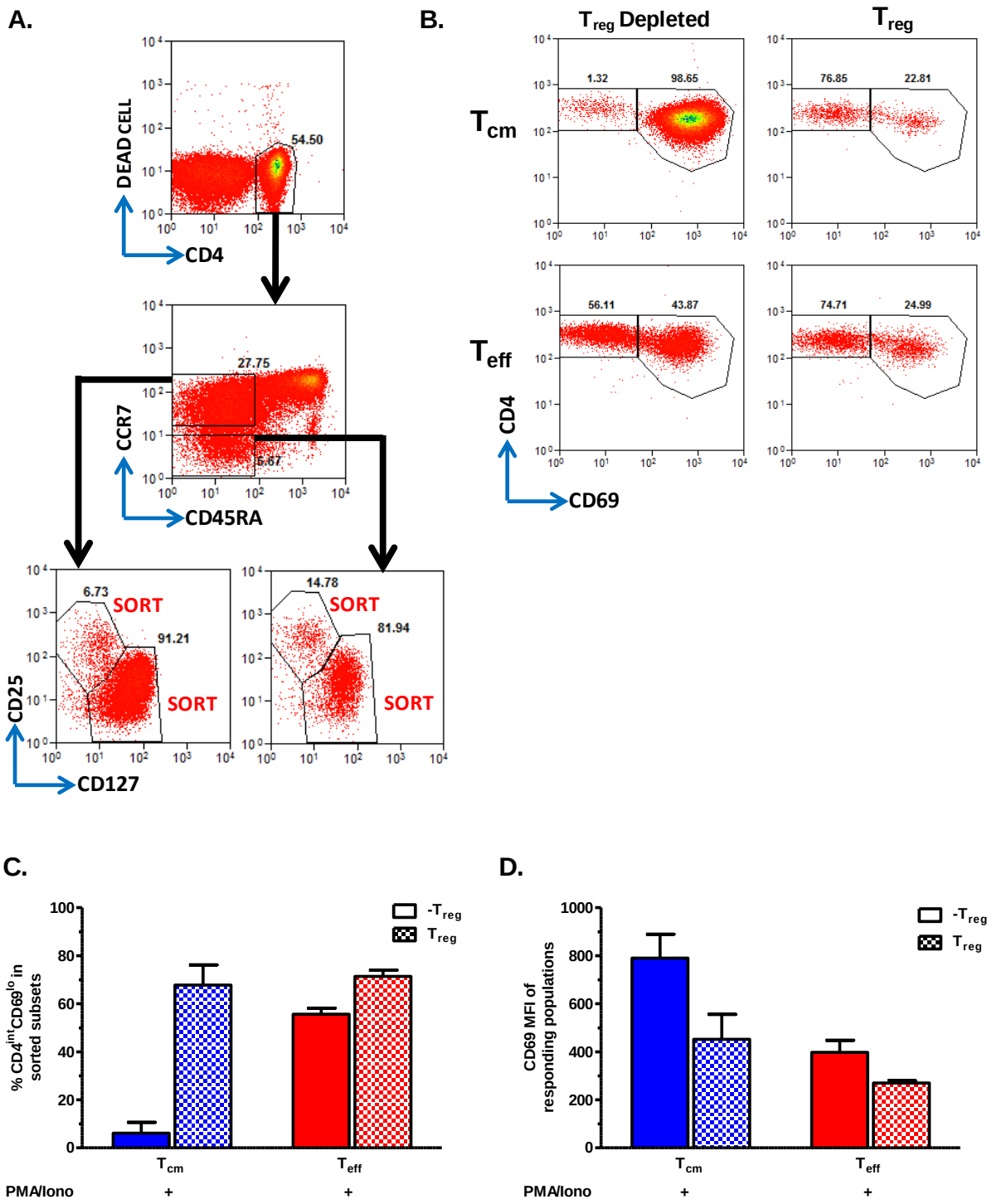

Figure 3.21 Analysis of an unresponsive phenotype in regulatory verses non-regulatory CD4$^+$ T cell subsets. T_{reg} ($CD25^{hi}CD127^{lo}$) and non-T_{reg} ($CD25^{int}CD127^{int}$) populations in central and effector memory $CD4^+$ T cell subsets were purified by fluorescence activated cell sorting (Gating is shown in **A.**). The four populations were cultured for 6h with PMA/ionomycin and analysed for the absence of CD69 upregulation. **B.** Representative flow cytometry plots showing the proportion of each population which responded to the stimulation ($CD69^{hi}$) and that failed to upregulate CD69. **C.** Graphical representation of the percentage of each sorted subset that failed to upregulate CD69. **D.** The CD69 median fluorescence intensity (MFI) of cells responsive to stimulation ($CD69^{hi}$). Data representative of n=2 healthy donors in n=1 experiment.

where engagement with PD-L1 can render cells hyporesponsive[196,197]. Therefore, PD-1 expression was measured by flow cytometry as a candidate marker for the non-responsive phenotype. To establish a baseline of PD-1 expression by $CD4^+$ T cells flow cytometry was performed on freshly isolated PBMC cultures gated on $CD3^+CD8^-CD4^+$ lymphocytes (Figure 3.22A, Figure 3.22B). The vast majority of the T_{naive} $CD4^+$ subset did not express PD-1 but in the memory ($CD45RO^+$) subset there was more varied expression of the receptor. As for memory cells there was no clear definition between PD-1^{lo} and PD-1^{hi} populations a gating threshold was set where PD-1^{hi} expression was defined as staining intensity above the level of the T_{naive} population. Although significantly more memory cells were PD-1^{hi} (38.2% (37.4-51.3) (median and IQR)) it was noted that the MFI in the PD-1^{lo} fraction was slightly elevated compared to the T_{naive} population. This may indicate that all memory $CD4^+$ T cells express PD-1 to a varying degree and the increase in its expression is progressive rather than phasic.

It was then investigated whether PD-1^{hi} memory T cells less readily downregulated $CD4^+$ and upregulated CD69 than their PD-1^{lo} counterparts following PMA/ionomycin treatment. PBMC cultures were stimulated and the PD-1^{lo} and PD-1^{hi} memory T cell populations examined for the percentage of unresponsive cells. T_{naive} cells which upregulate CD69 readily were included in the analysis as an internal control for the stimulation (Figure 3.22C, Figure 3.22D). As expected both memory populations had significantly more non-responsive cells than the control naïve subset. However, despite a slight increase in the non-responsive phenotype in the PD-1^{hi} fraction this was not statistically significant compared with PD-1^{lo} cells (Figure 3.22C, Figure 3.22D).

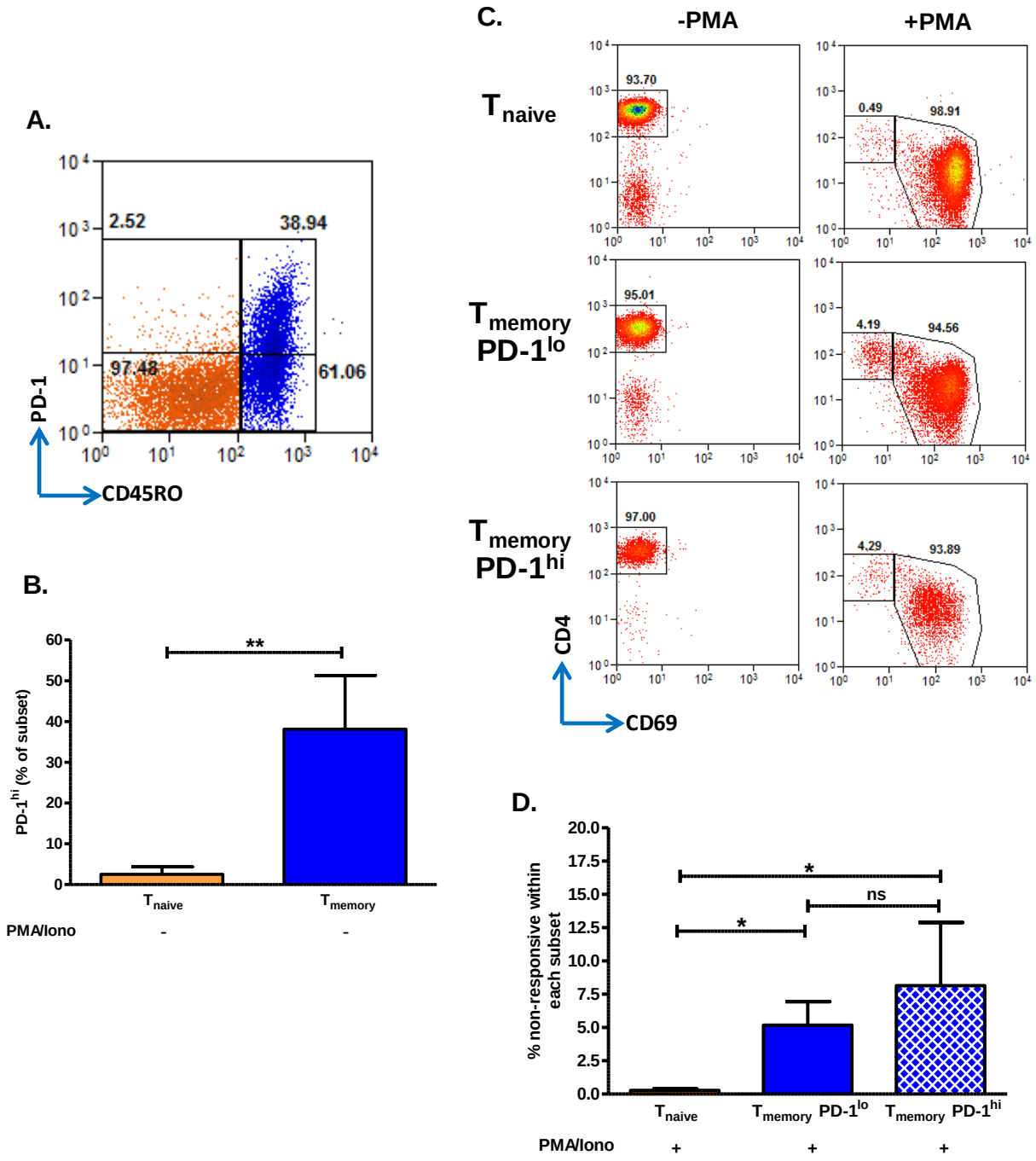

Figure 3.22 PD-1 expression by CD4$^+$ T cell subsets and the effect of differential expression on T cell activation. CD4$^+$ T cells from PBMC cultures were analysed for expression of PD-1 by flow cytometry. Additionally, cultures were stimulated for 6h with PMA/Ionomycin and upregulation of CD69 was measured. **A.** Representative flow cytometry plot showing PD-1 expression by naïve (orange) and memory (blue) CD3$^+$CD8$^-$CD4$^+$ T cell subsets in freshly isolated PBMC samples. Numbers represent the percentage of PD-1^{hi} and PD-1^{lo} cells per individual subset. **B.** Graph shows the median percentage of PD-1^{hi} cells in each subset. Error bars represent the IQR. **C.** Expression of CD69 in naïve, and PD-1$^{hi/lo}$ memory T cells ± stimulation. **D.** The percentage of subsets identified in in **C.** that fail to upregulate CD69 following stimulation. ns= no significance at $p<0.05$, *$p<0.05$ (Friedman statistical test followed with Dunn's multiple comparison analysis). **$p<0.01$ (Mann Whitney U statistical test). Data is representative of n=5-6 healthy individuals measured across 3 experiments.

As work in PBMC cultures suggested that PD-1 status is not related to non-responsiveness an alternative approach using FACS was applied to substantiate these observations (Figure 3.23). T_{cm} and T_{eff} $CD4^+$ T cell subsets were separated into their PD-1^{lo} and PD-1^{hi} fractions by FACS (for gating strategy see Figure 3.23A).Each population was stimulated for 6h with PMA/ionomycin and analysed for the percentage of $CD4^{int}CD69^{lo}$ non-responsive cells (Figure 2.23B, Figure 2.23C). In the T_{cm} sorted subsets there were more non-responsive cells in the PD-1^{hi} fraction than in the PD-1^{lo} culture. In contrast, in the T_{eff} subset where non-responsive cells have been shown to be most prevalent differential PD-1 expression had little bearing on the frequency of the non-responsive population (Figure 3.23C).

The MFI of CD69 expression was also analysed for the responding ($CD4^{lo}CD69^{hi}$) cell fraction. In the T_{cm} PD-1^{hi} culture the CD69 MFI of responding cells was lower than in the corresponding PD-1^{lo} culture. This is consistent with previous data in suggesting that the PD-1^{hi} fraction is less responsive. However, the reverse of this trend was seen in the T_{eff} population where the responsive PD-1^{hi} had a greater CD69 MFI, but there were no statistically significant differences attached to these observations. In conclusion, these findings support some association between PD-1^{hi} expression and diminished responsiveness to PMA/ionomycin in the T_{cm} subset. However, PD-1 expression is not related to the non-responsive phenotype in the T_{eff} subset and is an insufficient marker to define non-responsive $CD4^+$ T cells prior to stimulation.

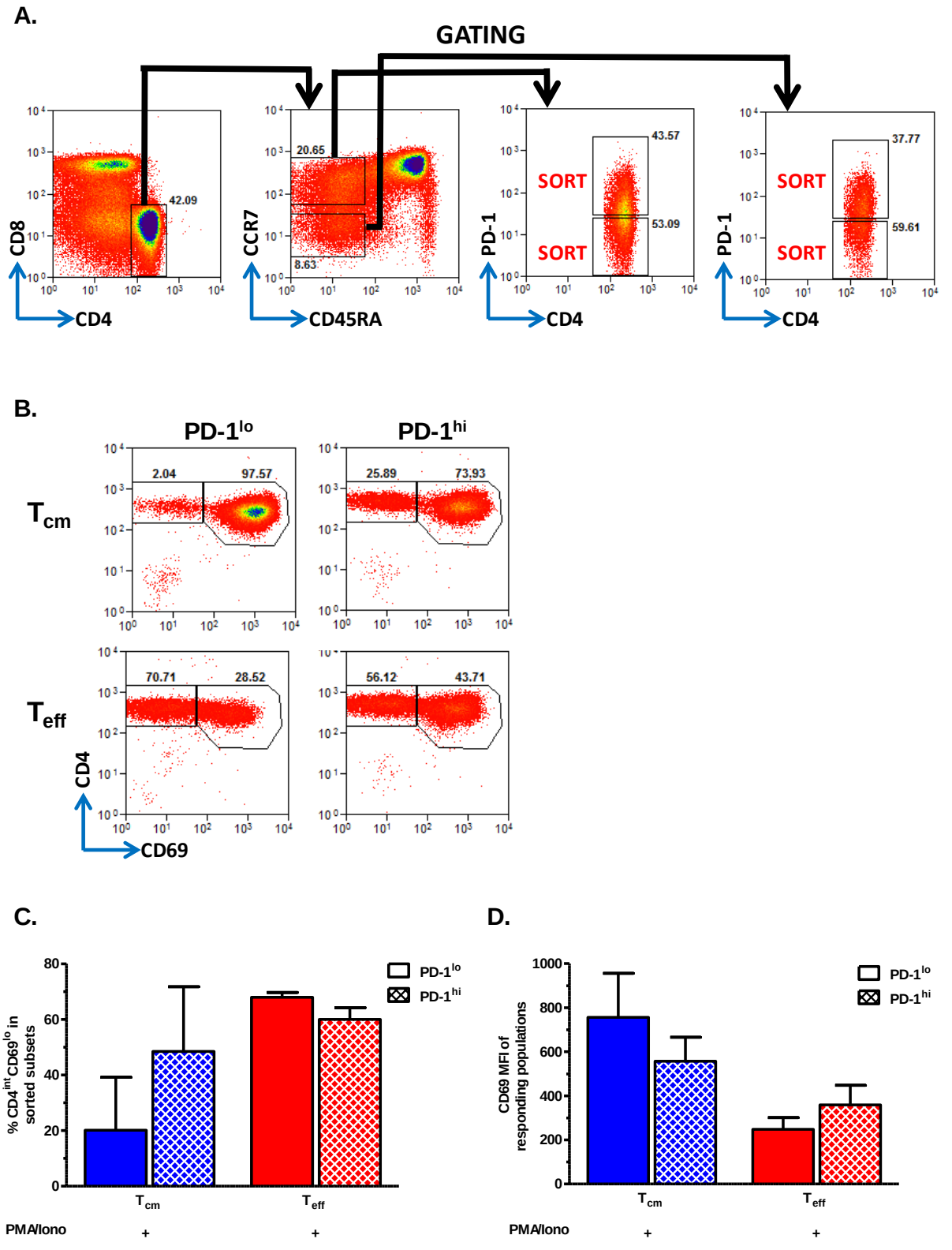

Figure 3.23 The relationship between PD-1 and CD69 expression in sorted CD4$^+$ memory T cell subsets. PD-1^{hi} and PD-1^{lo} CD4$^+$ memory T cell populations were purified by fluorescence activated cell sorting (gating strategy from the CD4$^+$ T cell stage forwards is shown in **A.**). Populations were cultured for 6h ± PMA and analysed for the absence of CD69 upregulation (representative flow cytometry plots shown in **B**, graphical representation is shown in **C.**). **D.** The CD69 median fluorescence intensity (MFI) of cells responsive to stimulation. Data representative of n=2 healthy donors in n=1 experiment.

3.11.2 The effect of exogenous gamma chain cytokine on the non-responsiveness of $CD4^+$ T cells.

As examination of PD-1 expression did not conclusively link the non-responsive population to T cell exhaustion it was investigated whether these cells exhibited 'anergic' as opposed to 'exhausted' characteristics. There are currently no positive markers that identify anergic T cells *in vivo*. However, the hyporesponsiveness elicited by anergic T cells can be reversed through the addition of exogenous IL-2 in *in vitro* cultures[189,381]. Prior work in my study had shown IL-2 did not influence the non-responsive population in stimulated T_{reg}, and T_{reg}-depleted cultures. Never-the-less this line of investigation was extended with the addition of other common gamma chain family cytokines (IL-7 and IL-15) in combination with IL-2. PBMC were cultured for 6h with PMA/ionomycin in the presence of IL-2, IL-7, IL-15 and a combination thereof (Figure 3.24). The percentage of non-responsive cells in the $CD3^+CD4^+$ T cell compartment was analysed by flow cytometry (Figure 3.24A). Addition of IL-2 to stimulated PBMC cultures again had no impact on the non-responsive $CD4^+$ T cell population and its persistence suggests these cells are not anergic (Figure 3.24B). In separate experiments where all three cytokines were investigated there was a small decrease in the median non-responsive frequency noted when IL-2 alone or the combination of IL-2, IL-7 and IL-15 was added to the cultures (Figure 3.24C). This trend was not statistically significant and there was no change in the non-responsive cell frequency when IL-7 and IL-15 were added alone. The overall effect of exogenous cytokine in this system was minimal and suggests anergy does not contribute to the hyporesponsiveness observed in these assays.

3.11.3 Intracellular expression of CD69 in the non-responsive $CD4^+$ T cell population.

A documented mechanism behind the hyporesponsiveness of anergic T cells is the sequestration of T cell signalling components[176,177,179]. This is achieved via the targeting of signalling mediators for degradation and an accelerated rate of proteolysis through increased ubiquitin ligase activity[172]. To assess whether the non-responsive $CD4^+$ T cell population

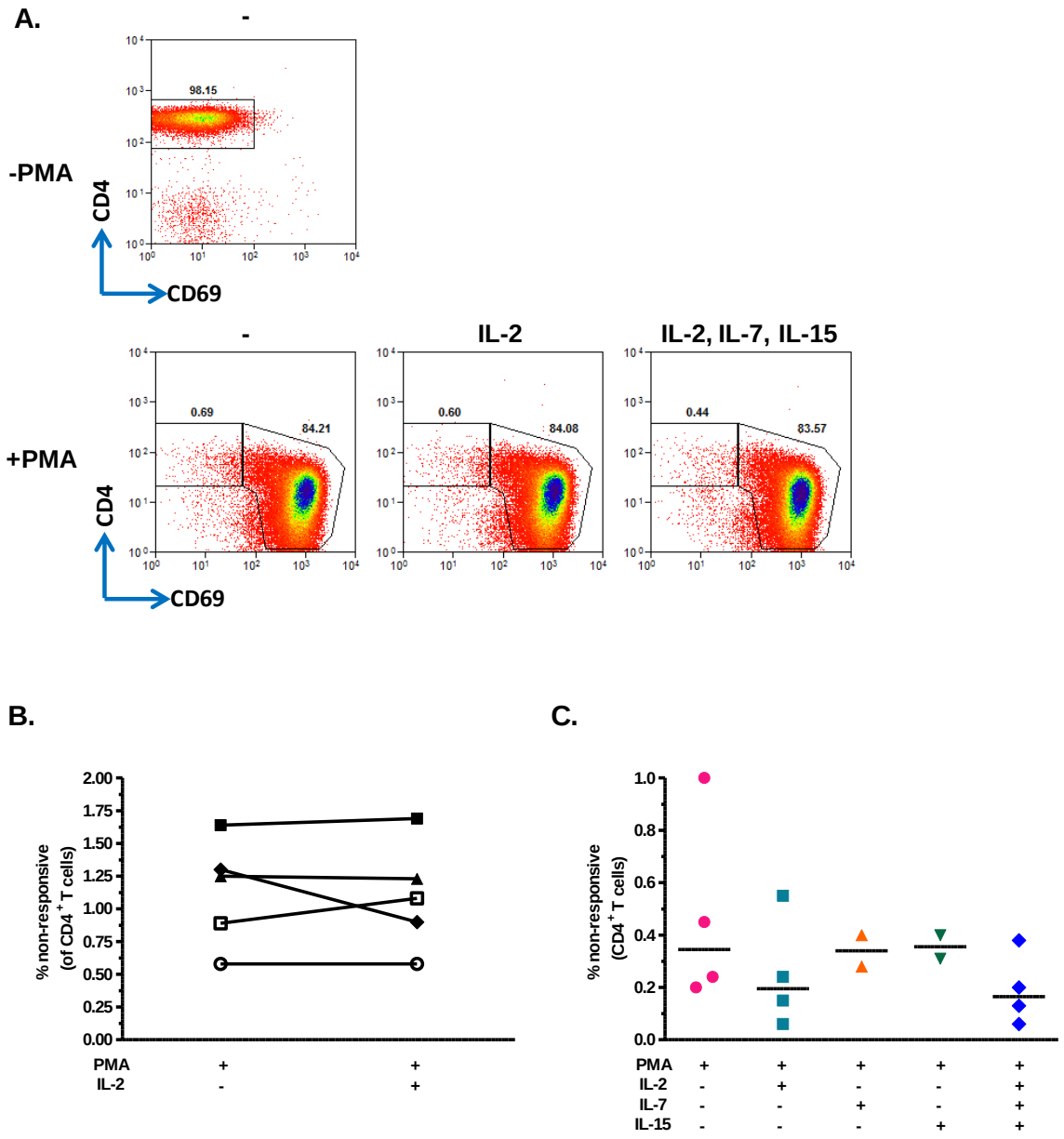

Figure 3.24 CD69 expression by $CD4^+$ T cells is not affected by presence of of γ_c chain cytokine *in vitro*. PBMC were cultured for 6h with PMA/Ionomycin ± IL-2, IL-7 and IL-15. $CD4^+$ T cells were analysed by flow cytometry for cells lacking CD69 expression. **A.** Representative plots showing CD69 expression by unstimulated (top panel) and simulated (bottom panel) CD4 T cells (gated on $CD3^+$ lymphocytes) with and without combinatorial γ_c chain cytokine. **B.** Comparison of the percentage of T cells unresponsive to stimulation ($CD4^{int}CD69^{lo}$) in the absence and presence of IL-2. **C.** In experiments independent to those shown in **B.** the absence CD69 upregulation in the presence of multiple cytokines was also tested.

demonstrated these characteristics staining for both surface and intracellular CD69 was performed consecutively. Surface and intracellular CD69 was labelled using different fluorochromes to identify whether non-responsive cells expressed CD69 intracellularly (Figure 3.25). A proteasome inhibitor (Velcade®) was then added to the PBMC cultures at increasing concentrations. By blocking proteasomal degradation it was proposed that any translated CD69 would accumulate in the cytosol. Therefore, it could be detected whether non-responsive cells translated CD69 protein that was targeted for lysosomal compartments before reaching the cell membrane.

PBMC were cultured for 6h with PMA/ionomycin and the $CD3^{+}CD8^{-}CD4^{+}$ T cell population analysed for surface and intracellular expression of CD69 (Figure 3.25A). When CD69 was stained intracellularly the background staining for CD69 was increased even in the absence of PMA/ionomycin (Figure 3.25A top panel). Due to this shift the gating of the intracellular non-responsive population was based on intracellular staining from the unstimulated control culture. Although there was a slight reduction in the non-responsive cell frequency when CD69 was measured intracellularly compared to at the surface (0.4% difference in median frequencies) results suggested that the population of $CD4^{int}CD69^{lo}$ cells persisted (Figure 2.25A middle panel, Figure 2.25C). This finding is based on the fact that not all cells were $CD69^{hi}$ when stained intracellularly and thus the non-responsive population does not express CD69 protein in the cytosol. When the proteasome inhibitor was added to the cultures there was a small percentage increase of non-responsive $CD4^{+}$ T cells at high concentrations (Figure 3.25C). This was unexpected as it was anticipated that by blocking protein degradation CD69 expression would increase and thus reduce the $CD4^{int}CD69^{lo}$ population. The CD69 MFI of the responding fraction also reduced with increasing concentrations of inhibitor (Figure 3.25D). In light of these observations the percentage of $IFN\gamma^{+}$ cells was measured to control for the effect of the inhibitor and T cell activation. Increasing doses of

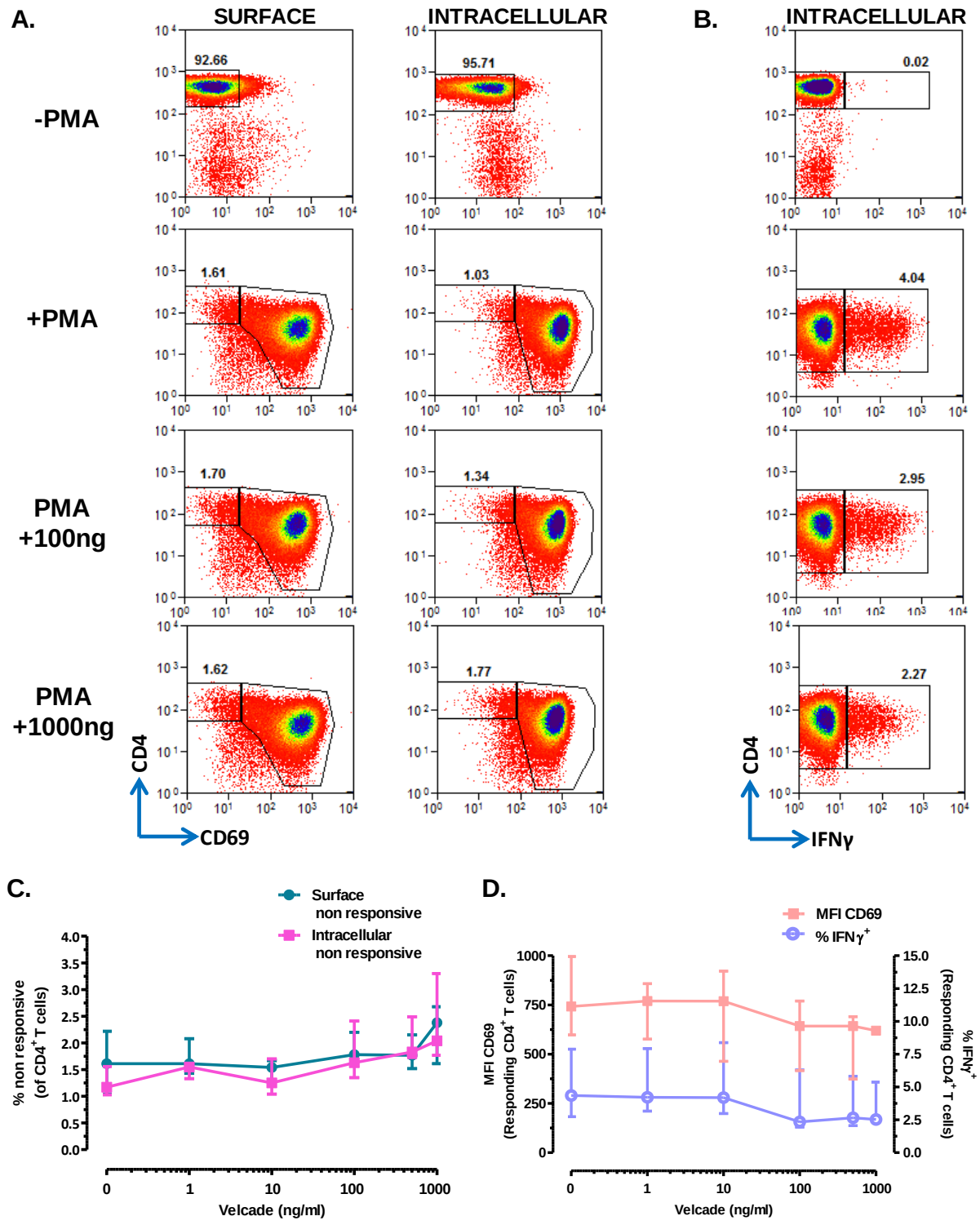

Figure 3.25 The effect of proteosome inhibition on CD69 expression by stimulated CD4$^+$ cells. PBMC were cultured with PMA/Ionomycin and increasing concentrations of Velcade (Bortezomib). The CD3$^+$CD8$^-$CD4$^+$ T cell population was analysed for CD69 upregulation relative to unstimulated cultures. **A.** Flow cytometry plots represent the percentage of CD4^{int} CD69^{lo} cells in each condition when staining for surface (left panel) and intracellular (right panel) CD69 expression. **B.** Plots represent the percentage of IFNγ$^+$ CD4$^+$ T cells. **C.** Surface and intracellular analysis of the CD4^{int} CD69^{lo} population with increasing concentrations of inhibitor. **D.** Median (and range) fluorescence intensity (MFI) of surface CD69 expression and the median (and range) percentage of IFNγ$^+$ CD4$^+$ T cells within the responsive fraction. Data is representative of n=3 healthy donors.

proteasome inhibitor resulted in a decrease of IFNγ$^+$ cells especially at high concentrations (Figure 3.25B, Figure 3.25D).This indicated that the proteasome inhibitor had more ubiquitous effects on CD4$^+$ T cell activation than anticipated.

3.12 Gene expression analysis of PMA/ionomycin-stimulated CD4$^+$ T cell populations.

3.12.1 Investigation of CD69 gene expression by the non-responsive CD4$^+$ T cell phenotype.

As no intracellular stores of CD69 protein were detected in the non-responsive population (Figure 3.25) it was investigated whether the root of this deficiency was a lack of CD69 mRNA expression. For this investigation cDNA was prepared from mRNA isolates of the desired cell cultures. Multiplex real time PCR (qPCR) was then used to compare the expression of the CD69 gene to a housekeeping gene to normalise differences in the starting amount of cDNA material. GAPDH (Glyceraldehyde 3-phosphate dehydrogenase) was chosen as a housekeeping gene and was initially tested to confirm that the cycle threshold (Ct) value measured was directly proportional to the amount of material added. CD4$^+$ T cells were isolated from PBMC using microbead MACS technology and the purity of the CD4$^+$ population was confirmed by flow cytometry (95.4% CD4$^+$) (Figure 3.26A). A titration based on equivalent cell numbers from the CD4$^+$ cell isolation cDNA prep was performed and the corresponding GAPDH qPCR amplification curves analysed for each Ct value (Figure 3.26B, Fig3.26C). Results showed that the Ct value was inversely proportional to the Log_2 cell number added which was consistent with a doubling of cDNA material per amplification cycle. Therefore, the GAPDH primer was considered free of contaminants and suitable for use as a housekeeping gene in multiplex experiments.

Work in this study had thus far failed to identify surface markers (or combination thereof) that could identify the non-responsive CD4$^+$ T cell population prior to PMA/ionomycin stimulation. A complex cell sorting strategy was devised in order to isolate non-responsive

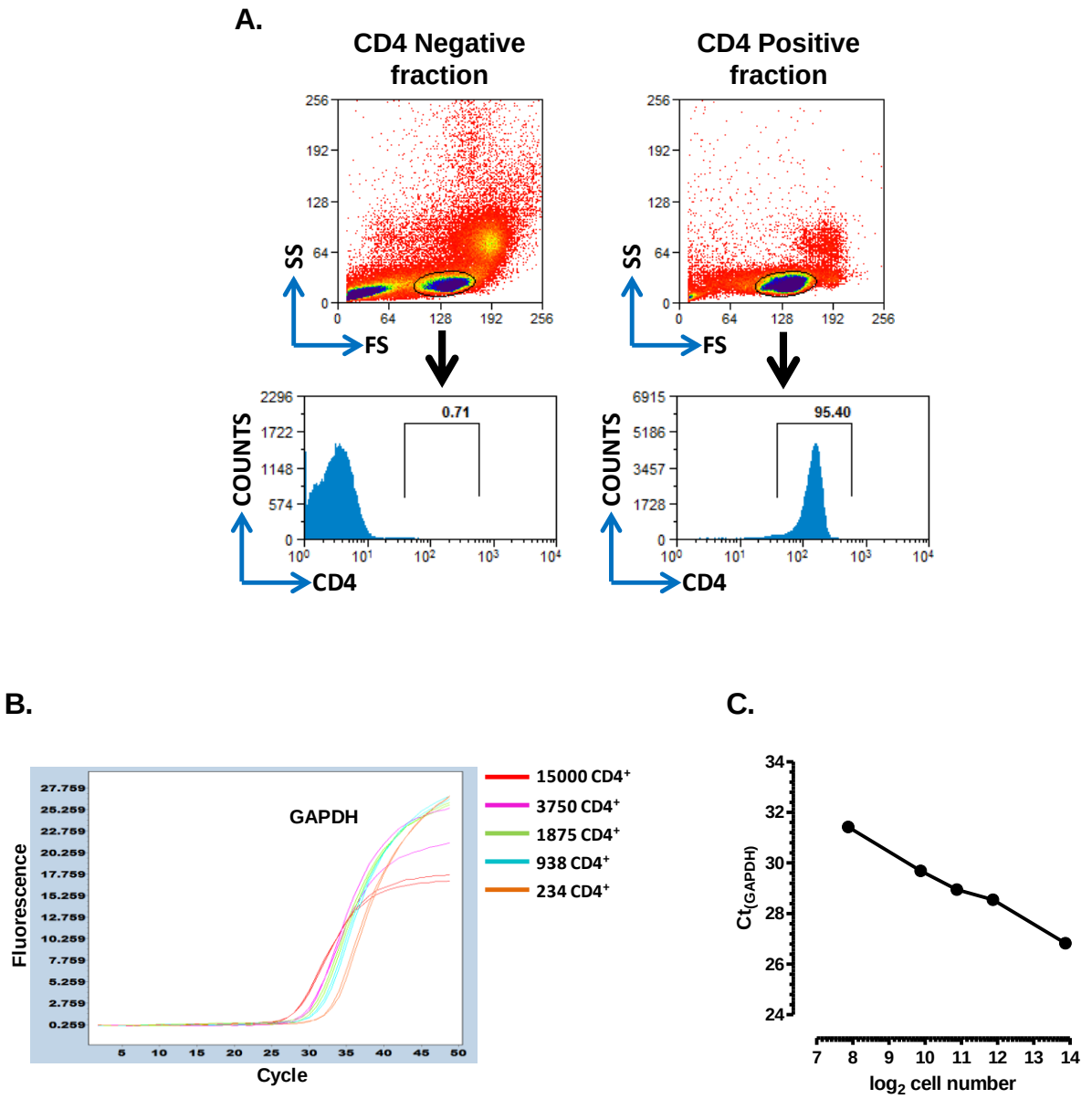

Figure 3.26 qPCR analysis of GAPDH gene expression in a cell number titration assay. $CD4^+$ T cells were purified from peripheral blood mononuclear cells by magnetic-activated cell sorting (MACs)**.** cDNA was prepared from a known number of $CD4^+$ T cells and a dilution series performed to yield a quantity of cDNA from a calculated equivalent cell number. qPCR was performed to assess the relative amount of GAPDH gene in each sample. **A.** Flow cytometry was used to confirm the purity of the CD4 MACS isolation. Plots represent the forward/side scatter profiles (top panel) and the percentage of $CD4^+$ cells (bottom panel) in the separated CD4 negative and positive fractions. **B.** qPCR amplification curves showing the amplification of GAPDH for each cell equivalent amount of cDNA (legend indicates the number of $CD4^+$ T cells per PCR reaction). Technical replicate's (duplicate) curves are shown for each cell number. **C.** Graph showing the relationship between the cycle threshold (Ct) of GAPDH and the applied cell number (log_2). Data is representative of n=2 technical replicates n=1 experiment.

cells at a purity sufficient for gene expression analysis (Figure 3.27A). As work on sorted T cell subset had shown that non-responsive cells were predominantly an effector memory phenotype (Figure 3.13) $CD4^{+}CCR7^{-}CD45RA^{-}$ cells were purified from PBMC by FACS. This population was stimulated for 4h with PMA/ionomycin and then separated into $CD4^{int}CD69^{lo}$ non-responsive and $CD4^{lo}CD69^{hi}$ responsive fractions by a second round of FACS (Figure 3.27A Figure 3.27B). Multiplex qPCR for CD69 and GAPDH was performed for both fractions in technical triplicates and the mean Ct analysed for n=5 donors (Figure 3.27C). Strikingly, when the fold change between CD69 expression and GAPDH expression was analysed (calculated by $2^{\wedge\text{-}\Delta Ct}$) it showed that the non-responsive population had approximately double the fold change in CD69 gene expression compared with the responsive fraction (Figure 3.27D). Although the elevated CD69 gene expression in the non-responsive fraction was not statistically significant this trend was counter-intuitive, as it was expected that the highest CD69 mRNA expression would be found in the responding population which expressed the highest level of CD69 protein. Additionally, the non-responsive population had previously been shown to have no notable intracellular expression of the receptor and it was not anticipated that the population would display greater levels of message with no evidence of translation (Figure 3.25).

In light of these findings CD69 gene expression was examined in unstimulated and stimulated total memory $CD4^{+}$ T cell cultures. This way it could be assessed if the differential CD69 expression between the sorted non-responsive and responsive T_{eff} fractions was population specific or a consequence of PMA/ionomycin stimulation. For these experiments memory ($CD45RA^{-}$) $CD4^{+}$ T cells were purified from PBMC by MACS and the purity of the retrieved fractions confirmed by flow cytometry (Figure 3.28A). The memory T cells were cultured with and without PMA/ionomycin and cDNA prepared from the unstimulated and stimulated cultures. Multiplex qPCR was used to compare the expression of CD69 to the internal GAPDH control as previously described.

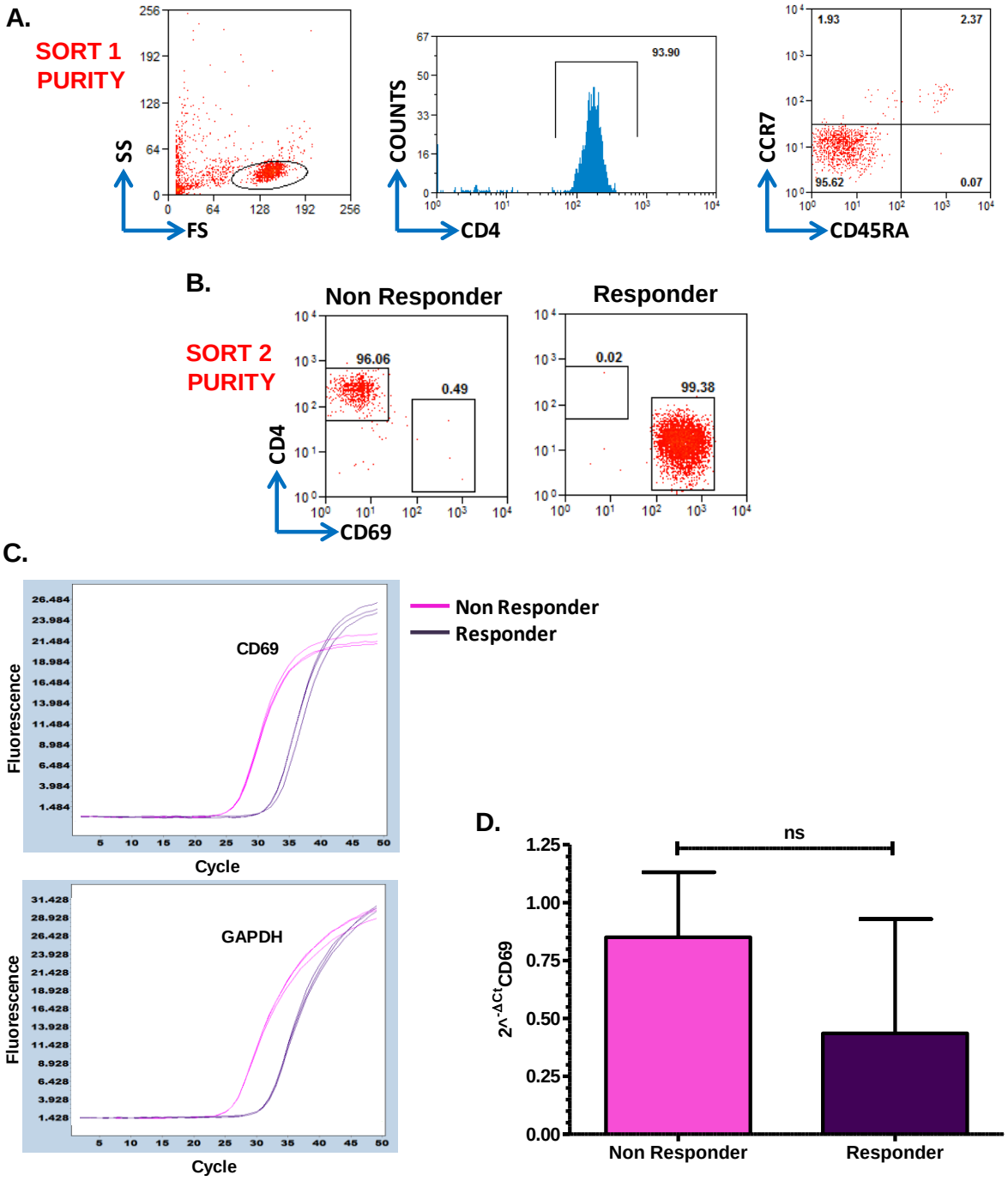

Figure 3.27 Analysis of CD69 gene expression by responsive and non responsive effector memory CD4$^+$ T cells. CD4$^+$ effector memory (CD45RA$^-$CCR7$^-$) T cells were purified by FACS. Following PMA/Ionomycin stimulation these cells were re-sorted into responsive (CD4^{lo}CD69^{hi}) and non-responsive (CD4^{int}CD69^{lo}) populations. cDNA preparations from each population were then analysed by qPCR to relatively quantify expression of the CD69 gene. **A.** Representative flow cytometry plots showing the purity of CD4$^+$ effector memory T cells following the pre stimulation separation. **B.** Plots show the purity of the non-responsive and responsive populations after the post stimulation separation. **C.** qPCR amplification curves show the specific amplification of the CD69 gene (top panel) and the matched control gene GAPDH (bottom panel) for each population. Technical replicate's (triplicate) curves are shown for each condition. **D.** Graph shows the median (And IQR) fold change ($2^{\wedge-\Delta Ct}$) between the CD69 and GAPDH gene for in responsive and non-responsive cells. ns= no significance at $p<0.05$ (paired student T test). Data is representative of n=5 independent experiments.

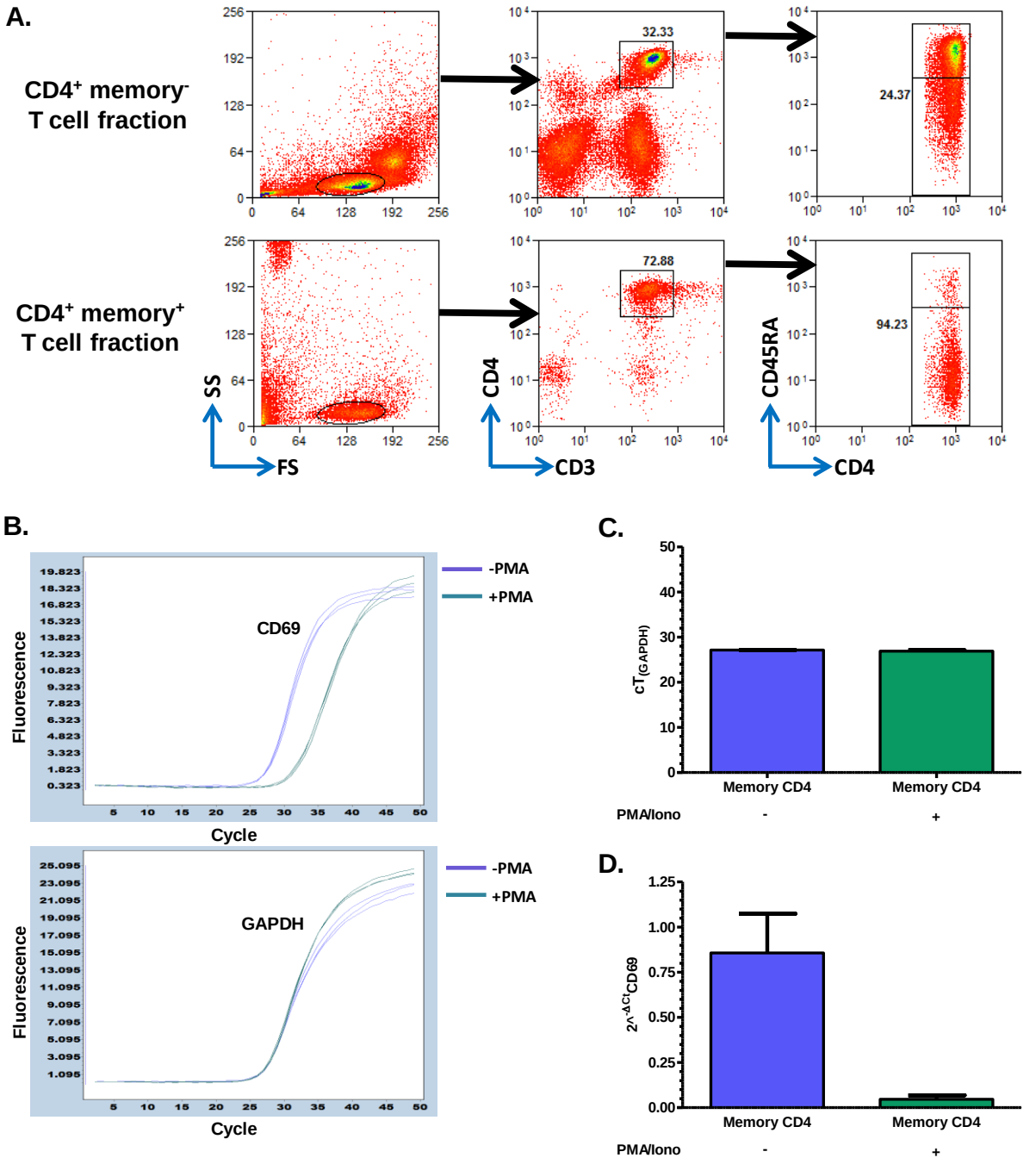

Figure 3.28 Analysis of CD69 gene expression by effector memory CD4$^+$ T cells following *ex vivo* stimulation. Memory CD4$^+$ T cells (CD45RA$^-$) were purified from PBMC by magnetic-activated cell sorting (MACs) and cultured with and without PMA/ionomycin. cDNA preparations were analysed by qPCR for expression of the CD69 gene relative to the control gene GAPDH. **A.** Flow cytometry was used to measure the purity of the MACS separation. Plots show the forward/side scatter profiles, the percentage of cells that are CD4$^+$, and the percentage of CD4$^+$ cells that are memory (CD45RA$^-$) in the fractions produced following separation. **B.** qPCR amplification curves show the specific amplification of the CD69 gene (top panel) and the matched control gene GAPDH (bottom panel) for unstimulated and stimulated memory CD4$^+$ T cell cDNA. Technical replicate's (triplicate) curves are shown for each condition. **C.** Graph shows the mean Ct value for GAPDH for each culture condition (cell numbers were equivalent). **D.** Graph shows the mean fold change ($2^{\wedge -\Delta Ct}$) between the CD69 and GAPDH gene expression in unstimulated and stimulated memory CD4$^+$ T cells. Data is representative of n=1 donor measured in 2 technically replicated experiments.

It was found that the Ct values of GAPDH were the same for the unstimulated and stimulated cultures, thus confirming the same amount of genetic material had been applied to each assay (Figure 3.28B bottom panel, Figure 3.28C). However, the fold change in CD69 expression showed that the unstimulated culture had approximately seventeen times greater CD69 expression than the matched stimulated culture (Figure 3.28D). This result confirmed that a 6 hour PMA/ionomycin stimulation induces a reduction in CD69 gene expression in $CD4^+$ memory T cells. Additionally this suggests that incomplete downregulation of CD69 mRNA expression in the sorted non-responsive population is consistent with an inability of these cells to activate.

3.12.2 Analysis of IFNγ cytokine gene expression.

The expression of the cytokine IFNγ was also analysed at mRNA level in the purified non-responsive and responsive populations defined in section 3.12.1. As with analysis of the activation marker CD69 the expression of IFNγ was also measured in purified unstimulated and stimulated total memory $CD4^+$ T cell populations. Similarly, such experiments could reveal changes solely resulting from the effects of the stimulation and be informative in the analysis of the sorted non-responsive and responsive T_{eff} phenotypes.

PMA/ionomycin stimulation induces some memory $CD4^+$ T cells to produce IFNγ protein (as shown in Figure 3.1E, Figure 3.2M) but no protein production occurs in resting cells. Therefore it was expected that cDNA preparations from stimulated cultures would show greater levels of IFNγ mRNA. However, findings showed that expression of the IFNγ gene in stimulated cultures was barely within the detectable range by qPCR as indicated by a very high Ct value (Figure 3.29A). The relative fold change in IFNγ gene expression was also around $4.2x10^4$ times greater in unstimulated cDNA preps as compared to stimulated preps (Figure 3.29A). These findings suggests that unstimulated (resting) memory $CD4^+$ T cells have greater stores of IFNγ mRNA than cells stimulated for six hours with PMA/ionomycin.

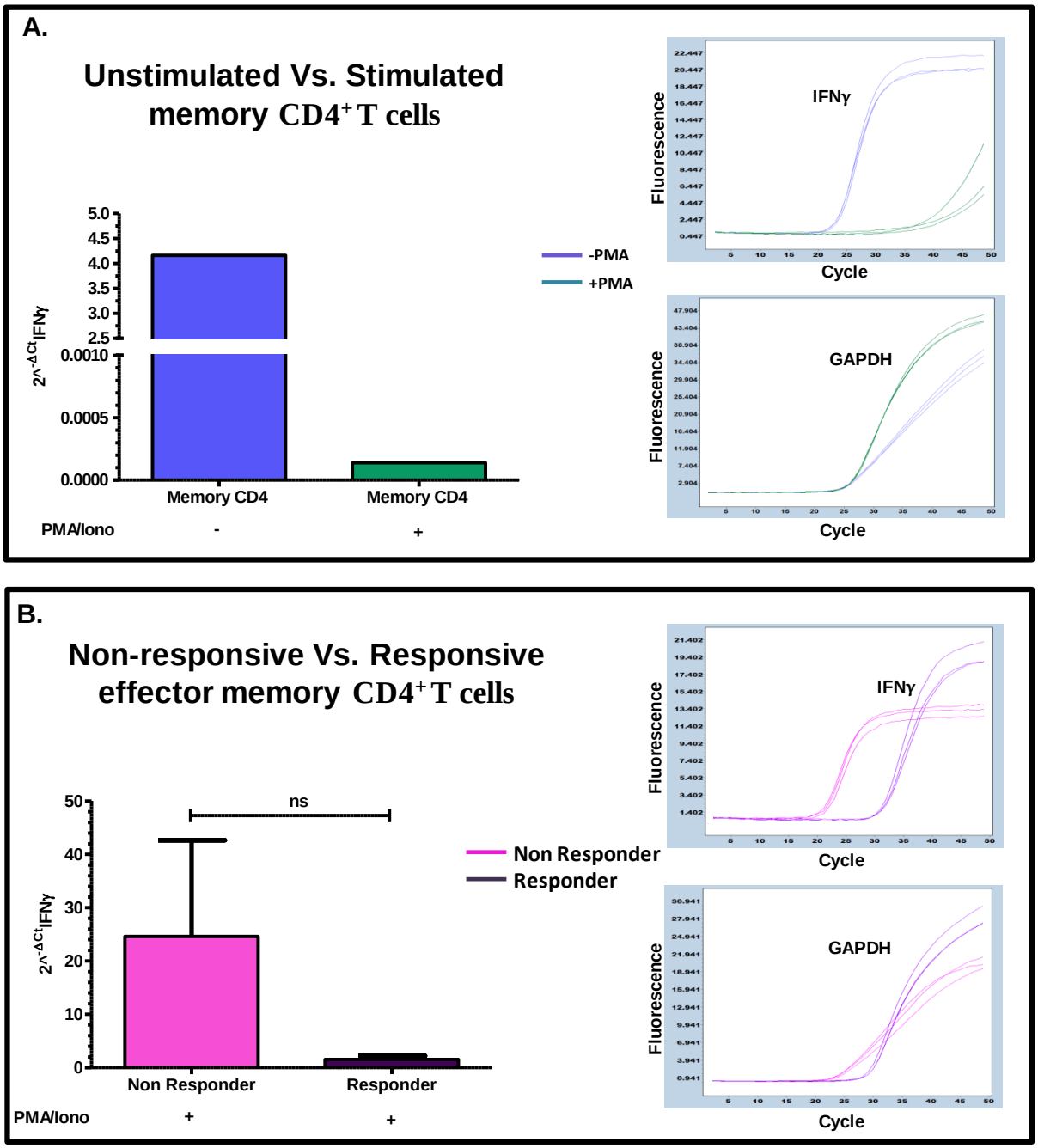

Figure 3.29 Analysis of IFNγ gene expression by effector memory CD4$^+$ T cell populations. A. Purified CD4$^+$CD45RA$^-$ memory T cells were cultured with and without PMA/ionomycin for 6h. Expression of IFNγ (relative to the control gene GAPDH) was measured from unstimulated and stimulated cultures by qPCR. Data is indicative technical triplicate amplification curves in n=1 experiment. **B.** Expression of IFNγ was measured in two effector memory CD45RA$^-$CCR7$^-$ populations that did and did not respond to PMA/ionomycin stimulation (CD4^{lo}CD69^{hi} and CD4^{int}CD69^{lo} surface expression respectively). Data is indicative of technical triplicate amplification curves for n=3 donors. ns; no significance at $p<0.05$. **A-B.** qPCR amplification curves for IFNγ and GAPDH are shown for all populations investigated. Graphs (left) indicate the fold change ($2^{\wedge -\Delta Ct}$) between IFNγ and GAPDH expression for each population.

Similar to the analysis of CD69 mRNA levels the T_{eff} non-responsive population had greater relative IFNγ expression comparative to the match responsive fraction (Figure 3.29B). This trend matched those observations from total memory $CD4^+$ T cell cultures (Figure 3.29A), although the difference in relative gene expression was nowhere near as profound (18 fold as opposed to $4.2x10^4$ fold). This was predominantly because IFNγ gene expression by the T_{eff} responsive fraction was not diminished to the level observed in the stimulated memory culture. Together these results suggest that the behaviour of the non-responsive $CD4^+$ T cells mirrors that of unstimulated cells, but in responsive (or stimulated) populations IFNγ mRNA expression is attenuated following exposure to PMA/ionomycin for 4 hours.

3.12.3 Expression analysis of T cell receptor signalling genes.

It was considered that the $CD4^{int}CD69^{lo}$ non-responsive phenotype may be induced through deficient intracellular signalling pathways triggered by PMA/ionomycin activation. Therefore, the expression of four key genes associated with T cell activation was measured to identify changes in the non-responsive population. The candidate genes included three T cell signalling genes (for LCK, PKCϴ, VAV-1) and one metabolic regulator (AMPK) which were measured independently by multiplex qPCR.

To get a baseline expression from each gene qPCR was initially performed on unstimulated and stimulated $CD4^+$ memory T cell cultures as described in Figure 3.28A. qPCR amplification curves were analysed for the Ct values of each gene and internal GAPDH control, then the fold change between these values calculated for each culture condition (Figure 3.30). The AMPK gene showed negligible amplification in qPCR reactions performed using cDNA preparations from both unstimulated and stimulated cultures. As its expression was beyond the detection range in such test cultures where there was ample input of genetic material this gene was excluded from subsequent analysis using sorted non-responsive cells (data not shown).

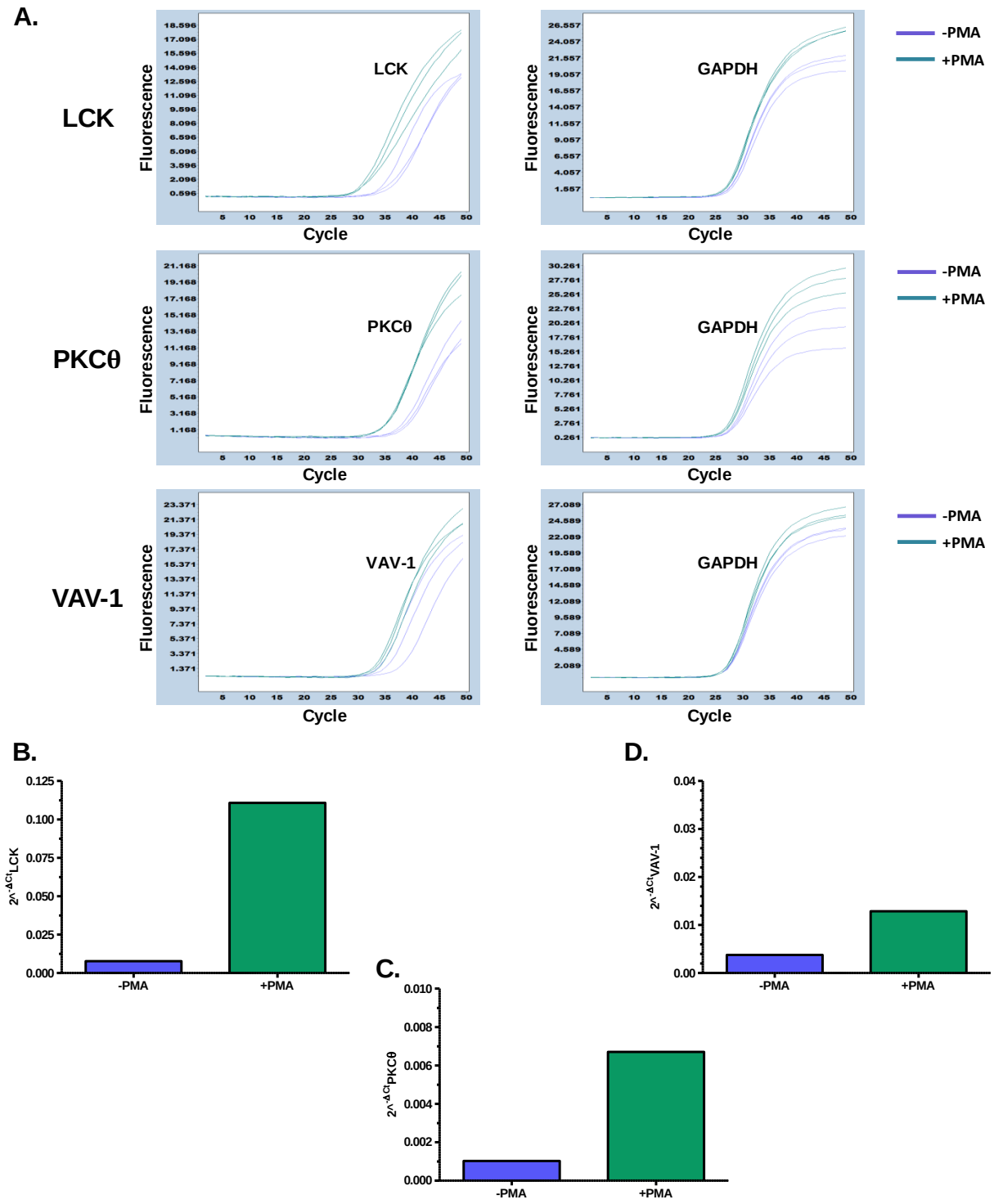

Figure 3.30 Expression of T cell receptor signalling genes in memory CD4$^+$ T cells. Memory CD4$^+$ T cells (CD4$^+$CD45RA$^-$) were purified from peripheral blood mononuclear cells by magnetic-activated cell sorting (MACs)**.** Cells were cultured for with and without PMA/ionomycin and cDNA prepared from each condition. qPCR analysis was performed to measure the gene expression of three T cell signalling associated genes (LCK, PKCθ, VAV-1) relative to the control gene GAPDH. **A.** qPCR amplification curves show the specific amplification of each signalling gene (**left panel**) and the matched control gene GAPDH (**right panel**) for unstimulated (blue) and stimulated (green) memory CD4$^+$ cell cDNA. Technical replicate's (triplicate) curves are shown for each cell number. **B-D.** Graphs show the fold change ($2^{\wedge -\Delta Ct}$) between the gene expression of each signalling gene and GAPDH in unstimulated and stimulated memory CD4$^+$ T cell cultures. Data is representative of n=1 experiment.

The T cell receptor signalling-related genes were all shown to amplify exponentially in each PCR reaction albeit towards the lower end of the range of detection (Figure 3.30A). There was an increase in expression of all three signalling genes in the stimulated memory T cell cultures when compared to those cultures not exposed to PMA/ionomycin (Figure 3.30B-D). In the case of PKCΘ and VAV-1 the fold increase in gene expression between the unstimulated and stimulated cultures was relatively small, measuring in at 7-fold and 3.5-fold respectively (as calculated by $2^{\wedge-\Delta Ct}$) (Figure 3.30C, Figure 3.30D). However, the difference in LCK gene expression was more substantial, with a 13.75-fold increase in expression following PMA/ionomycin treatment (Figure 3.30B). Together this data indicates that PMA/ionomycin stimulation itself increases mRNA expression of the three tested signalling components with LCK most influenced by the stimulation.

When the three T cell signalling genes were measured in FACS sorted T_{eff} non-responsive and responsive populations the trends observed in the stimulation control experiments were not recapitulated (Figure 3.31). Here there were minimal differences in the expression of LCK, PKCΘ and VAV-1 between each fraction, although the low expression of these genes combined with minimal starting material (restricted by the infrequency of the non-responsive population) rendered analysis of this data challenging. However, findings indicate that deficiencies in these genes are not responsible for the $CD4^{int}CD69^{lo}$ non-responsive phenotype as comparable expression levels were observed in the corresponding responsive fractions.

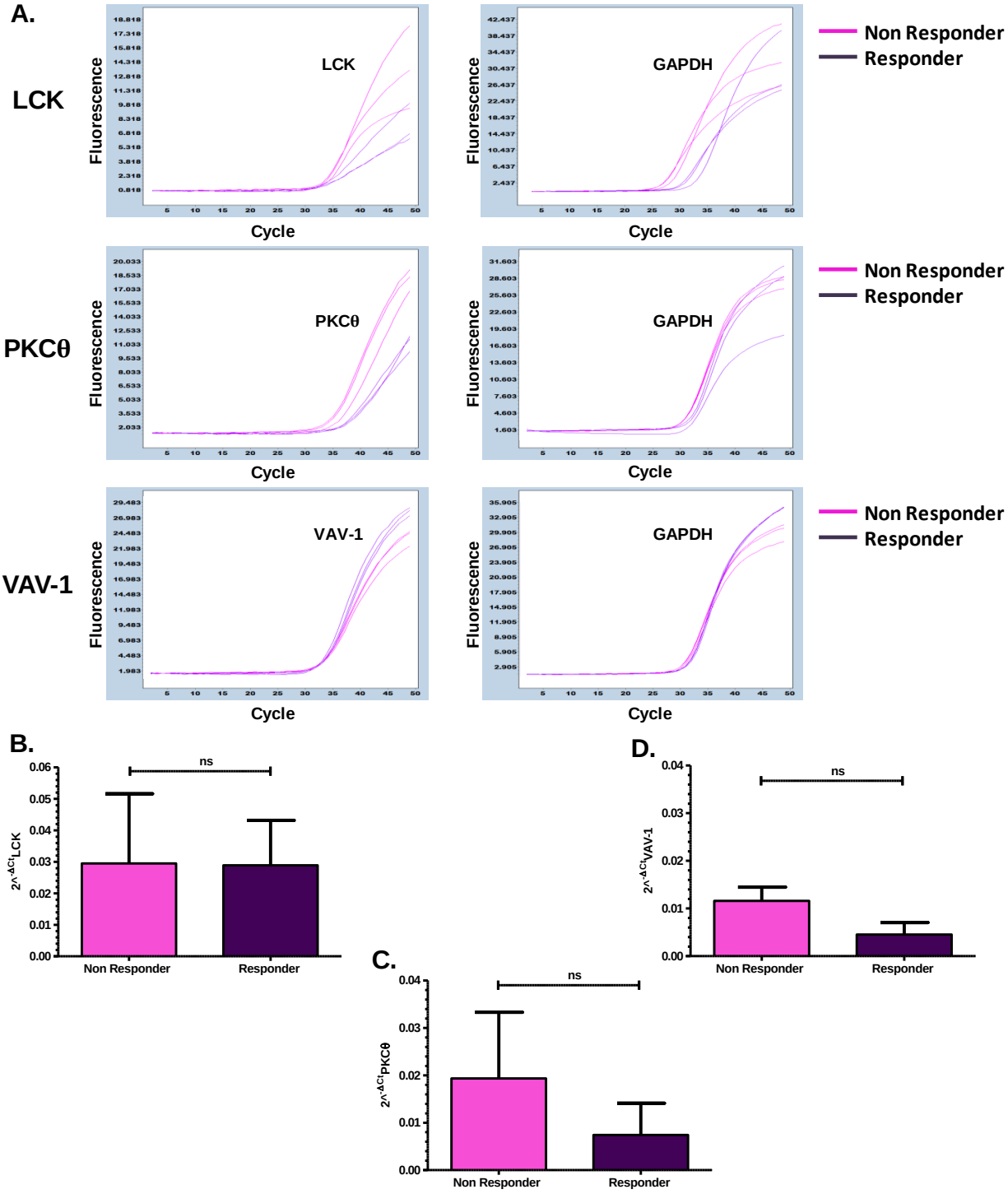

Figure 3.31 Expression of T cell receptor signalling genes in responsive and non responsive effector memory CD4$^+$ T cells. Purified CD4$^+$ effector memory T cells (CD45RA$^-$CCR7$^-$) were stimulated with PMA/Ionomycin. Cells were separated into responsive (CD4^{lo}CD69^{hi}) and non-responsive (CD4^{int}CD69^{lo}) populations by FACS. Expression of LCK, PKCθ and VAV-1 genes was examined relative to the control gene (GAPDH) by qPCR. **A.** qPCR amplification curves show the amplification of each signalling gene (**left panel**) and the control gene GAPDH (**right panel**) from each cDNA preparation. Technical triplicate amplification curves are shown for each population. **B-D.** Graphs show the fold change ($2^{\wedge-\Delta Ct}$) between the each signalling and control gene pair (and thus the relative gene expression) for both the non-responsive and responsive populations. Data is representative of n=3 paired non-responsive and responsive cell samples repeatedly measured in n=2-3 independent qPCR reactions. ns; no significance at $p<0.05$.

3.13 Discussion

Although naive $CD4^+$ T cells do express some effector cytokines when activated (most notably IL-2) the majority of T cell cytokines are produced by differentiated, antigen-experienced memory populations[382,383]. This investigation identified a subpopulation of cells within the two main memory subsets (T_{cm} and T_{eff}) which failed to produce any of thirteen effector cytokines when simulated *in vitro* (Figure 3.3). Findings suggest that a considerable proportion of the memory population has a function that cannot be accounted for following exposure to PMA/ionomycin. It may be assumed that these cells have some biological purpose or their persistence *in vivo* would be futile. A summary of the potential function and identity of these cells are explored below;

1) Cells have an atypical cytokine profile - although the panel of cytokines tested in these experiments was extensive it remains possible that the 'cytokine^{-ve}' cells express other effector molecules untested here. Two notable examples of these include the Th_1 and Th_{17}-associated cytokine lymphotoxin alpha (LT-α) and IL-25 which associated with Th_2 differentiation[384,385]. Given that flow cytometers now have more fluorescence channels available than at the time of these experiments there is more scope to expand the cytokine panel to include further markers in the future.

2) Cells have an atypical cytokine response to PMA/ionomycin – It is possible that the 'cytokine^{-ve}' population are fully functional cytokine producing cells but their cytokine gene expression is not driven by PMA/ionomycin-induced PKCϴ signalling. The nature of a stimulus can influence a cells cytokine profile in *in vitro* systems, which is shown by concurrently comparing the cytokine expression in response to multiple stimuli such as PMA/ionomycin, PHA and CD3/CD28 ligation[373,386,387]. For example, *I. Olsen and L.M Sollid (2013)* recently showed IL-17 and IFNγ production by T cell clones in response to PMA/ionomyin that only expressed IFNγ upon CD3/CD28 activation[373]. In *in vitro* systems

cytokine secretion kinetics (and thus the length of a stimulation assay) are also a consideration in revealing a populations total effector cytokine potential. Although the optimal time point for cytokine secretion was tested (Figure 3.1) it cannot be discounted that subpopulations of cells exhibit a delayed response beyond the measured duration.

3) Cells are truly cytokine negative – If the 'cytokine negative' population defined here truly produce no effector cytokine it is reasonable to consider their alternative function or identity. It is possible that such cells are purely proliferative and may even represent cells in the earliest transition from T_{naive} to T_{memory}. A definition of Th_0 is assigned to intermediary cells generated from activated T_{naive} populations prior to T_{memory} differentiation. However, in this model the Th_0 phenotype is transient and shown to produce multiple cytokines associated with both Th_1 and Th_2 lineages[112,388]. More recently a highly proliferative population of stem cell-like memory T cells (T_{SCM}) has been defined in both $CD4^+$ and $CD8^+$ T cell subsets[64,65]. These cells are also unsuitable candidates for the 'cytokine^{-ve}' phenotype as they retain the naïve-like CD45RA expression and produce intermediate levels of IFNγ, IL-2 and TNFα[64].

Plasticity between the differentiation pathways of $CD4^+$ T_{helper} lineages is well described both *in vitro* and *in vivo.* For example, cells derived from a Th_{17} lineage upregulate Th_1-associated transcription factors and cytokines (notably IFNγ) under appropriate polarising conditions[343,389]. It is conceivable that molecular mechanisms governing such shifts in cytokine expression such as transcriptional repression and epigenetic gene silencing[390] can shut down a cell's cytokine armoury entirely. Therefore, it cannot be discounted that cytokine^{-ve} cells may have expressed cytokine at some point in their history. The temporal aspect of cytokine expression and plasticity can be investigated through fate mapping experiments in mice and could be adapted for the purpose of this investigation[122].

Moving towards the more terminally differentiated end of the T_{memory} spectrum it is possible that cytokine^{-ve} cells have become 'anergised' to the effects of stimulation or are quiescent

through processes related to immune senescence. As processes which result in cytokine expression are highly complex it was first investigated whether cytokine^{-ve} cells were capable of activating with PMA/ionomycin exposure at all. As no transcription of cytokine genes can occur without activation this was easily ascertained by measuring CD69 upregulation. A population of cytokine^{-ve} memory CD4^{+} T cells was identified that did not upregulate CD69 and showed minimal downregulation of CD4 (a typical feature associated with PMA stimulation[372]). As PMA readily passes through phospholipid cell membranes and triggers PKCθ signalling from the inside of the cell[366] it is improbable that these cells had not encountered the stimulus in a 6h culture and their small decrease in CD4^{+} expression was indicative of this. Their hyporesponsiveness was striking and so the biology of these 'non-responsive' cells was analysed in depth to ascertain what they represented. It is acknowledged that there was also a CD4^{+} cytokine^{-ve} population that did activate readily but these cells were not investigated further in this study. Potential characteristics of these cells are alluded to in the discussion of cytokine^{-ve} cell biology above.

Based on initial analysis of PBMC cultures the non-responsive CD4^{+} T cell population had a T_{cm} (CD45RA^{-}CCR7^{+}) phenotype (Figure 3.11C). It was unexpected that a subpopulation with such quiescent-like characteristics would be found within the T_{cm} subset. However, this finding was refuted through retrospective examination of T_{cm} frequency in the blood. It appeared that T_{cm} cells were the main contributors to the non-responsive fraction because numerically they are represented almost 4 times greater than T_{eff} cells in the blood (Figure 3.12). This was confirmed by removing the T_{cm}/T_{eff} population bias via an alternative gating strategy, which showed that non-responsive cells were a heterogeneous mix of T_{cm} and T_{eff} phenotypes (Figure 3.11D). However, this heterogeneity was not recapitulated when T cell memory subsets were separated and stimulated independently. Here the T_{eff} subset had by far the largest non-responsive population whereas there was minimal representation in purified T_{cm} cell cultures (Figure 3.13).

A possible explanation for this disparity is that T_{eff} cells upregulated CCR7 expression in the PBMC cultures and made it appear like more T_{cm} did not respond. However, there is no published data suggesting that PMA/ionomycin stimulation induces CCR7 expression in the T_{eff} population. An alternative explanation is that some T_{eff} cells expressed CCR7 prior to the culture which also would have been undetectable in post-stimulation analysis. Since the CCR7/CD45 definition of memory was established *by F. Sallusto et al (1999)* subsequent studies have demonstrated that CCR7 expression by T_{eff} cells is necessary for peripheral tissue egress and their re-entry into the circulation [57,95]. Therefore the CCR7/CD45 isoform definition is not stringent and T_{eff} cells can transiently express CCR7[391]. Experiments here where T_{cm} and T_{eff} cells with varying expression of CD62L were stimulated independently supported this explanation as to why more non-responsive cells appeared to have a T_{cm} phenotype in PBMC cultures (Figure 3.14). Findings showed that a high proportion of the T_{cm} ($CD62L^{lo}$) cell cultures were non-responsive. Given that T_{cm} are classically associated with both $CCR7^{+}$ and $CD62L^{hi}$ expression it is possible that this purified $CD45RA^{-}CCR7^{+}CD62L^{lo}$ population was highly non-responsive because it actually represents a $CCR7^{+}$ T_{eff} subset. However, work examining the expression of CD27 on sorted T_{cm} and T_{eff} $CD62L^{hi/lo}$ sorted fractions counter argues this theory (Figure 3.15). CD27 expression is progressively lost during T cell differentiation[379] so it was anticipated that CD27 expression by the T_{cm} $CD62^{lo}$ population would be analogous to the T_{eff} subset if they were truly $CCR7^{+}$ T_{eff} cells. This was not the case and loss of CD27 correlated with the progressive loss of CCR7 and CD62L from T_{cm} to T_{eff}. However, the non-responsive fractions did have reduced CD27 expression regardless of their concurrent phenotype indicating that these cells may have undergone more proliferation than their subset-matched responsive counterparts. This may not necessarily be antigen-driven as high levels of homeostatic proliferation in the T_{cm} subset can drive a conversion through to a $CD27^{lo}$ phenotype[392]. $CD27^{lo}$ expression is amongst the defining feature of senescent T cells which have reached the limit of their replicative potential[393].

However, without additional markers of senescence such $CD28^{lo}$ and $CD57^{hi}$ expression it cannot be definitely established that the non-responsive population is representative of senescence T cells.

Collectively evidence from this study suggests that the non-responsive population is a differentiated effector memory phenotype. This population did not belong to a non-classical T_{helper} lineage (such as NK-like cells, $CD4^+CD8^+$ lymphocytes and TCRγδ T cells) which may have contributed to their differential response to PMA/ionomycin. CD69 expression by $CD4^+$ T cells is shown to peak by 12 hours following PMA exposure[394]. Other studies report maximal CD69 expression by 6 hours in response to various stimuli[42,395,396] which is consistent with data presented here and reflected in a stabilisation of the non-responsive population between 4-6h. The non-responsive population had no cytosolic stores of CD69 receptor at this time point as the $CD69^{lo}$ signal persisted when $CD4^{int}CD69^{lo}$ cells stained intracellularly (Figure 3.25). Expression of CD69 protein is dependent on translation of mRNA that is expressed *de novo* following activation[397]. The absence of CD69 expression by non-responsive cells is likely to be a consequence of deficient signal transduction upstream of gene transcription. This is supported by gene expression analysis which showed that CD69 expression by non-responsive T_{eff} cells was comparable to that of unstimulated memory cells that do not express CD69 protein (Figure 3.27-3.28). Surprisingly, the expression of CD69 transcript was greater in non-responsive and unstimulated memory populations than in the corresponding responsive or stimulated fractions (Figure 3.27-3.28). However, published data measuring the kinetics of CD69 transcription from both peripheral blood lymphocyte and T cell cultures shows CD69 transcript is detectable at 30min but levels decline rapidly from 6-8 hours[397,398]. Therefore, although the end point of this assay was at 4 hours it is possible that CD69 mRNA expression is already declining in the responding and stimulated T_{memory} populations in this system. In these populations CD69 expression may dip below that seen in unstimulated cultures due to overuse or degradation of mRNA transcripts to a refractory level.

To confirm these theories the transcriptional kinetics of this system could be measured by performing a time course of CD69 mRNA expression in activated T_{eff} cultures every 2h for a 12h period.

Surprisingly, expression of IFNγ at the message level followed the same trend as CD69 with the stimulated (and responsive) fractions showing diminished mRNA expression comparative with unstimulated (and non-responsive) cells (Figure 3.29). This is inconsistent with published findings and could not be explained by the cytokine's expression kinetics. It is well reported that IFNγ message is undetectable in resting $CD4^+$ T cells but levels rise immediately following activation[387,399]. IFNγ mRNA expression is shown to be monophasic and persistent for over 72h in response to various polyclonal and antigen specific stimuli[400]. However, PMA/ionomycin is underrepresented as a method of stimulation in such studies and alternative stimuli such as phytohemagglutinin and anti-CD3/CD28 are more frequently reported. In T_{memory} populations *W. Lai et al (2011)* show that NF-κB interaction with the IFNG gene promotor rapidly drives IFNγ expression to high levels[399]. This T-bet independent process underpins the rapid recall responses of memory $CD4^+$ cells in a manner reminiscent of innate immune cell responses. However, others maintain that IFNγ induction is T-bet dependent, as is supported by significant levels of Tbet nuclear localisation pre-activation[401]. It is hard to relate the analysis of IFNγ expression from my investigation to either of these scenarios and my results remain unexplained. From a technical perspective it was considered whether PMA/ionomycin stimulation caused changes in the control gene GAPDH and aberrantly influenced the gene expression calculations. However, experiments where unstimulated and stimulated cells were compared confirmed that PMA/ionomycin exposure did not affect GAPDH expression (Figure 3.28). Despite this, it would be beneficial to repeat this analysis perhaps with the inclusion of an alternative control gene such as β-actin to reassess findings related to IFNγ gene expression.

The frequency of non-responsive cells was highly variable between donors; particularly in the T_{eff} compartment (Figure 3.9, Figure 3.13). Non-responsive cell frequency was unrelated to gender which suggests that the population is not influenced by levels of androgens, oestrogens or progestogens. However, a small increase in non-responsive cell frequency was noted with increasing age, although the age range tested was limited. If the non-responsive population are senescent their frequency would be expected to increase with age, so measuring their frequency in an elderly population may be informative. In addition to these variables the distribution and function of memory T cells is known to be affected by physical activity. Strenuous exercise can reduce the Th_1-associated cytokine responses of circulating $CD4^+$ T cells to PMA/ionomycin and this decrease correlates to levels of plasma epinephrine[402]. $CD4^+$ T cells express beta adrenergic receptors (notably the β_2 isoform) which can transduce signalling upon the binding of serum catecholamines[403] and levels of these increase during exercise or stress[404]. It is shown that circulating T cells increase during exercise which is followed by a paradoxical decrease on activity cessation achieved via their redistribution into the peripheral tissue [405]. This is partially attributed to the effect of glucocorticoid changes on chemokine receptors associated with homing[406]. Serum cortisol also fluctuates with time of day as part of natural circadian rhythm and also alters distribution of lymphocyte populations and their activity[407]. In this investigation the time of blood sampling and activity levels of the donors were controlled variables so the significance of such effects is questionable in this system. However, to directly negate the influence of cortisol and adrenomedullary hormones upon non-responsiveness serum levels could be measured directly and correlated to the population's frequency.

There are other potential causes of the intra-donor variability in non-responsive cell frequency. Infection can have implications for T cell functionality that persist long after that infection is resolved. There is significant work in the literature describing a refractory period exhibited by activated $CD4^+$ T cells[408–410]. *C.T Duthoit et al (2004)* have documented that in

both *in vitro* and *in vivo* adoptive transfer models once stimulated with antigen, $CD4^+$ T cells are resistant to restimulation for a considerable period and may acquire suppressive functionality during this inactive phase[410]. However, my work suggested that the non-responsive population is not recently activated *in vivo* as the population persisted when those cells with physiological expression of CD69 were removed (Figure 3.16). That said, the expression of CD69 in T cell activation is phasic and it cannot be discounted that these cells have undergone *in vivo* activation some days previous and have subsequently lost CD69 expression. In *in vitro* cultures CD69 expression can be maintained for up to 72h whereas others show CD69 expression decreases to baseline between 24-72h in experiments using PBMC[42,411]. Therefore, the T cell hyporesponsiveness defined in my study may be due to a previous activation event and account for the variability in their frequency.

Like CD69, CD25 expression is also elevated on activated $CD4^+$ T cells as well as its association with T_{reg} biology. Initial experiments here examining whether the non-responsive population had a T_{reg} phenotype were based on a $CD25^{hi}$ phenotype alone (Figure 3.20). The $CD25^{hi}$ population had a greater proportion of non-responsive cells so it could be questioned whether these cells were true T_{reg} or actually activated conventional $CD4^+$ T cells. Work in mouse models suggests that IL-2 is essential for the functionality and maintenance of the T_{reg} population[156,412,413]. In mouse models animals deficient in the IL-2 signalling pathway (IL-$2R\beta^{-/-}$) lack $CD25^{hi}$ T_{reg} and $CD25^{hi}$ T_{reg} adoptively transferred IL-$2R\beta^{-/-}$ knockout mice cannot successfully expand[414]. In other studies addition of IL-2 to T_{reg} cultures from $CD69^{-/-}$ mice is shown to restore activation of the TCR pathway via phosphorylation of STAT5[415]. Addition of exogenous IL-2 did not perturb the non-responsiveness of the $CD25^{hi}$ population in my investigation which may suggest these cells are not a true T_{reg} phenotype. However, the poor purities of the T_{reg} and non-T_{reg} fractions in these experiments made subsequent analysis difficult to interpret.

The proportion of cells with a non-responsive phenotype in the T_{eff} subset was comparable in the T_{reg} and non-T_{reg} populations when these subsets were defined by CD25 with CD127 expression (Figure 3.21). Although T_{reg} were marginally less responsive than non-T_{reg} in this system they do not numerically predominate the non-responsive population due to their low frequency in the blood. Therefore, the non-responsive population is a mix of $CD25^{int}CD127^{int}$ and $CD25^{hi}CD127^{lo}$ subsets and this implies that T_{eff} are more non-responsive irrespective of their CD25/CD127 status. It is not possible to determine what the contribution of iT_{reg} or effector nT_{reg} is to the non-responsive populations described here as these subsets are phenotypically similar in terms of their CD25 and CD127 expression. However, it would be interesting to investigate whether the non-responsive cells in the non-T_{reg} compartment actually represent more atypical T_{reg} such as $Tr_{1.}$ Tr_1do not putatively express CD25 at rest and although surface markers to identify this rare subset are not firmly established candidate examples include CD49b and LAG-3 together with low FOXP3 expression[416].

Historically T_{reg} biology has been synonymous with the T cell tolerance and anergy but endogenous anergic T cells have not been identified *ex vivo*. In *in vitro* studies a feature of anergic T cells is the reversal of hyporesponsiveness through addition of exogenous IL-2[189,381]. In my investigation the presence of IL-2 did not reverse the non-responsive phenotype (Figure 3.20, Figure 3.24). IL-2 signalling reverses anergy through restoring the activity of AP-1[381]. As AP-1 deficiency (via lack of co-stimulation) is a key feature of anergy this suggests that the non-responsive phenotype is not anergic by the classical definition. The fact that the population was induced following anti-CD3/CD28 signalling where adequate co-stimulatory signalling was provided supports this assumption (Figure 3.6, Figure 3.14-3.15). However, an alternative form of hyporesponsiveness that is distinctive from 'anergy' is defined in the literature as 'adaptive tolerance' by *Schwartz R. H et al* and is not reversible by IL-2 signalling[188,190]. In adaptive tolerance cells are less responsive with respect to effector cytokine production and require the persistence of stimuli to remain

tolerised[190]. It is possible that the non-responsive phenotype is more consistent with adaptive tolerance than anergy although interrogation of their biochemical signalling pathways would be required to support this. Currently such work would be challenging given the populations low frequency and the inability to purify them without prior stimulation.

A feature shared between anergy and adaptive tolerance is the incomplete degradation of IκBα[190]. In anergised or tolerised cells release of NF-κB for nuclear translocation is prevented and its downstream effects are lost. It was suspected that this phenomenon was reproduced when a proteasome inhibitor was added to stimulated 6h cultures in this study (Figure 3.25). At high concentrations of this proteasome inhibitor Bortezomib (Velcade®) the non-responsive cell frequency was elevated and the expression of CD69 and IFNγ by responding cells decreased. This may indicate inhibition of the proteolytic degradation of IκBα amongst other NF-κB regulators and this is previously described in the context of Bortezomib as a therapy for multiple myeloma[417]. Such findings were a collateral effect of my assay design as it was intended to assess whether non-responsive cells had increased proteasome trafficking of activation-associated proteins. This is a feature associated with anergy via increased activity of ubiquitinase enzymes[172]. However, given the proteasome inhibitors effects on T cell activation this could not be appropriately measured in this system and this question requires an alternative strategy for investigation.

An additional mechanism of peripheral T cell tolerance is the deletion of self-reactive cells by apoptosis[418]. The induction of anergy and apoptosis are distinctive phenomenon on a signalling level and here I show that the non-responsive population was highly prone to the latter fate (Figure 3.17). PMA/ionomycin stimulation induced a considerable degree of cell death in both the non-responsive and responsive $CD4^+$ T cell populations particularly in cultures over 12 hours (Figure 3.7). This may be unsurprising as the effects of PMA/ionomycin stimulation are irreversible and excessive stimulation causes activation-

induced cell death (AICD). Compared with PBMC based assays the degree of T cell apoptosis did not reduce when subsets were purified prior to stimulation (Figure 3.19D). This suggests that the induction of apoptosis was a T cell intrinsic phenomenon and was not influenced by non-T cell subsets or soluble mediates released into PBMC cultures.

PMA/ionomycin exposure may be considered a cellular stressor given the metabolic requirements of the T cell response that it invokes[419]. It can be speculated that the non-responsive state is induced by abnormal metabolic processes as a result of activation. AMPK (5' AMP-activated protein kinase) is shown to activate the p38MAPK pathway in response to cellular stress, low glucose or DNA damage[420,421]. Therefore, in my investigation expression of AMPK was measured in stimulated cultures as a measure of metabolic regulation. AMPK was also a suitable candidate for analysis as the non-responsive population had demonstrated an increased fragility and diminished CD27 expression. *A. Lanna et al (2014)* show that increased AMPK induces p38 activation and is associated with $CD27^{-}CD28^{-}$ senescent $CD4^{+}$ T cells[422] . This is attributed to DNA damage in senescence and is reproducible through inducing DNA damage in more undifferentiated cells. The authors demonstrated the presence of unphosphorylated AMPK protein by western blot in primary $CD4^{+}$ T cells[422]. However, in my investigation no AMPK expression by memory CD4 T cells was detected by qPCR irrespective of PMA/ionomycin exposure. It cannot be distinguished whether this result reflects a genuine instability of AMPK mRNA at the message level, absence of constitutive transcription or accelerated degradation. A failure of the AMPK gene primers cannot be discounted in these experiments as no positive control for AMPK was tested.

The homeostatic cytokines IL-7 and IL-15 have an important role in the maintenance of the memory $CD4^{+}$ T cell population[423,424]. Addition of IL7, IL-15 or IL-2 to stimulation assays could neither reverse nor assist the survival of non-responsive cells (Figure 3.24). Even when removing the stimulus at 6 hours and allowing the cells to rest the population could not be maintained for over 24 hours irrespective of homeostatic cytokine. With acknowledgement to

the fragility of the population it was speculated whether it represented a collection of dying cells and thus a non-physiological by-product of the *in vitro* system. However, this can be refuted on a number of levels. Firstly, the non-responsive population was a homogeneous memory phenotype. If it represented apoptotic cells more heterogeneity and the inclusion of T_{naive} cells may have been expected. Secondly, with consideration to morphological changes that occur in early apoptosis those cells that were apoptotic *in vivo* would not fall within a viable lymphocyte gate in flow cytometry experiments after 6 hours of culture. Lastly, when dead cell exclusion dyes were used in these assays the majority of non-responsive cells were viable indicating that failure to upregulate CD69 was not a consequence of cell death. In summary, although the non-responsive population is more prone to apoptosis this is an effect of their lack of response to PMA/ionomycin as opposed to a cause of it. Therefore, PMA/ionomycin is revealing a set of cellular characteristics that are distinctive in this population and require further investigation.

Anti-CD3/CD28 Dynabead® stimulation also revealed a hyporesponsive population analogous to that revealed by PMA/ionomycin (Figure 3.6, Figure 3.14-3.15). However, non-responsive cells in these assays did not downregulate CD4 and were more frequent in analysis of both T_{naive} and T_{memory} populations. The latter may be explained by the methodology of stimulating T cells with CD3/CD28 coated beads, as unlike with PMA/ionomycin it cannot be guaranteed that every cell in the culture has engaged the stimulus. Therefore, the non-responsive population in these assays is likely to be contaminated with unstimulated cells. Despite this discrepancy in frequency the similarities in CD69 kinetics, lack of CD69 upregulation and analogous differentiation status is supporting evidence that the non-responsive population can be induced physiologically and has relevance *in vivo*.

Studying the non-responsive population and their intracellular signalling was associated with various challenges in this investigation partially due to low cell counts and the inability to maintain them in long-term cultures. It would have been favourable to examine

phosphorylation events in PMA/ionomycin-induced signalling pathways by western blot but there were insufficient cell numbers to do this. From a gene expression perspective the desired approach was to perform a T-cell receptor-specific gene array to analyse differential expression of 96 genes between responding and non-responsive T_{eff} populations. Recovered cDNA preparations were again insufficient in quantity for this extensive analysis. Due to these technical barriers an alternative approach was adopted where the expression differentials of three candidate T cell signalling genes (for LCK, PKCϴ, VAV-1) were measured independently by multiplex qPCR (Figure 3.30-3.31). PKCϴ is the main target for PMA binding and PKCϴ expression is an absolute requirement for CD69 upregulation[365,425], so it was considered whether PKCϴ deficiency was responsible for the non-responsive state. Conversely, PKCϴ activation drives AICD through caspase-8 induced FAS/FASL related interaction[426] so it's over expression may be driving apoptosis in the non-responsive state. LCK was investigated due to the minimal downregulation of CD4 in the non-responsive population. In appropriately activated cells PMA induces CD4 downregulation via the uncoupling of CD4 to $p56^{lck}$ (protein product of the LCK gene) through PKCθ-driven phosphorylation of Ser^{408} and Ser^{415} on the CD4 cytoplasmic tail[427,428]. This leads to increased clathrin-mediated endocytosis of the CD4 receptor and its diversion away from the endosomal membrane recycling pathways once internalised[372]. With regards to the activity of VAV-1 this guanosine nucleotide exchange factor is required for PKCϴ translocation to the immunological synapse in T cell activation[429]. In other reports phosphorylation of VAV-1 is a prerequisite for calcium flux which is an integral requirement for complete T cell activation[430,431]. VAV-1 expression was also investigated as the ubiquitin ligase Cbl-b negatively regulates VAV-1 activity and this relationship is a proposed mechanism of T-cell tolerance[180].

PMA/ionomycin induced increased expression of all three signalling genes comparative to baseline with LCK most notably upregulated (Figure 3.30). This may imply that a feedback

loop operates to stabilise these mRNA's or increased their transcription following PMA/ionomycin-induced activation. There were no such differences in expression observed between the purified non-responsive and responsive fractions (Figure 3.31). This was unexpected although the non-responsive and responsive populations did not exactly match the control cultures in terms of memory phenotype which may have contributed to this inconsistency. However, the data suggests that differential expression of LCK, PKCϴ and VAV-1 does not contribute to the differential response to PMA/ionomycin seen in these assays. Despite this, some involvement of these signalling components cannot be discounted as changes in their phosphorylation status or localisation were not measured in these assays.

Although informative the expression analysis of the non-responsive population was not completed in this investigation. To move experiments forward the requirement for a concise definition of surface markers to identify the non-responsive population is essential. Currently experiments are limited by the inability to purify the population without revealing the phenotype through PMA/ionomycin stimulation. This stimulation ultimately induces cell death and the material recoverable through post-stimulation sorting strategies is limited. cDNA amplification techniques could be applied to future studies to boost the amounts of genetic material obtainable from purified non-responsive cells. Through this a more wide scale gene array approach could reveal a detailed surface receptor profile associated with the non-population to take forward subsequent strategies.

CHAPTER SUMMARY

This work identified a subpopulation of $CD4^+$ cells whose phenotype was revealed through a hyporesponsiveness to PMA/ionomyin and anti-CD3/CD28 stimulation. These cells were characterised by the surface expression of $CD4^{int}CD69^{lo}CCR7^{+/-}CD45RA^-CD62L^{lo}CD27^{lo}$ which suggests they are a highly differentiated memory phenotype. However, their PD-1 expression was associated with their memory status and not their hyporesponsiveness *per se*, indicating that these cells are not 'exhausted' by means of the classical definition.

PMA/ionomycin is routinely used universally to reveal the cytokine potential of T cells and here I demonstrate that a notable proportion of T_{eff} cells are programmed to be driven towards apoptosis by this stimulus. This investigation highlights that the effect of PMA/ionomycin on T cells is not equivocal even within a particular subset and subsequent analysis should thus be treated with caution.

The non-responsive population did demonstrate features associated with *in vivo* adaptive tolerance as opposed to clonal anergy, meaning further understanding of this population's biology is highly relevant to these fields. It would be of interest to investigate the clonality of the population and access whether they were driven to an irreversibly hyporesponsive state through chronic viral infection. This work may also have implications in tumour immunology, with respect to the evasion of cancerous cells from the immune system through chronic antigen presentation to T cells. It could be argued that these cells must activate in response to some stimulus but the relevant signals required to facilitate activation are yet to be identified.

CHAPTER 4

RESULTS

CHARACTERISATION OF CEREBROSPINAL FLUID DERIVED $CD4^+$ T CELLS IN HEALTH AND DISEASE.

4 CHARACTERISATION OF CEREBROSPINAL FLUID DERIVED CD4$^+$ T CELLS IN HEALTH AND DISEASE.

4.1 Rationale.

Many studies have described the cellular components of CSF in various neuroinflammatory patient cohorts[248,271,432]. Despite such work there has been little focus upon CSF cells in the context of human health until relatively recently. CD4$^+$ T cells are now recognised as the predominant CSF leukocyte subset in both the absence and presence of disease and are largely a central memory phenotype in humans (CD45RO$^+$CCR7$^+$)[247,288]. However, fundamental aspects of CSF CD4$^+$ T cell biology are under defined. These include the specificity of homeostatic CD4$^+$ T cell migration from blood to CSF under resting conditions and the anatomical localisation of these cells within the fluid and associated stromal compartments. Analysis of 'normal' human CSF is restricted as the sampling procedure is highly invasive and cannot be performed ethically in healthy individuals. Therefore to study normal CSF it is often modelled in patients who lack inflammatory disease but require this procedure for diagnostic or therapeutic purposes. An alternative system is to model normal CSF and its associated compartments in naïve rodents that do not have any underlying pathology. At present there are minimal publications that make use of this method to investigate homeostatic CNS migration. In this chapter T cell subsets associated with unchallenged mouse and rat CNS are characterised by their surface marker expression and anatomical distribution within the brain. Such work compliments a comparative analysis of peripheral blood and CSF-derived T cells from a patient cohort without inflammatory disease. In parallel with this investigation inflammation-driven changes to CD4$^+$ T cell populations are measured in patients with multiple sclerosis and other neuroinflammatory pathologies.

Hypotheses applicable to this work are that in man central memory (CCR7$^+$CD45RO$^+$) CD4$^+$ T cells are enriched in the CSF through selective recruitment from the blood and this trend is upheld through the analogous central memory population in mouse (CD44^{hi}CD62L^{hi}).

Additionally, $CD4^+$ T cells associated with unchallenged mouse CNS are localised to the choroid plexus regions which is described as the primary location of $CD4^+$ T cell migration into brain in many publications[253,271,433] . As it is proposed that the *glia limitans* limits T cell entry into the brain parenchyma in the absence of inflammation[257] it is hypothesized that no $CD4^+$ T cells will be associated with the parenchymal compartments in this study.

4.2 Validation of the immunofluorescence protocol for detection of $CD4^+$ T cells in mouse CNS tissue.

Experiments were performed to identify $CD4^+$ T cell niches in unchallenged murine brain. Confocal microscopy was the appropriate analytical tool for this exercise, but given that the anticipated frequency of $CD3^+CD4^+$ T cells in brain was extremely low it was important to establish that these cells were reliably detectable. The staining and imaging process was validated by imaging sections of murine spleen, which were treated identically to CNS preparations and acted as a positive control for the immunofluorescence procedure (Figure 4.1). Figure 4.1A shows isotype control images of murine spleen stained with irrelevant IgG and with the nuclear counterstain DAPI. Imaging parameters applied to the isotype control staining were used to set the threshold of specific positive staining for CD3, CD4 and B220 (Figure 4.1B). In these experiments T cell zones of the spleen were clearly identified by co-localisation of $CD3^+$ and $CD4^+$ staining. In addition, images showed $B220^+$ cells within B cell areas which were largely distinct from CD3 or CD4 staining. These experiments demonstrated the ability to detect $CD4^+$ T cells in this system.

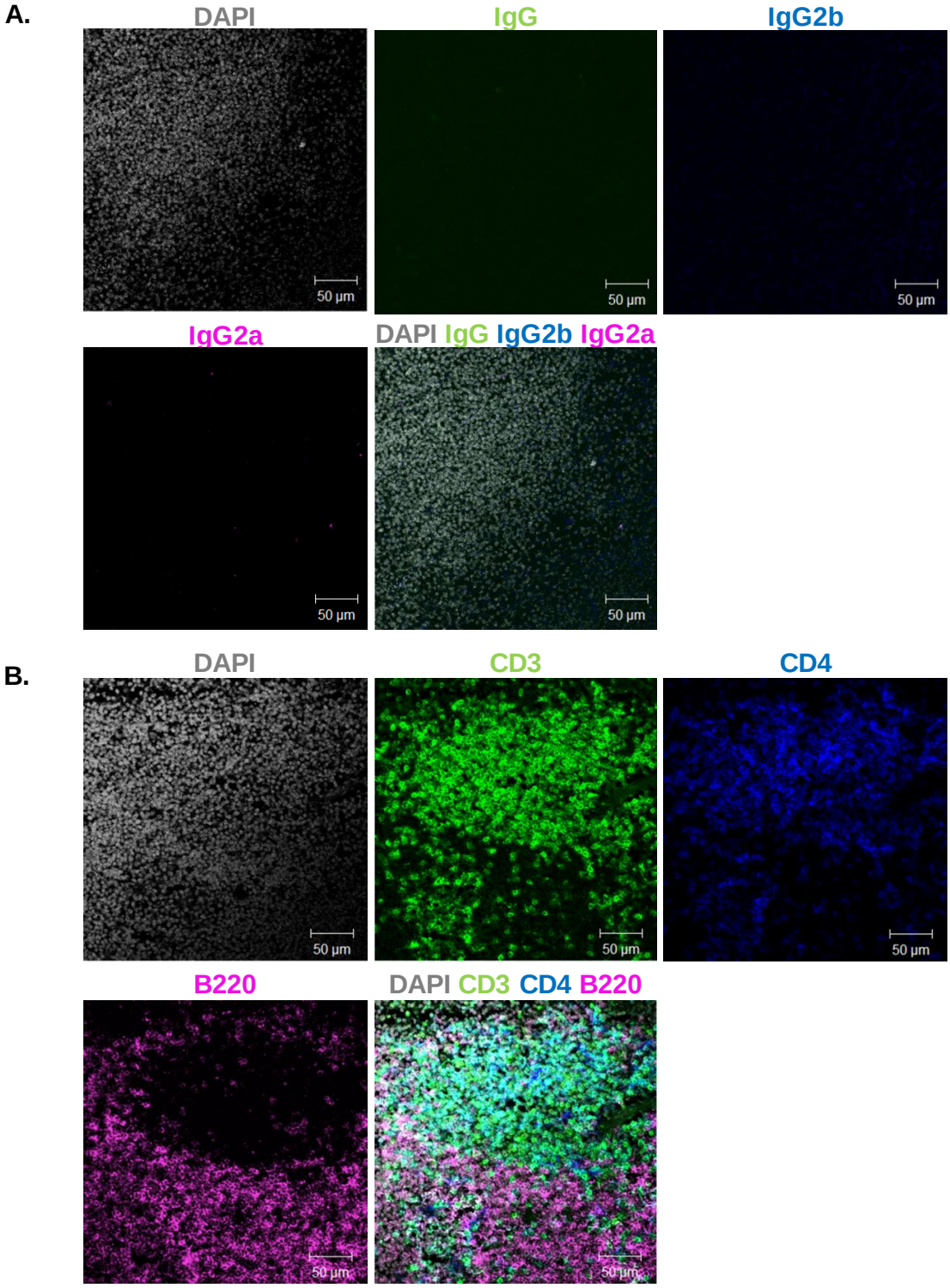

Figure 4.1 Confocal imaging of T and B cell areas in murine spleen tissue. C57BL/6 mice were intra-cardially perfused post mortem with PBS and fixative. Brain tissue was harvested for confocal analysis of infiltrating $CD4^+$ lymphocytes ($CD3^+CD4^+$). As a positive control for each brain imaging experiment spleen were also harvested, sectioned and stained for CD3 and CD4 using the same protocol. Spleen was also stained with B220 to differentiate between T and B cell areas of the tissue. **A.** Single colour and composite confocal images of the isotype control staining performed on spleen sections. **B.** Confocal images of specific lymphocyte staining taken under the same parameters as the isotype controls shown in **A.** A nuclear counterstain (DAPI) was used in both isotype control and specific staining experiments. Data is representative n=2 independent experiments with 6-10 images taken per experiment.

Isotype control parameters set on spleen sections could not be applied to the imaging of brain sections due to differences in the intensity of non-specific staining and background autofluorescence. Therefore single colour isotope control staining for CD3 and CD4 was performed on brain sections to set the threshold for a positive signal (Figure 4.2). The autofluoresence of different anatomical areas of the brain was variable and confirmed by imaging the sections without performing any staining (data not shown). Therefore, regional isotype control staining was performed in multiple brain areas and specific staining was indicated in accordance with the corresponding isotype parameters.

4.3 Image analysis of $CD4^+$ T cells in murine choroid plexus tissue

Imaging of murine CP was performed on lateral ventricle CP located within sections of the midbrain region. The CP structure was occasionally pressed against the wall of the ventricles due to effects of the sectioning procedure, but more often it was observed free hanging into the ventricular space. The tissue was clearly recognisable through the organisation of its distinctive large cuboidal epithelium layers arranged in elongated villous projections (Figure 4.3). Embedded within the CP tissue positively stained $CD3^+$, $CD4^+$ and $CD3^+CD4^+$ cells were observed (Figure 4.3). Co-localisation of CD3 and CD4 positive staining indicated the presence of $CD4^+$ T cell associated with the tissue. However, this was only just detectable above the level of the background autofluorescence.

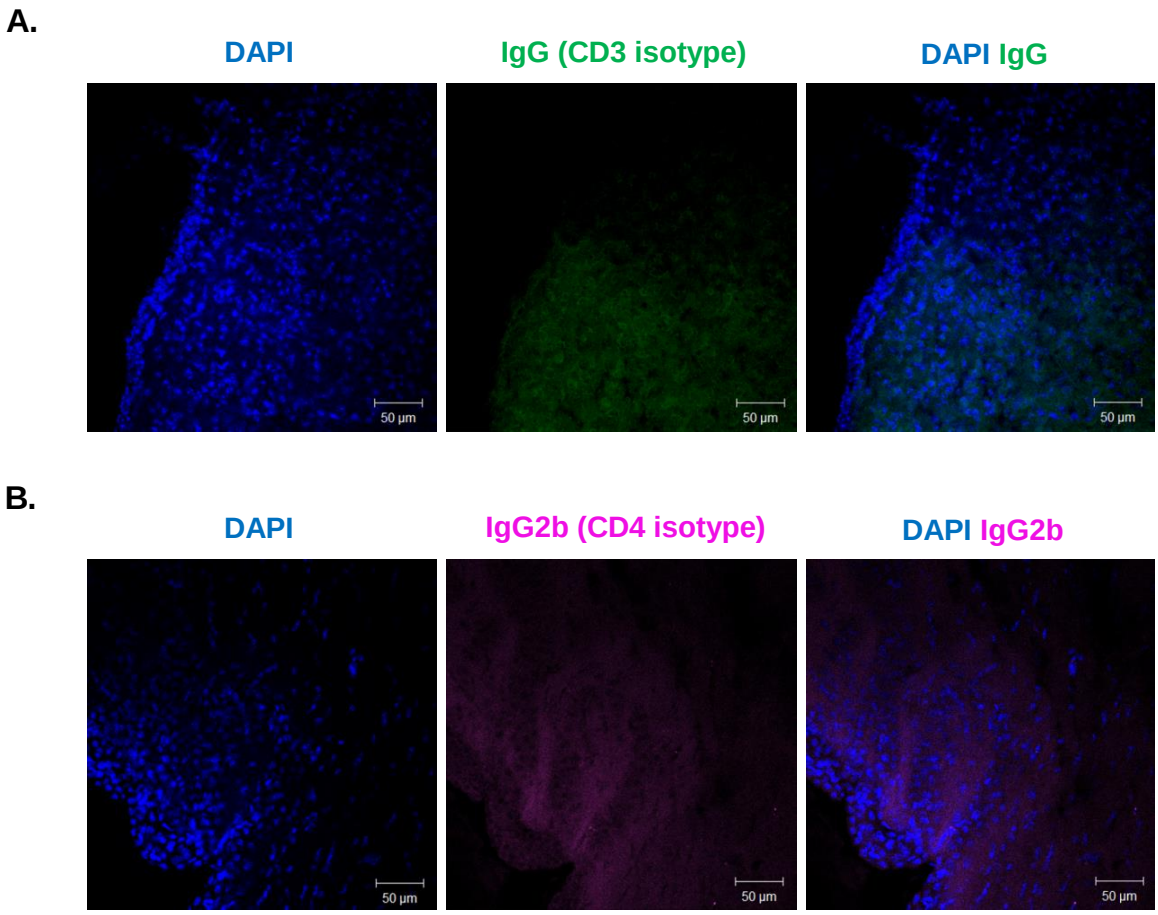

Figure 4.2 Isotype control imaging for lymphocyte staining in CNS. C57BL/6 mice were intra-cardially perfused post mortem with PBS and fixative. Harvested intact brain tissue was fixed frozen, sectioned and stained for CD3 and CD4 with a nuclear counterstain (DAPI). Single colour isotype control staining was performed to set the fluorescence intensity threshold of specific positive staining. **A.** Representative image of brain outer cortex showing the level of background staining from a CD3 isotype control. **B.** Representative image of the periventricular region of the midbrain (ventricle is shown left bottom corner of frame), showing isotype control staining for CD4. Images are representative of 3-5 images taken in n=3 independent experiments.

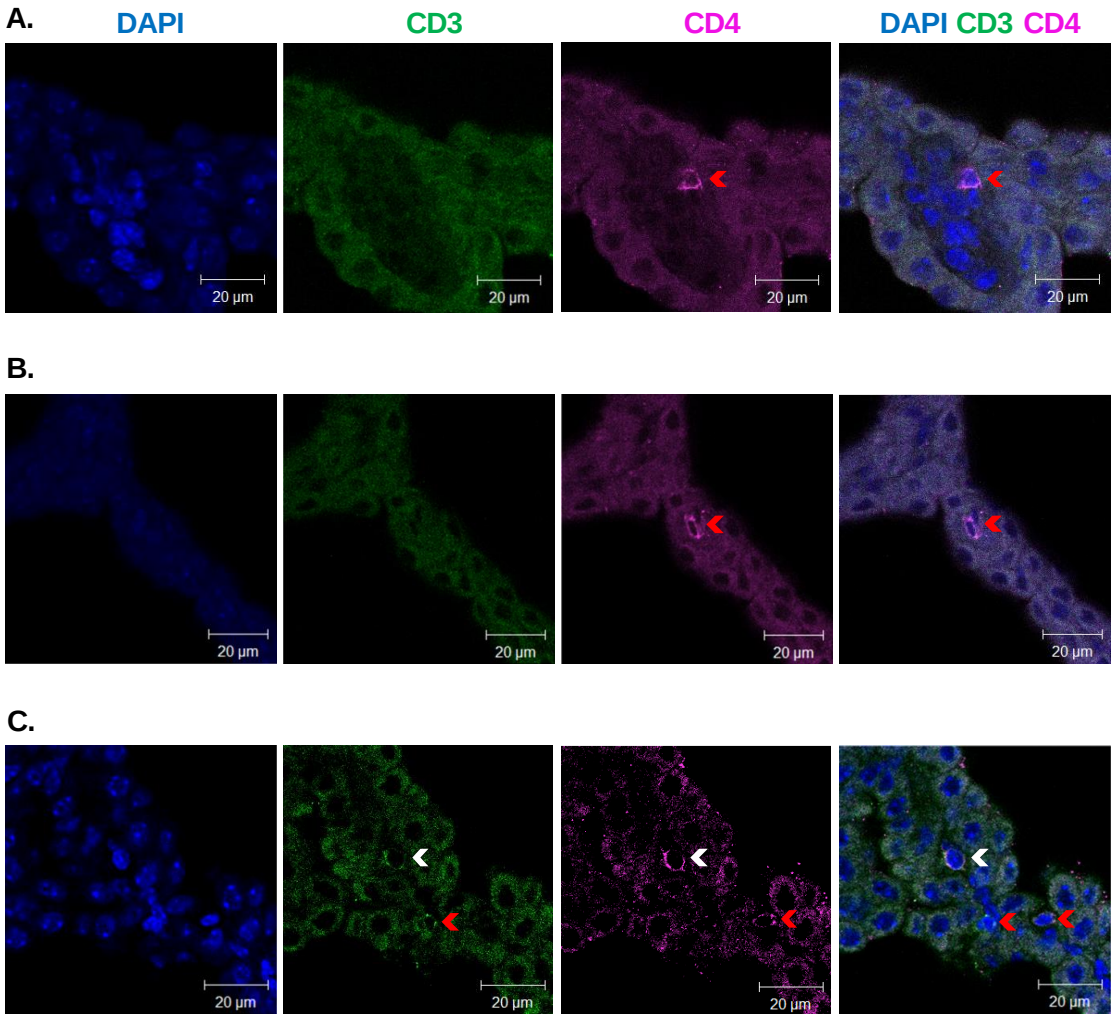

Figure 4.3 Confocal imaging of $CD3^+$ and $CD4^+$ cells associated with murine choroid plexus tissue. C57BL/6 mice were intra-cardially perfused post mortem with PBS and fixative. Harvested in tact brain tissue was fixed frozen, sectioned at 20µm thickness and stained for CD3 and CD4. Midbrain sections were mounted using medium containing DAPI (nuclear stain) and confocal images were captured of the choroid plexus tissue at a x40 objective magnification. **A,B.** Images show single stained (red arrows) $CD4^+$ cells in the choroid plexus tissue. **C.** Images show a single stained $CD3^+$ cell (red arrow) and co-localised staining by a $CD3^+CD4^+$ T cell (white arrow). Positive staining was set as an intensity above the threshold of single stained matched isotype controls. Images shown are of representative of n=2 experiments were n=6-8 images captured at this magnification per experiment.

4.4 Quantification of $CD4^+$ T cells in unchallenged murine CNS by confocal microscopy.

The frequency of $CD4^+$ T cells associated with CP was then measured with respect to other regions of the brain. Figure 4.4 shows nuclear staining performed on a whole mouse coronal brain section. This image represents multiple images captured on an epifluorescence microscope that are digitally reconstructed to recreate a map of the brain section. The associated extracted regions show the four brain areas selected for analysis of lymphocyte infiltration. As epifluorescence microscopy was found to be insufficient for this purpose, the meninges, cortex, periventricular, and CP regions were analysed individually by confocal microscopy (Figure 4.5A-D)). In these experiments, multiple images were taken of each region and the $CD3^+$, $CD4^+$ and $CD3^+CD4^+$ cells counted in each field of view. The average frequency of each phenotype per field of view was recorded and these values were recalculated to represent the frequency of each cell type per mm^2 of tissue (Figure 4.6). Results showed representation of all three phenotypes was extremely low with no evidence for any positive cells embedded within the cortex parenchyma (Figure 4.5B, Figure 4.6). $CD3^+$ and $CD4^+$ single positive cells had the greatest representation in the meninges and these populations tended to be clustered together rather than dispersed across multiple captured images (Figure 4.6A). A very low frequency of $CD3^+$ cells were also identified in the periventricular and CP regions (Figure 4.6A), whereas $CD4^+$ cells were restricted to the meninges and CP (Figure 4.6B). It is likely that a $CD3^+CD4^-$ signal represented the presence of $CD8^+$ T cells but direct staining for CD8 was not performed to confirm this. $CD3^+CD4^+$ cells were only identified in the CP and periventricular regions, albeit at a lower frequency than the single positive cells (Figure 4.6C). This result showed that $CD3^+CD4^+$ T cells were predominantly associated with the CP and ventricular system in these experiments.

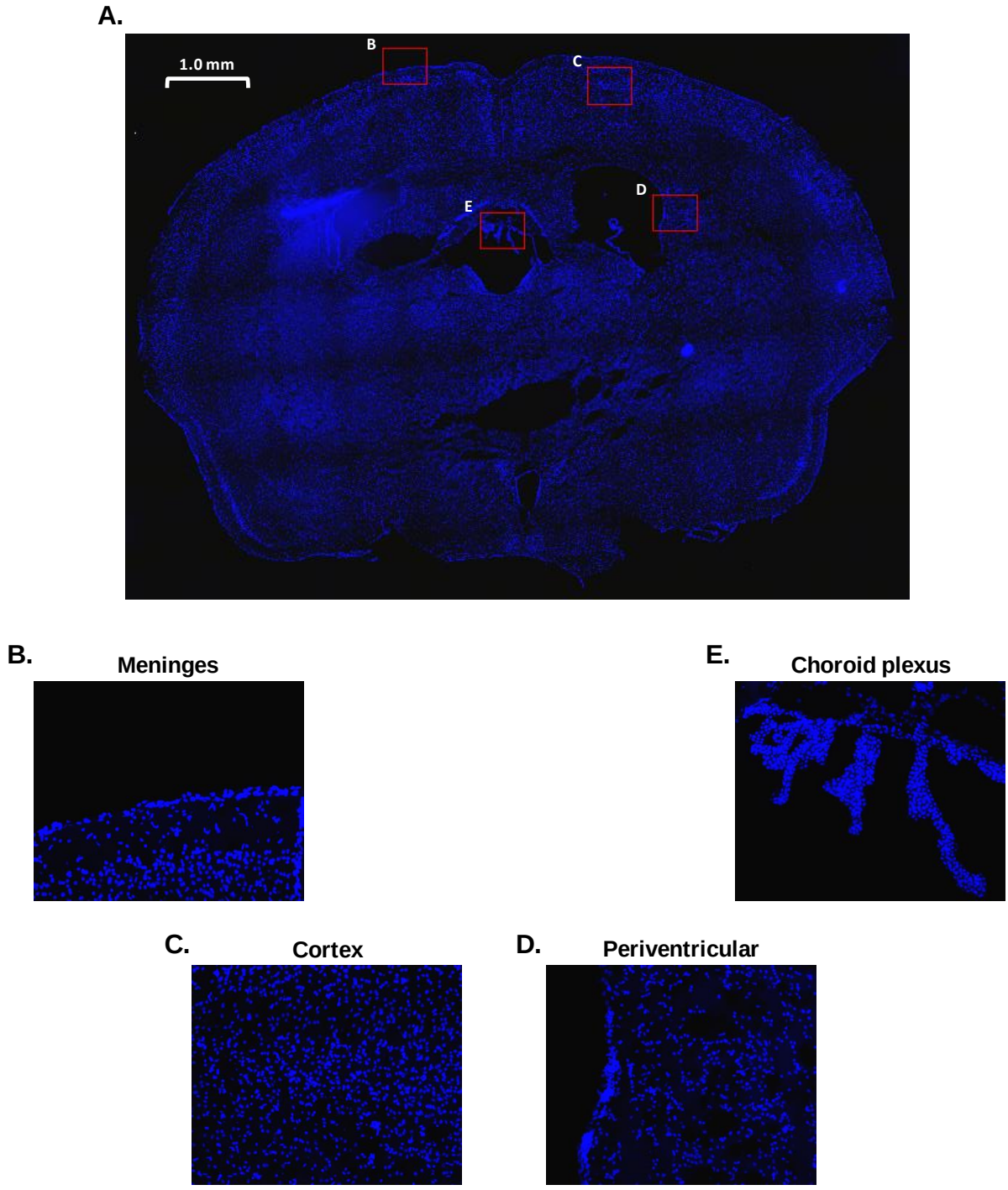

Figure 4.4 Imaging strategy for identification of CNS-associated CD4$^+$ T cells. C57BL/6 mice were intra-cardially perfused post mortem with PBS and fixative. Harvested in tact brain tissue was fixed frozen, sectioned at 20μm thickness and stained for CD3 and CD4. Sections were mounted using medium containing DAPI (nuclear stain). Four brain regions were selected to quantify the frequency of lymphocytes in each area. **A.** Image shows nuclear staining (DAPI) of a whole midbrain coronal section. Image represents multiple fields captured by an epifluorescence microscope that are digitally reconstructed to produce the complete image. Four selected brain regions for subsequent analysis are shown (B-E). **B-E.** Images show enlarged extracted regions from areas indicated in **A.** and demonstrate nuclear staining in the regions later analysed for T cell infiltration. Images are representative of serial midbrain sections taken from n=1 brain dissection.

A.

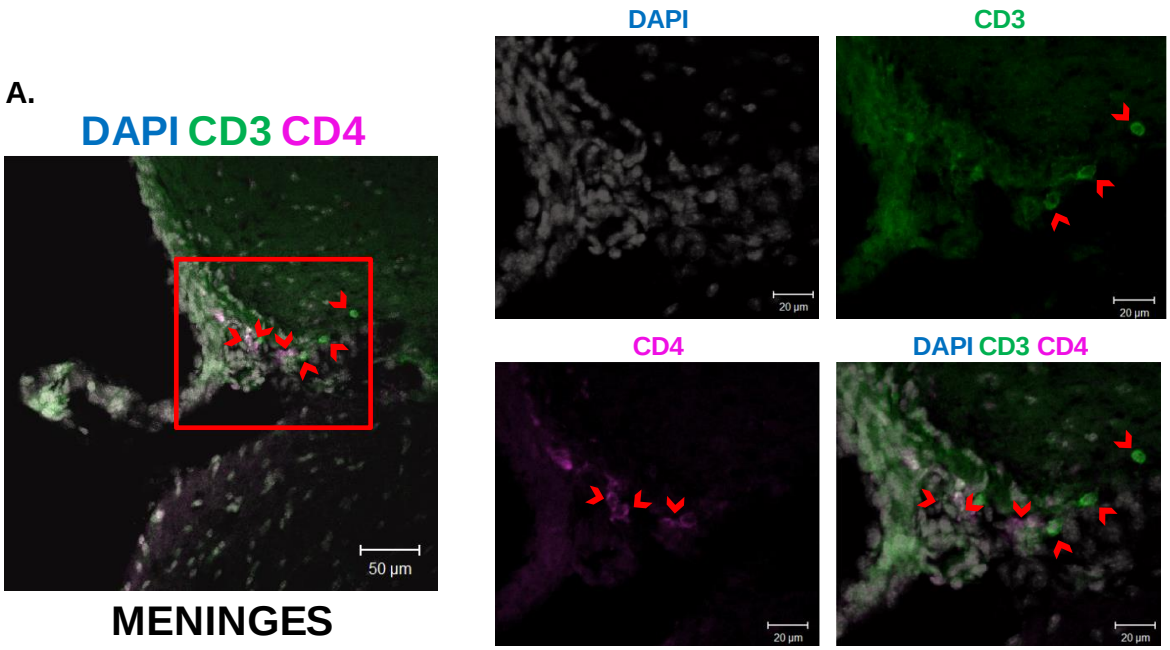
DAPI CD3 CD4
50 µm
MENINGES
DAPI
CD3
CD4
DAPI CD3 CD4
20 µm

B.

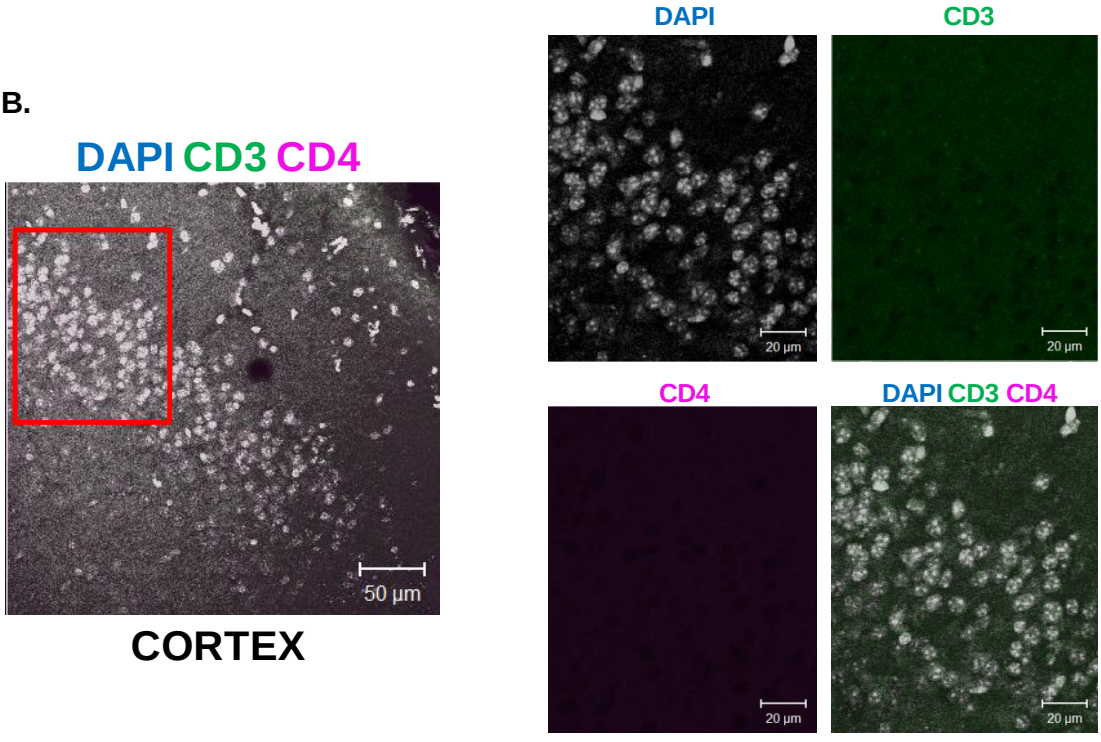
DAPI CD3 CD4
50 µm
CORTEX
DAPI
CD3
CD4
DAPI CD3 CD4
20 µm

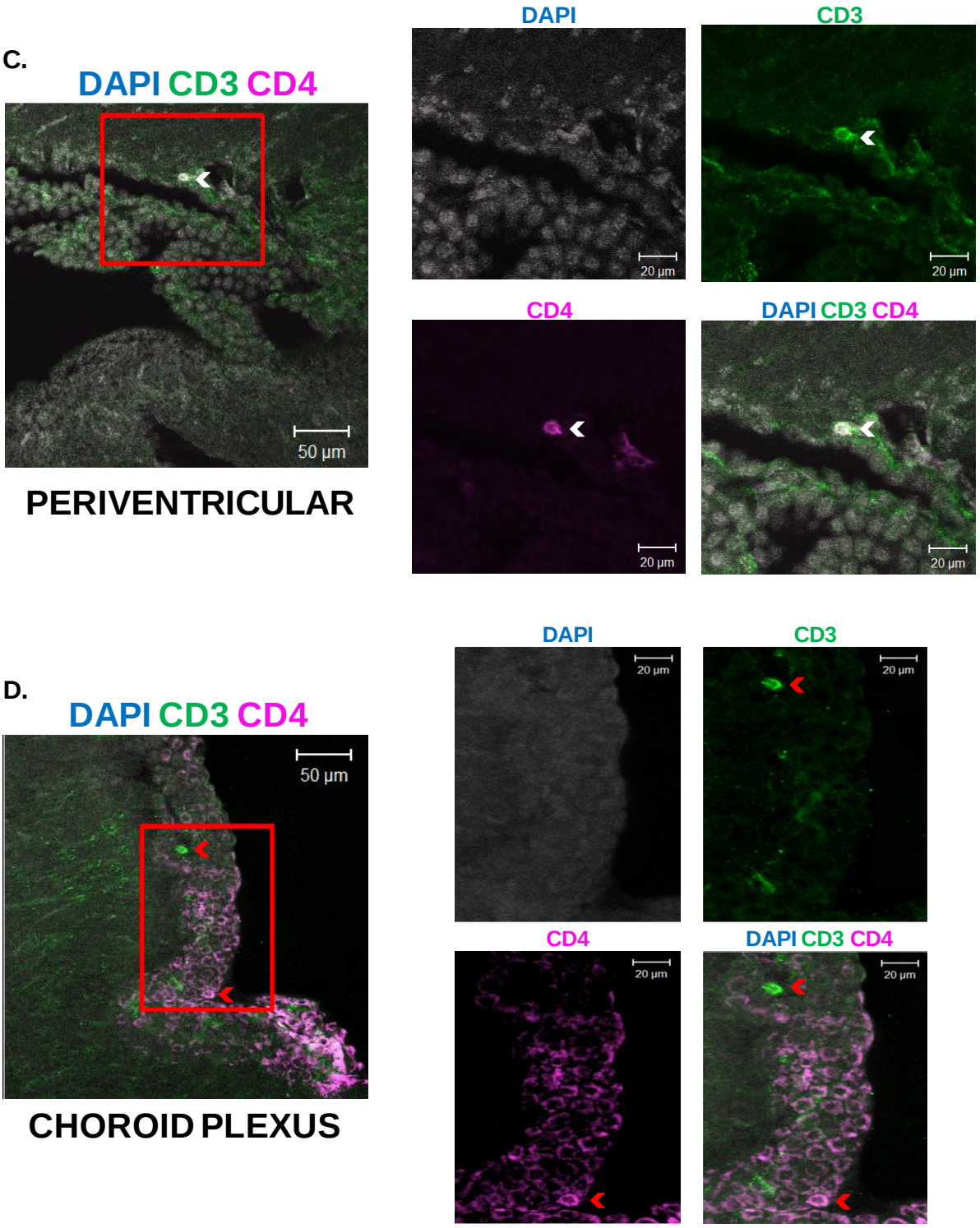

Figure 4.5 Confocal images associated with the quantification of $CD3^+$ and $CD4^+$ cells in murine CNS. C57BL/6 mice were intra-cardially perfused post mortem with PBS and fixative. Harvested in tact brain tissue was fixed, sectioned and stained for $CD3^+$ (green) and $CD4^+$ (magenta) then counterstained with DAPI (nuclear stain). Representative confocal images of four investigated brain regions are shown **A-D.** (**Left panel**). $CD3^+$ and $CD4^+$ cells are indicated by red arrows. The red box (left) indicates an enlarged extracted region, with associated single colour and composite images shown in the right panel. Images are representative of n=2 independent experiments with 5-12 images captured per experiment.

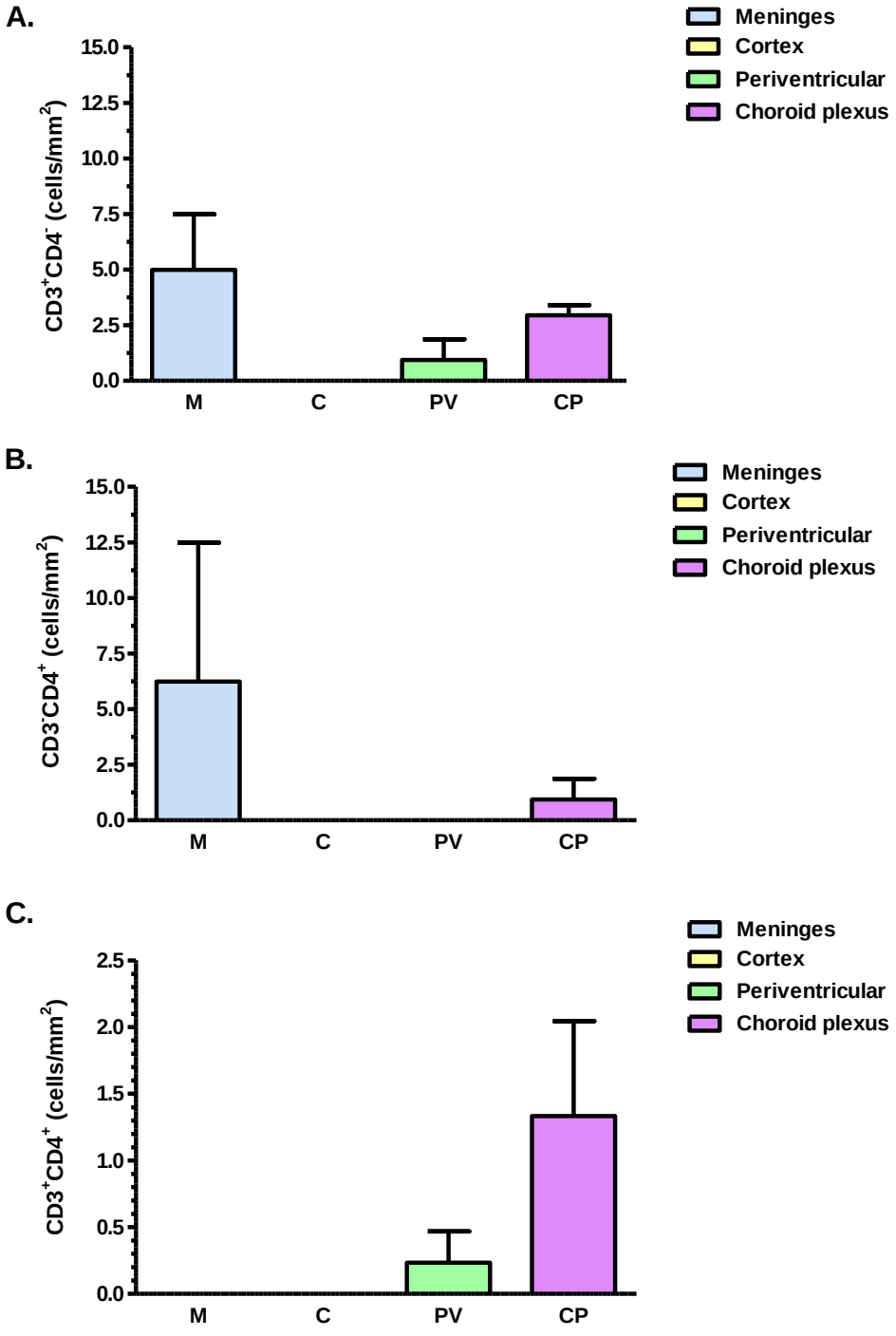

Figure 4.6 The frequency of cells with a $CD3^+$, $CD4^+$ or $CD3^+CD4^+$ dual expression phenotype in four regions of murine brain tissue. C57BL/6 mice were intra-cardially perfused post mortem with PBS and fixative. Harvested in tact brain tissue was fixed and serial sections taken of the midbrain region. Sections were stained for CD3 and CD4 with a nuclear counter-stain. Multiple confocal images were captured of the meningeal layer, the cortical region, the periventricular area and the choroid plexus. The frequency of $CD3^+$, $CD4^+$ and $CD3^+CD4^+$ in each random field of view was quantified and multiplied to give a cell count per unit area for each phenotype. **A.** Graph showing the mean ± SEM frequency of $CD3^+$ single stained cells per mm^2 in each brain region measured. **B.** Graph showing the mean ± SEM frequency of $CD4^+$ single stained cells per mm^2 in each region. **C.** Graph shows the mean ± SEM frequency of $CD3^+$ $CD4^+$ dual stained cells per mm^2. Data is representative of n=2 independent experiments with 4-12 images taken per region in each experiment.

4.5 Dissection of rodent CNS tissue for analysis of associated $CD4^+$ T cells.

Having used imaging to investigate the location of $CD4^+$ T cells within murine CNS compartments, flow cytometry was considered more appropriate for detailed phenotypic analysis of CNS-associated T cell subsets in rodent. For these experiments CNS-associated lymphocytes were analysed from whole brain tissue, CP and CSF. The T cell composition of each compartment was then compared to matched peripheral blood and a preparation of splenocytes (the latter acting as a positive control of the system). Brain and CP samples required tissue digestion and lymphocyte isolation processes prior to analysis. It was essential that the CNS vasculature was completely flushed with saline to evacuate contaminating blood lymphocytes. To achieve this, a whole body cardiac perfusion with saline was performed post mortem to flush blood out the vasculature. The efficacy of such as procedure was demonstrated by addition of Evan's blue dye to the perfused saline solution (Figure 4.7A). As this dye is retained within blood vessels it clearly demarcates successfully perfused areas. The staining of meningeal vessels strongly indicated successful perfusion of brain tissue (Figure 4.7A). Evan's blue perfusion also highlighted the extent of the heavy vascularisation of the CP structure, as seen by the intense blue staining in Figure 4.7C. This staining was particularly useful in honing CP dissection techniques as the vasculature of the CP structure is its most recognisable feature but in perfused animals this is not visible. CP was most successfully dissected from the 4^{th} ventricle, with intact structures measuring approximately 4mm in diameter in unfixed mouse brain (Figure 4.7B). Under high magnification the distinctive ruffled villous structure of perfused choroid tissue was visible on a dissection microscope (Figure 4.7D). Lateral ventricle CP was also obtained in both mice and rats, albeit less consistently due to its smaller size and anatomical location. Therefore for subsequent experiments analysis of this tissue was predominantly restricted to the 4^{th} ventricle structure only.

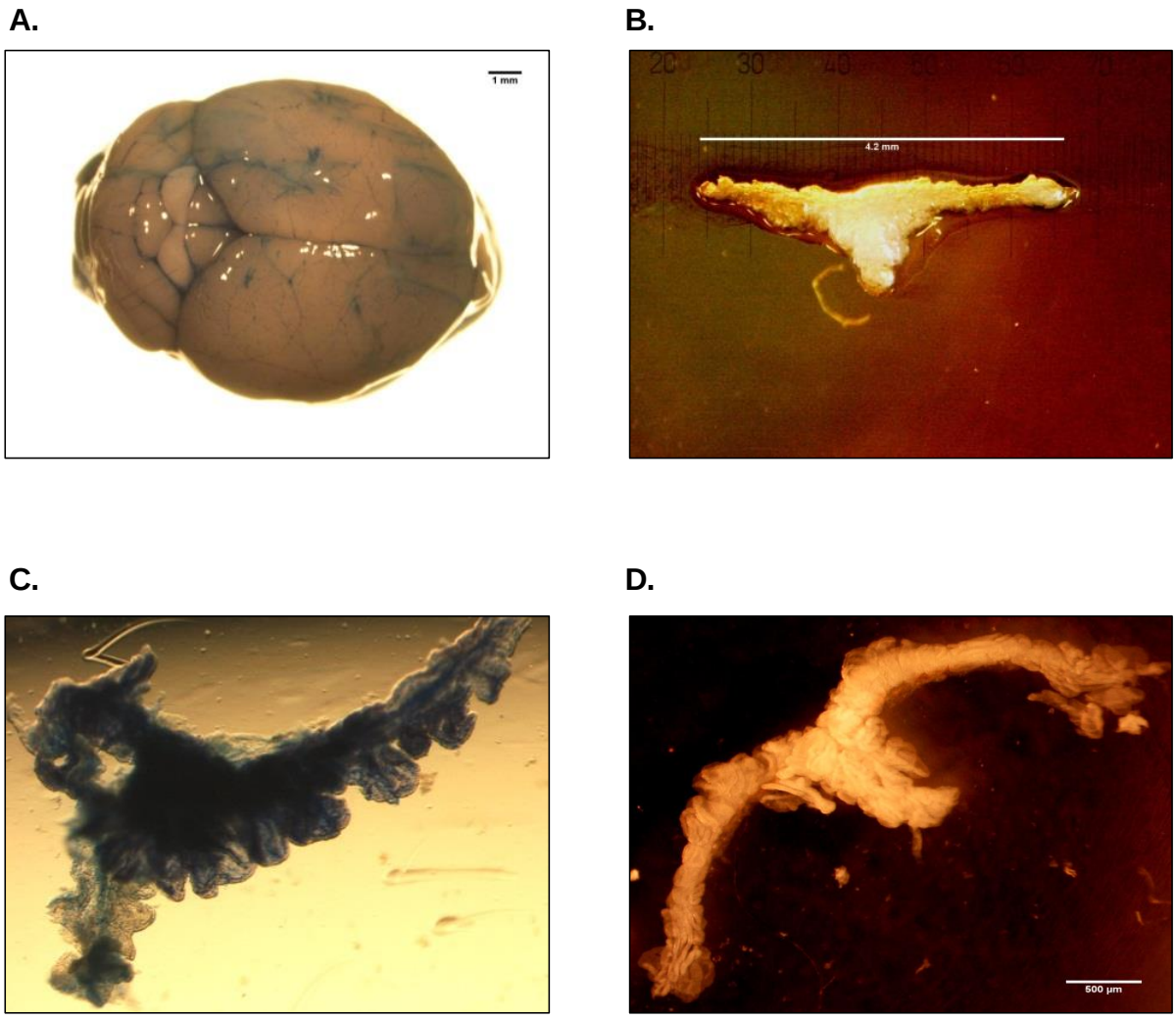

Figure 4.7 The perfusion of rodent brain and dissection of choroid plexus. C57BL/6 mice were intra-cardially perfused post mortem with 0.5% w/v Evan's Blue in PBS or PBS alone. The brains were removed whole and choroid plexus from the 4th ventricle dissected under a dissection microscope. **A.** Whole mouse brain showing the meningeal vasculature stained blue following perfusion with Evan's Blue dye. **B.** Intact choroid plexus tissue dissected from the 4th ventricle post PBS perfusion. **C-D.** Magnified images of 4th ventricle choroid plexus showing its ruffled villous structure. The extent of the tissues dense vascularisation is revealed following Evan's Blue perfusion (**C**).

4.6 Analysis of CNS associated T cells in an unchallenged rat model.

The $CD3^+$ T cell compartment associated with whole perfused brain, CP, CSF, peripheral blood and spleen was analysed by flow cytometry in the rat. The methodologies associated with the processing of each tissue prior to analysis are detailed in Chapter 2, Sections 2.10-2.12. The gating of lymphocytes was set using the forward and side scatter profile of lymphocytes in the blood and was kept consistent for each tissue (Figure 4.8A). Due to the very high proportion of non-lymphoid cellular matter in the whole brain sample a live gating strategy was used to minimise the recording of irrelevant material (Figure 4.8A bottom panel). Firstly, the percentage of T cells ($CD3^+$) that were $CD4^+$ was measured in each compartment (Figure 4.8B, Figure 4.8D). The proportion of T cells with a $CD4^+$ phenotype was significantly reduced in all three CNS compartments (CSF, CP and CNS) when compared to peripheral blood (Figure 4.8D), thus indicating that $CD4^+$ T cells do not predominate the T cell infiltrate into rat CNS. It was also noted that there was little difference in the representation of $CD4^+$ T cells between the CNS compartments. The memory status of the $CD4^+$ T cell population in each tissue was also recorded (Figure 4.8C, Figure 4.8D). Low expression of the CD45R isoform CD45RC is associated with a memory-like phenotype in rat[434,435]. The proportion of $CD4^+$ T cells with a $CD45RC^{lo}$ phenotype in the CSF was significantly greater than in the blood and the spleen (68.9% ±13.7 as compared to 33.6% ±2.85 and 38.8% ± 2.9 respectively (mean ± SEM)). A trend of increased memory $CD4^+$ T cell representation was also observed in the CP and whole brain preparations although these observations were not statistically significant.

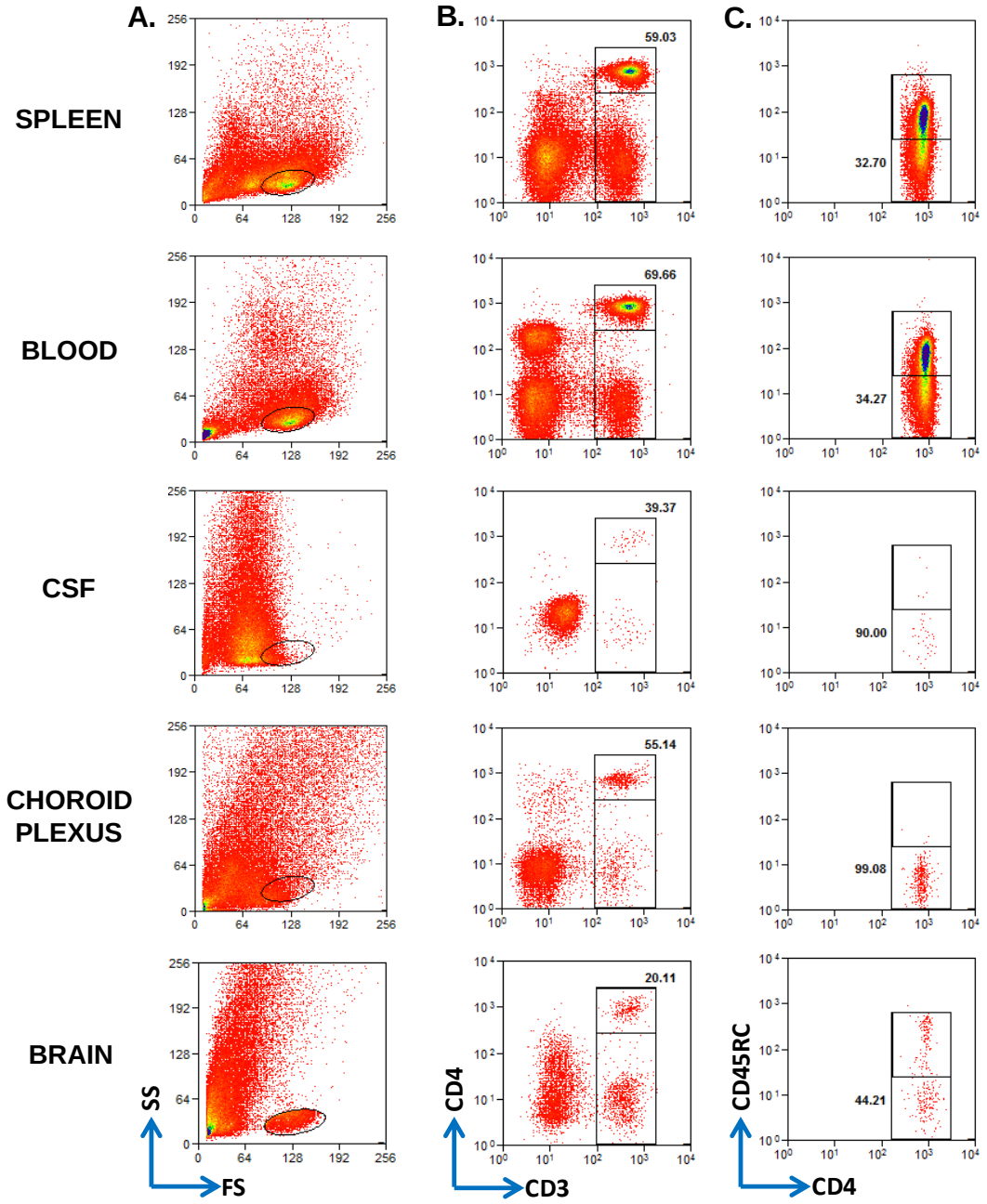
A.
B.
C.
SPLEEN
BLOOD
CSF
CHOROID PLEXUS
BRAIN
59.03
32.70
69.66
34.27
39.37
90.00
55.14
99.08
20.11
44.21
SS
FS
CD4
CD3
CD45RC
CD4

D.

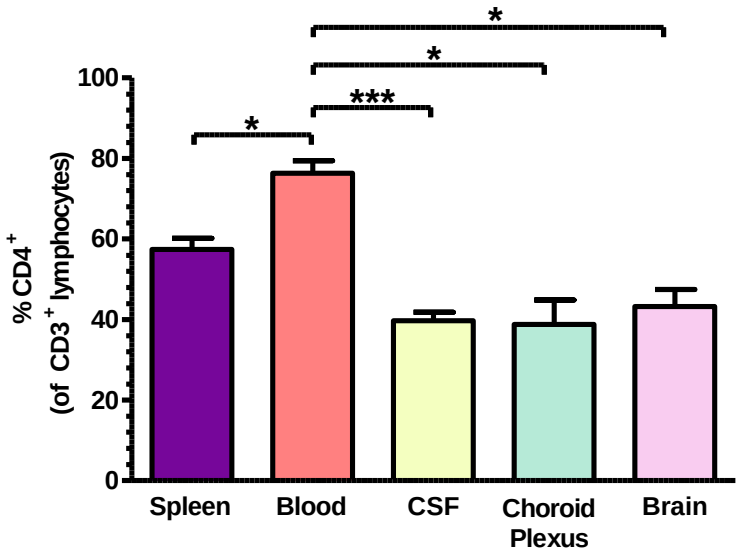
% CD4+ (of CD3+ lymphocytes)
Spleen
Blood
CSF
Choroid Plexus
Brain
*
*
***
*

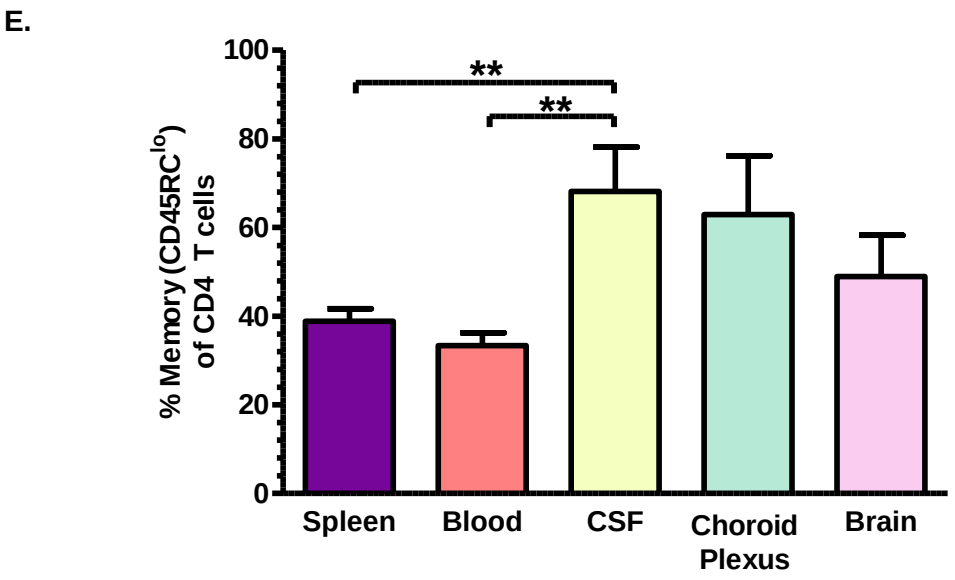

Figure 4.8 Identification of CD4$^+$ T cell subsets in the central nervous system of an unchallenged rat model. Cerebrospinal fluid (CSF), saline perfused choroid plexus and brain tissue were harvested from terminally anesthetised rats. Cell preparations from each compartment were analysed by flow cytometry for the presence of CD4$^+$ T cells and compared with matched peripheral blood and spleen derived samples. **A.** Representative flow cytometry plots showing the forward and side scatter profiles of the different tissue preparations. Gating was set consistent with the lymphocyte profile observed in peripheral blood samples. In whole brain samples a live gating strategy was used to reduce the cell counts (due to the high cell number). **B.** Plots show the presence of lymphocytes (CD3$^+$) in each tissue. Numbers represent the percentage of the CD3$^+$ lymphocytes that are a CD4 phenotype. **C.** Plots show the representation of memory (CD45RC^{lo}) within the CD4 T cell population each tissue. Numbers indicate the percentage of CD4 T cells that are memory. **D.** Graph of the mean ± SEM percentage of CD3$^+$ cells that are CD4$^+$. **E.** Graph of the mean ± SEM percentage of CD4 T cells that are a memory phenotype (CD45RC^{lo}). *p<0.05, **p<0.01, ***P<0.001 (one way ANOVA statistical analysis followed by Bonferroni's multiple comparisons test). **A-C.** Data is representative of n=4 rats measured in 2 independent experiments. **D,E.** Data is representative of n=3-4 rats measured in 4-8 independent experiments.

4.7 Analysis of CNS-associated T cells in an unchallenged mouse model.

The phenotype and memory status of CNS-derived $CD4^+$ T cells was then investigated in naïve C56BL/6 mice. $CD45^+$ leukocytes were isolated from fresh mouse brain and the cellular component of CSF pooled from six mice. It was not possible to retrieve sufficient cellular material from murine CP to perform accurate analysis of the $CD4^+$ T cell content. Therefore this analysis was omitted and the brain and CSF-derived T cell populations were compared to those from peripheral blood and spleen. Firstly, the representation of $CD4^+$ T cells within the total T cell population was analysed by flow cytometry (Figure 4.9). In contrast to experiments performed in rat, T cells were identified by expression of the leukocyte marker CD45 in addition to CD3. Further addition of a CD8 marker then enabled a direct ratio between $CD4^+$ to $CD8^+$ T cell subsets to be measured in the $CD45^+CD3^+$ population (gating strategy is shown in Figure 4.9A). As was observed in the rat there was a decrease in $CD4^+$ representation in the brain and CSF-derived T cell populations in comparison to those from the peripheral blood and spleen (Figure 4.9B, Figure 4.9C). Here this was seen as a bias towards a $CD8^+$ phenotype and shift away from a $CD4^+$ phenotype in the two CNS compartments measured. However, the differences in $CD4^+$/CD8 ratio between the tissues were more variable than in the rat system and this trend was not statistically significant. With consideration to CSF samples this was in part due to an experimental outlier where $CD4^+$ T cells dominated the T cell population and very few CD8 cells were measured (Figure 4.9C).

The memory status and phenotype of $CD4^+$ T cells from the brain digests and CSF samples were then interrogated by flow cytometry. Due to the technical challenges of sampling CSF from mouse without perturbing surrounding CNS tissue phenotyping experiments for brain and CSF were performed independently. In mouse, the memory (antigen experienced) T cell phenotype is characterised by $CD44^{hi}$ expression with the definition between T_{cm} and T_{eff} subsets indicated by $CD44^{hi}CD62L^{hi}$ and $CD44^{hi}CD62L^{lo}$ respectively[436–438].

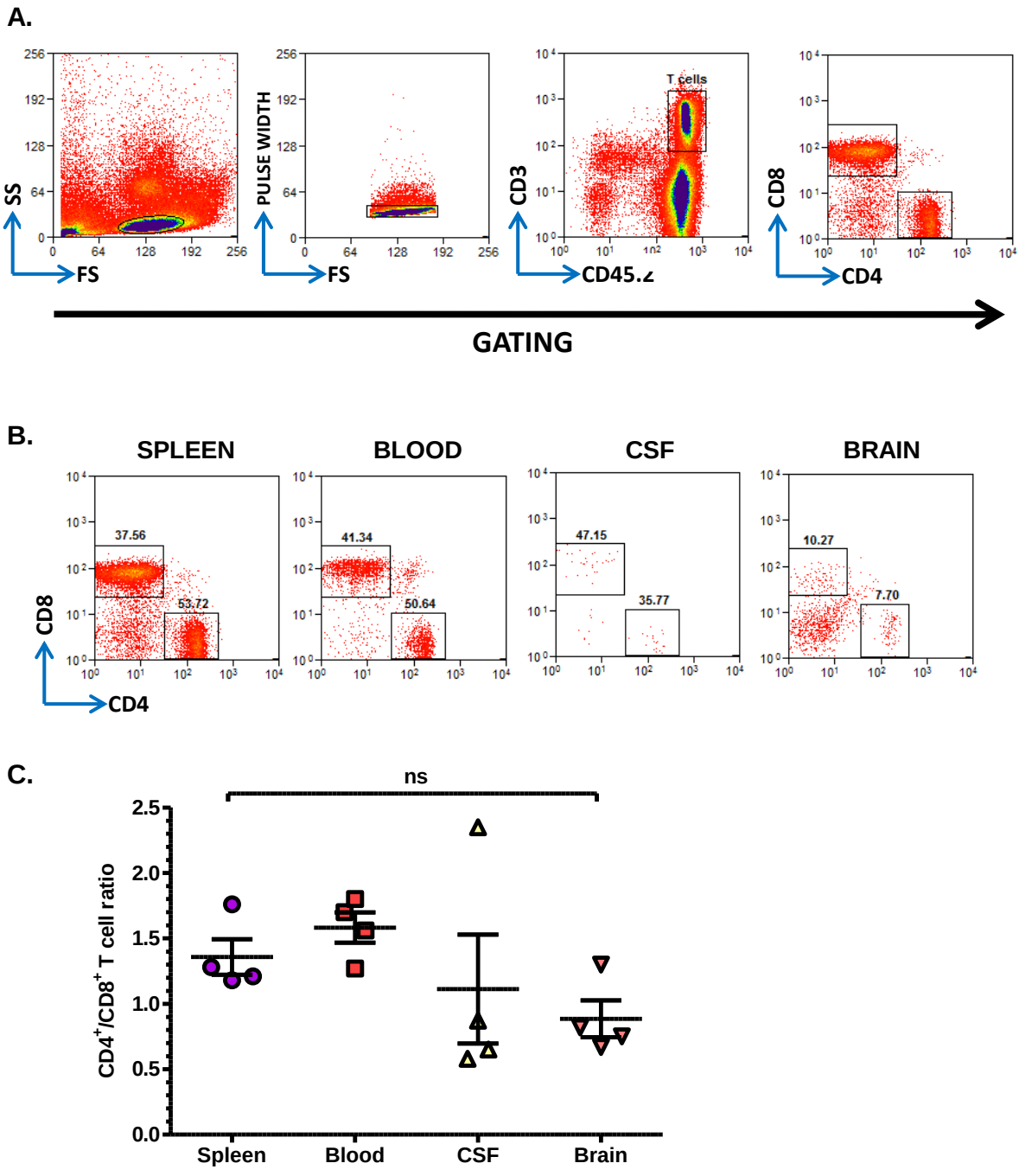

Figure 4.9 Changes in the distribution of CD4 and CD8 lymphocytes between the CSF, brain and peripheral compartments. The cellular component of CSF and brain-derived CD45$^+$ leukocytes from unchallenged C57BL/6 mice were analysed by flow cytometry. The ratio of CD4 to CD8 T cells was compared to T cells from peripheral blood and spleen-derived cell isolates. **A.** Gating strategy for the identification of T cells (CD45$^+$CD3$^+$ lymphocytes) within each compartment. Gating strategy is demonstrated by flow cytometry plots from a murine spleen sample. **B.** Representative plots show populations of CD4 and CD8 T cells within murine spleen, blood, CSF and brain (plot numbers indicated the percentage of cells in each gate). **C.** Graph shows the mean ± SEM ratio of CD4$^+$ to CD8$^+$ T cells in each compartment (CD4/CD8). ns = no significance at $p<0.05$ (one way ANOVA followed by Bonferroni's multiple comparisons test). Data is representative of n=6 mice measured in 3 independent experiments. CSF data is representative of one sample pooled from n=6 mice per experiment.

Firstly, the percentage representation of memory ($CD44^{hi}$) cells in the total $CD4^+$ population was investigated (the gating strategy for $CD4^+$ T cells is shown in Figure 4.10A). The representation of memory T cells in the CSF fluid was significantly greater than in the peripheral blood and spleen with 69.9% ± 6.7 (mean ± SEM) of CSF T cells exhibiting $CD44^{hi}$ expression (Figure 4.10B, Figure 4.10C). The $CD44^{hi}$ memory pool in the blood and spleen was vastly dominated by a T_{eff} phenotype with very little representation of the T_{cm} subset (Figure 4.10D). This T_{eff} dominance was slightly more pronounced in the CSF compartment, although statistically there was no difference in the memory distribution in CSF when compared to the blood and spleen populations (Figure 4.10D).

The memory status of brain-derived $CD4^+$ T cells was then analysed for comparative analysis with the CSF experiments (Figure 4.11). Brain-derived leukocytes ($CD45^+$) were enriched by MACS by applying a suspension of enzymatically digested brain tissue labelled with anti-CD45 microbeads through two magnetic columns (Figure 4.11A). Although the purity of the eluted $CD45^+$ suspension was low (approximately 6% of cells within a lymphocyte gate), this approach was successful as it removed a vast amount of debris and irrelevant material from cell preparation (Figure 4.11A). Although the general trend in memory status observed in the CSF was recapitulated in the whole brain digests memory T cells were less well represented in the brain than in CSF samples (37.1% ± 4.3 compared with 69.9% ± 6.7 (mean±SEM)). However, the memory phenotype was still significantly more prevalent in the brain-derived population than in matched peripheral blood and spleen (Figure 4.11B, Figure 4.11C). The memory $CD4^+$ T cell population associated with brain were predominantly a T_{eff} phenotype (Figure 4.11D) as was observed in the CSF. However, in contrast there was a small but significant percentage increase of the T_{eff} phenotype in the brain when compared to a matched analysis of peripheral blood (95.8% ±2.1 and 84.4% ± 4.1 respectively) (Figure 4.11D).

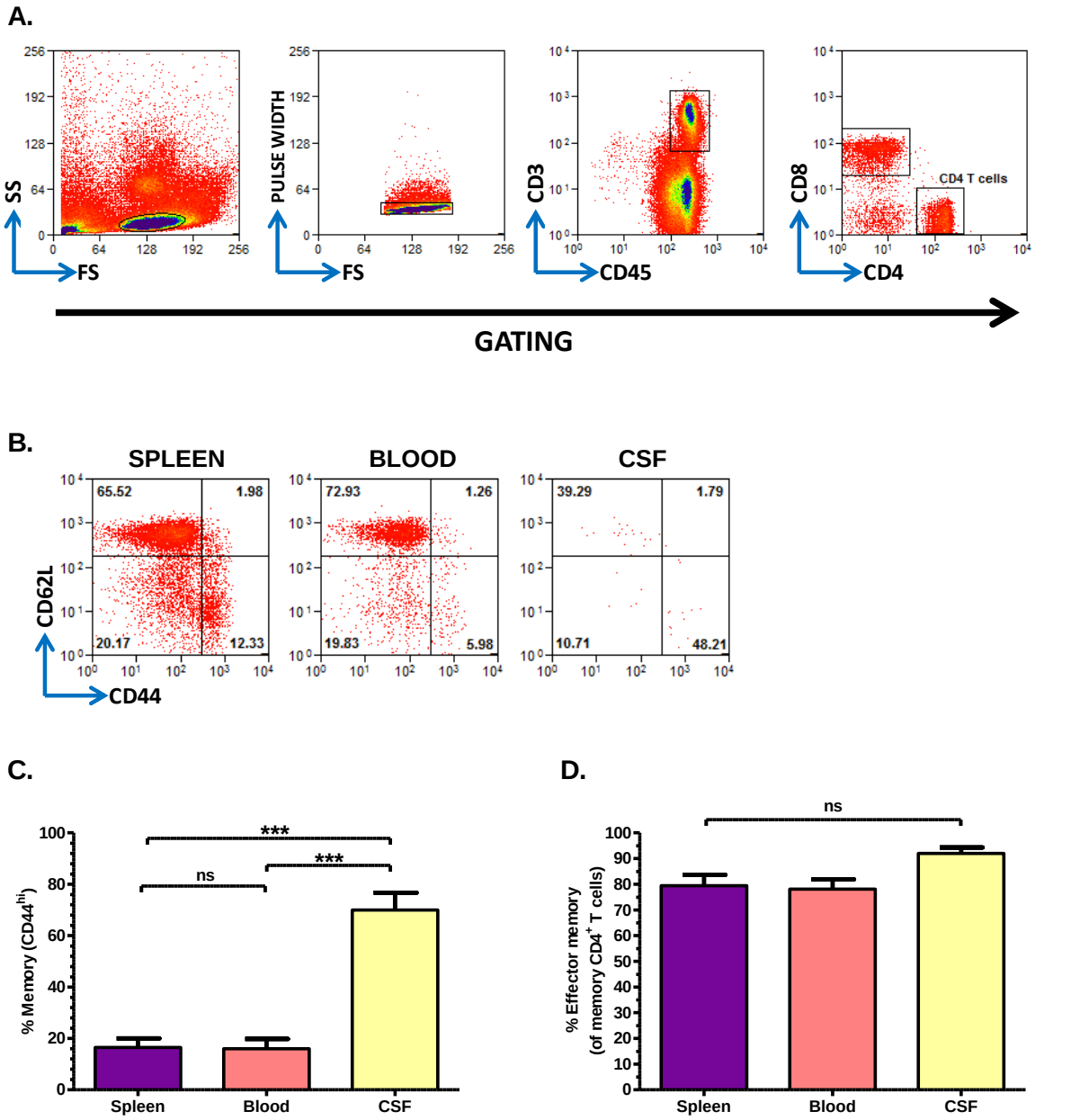

Figure 4.10 Distribution of naïve and memory CD4 T cell subsets in murine CSF. Cerebrospinal fluid (CSF) was pooled from unchallenged C57BL/6 mice and cellular compartment was analysed by flow cytometry. The distribution of naïve and memory CD4 T cells from CSF was compared with matched peripheral blood mononuclear cells and spleen-derived cell isolates. **A.** Gating strategy for the identification of CD4 T cells ($CD45^+CD3^+CD8^-CD4^+$ lymphocytes) within CSF. Gating strategy is demonstrated using a murine spleen sample. **B.** Representative plots show the distribution of naïve ($CD62L^{hi}CD44^{lo}$), central memory ($CD62L^{hi}CD44^{hi}$), and effector memory ($CD62L^{lo}CD44^{hi}$) $CD4^+$ T cells in murine spleen, blood and CSF. **C.** Graph shows the percentage of CD4 T cells with a memory phenotype ($CD44^{hi}$). **D.** The percentage of the memory ($CD44^{hi}$) CD4 population that is central memory phenotype ($CD62L^{hi}$). ***$p<0.001$, ns= no significance at $p<0.05$ (one way ANOVA followed by Bonferroni's multiple comparisons test). Data is representative of n=6 mice in measured in 3 experiments.

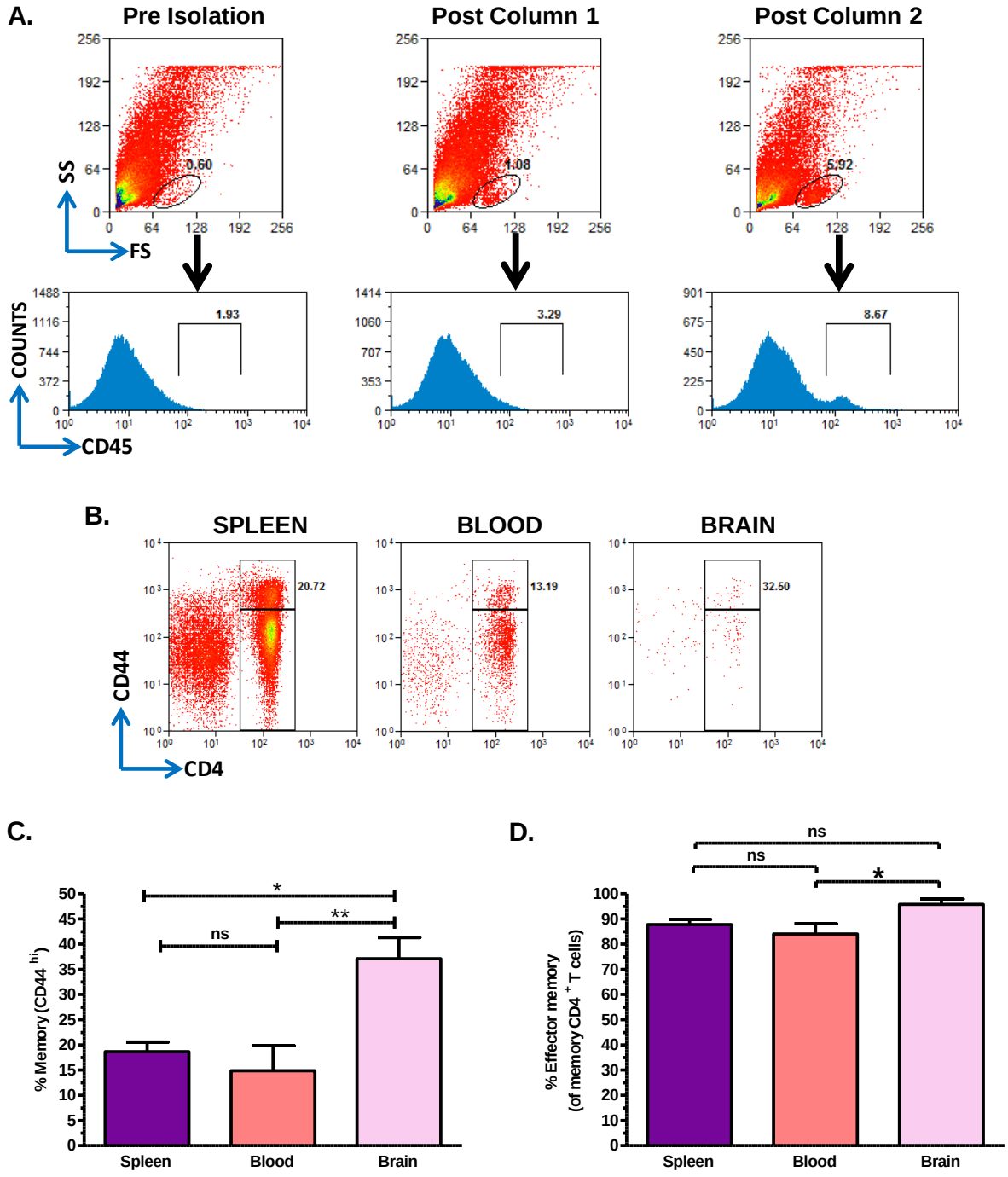

Figure 4.11 Leukocyte isolation from murine CNS tissue and the representation of memory cells in the CD4 T cell population. Brain tissue was harvested from unchallenged, saline perfused C57BL/6 mice and the associated leukocytes ($CD45^+$) enriched through magnetic activated cell sorting (MACS). T cells ($CD45^+CD3^+CD8^-CD4^+$) from the brain, peripheral blood and spleen cell were analysed by flow cytometry for the distribution of memory cells ($CD44^{hi}$). **A.** Representative plots show the leukocytes ($CD45^+$) present in digested brain tissue prior to enrichment, and following each stage of a consecutive two-step MACS column filtration process. **B.** Representative plots indicate the percentage of the CD4 T cells (all gated) that are a memory phenotype ($CD44^{hi}$) in each tissue. **C.** Graph shows the mean ± SEM percentage of CD4 T cells that are memory. **D.** Graph shows the percentage of memory cells that are an effector memory phenotype ($CD44^{hi}CD26L^{lo}$). *p<0.05, **p<0.01 ns= no significance at p<0.05 (one way ANOVA followed by Bonferroni's multiple comparisons test). Data is representative of n=6 mice.

4.8 The frequency and distribution of CSF-derived T cells in multiple human disease cohorts.

Having analysed peripheral blood and CSF-derived T cell populations in rodent models work was translated into human patient cohorts presenting both non-inflammatory and inflammatory neurological disorders. It should be noted that the processing of these samples was performed by another member of the group (Miss Lindsay Durant). The raw data collection was reanalysed by me (the investigator) for the purpose of this study. Central to this analysis was a mixed cohort of patients diagnosed with non-inflammatory neurological disease (OND) as sampling from this group most closely represented 'normal' matched CSF and blood. In addition, patients falling under multiple sclerosis (MS) diagnostic criteria were categorised into three cohorts in accordance with the clinical course of the disease. These included clinically isolated syndrome (CIS), primary progressive MS (PP-MS) and relapsing remitting MS (RR-MS). Lastly, a mixed patient cohort with other inflammatory neurological diseases (ONID) was included in the comparative analysis. The clinical diagnoses of all patients assigned to the OND and ONID groups for this work are described in Section 2 Table 2.1. The median patient age (with range) for each group is also shown in this table.

The representation of $CD4^+$ and $CD8^+$ T cells in the CSF and peripheral blood of each cohort was analysed by flow cytometry (gating strategy is shown in Figure 4.12A). When the $CD4^+/CD8^+$ ratio of T cells in the CSF was compared to matched peripheral blood samples the general trend indicated an increase in $CD4^+$ representation in the CSF (Figure 4.12B). The exception to this was in the PP-MS cohort where the proportion of T cells with the $CD4^+$ phenotype was elevated in the peripheral blood (as opposed to a decrease in CSF representation). Interestingly the $CD4^+$/CD8 ratio in the CSF was fairly consistent across all the groups measured, with the highest ratio in the CIS group (4.5 (2.6-6.0) median (IQR)) and the lowest in the OND group (3.9 (2.7-5.7) median (IQR)).

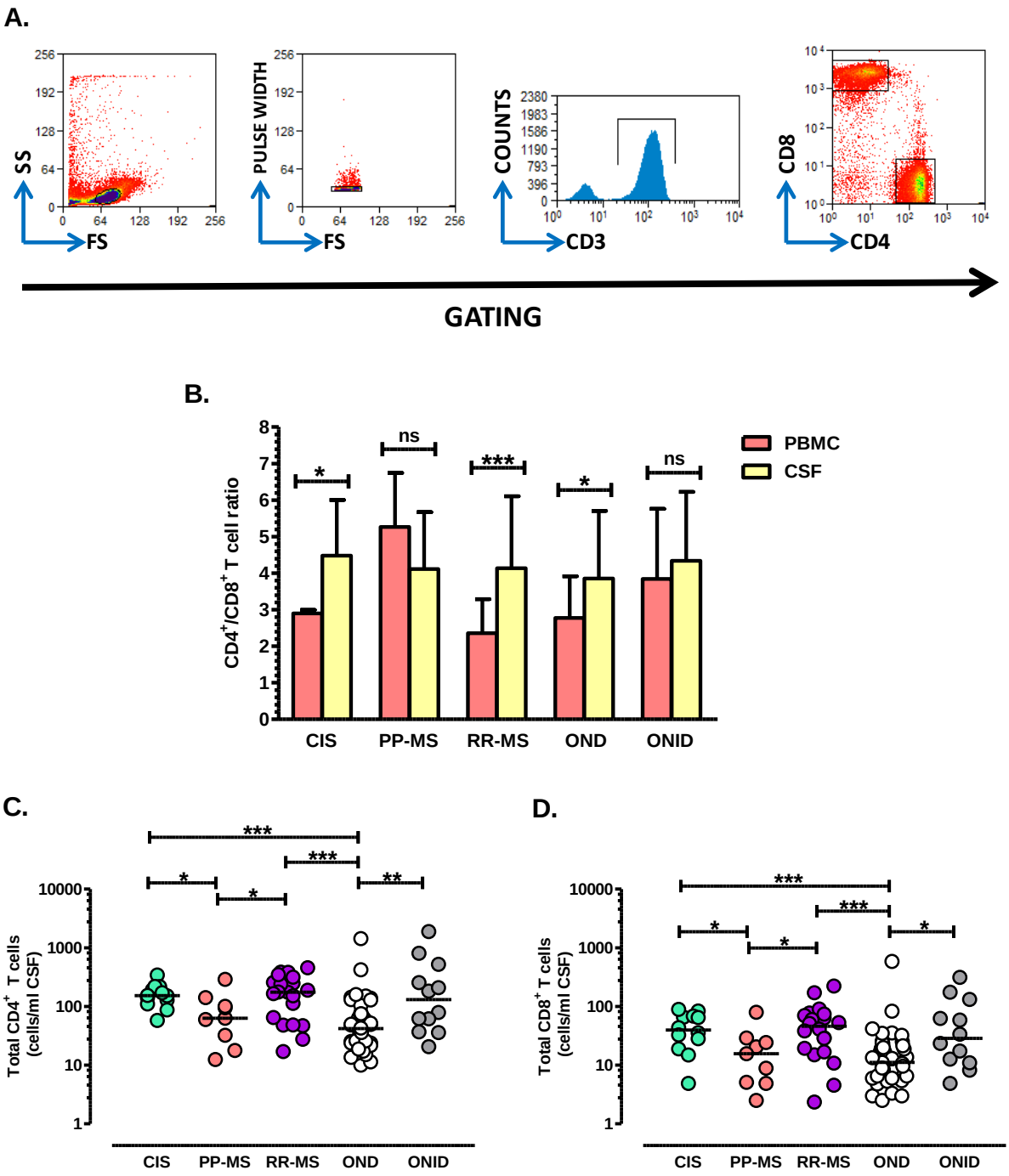

Figure 4.12 Representation of CD4 and CD8 T cells in the cerebrospinal fluid of multiple patient cohorts. Peripheral blood and CSF samples were taken from multiple patient cohorts[±]. The distribution of CD4 and CD8 T cell subsets in each compartment was analysed by flow cytometry. **A.** Gating strategy for the analysis of $CD4^+$ and $CD8^+$ T cell distribution. **B.** The ratio of $CD4^+/CD8^+$ T cell subsets from matched blood and CSF samples in five patient groups. **C, D.** The absolute frequency of CD4 T cells (**C.**) and CD8 T cells (**D.**) in the CSF of each patient group. Each point represents one patient sample, with the line representing the median frequency of each T cell phenotype per ml of CSF. *p<0.05, **p<0.01, ***p<0.001, ns = no significance at p<0.05 indicating statistical significance by Wilcoxon matched-pairs signed rank test (**B.**) and Mann-Whitney U statistical test (**C, D.**). [±] **CIS**; clinically isolated syndrome (n=12), **PP-MS**; primary progressive multiple sclerosis (n=9), **RR-MS**; relapsing remitting multiple sclerosis (n=20), **OND**; other neurological disease (n=51), **ONID**; other neurological inflammatory disease (n=12).

This consistency suggests that the ratio of $CD4^+/CD8^+$ T cell in the CSF is largely independent of inflammatory or disease status (Figure 4.12B).

The absolute frequency of both $CD4^+$ and $CD8^+$ T cell populations was also measured in the CSF (Figure 4.12C and Figure 4.12D respectively). With the exception of the PP-MS group the OND cohort had significantly fewer $CD4^+$ T cells per ml/CSF than the other inflammatory disease groups (both MS and non-MS). In addition, the PP-MS group had significantly fewer $CD4^+$ T cells than the CIS and RR-MS groups (Figure 4.12C). These trends were reproduced when the frequency of $CD8^+$ T cells was measured, where again fewer cells were found in the CSF of the OND and PP-MS groups comparative to the other inflammatory disease cohorts (Figure 4.12D).

Next the distribution of subsets within the memory compartment of the $CD4^+$ T cell population was assessed. The representation of the central memory phenotype ($CCR7^+$) within the $CD45RO^+$ memory pool was consistent across all of the patient groups (Figure 4.13). This trend was observed both in the blood and CSF compartments where there was consistently a strong bias towards a T_{cm} phenotype. A slight decrease in the T_{cm} population (or increase in T_{eff} representation) in the RR-MS group was noted but this was not statistically significant. The T_{cm} bias observed in this analysis was the reverse of what was shown in mouse studies, where a T_{eff} population dominated both the blood and CSF (Figure 4.10D, Figure 4.11D). Given that the predominating blood population was best represented in the CSF of both species the relationship between each compartment was then investigated further in humans. A correlation analysis was performed where the percentage of memory cells (T_{cm} + T_{eff}) that were a T_{cm} phenotype was measured in match peripheral blood and CSF samples (Figure 4.14). When OND and ONID (non-MS) cohorts were analysed, results showed that the percentage of T_{cm} cells within the blood memory pool positively correlated with those found in the CSF (Figure 4.14A-B, Figure 4.14F).

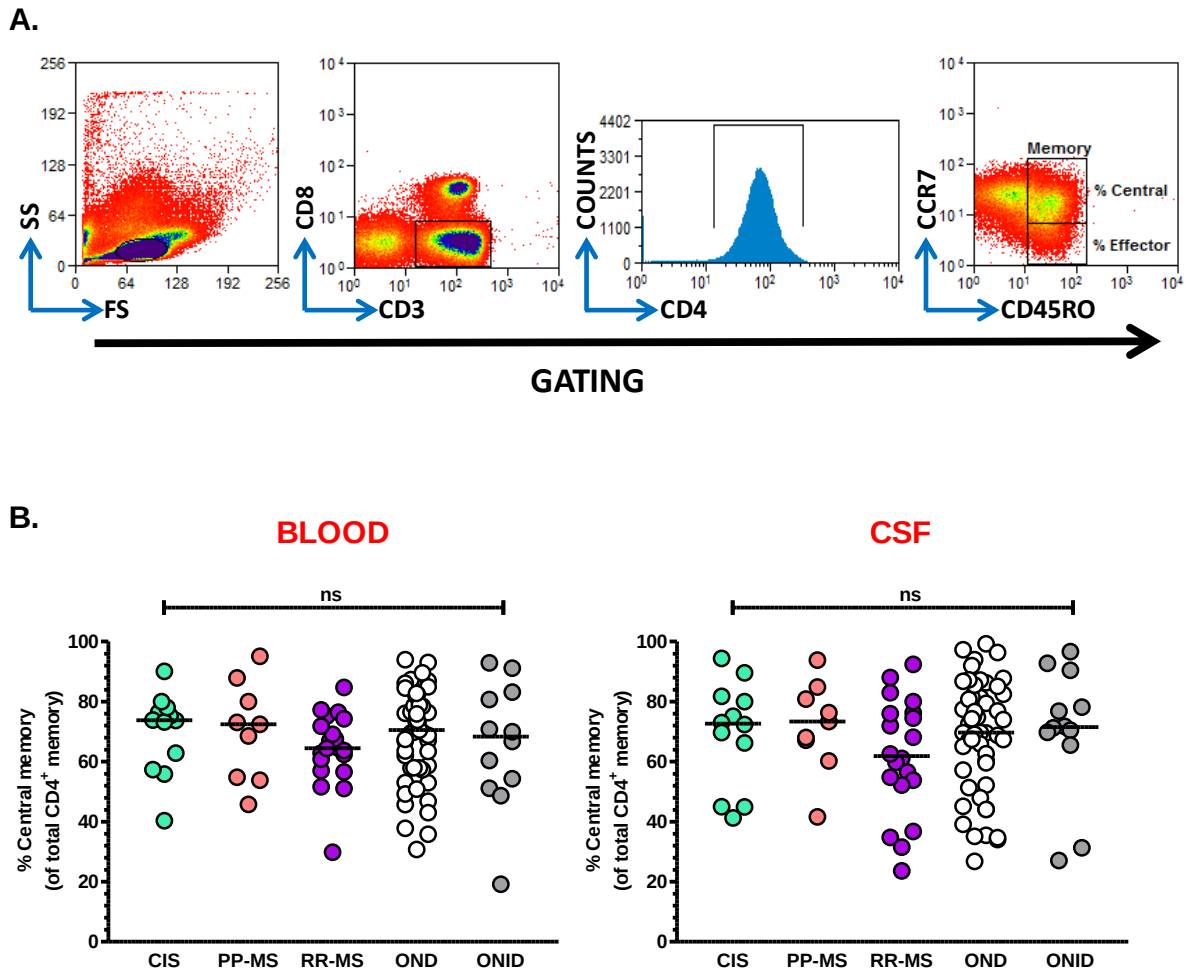

Figure 4.13 The distribution of memory subsets in CD4$^+$ T cell populations from human peripheral blood and cerebrospinal fluid. Peripheral blood and CSF samples were taken from multiple patient cohorts$^{\pm}$. In the CD4$^+$ T cell population, the representation of CCR7$^+$ cells (central memory) within the total memory pool (CD45RO$^+$) was analysed by flow cytometry. **A.** Gating strategy for the identification of central and effector memory CD4 T cells. **B.** The percentage of the memory compartment that is a central memory phenotype in the blood and CSF. Each point represents one patient sample, with the line representing the median percentage representation of central memory. ns = no significance at $p<0.05$ (Mann-Whitney U statistical test between pairs of patient groups). $^{\pm}$**CIS**; clinically isolated syndrome (n=12), **PP-MS**; primary progressive multiple sclerosis (n=9), **RR-MS**; relapsing remitting multiple sclerosis (n=20), **OND**; other neurological disease (n=51), **ONID**; other neurological inflammatory disease (n=12).

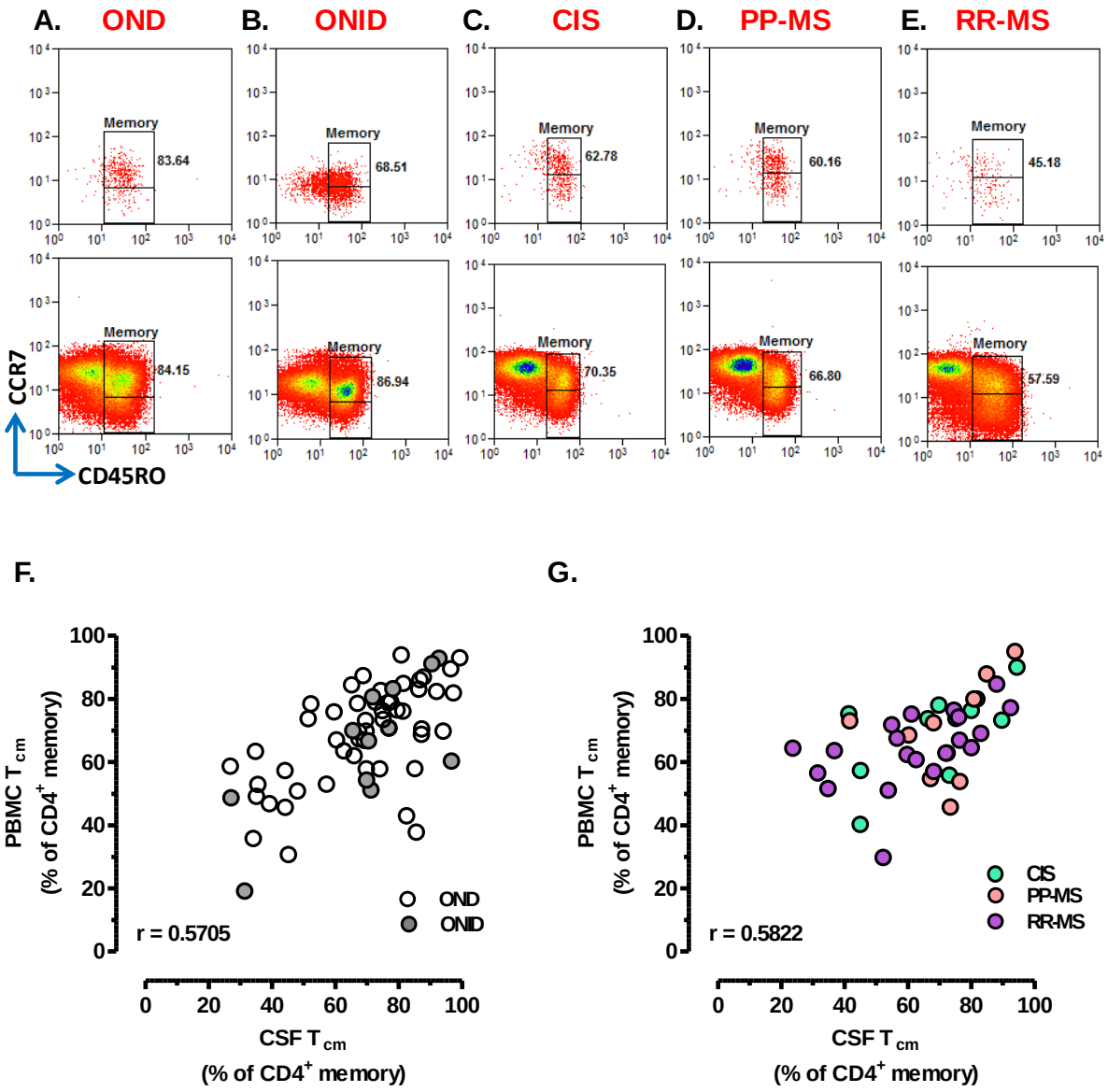

Figure 4.14 The memory status of CD4 T cell from the blood and matched cerebrospinal fluid of patients with and without neuroinflammatory disease. Peripheral blood mononuclear cells and the cellular component of CSF were analysed from multiple patient groups[±]. The representation of central memory cells ($CD45RO^{+}CCR7^{+}$) within the memory CD4 T cell population ($CD45RO^{+}$) was analysed by flow cytometry. **A-E.** Representative plots gated on the memory population of CD4 T cells indicating the percentage that are central memory in each patient group. Plots represent a CSF (top panel) and matched blood (bottom panel) T cell analysis from one patient per disease cohort. **F.** Correlation between the distribution of central memory in the peripheral blood and CSF memory T cell pool from patients without a multiple sclerosis diagnosis (**OND**; other neurological disease (n=51), **ONID**; other neurological inflammatory disease (n=12)). **G.** Graph indicates the same correlation performed in patients with three clinical disease courses of multiple sclerosis (**CIS**; clinically isolated syndrome (n=12), **PP-MS**; primary progressive multiple sclerosis (n=9), **RR-MS**; relapsing remitting multiple sclerosis (n=20)). **E,F.** r number represents the spearman correlation value (correlation is significant at the level $p<0.001$).

This trend was also observed across all MS groups, where again the CSF memory distribution was a direct reflection of that measured in matched blood (Figure 4.14C-E, Figure 4.14G). These results demonstrate that the proportion of T_{cm} in the CSF is related to that in the peripheral blood in the absence of inflammation and that this relationship is not perturbed by underlying neuroinflammatory pathology.

4.9 Discussion.

The first aim of this investigation was to model 'normal' CSF and CNS compartments in naïve mice and examine the associated $CD4^+$ T cell composition. There are two main advantages of using animal modelling for this purpose. Firstly, in the rodent system CSF can be sampled in parallel with matched CNS tissue post-mortem. This gives a more complete insight into the T cell distribution in multiple CNS compartments simultaneously which is not often possible in human histopathological studies. Secondly, obtaining completely normal CSF from healthy participants cannot be justified ethically. Therefore, the closest definition of a 'normal' CSF cellular composition typically comes from spinal anaesthesia procedures[247] or diagnostic sampling where the suspected pathology is not inflammatory in nature[248,288]. Diagnostic sampling is commonly used to characterise 'normal' CSF in the literature and so this was utilised for the purpose of this study (OND group). However, it is acknowledged that non-inflammatory disorders may have systemic effects that indirectly influence immune function in a CNS context.

The main disadvantage of studying CNS derived T cell populations in rodents is the low number of cells that are retrievable from the various compartments for analysis. In the absence of inflammation or infection the migration of T cells from the blood into the CSF spaces is limited to a very low level recruitment. Studies which investigate T cell association with rodent brain are largely restricted to models where activated or CNS-antigen specific T cell clones are adoptively transferred in a naïve host[252,270,439]. Transferred cells are identified

via fluorescent labelling to track their migration, be that through intravital microscopy or whole brain sectioning procedures. However, endogenous CNS associated $CD4^+$ T cells have not been quantified without such experimental intervention. My investigation intended to address this question via image capture of serial brain sections to map and quantify T cells associated with whole unchallenged mouse brain. Mapping of a whole brain could be achieved by capturing multiple images per tissue section and digitally reconstructing the images on an epifluorescence microscope as is shown by the nuclear staining in Figure 4.4. However, the lack of confocality of this system proved problematic as the serial brain sections cut for this exercise were thick (20µm) in order that the whole brain could be represented within the analysis. As a result, the high background signal from the out of focus tissue masked any signal from specific lymphocyte staining in the epifluorescence system. Therefore, an alternative strategy was devised where four brain regions were selected and analysed on a confocal microscope to alleviate these issues. Immunofluorescence techniques were favoured over immunohistochemistry for this exercise as it permitted the use of more markers for cellular identification. It was originally intended that the location of multiple T cell subsets could be shown in relation to the CNS vasculature and choroid plexus epithelium through additional staining with PECAM-1 and cytokeratin-8 respectively. However, staining for up to six markers proved technically challenging and was hampered by high tissue autofluorescence and non-specific staining. Although such images of an interpretable quality were not produced during this investigation, it is acknowledged this exercise would provide a more detailed insight into the localisation of T cells within CNS tissue.

Results from this investigation did identify a low number of $CD3^+$, $CD4^+$ and $CD3^+CD4^+$ associated with distinct gross anatomical locations within the mouse midbrain sections (Figure 4.4-4.5). Whereas $CD3^+CD4^+$ surface expression strongly indicated the presence of $CD4^+$ T cells it may be assumed that $CD3^+$ population represented the CD8 phenotype. However NK and $CD4^+CD8^+$ cells have been described in association with human CNS and

an increase in these subsets is associated with inflammatory pathologies[440,441]. In my experiments the frequency of $CD3^+$ cells was greater than the $CD3^+CD4^+$ population, which is consistent with the inverted $CD4^+/CD8^+$ ratio in the CNS that was also identified by flow cytometry (Figure 4.9). Interestingly, $CD3^+$ single positive cells were observed in the meninges, choroid plexus and periventricular regions, whereas $CD3^+CD4^+$ T cells were not observed in the meninges. A leptomeningeal route of T cell migration from the blood into the perivascular CSF-filled spaces of the leptomeninges has been described *by Carrithers et al (2000)*[252]. However, intravital studies of the leptomeninges via a cranial window have failed to identify T cell capture and migration here in the absence of inflammation[274]. Given that the perivascular spaces are continuous with the CSF flow it is not possible to say whether these $CD3^+$ (assumed $CD8^+$) T cells represent cells that have migrated via a meningeal route or they are derived from another BCSFB pathway and are retained in the meningeal spaces.

The fact that $CD3^+CD4^-$ ($CD8^+$) cells were readily detected in choroid plexus tissue in the rat by flow cytometry is evidence against choroid plexus T cell migration being exclusive to the $CD4^+$ subset (Figure 4.5-4.6). With the assumption that the meningeal and CP-derived T cells were behind the BBB/BCSF barrier (inclusion of an endothelial marker would be required for conformation), this result suggests differential T cell distribution between these CSF-filled compartments. Such a phenomenon has not been previously documented under homeostatic conditions in mice and in contrast human studies show that the cellular composition of CSF is consistent in both the lumbar and ventricular regions[283]. More detailed analyses of T cells co-localisation with meningeal and CP barriers are required to take these findings forward, in addition to more comprehensive T cell phenotyping in these microscopy experiments.

Anecdotally, $CD3^+$ cells were often seen in proximity to $CD4^+$ cells in the meninges. These $CD4^+$ single positive cells may represent a population of perivascular macrophages in the meningeal space; an observation which was supported by their size and morphology. Low

CD4 expression by both resting macrophage and microglial populations is reported in rodent brain, with increased expression in response to activation or in the context of EAE[442,443]. $CD4^+$ expression by CP macrophages (epiplexis cells) is not described in the literature. However, $CD3^-CD4^+$ cells were also found to reside in the CP and were again often in the same field of view as $CD3^+$ T cells (irrespective of CD4 status; Figure 4.5D). These findings together with the absolute absence of $CD4^+$ T cells or $CD4^+$ monocyte lineage in brain parenchyma (cortex) suggest that these cells are involved in homeostatic immune surveillance in line with a model described by *Engelhardt et al (2011)* [257]. Immune surveillance is performed by T cells residing in the CSF-filled spaces behind the BBB and BCSFB and here they interact with perivascular APC. However, in the absence of specific antigen recognition the outermost parenchymal basal lamina of the brain (*glia limitans*) is not breached. With these concepts in mind it is acknowledged that $CD3^+$ and $CD3^+CD4^+$ cells were identified in the periventricular region adjacent to the CP, thus contradicting this model (Figure 4.5C). However, it is unlikely that this region of brain represents true parenchymal tissue and is more likely representative of circumventricular organ (CVO) structures. The CP is part of a CVO network in the 3rd and 4th ventricles and both structures lack endothelial tight junctions and have fenestrated vasculature[444]. T cell migration across CVO which lines the ventricles is documented, most notably as a proposed route of T cell migration in EAE[445]. It is in such instances where more comprehensive markers of epithelial and endothelial barriers would be useful in this analysis to more accurately define the borders of the parenchyma and ventricular structures. It is also acknowledged that my work is only representative of the midbrain region and therefore additional sampling of the forebrain and hindbrain structures would be highly appropriate in further experiments.

Flow cytometry was used to investigate the phenotype of CNS-derived T cells in more detail than was permissive by microscopy analysis (rodent) and to examine T cell subsets within the CSF and blood compartments (rodent and human). In humans, the ratio of $CD4^+/CD8^+$ T cells

in the CSF was increased compared to the blood in the non-inflammatory disease cohort which is consistent with what is reported elsewhere[248,446]. Interestingly, I found that this ratio was reversed in both the mouse and rat CSF models and was consistent with analysis in rodent CNS tissue preparations. This finding is contrary to reports by *K. Baruch et al (2012)* who have demonstrated a $CD4^+$ T cell bias in unchallenged murine CP (62% ± 2.76 (mean ± SEM) in the same mouse strain utilised in this investigation[447]. However, this group have not reported the $CD4^+/CD8^+$ ratio in the CSF compartment of normal mice. My work may indicate a more dominant role of the $CD8^+$ T cell subset in normal rodent CNS surveillance. Whether this is a result of differential recruitment or increased retention of this subset is open to speculation. It may also be indicative of more resident $CD8^+$ T_{RM}-type population associated with the CNS as is reported post influenza and vesicular stomatitis virus infection in mice[448,449]. Alternatively, it may simply be reflective of alternative requirements of the species for protection against endemic CNS pathogens.

In line with current understanding of human CSF biology there was a shift in favour of the $CD4^+$ T cell phenotype in the CSF irrespective of inflammatory disease with the exception of the PP-MS group (Figure 4.12). Within the CSF compartment, it is reported that the $CD4^+/CD8^+$ T cell ratio is significantly great in MS cohorts[450]. I found that the $CD4^+$ T cell bias in the CSF was only marginally increased in the CIS and RR-MS groups compared with the OND cohort, but the difference between the blood and CSF ratios was accentuated (Figure 4.12B). These findings do not necessarily indicate that migration into CNS is more $CD4^+$ biased in inflammation as a heavy enrichment of $CD8^+$ T cells are identified within active MS lesions[451]. Therefore, it cannot be excluded that migration across the *glia limitans* favours the $CD8^+$ subset when there is parenchymal inflammation. Such a phenomenon is also observed in inflamed perivascular cuffs where $CD4^+$ T cells are retained adjacent to the vessels whereas the $CD8^+$ subset preferentially migrates into the tissue[354,355].

As previous studies have proposed that the $CD4^+$ T cell population has a significant role in CNS immune surveillance[257,452] the memory status of this population was characterised further in this study. Initial animal experiments were performed in rat due to the increased volume of CSF and amount of CP tissue obtainable per animal. Results showed that there was an increased proportion of $CD4^+$ T cells with $CD45RC^{lo}$ expression in the CSF, CP and whole brain (Figure 4.8D). This was consistent with BCSFB migration being restricted to the memory phenotype as in the rat antigen experienced $CD4^+$ T cells are classically defined by $CD45RC^{lo}$ expression whereas naïve cells express $CD45RC^{hi}$[434,435]. However, this definition has been repeatedly challenged by evidence that antigen experienced $CD45RC^{lo}$ cells revert back to the $CD45RC^{hi}$ isoform in the absence of persistent antigen[453]. This implies that $CD45RC^{lo}$ expression is more representative of an 'activated' as opposed to a true 'memory' phenotype. In support of this, when rat $CD4^+$ T cells were stimulated with PMA/ionomycin as part of this investigation all cells lost $CD45RC^{hi}$ expression (as discussed later in Chapter 5). Given that a clear definition of memory and distinction between central and effector phenotypes was pivotal to this enquiry further use of rat models was restricted. Therefore, more detailed investigation was taken forward in the mouse where memory markers are better established and more translatable to human immunology.

The absolute number of T cells in murine CSF and brain was not quantified numerically in this investigation and analysis focused on the distribution of T cell subsets. The estimated number of $CD4^+$ T cells retrieved from CSF was similar to parameters described by *Kunis et al* who previously reported $CD4^+$ T cell frequencies at approximately 1.25 cells/ul of CSF[282]. Given that only 10-20ul of CSF can be collected per mouse this can render the very small number of CSF-derived lymphocytes difficult to interpret on flow cytometry plots. As in the rat system, mouse CSF from multiple siblings was pooled in these experiments to increase the cell numbers and add power to the subsequent statistical analysis (Figure 4.9-4.11). In addition, flow cytometry gates were kept consistent and set on the parameters of peripheral

blood derived lymphocytes. In mouse the percentage of memory cells ($CD44^{hi}$) in the blood was low, which may be expected given that these animals were housed in specific pathogen free conditions (Figure 4.10-4.11). As anticipated there was significant enrichment of memory T cells in the CSF and brain which is indicative of memory specific migration. It should be noted that in these experiments the brain-derived $CD4^+$ T cells included CP associated populations, as this tissue was not removed from the preparations. Given that microscopy identified CP to be the primary site of residing $CD4^+$ T cells in the brain, it is likely a significant proportion of brain derived cells were of a CP origin.

In mouse peripheral blood the predominant memory phenotype was effector memory ($CD44^{hi}CD62L^{lo}$) with little representation of a central memory population ($CD44^{hi}CD62L^{hi}$) and this distribution was reflected in the both the CSF and brain (Figure 4.10-4.11). There was a slight increase in T_{eff} in the brain but this difference may not directly indicate an absence of T_{cm} recruitment but may suggest an apparent under representation of the T_{cm} due to their low frequency combined with the low cell numbers in CSF. Reported findings from *Baruch et al (2012)* describe an enrichment of $CD4^+$ T_{eff} phenotype in the CP under the assumption that these cells are retained in the CP whilst T_{cm} migrate away into the CSF[447] (the authors reference to the T_{cm} predomination in humans). The domination of the T_{eff} subset in the CSF in my study challenges this proposal and is more consistent with a lack of specific subset recruitment across the BCSFB. Together these findings provoked revision of the proposal that the $CD4^+$ memory T cell subset distribution in normal CSF is a result of direct T_{cm} recruitment. Instead it was considered whether the memory subset distribution in the CSF is reflective of the memory status of the blood. This was tested by examining the corresponding memory subsets in the human patient cohorts (Figure 4.13-4.14). The T_{cm} phenotype dominated the memory population in both the blood and the CSF irrespective of underlying disease. In the OND group it was found that T_{cm} representation within the blood memory pool was directly proportional to the levels measured from matched CSF. This data

indirectly supports a similar analysis previously reported by *P. Kivisäkk et al (2004),* where the opposing T_{eff} memory phenotype is examined[249]. The authors show that the percentage of T_{eff} in the peripheral blood is proportional to that in matched CSF in patients without inflammatory disease, but here the distinction between T_{cm} and T_{eff} is defined by expression of $CD27^{hi/lo}$ as opposed to $CCR7^{+/-}$[249]. Given that my work shows $CCR7^{-}$ T_{eff} cells are as equally well represented in the CSF as the periphery in the absence of inflammation this may suggest that homeostatic recruitment across the CP (and potentially leptomeningeal spaces) into CSF is not CCR7 dependent (Figure 4.14). The proposal that $CD4^{+}$ T cell recruitment into the CSF is dependent upon CCR7 expression is supported by studies where lymphoblastic leukaemia is modelled in mice. Here transformed lymphoblastic cells from $CCR7^{-/-}$ haemopoietic progenitors are incapable of infiltrating into CNS whereas those from wild type progenitors migrate readily[454]. However, this work is not necessarily representative of homeostatic migration in mice and in response it may be favourable to directly measure CCR7 expression in the mouse system presented in this chapter. In humans, the CCR7 ligand CCL19 is constitutively expressed on brain post-capillary venules and is detectable in the CSF[285,286]. Additionally, constitutive expression of the alternative ligand CCL21 is reported on choroid plexus epithelium from cadavers without neuroinflammatory disease[249]. However, the argument that homeostatic CNS migration must involve CCR7 simply because it is expressed by the numerically dominant CSF T cell population does not hold in accordance with findings present as part of this thesis. A similar argument is presented in a recent study by *B. Vander Lugt et al (2013)* in the context of lymph node migration[455]. Despite universal understanding that T cells within secondary lymphoid organs are $CCR7^{+}$ when irradiated mice are reconstituted with mixed $CCR7^{+}$ and CCR7-deficient T cells, lymph node migration occurs independently of CCR7 expression. In line with my work, CCR7 expression may represent a bystander effect that is not essential in the CNS migration process *per se*.

The correlation between the memory subset distribution in the blood and CSF was consistent in every MS and non-MS inflammatory disease cohort tested, indicating that this relationship is independent of inflammatory disease status (Figure 3.14). This was contrary to finding from the *P. Kivisäkk et al (2004)* study was based on linear regression analysis no such relationship was found in an MS patient cohort[249]. My results suggest that proportionally there was no enrichment of T_{eff} cells in the CSF of any MS cohorts or inflammatory disease groups through increased $CCR7^-$ T_{eff} recruitment. Conversely, an absence of T_{eff} depletion in CSF memory pool is evidence against their preferential migration into the CNS parenchyma. However, although the distribution of T_{cm} and T_{eff} was not significantly altered in inflammation it cannot be discounted that their recruitment is via a pathway independent of the normal homeostatic routes. For example, a switch towards a more activation-driven chemokine dependent pathway could drive both T_{cm} and T_{eff} subset recruitment non-preferentially. $CXCR3^+$ T cells are enriched in the CSF in models of MS patients[360,361] and CXCR3 blockade is shown to inhibit the onset of disease in adoptive transfer models of EAE[456]. However, CXCR3 expression is not exclusive to the T_{eff} subset as shown by work examining anti-viral recall responses of T_{cm} in secondary lymphoid organs[457]. Here the CXCR3 ligands CXCL9 and CXCL10 are upregulated by activated DC at inflammatory foci. Expression of CXCR3 by T_{cm} is essential for the migration towards these areas and thus increases the kinetics of recall responses to viral antigen.

Enhanced migration of both T_{cm} and T_{eff} subsets through a concurrent upregulation of chemokine receptors could explain why the absolute frequency of CSF $CD4^+$ T cells increased in inflammation but the distribution of the subsets did not. In support of this there were significantly more $CD4^+$ and $CD8^+$ T cells in the CSF of CIS, RR-MS and ONID cohorts than in the non-inflammatory control group (Figure 4.12B). It cannot be discounted that in inflammation there is an increased reactivation and proliferation of $CD4^+$ and $CD8^+$ T cell populations behind the BBB and BCSFB *in situ*. Such T cell expansion has been

identified in the leptomeningeal spaces following the induction of EAE[289]. Interestingly, $CD4^+$ and $CD8^+$ frequencies from the PP-MS group were comparable to the OND cohort and may be reflective of a different disease aetiology compared with the other MS cohorts (Figure 4.12B). Overall, these findings suggest that differential T cell pleocytosis as opposed to memory status in various neuroinflammatory diseases could provide a useful diagnostic application. The significance of variable cellularity between disease states was also well documented in a meta-analysis of CSF composition by *Alvermann et al (2014)*[458].

CHAPTER SUMMARY

In summary, this line of investigation has challenged current understanding regarding the specificity of memory $CD4^+$ T cell migration into the CNS under homeostatic conditions. In contrast to human studies, enrichment of $CD8^+$ T cells was observed in mouse and rat CNS which may suggest a more dominant role of this subset in rodent immune homeostasis. However, $CD4^+$ T cells were identified in normal mouse brain and were predominantly localised to the CP regions and the meninges. Evidence suggests that migration from blood to CSF is permissive to both central and effector memory $CD4^+$ T cell subsets in the absence of inflammation. The memory phenotype of these subsets in the CSF is a reflection of their representation in the blood in both mice and men. In addition, the distribution of the memory subsets is not perturbed in neuroinflammatory pathology and the homeostatic migratory pathway persists. Therefore it is the frequency of CSF T cells that is best associated with active neuroinflammatory disease with particular respect to primary or reoccurring inflammatory episodes in MS.

CHAPTER 5

RESULTS

THE POTENTIAL OF $CD4^+$ T CELLS IN THE CNS TO ACTIVATE AND PRODUCE EFFECTOR CYTOKINES.

5 THE POTENTIAL OF CD4$^+$ T CELLS IN THE CNS TO ACTIVATE AND PRODUCE EFFECTOR CYTOKINES.

5.1 Rationale.

Many publications which review the immunological barriers in the CNS refer to the role of CD4$^+$ T cells in immune surveillance within the CSF space[253,257,452]. Findings that give probable cause for a role of adaptive immune surveillance within the CSF include; 1) the presence of various antigen presenting cells in the CSF space[289], 2) the circulation and outflow of CNS antigens from the CSF fluid[297,298], 3) a more dominant role of a lymphatic route of CSF drainage via the cervical lymph nodes than previously credited[294,295]. However, although memory CD4$^+$ T cells are the predominating adaptive immune cell in the CSF very few studies have directly examined their functionality in the absence of inflammatory pathology. Therefore, the robustness of CD4$^+$ T cell activation and cytokine production from healthy CSF has not been formally demonstrated. This void is particularly apparent in mouse studies where there is an extensive literature on CNS-associated T cell cytokine production in EAE and infection models, but few publications addressing T cell responsiveness in naïve animals. An exception to this is a study by Kunis et al (2013), who report an enrichment of IFNγ and IL-4 producing CD4$^+$ T cells in naïve CP but no such increase in IL-17 or GM-CSF secretors[282]. However, the authors do not report the cytokine secreting potential of CSF CD4$^+$ T cells as part of their study.

My investigation has previously described how CD4$^+$ T cells from healthy human peripheral blood were stimulated with PMA/ionomycin *in vitro* to reveal their cytokine potential (Chapter 3). In addition, upregulation of the activation marker CD69 was used to measure the responses of T cell populations to *in vitro* stimulation. As the effector function of homeostatic CD4$^+$ T cells in the CNS is poorly defined these analyses were applied to the CNS and CSF-derived CD4$^+$ T cell populations whose phenotype was examined in Chapter 4. As in experiments where the phenotype of these populations was examined, it was favourable to

model 'normal' CSF (and CNS) in rodent systems in addition to sampling from human patient cohorts. In this chapter the expression of CD69 and the proflammatory cytokine IFNγ were measured in two rodent systems. When sampling human data, CD69 expression was measured from blood and CSF-derived $CD4^+$ T cell populations in both non-inflammatory and inflammatory disease cohorts. This allowed for comparative analysis between a 'normal' and inflammatory pathological status in these compartments that could be measured in addition to examining intra-cohort differentials between the blood and CSF.

Preliminary studies prior to this investigation indicated that in the absence of inflammatory pathology the cytokine responses of $CD4^+$ T cells in the CSF were diminished comparative to the peripheral blood (Figure 1.5). Therefore, based on this data the hypotheses are that fewer $CD4^+$ T cells from non-inflamed human CSF will secrete cytokine but peripheral blood responses will remain robust. In addition, cytokine producing $CD4^+$ T cells will be enriched in the CSF of patients with neuroinflammatory disease. With regard to CD69 expression analysis, a hypothesis can be drawn based on evidence presented in the previous two chapters. In Chapter 3, a population of memory $CD4^+$ T cells that did not express CD69 upon *ex vivo* activation was identified in human peripheral blood. In addition, data presented in Chapter 4 argued in favour of selective memory $CD4^+$ T cell migration into the CSF compartment that was equally permissive to both T_{cm} and T_{eff} subsets in the absence of inflammation. Therefore it can be postulated that the representation of non-responsive ($CD69^{lo}$) $CD4^+$ T cells in the CSF memory compartment will be proportionally consistent with that seen in the peripheral blood memory pool.

5.2 Examination of differential CD69 expression by murine $CD4^+$ T cells in the CNS and peripheral blood.

Flow cytometry was used to examine the expression of CD69 in brain-derived $CD4^+$ T cells from unchallenged C57BL/6 mice. Findings were compared to analogous populations derived from the blood and the spleen. $CD4^+$ T cells in the brain were identified by gating on

$CD45^+CD3^+CD4^+$ lymphocytes from $CD45^+$ leukocyte preparations. $CD45^+$ leukocytes were isolated from a suspension of digested brain by MACS (see Chapter 4 Figure 4.11). All gating was set according to parameters identified in lysed peripheral blood cultures. Interestingly, in freshly isolated cell preparations it was noted that $CD4^+$ T cells in the brain had a slightly lower expression of CD4 than those populations in the blood and spleen. Uncultured cell isolates were then examined for their expression of CD69 *ex vivo* (Figure 5.1A, Figure 5.1C). Significantly more brain-derived $CD4^+$ T cells expressed physiologically elevated levels of CD69 than those cells from the peripheral blood and spleen (Figure 5.1C). However, the physiological expression of CD69 was notably lower than levels obtained following stimulation with PMA/ionomycin as was previously identified in human samples (Figure 3.16). There was little difference in the percentage of $CD69^{hi}$ $CD4^+$ T cells between the blood and spleen (11.5% ±2.7 and 13.5% ±1.5 (mean±SEM) respectively), whereas nearly a third of CNS-derived cells were of this phenotype (30.8% ± 5.9 (mean±SEM)).

In a separate analysis, cells from each tissue were cultured for 3 hours with PMA/ionomycin and the percentage of $CD4^+$ T cells that did not upregulated CD69 was measured (Figure 5.1B, Figure 5.1D). The classical downregulation of CD4 induced by PMA/ionomycin stimulation in human $CD4^+$ T cell cultures was not observed in the analogous murine population. In contrast, the difference in CD4 expression between $CD69^{lo}$ (non-responsive) and $CD69^{hi}$ (responsive) fractions was marginal. In these stimulation assays there was a decreased representation of non-responsive ($CD69^{lo}$) $CD4^+$ T cells in the brain compared to the peripheral blood and spleen. Only 15.0% ± 5.2 (mean±SEM) of brain-derived $CD4^+$ T cells did not respond to PMA/ionomycin as opposed to 35.9% ± 9.8 in the blood. Although this was not statistically significant, this shows that the brain-derived population were at least as responsive to the stimulus as the peripheral T cell pool.

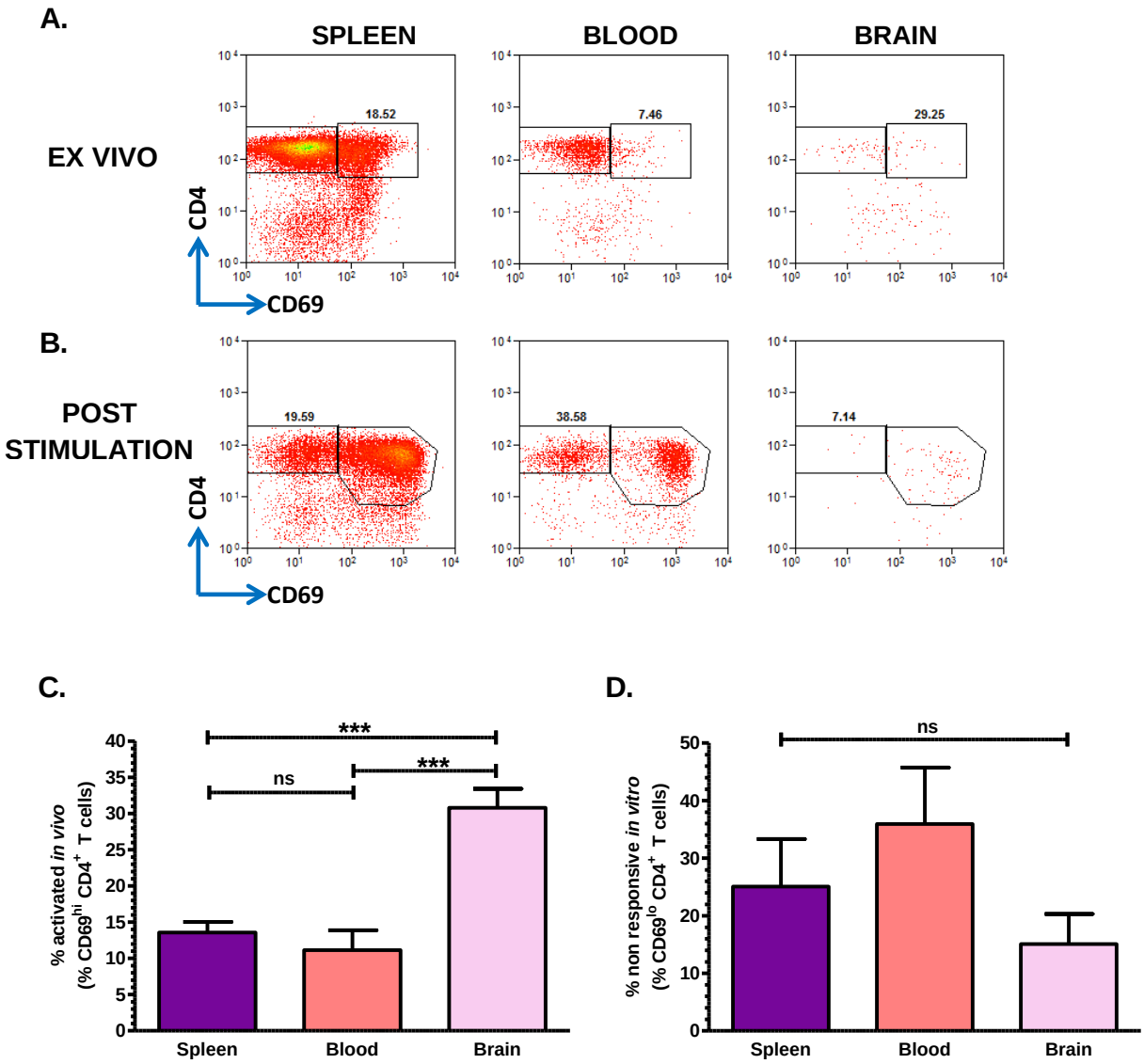

Figure 5.1 Analysis of CD69 expression by murine CNS derived CD4 T cells. Brain tissue was harvested from unchallenged, saline perfused C57BL/6 mice and the associated leukocytes ($CD45^+$) enriched through magnetic activated cell sorting (MACS). T cells ($CD45^+CD3^+CD8^-CD4^+$) from the brain-derived leukocytes, peripheral blood and spleen were analysed by flow cytometry for elevated CD69 expression as an indicator of recent activation *in vivo*. In additional experiments cell isolates were stimulated for 3h with PMA/ionomycin and analysed for the failure to upregulated CD69 (non-responsiveness). **A.** Representative flow cytometry plots show the percentage of $CD69^{hi}$ $CD4^+$ T cells in unstimulated assays. **B.** Plots show the percentage of non-responsive $CD4^+$ T cells ($CD69^{lo}$) in stimulated (+PMA) cell cultures. Plot numbers indicate each population as a percentage of total CD4 T cells (all gated cells). **C.** Graphs show the mean ± SEM proportion of $CD4^+$ T cells that are recently activated *in vivo* ($CD69^{hi}$). Data is representative of n=5 mice. **D.** The mean ± SEM percentage of non-responsive $CD4^+$ T cells ($CD69^{lo}$) following *in vitro* stimulation. Data is representative of n=6 mice. ***p<0.001, ns= no significance at p<0.05 (one way ANOVA statistical analysis followed by Bonferroni's multiple comparisons test).

The above findings were reproduced when endogenous and induced CD69 expression was examined in CSF-derived $CD4^+$ T cell populations (Figure 5.2). As was observed in brain-derived populations the percentage of CSF $CD4^+$ T cells that were recently activated *in vivo* ($CD69^{hi}$) was greater than those cells from the blood and spleen (Figure 5.2A, Figure 5.2C). Following stimulation fewer CSF $CD4^+$ T cells also failed to upregulate CD69 comparative to those in the periphery. Statistically this difference was not significant by means of ANOVA statistical testing comparing all three groups despite the apparent trend (Figure 5.2B, Figure 5.2D). Taken together these results may indicate that the $CD4^+$ T cell populations associated with the brain and the CSF compartment have a more activated phenotype *in vivo* and readily respond to PMA/ionomycin stimulation.

5.3 Quantification of 'non-responsive' $CD4^+$ T cells in the peripheral blood and CSF of patients with non-inflammatory neurological disease and multiple sclerosis.

The ability of peripheral blood and CSF $CD4^+$ T cells to activate in response to PMA/ionomycin was measured in two patient cohorts and one healthy control group. The healthy control group (HC) represented volunteers from the same population demographic as was investigated in Chapter 3 and for ethical reasons only blood was taken from these participants. To represent 'normal' CSF a group diagnosed with non-inflammatory neurological disease was examined as characterised in Table 2.3 and described in Chapter 4 (OND). However, for this experimental purpose sampling of patients with inflammatory disease was low and only individuals with a diagnosis of MS were included. Therefore, one patient with CIS, three with RR-MS, and four with PP-MS were grouped into a general MS cohort for this investigation (n=8).

In these experiments, cultures were stimulated for 6 hours to reveal the 'non-responsive' $CD4^{int}CD69^{lo}$ phenotype as described in Chapter 3. Firstly, the percentage of non-responsive cells in the $CD3^+CD8^-CD4^+$ T cell population in the blood was measured by flow cytometry and compared between the three groups (Figure 5.3A, Figure 5.3B).

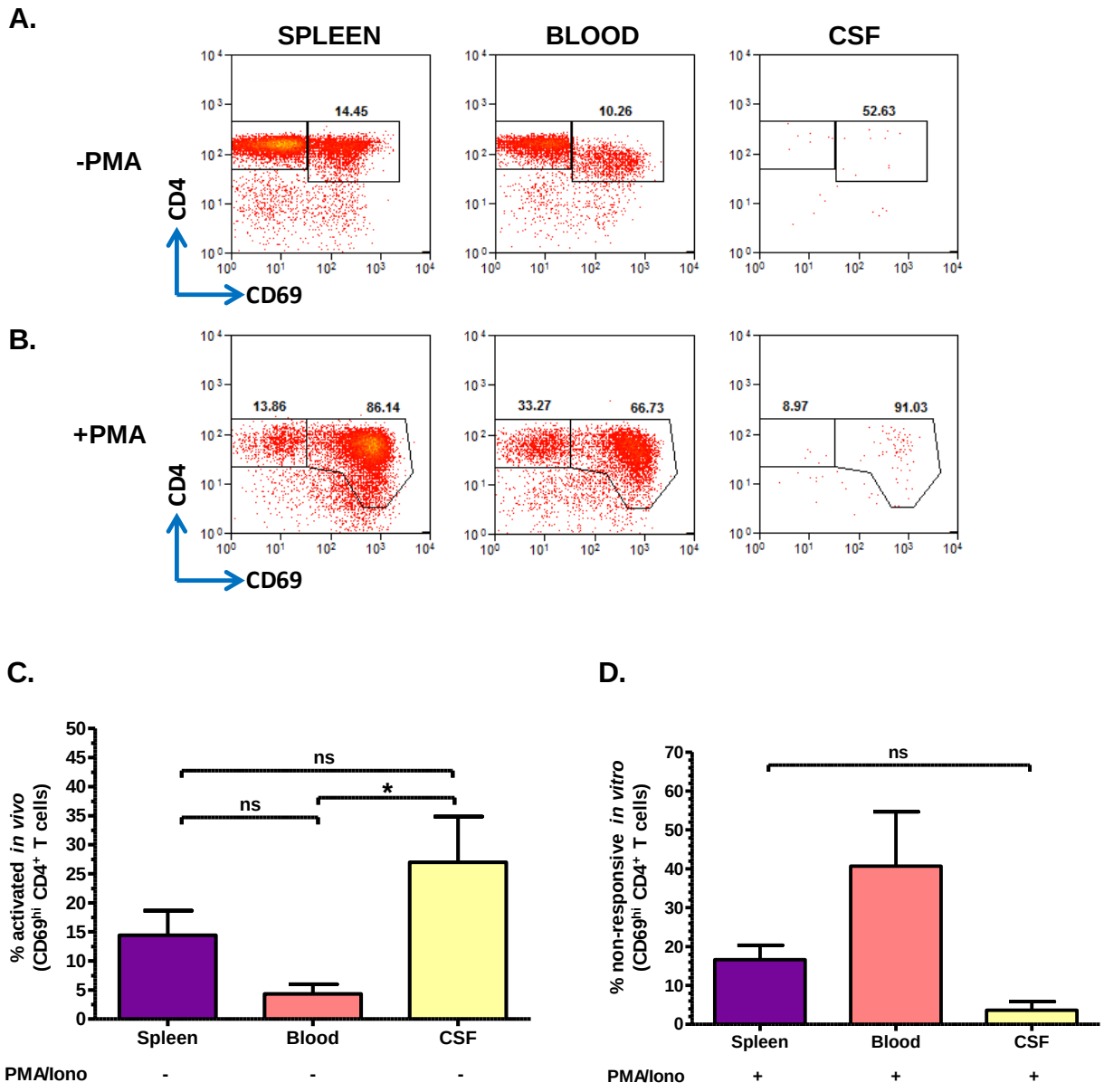

Figure 5.2 Analysis of CD69 expression by murine CSF derived CD4 T cells. Cerebrospinal fluid (CSF) was pooled from unchallenged C57/BL6 mice and the cellular compartment was analysed by flow cytometry. Uncultured T cells ($CD45^+CD3^+CD8^-CD4^+$) from CSF, peripheral blood, and spleen were analysed for expression of $CD69^{hi}$ as an indicator of recent activation *in vivo*. In additional experiments cell isolates were stimulated for 3 hours with PMA/ionomycin and analysed for the failure to upregulated CD69 (non-responsiveness). **A.** Representative flow cytometry plots show the percentage of $CD69^{hi}$ $CD4^+$ T cells in uncultured (-PMA) assays. **B.** Plots show the percentage of non-responsive $CD4^+$ T cells ($CD69^{lo}$) from stimulated (+PMA) cell cultures. Plot numbers indicate each population as a percentage of total $CD4^+$ T cells (all gated). **C.** Graphs show the mean ± SEM proportion of $CD4^+$ T cells that are recently activated *in vivo* ($CD69^{hi}$). Data is representative of n=6 mice measured in 3 independent experiments **D.** The mean ± SEM percentage of non-responsive $CD4^+$ T cells ($CD69^{lo}$) following *in vitro* stimulation. Data is representative of n=6 mice measured in 3 independent experiments. *$p<0.05$, ns= no significance at $p<0.05$ (one way ANOVA statistical analysis followed by Bonferroni's multiple comparisons test).

The percentage of $CD4^{int}CD69^{lo}$ non-responsive cells recorded in the healthy control group was low compared with the OND and MS groups (8.2% (3.6-17.3 IQR)). However, the representation of non-responsive cells in this control group was notably higher than when healthy individuals were analysed previously, where the median percentage was shown to be 1.2% (0.7-1.9 IQR) (Chapter 3 Figure 3.9). The proportion of non-responsive cells in the OND and MS groups was very high and measured at 3.2 times and 3.7 times greater than the healthy control group respectively (Figure 5.3B). This increase in the non-responsive cell frequency between the HC and both the OND and MS groups was statistically significant but there was no statistical difference between the two patient cohorts. When the representation of non-responsive cells in the CSF of OND and MS patients was compared there was a notable decrease observed in the MS group (Figure 5.3C). No statistical significance was associated with this difference due to both high variability in the population's frequency in the OND group and two outliers in the MS cohort where a very high percentage of non-responsive cells was recorded.

The representation of non-responsive cells in the blood was then compared to the corresponding frequency in the CSF in OND and MS patient groups (Figure 5.3D, Figure 5.3E). In the OND group, the frequency of non-responsive cells in the CSF ranged from 3.2-70.8% and was notably more variable than in the blood. However, the median percentage of the population was not significantly different between the blood and CSF (Figure 5.3A, Figure 5.3D). In contrast, the non-responsive phenotype in the CSF of the MS group was notably reduced comparative to the blood in most individuals (Figure 5.3A, Figure 5.3E). The exception to this trend was the two aforementioned outliers whose frequency of non-responsive cells in the CSF was extremely high.

To further characterise the non-responsive phenotype in each patient cohort the proportion of non-responsive cells in each $CD4^+$ T cell subset was measured in the blood and CSF (Figure 5.4). In Chapter 3 it was identified that the representation of the non-responsive population

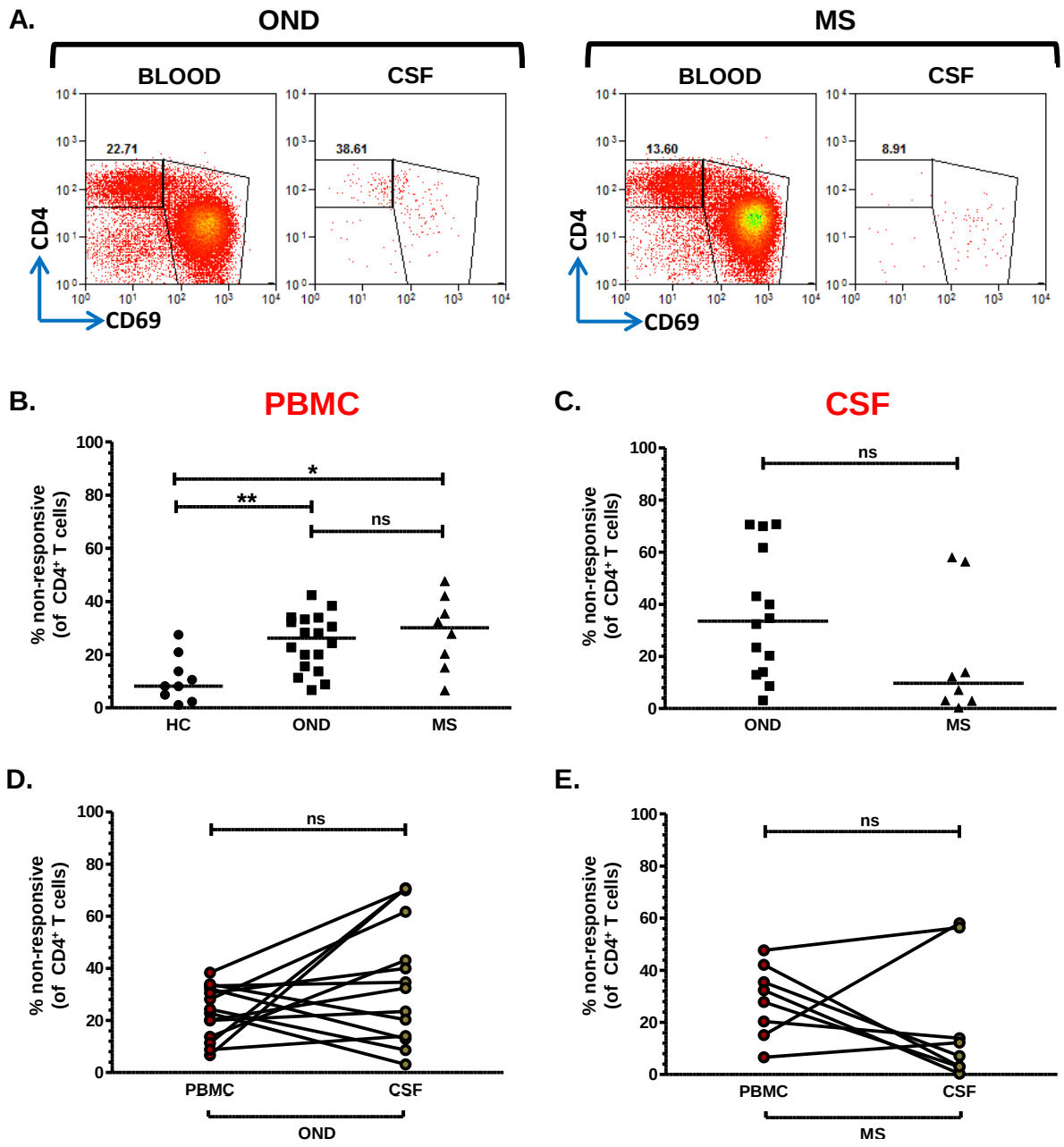

Figure 5.3 Investigation of hyporesponsive CD4$^+$ T cell frequencies in the blood and cerebrospinal fluid of patients with neurological and inflammatory neurological disease. Peripheral blood mononuclear cells and CSF cell isolates were collected from two patient groups (non-inflammatory neurological disease (OND) and multiple sclerosis (MS)) and stimulated for 6h with PMA/Ionomycin. The CD4$^+$ T cell population (CD3$^+$CD8$^-$CD4$^+$) was analysed by flow cytometry for the failure to upregulate CD69 following stimulation. CD69^{lo} expression was gated at the fluorescence intensity of unstimulated cultures. **A.** Representative plots show the responsive (CD4^{lo}CD69^{hi}) and non-responsive (CD4^{int}CD69^{lo}) CD4$^+$ T cell fractions in the blood and matched CSF of each disease cohort. Numbers indicate the percentage of unresponsive cells. **B-C.** The median percentage of non-responsive CD4$^+$ T cells in the blood **(B.)** and the CSF **(C.)** of each patient cohort and a healthy control (HC) group. **D-E.** The median non-responsive cell frequency in the blood and CSF was compared in the OND **(D.)** and MS **(E.)** groups. *p<0.05, **<p<0.01, ns = no significance at p<0.05 (Mann-Whitney statistical test (**B-C.**) Wilcoxon matched-pairs signed rank test (**D-E.**)). Data is representative of n=14 CSF and n=18 PBMC samples in the OND cohort and n=8 blood and CSF samples in the MS cohort.

may be biased by the frequency and distribution of each T cell subset. Therefore, a gating strategy was applied to measure the percentage of T_{naive} ($CD45RA^{+}CCR7^{+}$), T_{cm} ($CD45RA^{-}CCR7^{+}$) and T_{eff} ($CD45RA^{-}CCR7^{-}$) cells that were non-responsive, as opposed to examining the representation of each subset within the $CD4^{int}CD69^{lo}$ population (Figure 5.4A).

Firstly, peripheral blood samples were analysed to identify the $CD4^{+}$ T cell subset with the greatest representation of non-responsive cells. It was found that the T_{cm} population had the highest median frequency of non-responsive cells in both OND and MS groups (around 45% and 53% in the OND and MS groups respectively) (Figure 5.4B). There was also a high representation of these cells in the T_{eff} subset of both groups, with no statistically significant difference in frequency identified between the T_{cm} and T_{eff} subsets. Consistent with trends revealed where healthy controls were sampled in Chapter 3, minimal numbers of T_{naive} cells in the blood failed to respond to PMA/ionomycin stimulation in both patient groups (Figure 5.4B). There was also minimal representation of non-responsive cells in the T_{naive} compartment in the CSF of OND and MS patients (Figure 5.4C). The exception to this trend was two outliers in the MS group, but these patients were not shown to have the same clinical course of MS. As in the blood the T_{cm} subset had the highest proportion of the non-responsive population in both groups. However, non-responsive cells in the T_{cm} subset were 2.3 times more numerous than the T_{eff} subset in the OND group, whereas this differential 3.3 times in favour of the T_{cm} subset in the MS group (Figure 5.4C). This suggests that T_{eff} cells in the CSF of MS patients are proportionally more responsive than T_{cm} cells when compared with individuals that have no underlying inflammatory disease.

In an alternative analysis of the data set described in Figure 5.4 the percentage of non-responsive $CD4^{+}$ T cells in each subset was directly compared between the blood and CSF compartments within each patient group (Figure 5.5). In the OND group there were no statistically significant changes between the responsiveness of blood and CSF-derived T cells across all the subsets (Figure 5.5A).

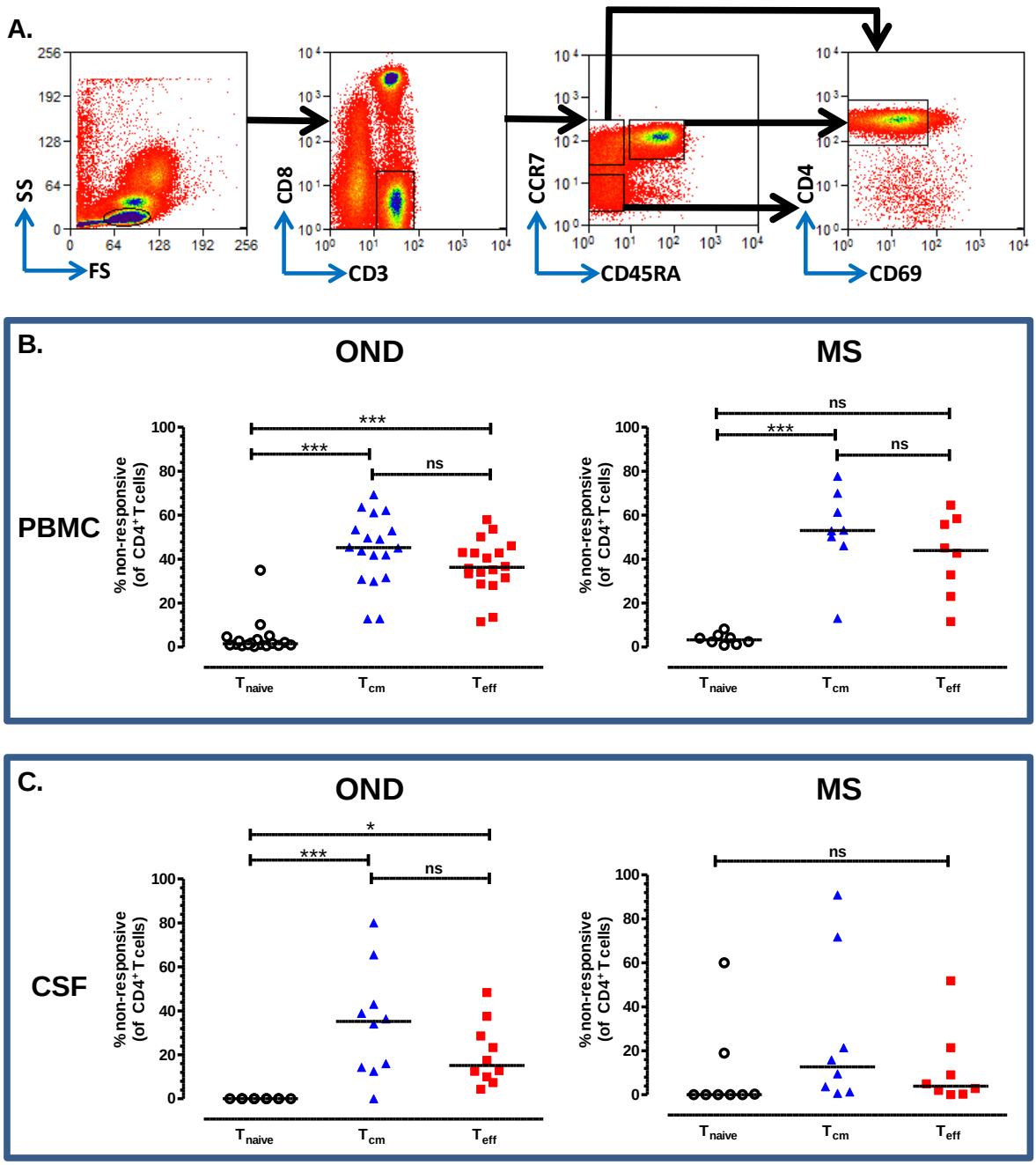

Figure 5.4 The effect of disease status upon the subset distribution of non-responsive CD4$^+$ T cells within the blood and cerebrospinal fluid compartments. Peripheral blood mononuclear cells and cerebrospinal fluid (CSF) cells were isolated from patients with non-inflammatory neurological disease (OND) and multiple sclerosis (MS). Cells were stimulated for 6h with PMA/Ionomycin and the naïve (CCR7$^+$CD45RA$^+$), Central memory (CCR7$^+$CD45RA$^-$) and effector memory (CCR7$^-$CD45RA$^-$) CD4$^+$ T cell populations analysed for the percentage of cells that did not upregulate CD69. **A.** Flow cytometry gating strategy for identifying unresponsive (CD4^{int}CD69^{lo}) CD4$^+$ T cells in each subset. CD69^{lo} expression was gated at the fluorescence intensity of unstimulated cultures. **B-C.** The percentage of unresponsive CD4$^+$ T cells from each subset in the blood **(B.)** and CSF **(C.)** of patients with non-inflammatory neurological disease and inflammatory neurological pathology. ***p<0.001, *p<0.05 ns = no significance at p<0.05 (Friedman statistical test, followed by Dunn's multiple comparisons analysis). Data is representative of n=10 CSF and n=18 PBMC samples in the OND cohort and n=8 blood and CSF samples in the MS cohort.

However, comparative to the blood there was a notable reduction of non-responsive cells in the T_{cm} and T_{eff} subsets in the CSF. In contrast, when the MS group was examined both the T_{cm} and T_{eff} non-responsive populations were markedly diminished in the CSF comparative to the blood (Figure 5.5B). Due to two outliers with a very high percentage of non-responsive cells in the CSF this decrease was not statistically significant in the T_{cm} subset. However, there were significantly fewer non-responding cells in the T_{eff} subset which strongly indicates a differential activation status of this subset in the CSF compartment (Figure 5.5B).

The dataset was then analysed to examine the effect of inflammation upon the frequency of non-responsive cells in each subset derived from the blood and CSF (Figure 5.5C, Figure 5.5D). In the blood the frequency of non-responsive cells in each subset was comparable between the OND and MS subsets (Figure 5.5C). This indicates that inflammatory changes associated with MS do not affect the responsiveness of $CD4^+$ T cells in the blood. However, notable changes in responsiveness were observed between the groups when the CSF was examined (Figure 5.5D). The median frequency of non-responsive cells in the T_{cm} and T_{eff} subsets was diminished in the MS cohort comparative to the OND group. This result suggests that both memory subsets activate more readily in the CSF on a background of neuroinflammation, although no statistical inferences were drawn from these findings (Fig 5.5D). Surprisingly there were significantly more non-responsive CSF cells in the T_{naive} subset of MS patients. However, this is largely due to two outliers in the MS cohort that expressed very high numbers of non-responsive cells, whereas none of the OND patients had any non-responsive cells in their samples (Figure 5.5D). Together with the low cell numbers and the very low representation of T_{naive} cells in the CSF compartment it is unlikely that this difference between the groups is truly reflective of a difference in non-responsive cell status.

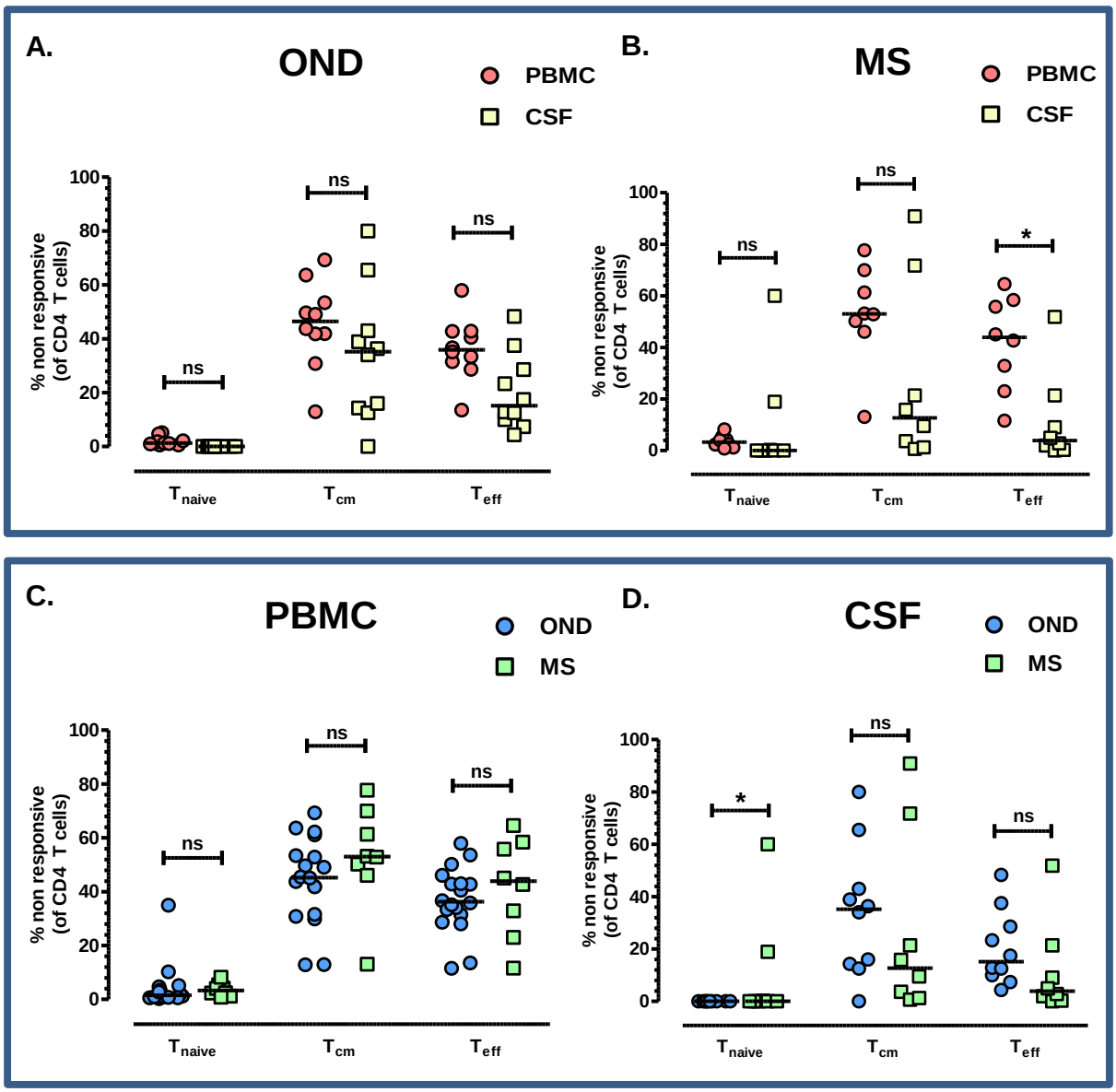

Figure 5.5 Comparative analysis of hyporesponsive CD4$^+$ T cells in the blood and cerebrospinal fluid of patients with and without neuroinflammatory disease. Peripheral blood mononuclear cells and cerebrospinal fluid (CSF) cells were isolated from patients with non-inflammatory neurological disease (OND) and multiple sclerosis (MS). Cells were stimulated for 6h with PMA/Ionomycin and the naïve (CCR7$^+$CD45RA$^+$), Central memory (CCR7$^+$CD45RA$^-$) and effector memory (CCR7$^-$CD45RA$^-$) CD4$^+$ T cell populations were analysed for the percentage of cells that did not upregulate CD69 (non-responsive cells). **A-B.** Comparative analysis of the non-responsive cell frequency in each subset derived from the peripheral blood and CSF (**A.** OND group, **B.** MS group). **C-D.** Graphs show the non-responsive cell frequency in each subset identified in blood (**C.**) and CSF (**D**) of OND and MS patients. *p<0.05 ns = no significance at p<0.05 (Wilcoxon matched-pairs signed rank test (**A-B.**), Mann-Whitney statistical test (**C-D.**)). Data is representative of n=10 CSF and n=18 PBMC samples in the OND cohort and n=8 blood and CSF samples in the MS cohort. Graph error bars depict the interquartile range.

5.4 Analysis of cytokine expression by peripheral and CNS-derived $CD4^+$ T cells in the rat.

Having examined the ability of CSF (and CNS) derived $CD4^+$ T cells to activate in response to PMA/ionomycin stimulation in both human and mouse the expression of cytokine was analysed by flow cytometry to provide further insight into their effector function. Due to the low cellularity of CNS and CSF preparations in the mouse it was inappropriate to analyse cytokine expression in this system. Therefore, analysis of cytokine expression was performed in the rat as more CNS cells were obtainable. Following stimulation with PMA/ionomycin for three hours the expression of the archetypal Th_1 cytokine IFNγ by rat spleen, blood, CSF, CP and brain derived $CD3^+CD4^+$ T cells was analysed by flow cytometry (Figure 5.6). The percentage of IFNγ producing $CD4^+$ T cells in lysed blood and splenocyte cultures was low (0.9% ± 0.3 and 1.9% ± 0.5 respectively (mean ± SEM)). In contrast, the proportion of $IFN\gamma^+$ $CD4^+$ T cells in the CSF was dramatically increased with over a third of CSF-derived cells expressing the cytokine (34.2% ± 8.6 (mean ± SEM)). Consistent with this increase in IFNγ producing cells in the CSF there was also considerable enrichment of the $IFN\gamma^+$ $CD4^+$ T cells in CP and whole brain digests. However, due a limited number of experiments in these tissues no statistical inferences could be drawn from these findings. Together these findings indicate that in rodents IFNγ producing $CD4^+$ cells are enriched in the CNS compartments.

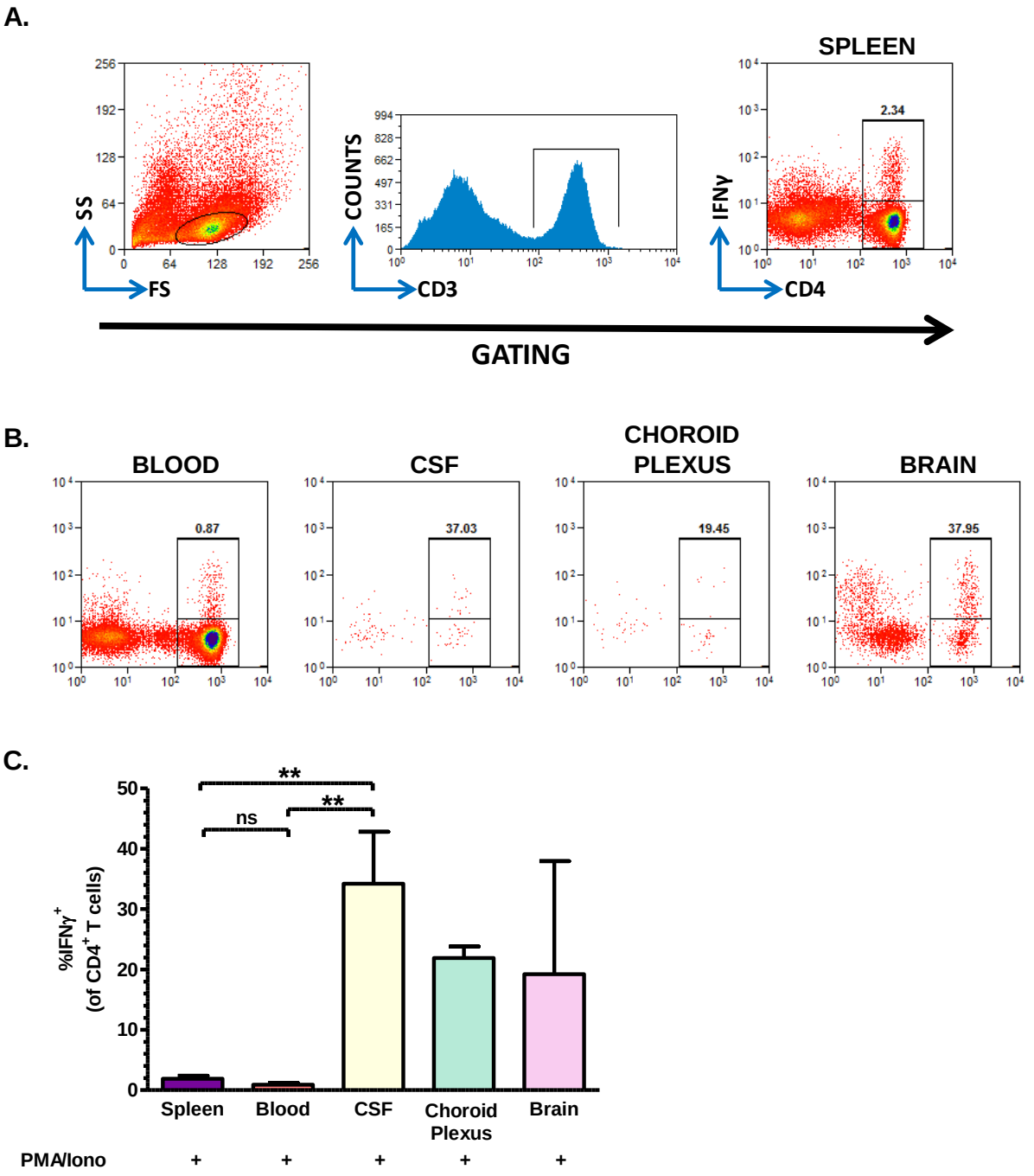

Figure 5.6 Expression of IFNγ by central nervous system CD4$^+$ T cells. Cerebrospinal fluid (CSF), saline perfused choroid plexus and brain tissue were harvested from terminally anesthetised rats, and cell preparations from each compartment were stimulated with PMA/Ionomycin for 3h. The CD4$^+$ T cell populations were analysed for expression of IFNγ by flow cytometry and the expression compared with matched peripheral blood and spleen derived samples. **A**. Gating strategy to define IFNγ expression by CD3$^+$CD4$^+$ T cells. Gating is demonstrated using a rat spleen sample. **B.** Representative plots showing IFNγ expression by CD4$^+$ T cells in each tissue compartment. Data is representative of n=2 independent experiments. **C.** Graph of the mean ± SEM percentage of CD4 T cells that express IFNγ. ns = no significance at $p<0.05$, *$p<0.05$, **$p<0.01$ (one way ANOVA statistical analysis followed by Bonferroni's multiple comparisons test). Data is representative of n=1-5 independent experiments.

5.5 Discussion.

A defining characteristic of memory $CD4^+$ T cells is the ability to produce effector cytokine in response to an immunogenic stimulus. Therefore, in order to have a role in CNS immune surveillance it may be anticipated that CSF $CD4^+$ T cells elicit a robust cytokine responses. In this chapter, 'normal' CSF was modelled in mice and rats to examine the activation status of the $CD4^+$ T cell compartment. In order to produce cytokine, $CD4^+$ T cells must be activated which can be measured by surface expression of CD69[51,411]. In the absence of an applied exogenous stimulus a greater number of $CD4^+$ T cells associated with the brain and CSF of unchallenged mice expressed the activation marker CD69 than those in the peripheral blood (Figure 5.1C, Figure 5.2C). In this investigation the analysis of *ex vivo* CD69 expression by human CSF CD4+ T cells was not examined as all samples were used for experiments where cells were stimulated *in vitro*. However, in support of findings in mouse a human study from by *P. Kivisäkk et al* has previously demonstrated an increased proportion of central memory $CD4^+$ T cell ($CD4^+CD45RO^+CD27^+$) in the CSF which exhibit a recently activated $CD69^+$ phenotype[271]. It can be speculated that the increase in $CD69^+$ $CD4^+$ T cells in the CSF (and brain) is brought about by either 1) selective migration of $CD69^+$ memory cells from the blood, 2) activation of the memory $CD4^+$ T cells during migration across the BCSFB or BBB, 3) intrathecal activation within the CSF space, 4) residency of $CD4^+$ T cells within the CP or CSF-filled cavities such as the subarachnoid space. With consideration to the first proposal, CD69 expression is not a prerequisite for migration in mature T cell subsets into peripheral tissues as shown by unaltered migration of $CD4^+$ T cells into intestine, lungs, liver and lungs in $CD69^{-/-}$ mice[459]. From a surveillance perspective CD69-dependent migration would severely restrict the repertoire of $CD4^+$ T cells with CSF access given the infrequency of $CD69^+$ T cells in the blood. However, as CD69 expression is associated with activation it may be that other receptors such as chemokines or integrins that are upregulated with activation mediate the migration progress, thus causing the apparent $CD69^+$ enrichment. This is

consistent with the long standing view that in passive models of EAE only T cells that are activated in the periphery can gain access to the CNS[460,461] .

$CD4^+$ T cell interaction with activated endothelium is reported to increase surface CD69 expression[462], but in the absence of inflammatory disease or infection it may be assumed the CNS endothelium is not activated. As the BCSFB represents a double barrier of endothelium and epithelium at the level of the CP it cannot be discounted that $CD4^+$ T cells acquire CD69 expression in the CP stroma. This may be considered more probable than CD69 acquisition in the intrathecal space unless interaction of $CD4^+$ T cells with the *pia mater* and ependymal lining of the CSF cavities is capable of triggering CD69 expression. This is also under the assumption that interaction with APC in the CSF space would not trigger CD69 expression without cognate antigen recognition via the TCR and that CD69 $CD4^+$ T cells are not selectively retained within the intrathecal compartment as part of a resident phenotype.

Aside from the association of CD69 with activation it is also reported to modulate the migration patterns of $CD4^+$ T cells within secondary lymphoid organs. Given that the CSF can be equated to a modified lymphatic of the CNS it can also be speculated that CD69 expression has a role in $CD4^+$ T cell migration behind the BCSFB and BBB. In the context of peripheral mucosal barriers, tissue resident $CD4^+$ T cells in the periphery are distinct from their circulating counterparts through the constitutive CD69 expression[463]. As CD69 expression by resident $CD4^+$ T cells within the skin mucosa is independent of activation status[95] it is possible that $CD69^+$ T cells within the CNS reside there more permanently than previously credited. Thus, $CD69^+CD4^+$ T cells may not necessarily represent peripherally-derived 'activated' cells *per se*. In support of this, virus-specific $CD8^+$ T_{RM} cells have been shown to reside within the CNS of mice for up to a year post infection[448,449]. These T_{RM} cells are $CD103^+$ and parabiosis experiments in mice show that they do not recirculate[93]. How applicable this model is to T_{RM} persistence without a prior heavy antigen load is not well reported. In addition, an analogous CNS $CD4^+$ T_{RM} population has not been identified. In a

study by *Kivisakk et al (2006)* where CSF from a small human cohort is sampled the author anecdotally describes how CSF $CD4^+$ T cells were found to be negative for expression of CD103[464]. Therefore, it is possible that $CD103^+$ T cells are maintained within the CP whilst $CD103^-$ subsets recirculate in the CSF. Ideally analysis of matched CP and CSF samples would be required to confirm this. A basis for this hypothesis could be achieved by examining the $CD103^+$ expression of those rodent CNS $CD4^+$ T cells identified in my investigation to test for $CD69^+CD103^+$ T_{RM} in the CP, CSF and whole brain compartments.

When murine cell cultures were stimulated with PMA/ionomycin $CD4^+$ T cells upregulated CD69 but did not downregulate CD4 as is characteristically observed in the analogous human population (Figure 5.1-5.2). This may suggest that in mouse the coupling of CD4 to $p56^{lck}$ or its recycling pathway is not perturbed by PMA in the way it is in humans[372]. Stimulation of murine CSF and brain-derived leukocyte cultures with PMA/ionomycin resulted in the activation of the majority of $CD4^+$ T cells. More cells upregulated CD69 than in the peripheral blood and spleen which was reflected by a decrease in the non-responsive population. This may be in part due to the fact that a greater proportion of the population expressed physiologically high levels of CD69 *in vivo* and therefore would not have fallen within the $CD69^{lo}$ non-responsive gate (Figure 5.1-5.2). Therefore, even though less of the $CD4^+$ population in the CSF and brain didn't respond to the stimulation this may not necessarily mean they are more responsive. Anecdotally, the level of CD69 expression on the cells that did respond was similar in the CNS and peripheral compartments as shown by an equivocal CD69 MFI. This suggests that CNS-associated $CD4^+$ T cells that do activate can upregulate CD69 at least as readily as cells in the blood and spleen. Together this is evidence that $CD4^+$ T cell in the CNS are at least as responsive as those cells in the periphery and the microenvironment of the CSF or CNS niches does not diminish their ability to activate. However, more work is required to investigate the acquisition of CD69 expression by CNS

$CD4^+$ T cells *in vivo* as this may be highly informative with respect to their origins and migratory behaviour in addition to their functionality.

When CD69 expression by $CD4^+$ T cells from OND and MS patient blood were examined the percentage of non-responsive cells was surprisingly high (5.3A, 5.3B). In addition, the non-responsive $CD4^+$ T cell frequency in the HC group was elevated by around 7% compared with the same population demographic sampled in Chapter 3. As another member of the group was responsible for processing the HC samples referred to in this chapter it was considered whether technical discrepancies between our preparations were accountable for the differential hyporesponsiveness between these data sets. As I reanalysed these samples in accordance with the gating strategy and parameters used in Chapter 3 our potential differential interpretation of flow cytometry plots was not responsible for the variation. To directly compare technical variation between individuals on two occasions the entire assay was performed in parallel using blood from the same donor. When our corresponding non-responsive populations were compared on both occasions there were negligible differences in the T cell phenotype and responsiveness between our samples. With such internal controls established the reasons why the non-responsive cell frequency varied in healthy donors between the data sets remains unknown. An untested variable was the time of day at which the samples were taken as in Chapter 3 all blood was sampled between 8-9am whereas in this data set the time varied according to when patient samples were taken.

As the OND cohort represented patients with no immunological component to their neuropathology it was expected that the percentage of $CD4^{int}CD69^{lo}$ non-responsive cells in OND blood should match that observed in healthy control (HC) patients. However, there was a much higher representation of the non-responsive population in the OND group despite these HC assays being performed in parallel to minimise the sampling error. As the HC samples were taken within the research lab facility and the OND/MS samples were taken in clinic it was questioned whether this differential processing was responsible for the variation

in hyporesponsiveness. Much effort was taken to ensure technical variables were not responsible for these changes, with independent experiments being performed to directly test differences in standard operating procedure (data not shown). In these tests, it was shown that the collection of blood into heparinised tubes versus the EDTA anti-coagulant used in the clinic had no influence on the responsive population. To account for the increased time that sample were held in clinic compared to the lab, the duration of time between blood sampling and cell culture was also tested. This also had no bearing on the outcome of CD69 expression.

Having minimised the impact of technical variation, it is difficult to pinpoint why the representation of non-responsive cells was elevated in the OND cohort compared with the HC group. It is possible that the increase was related to the co-morbidity of patients in the OND group but it is impossible to pinpoint an exact cause given the different disease aetiology in this mixed cohort. Despite this, a common feature all the OND patients share is the acute stress they were under at the time of sampling as blood was taken at the time of CSF collection by lumbar puncture. In addition, another consideration is the chronic stress and prolonged anxiety these patients may suffer as a result of their neurological illness. Although the impact of stress in this system is not measurable directly there is significant attention to the effects of psychological disorders upon immune function in the literature. In rat models it is documented that acute and chronic stress can decrease T cell numbers in the blood whilst reducing both their IL-2 production and proliferative capacity[465,466]. In humans, chronic psychological stress is commonly associated with immune suppression, increased infection rates and decreased tumour surveillance[467–469] which is fitting with the T cell hyporesponsiveness observed in these assays.

The same iatrogenic and psychological stressors applied to the MS group and OND group as all these patients were sampled in the same way. Therefore, in the context of assessing whether inflammation has an impact on the hyporesponsiveness of $CD4^+$ T cells the more appropriate comparative analysis is between the MS and OND group as opposed to between

the MS the HC cohort. Although the non-responsive population in the blood of MS patients was significantly greater than the HC group there was only a marginal increase between the MS and the OND cohorts (Figure 5.3B). In addition, the percentage of non-responsive cells in both the memory and naïve $CD4^+$ T cell subsets was comparable in PBMC cultures from OND and MS groups (Figure 5.5C). Therefore, the activation status of the T cell subsets in the blood was not skewed by inflammatory pathology. These findings suggest that an inflammatory background does not influence the upregulation of CD69 by the circulating $CD4^+$ T cell population in the blood and thus does not contribute to $CD4^+$ T cell hyporesponsiveness. This may imply that chronic antigenic stimulation (as a feature of ongoing neuroinflammatory pathology), does not drive the hyporesponsiveness of $CD4^+$ T cells that is revealed by *ex vivo* stimulation. This is evidence against the suggestion that the $CD4^{int}CD69^{lo}$ non-responsive phenotype represents cells driven into tolerised or exhausted state via persistent antigen exposure as discussed in Chapter 3. However, to add weight to these findings increased sampling in the MS group is required and would thus enable the multiple disease etiologies represented in the MS cohort to be analysed independently.

In contrast to findings in the blood, more notable differences in the non-responsive population were observed in CSF samples from the OND and MS cohorts (Figure 5.3-5.5). In the OND group there was a decreased representation of non-responsive cells within the T_{cm} and T_{eff} subsets in the CSF when compared with the blood, most notably in the T_{eff} subset (Figure 5.5A). This decrease in $CD4^+$ T cell non-responsiveness is consistent with the trends observed in mouse experiments (Figure 3.1-3.2) and suggests that in the absence of inflammation $CD4^+$ T cells in the CSF upregulate CD69 at least as readily as their peripheral blood counterparts. This is further evidence that without inflammation the CSF microenvironment does not promote the $CD4^+$ hyporesponsiveness as revealed by PMA/ionomycin stimulation. From an alternative perspective as the non-responsive phenotype is not enriched in the CSF this is evidence against its selective recruitment from the blood. However, it cannot be discounted

that the non-responsive population in the CSF was affected by an increased *in vivo* expression of CD69 in the intrathecal compartment as was identified in mouse (Figure 5.2C). The mouse models in this investigation has highlighted the importance of measuring *ex vivo* CD69 expression in human systems in the future to examine for features of residency and persistence in the CNS.

In the MS cohort there was a more pronounced reduction of non-responsive $CD4^+$ T cells in the CSF relative to the blood (Figure 5.3E, 5.5B). The source of this decrease was a reduction of cells that failed to respond in both the T_{cm} and T_{eff} subsets indicating that both intrathecal populations are more readily activated. It was also noted that the decrease in T_{eff} non-responsive cells between the blood and CSF was comparatively greater than in the T_{cm} subset (Figure 5.5B). Although the non-responsive frequency from the T_{cm} subset was subject to extreme variation these findings suggest that the T_{eff} subset was preferentially more readily activated in the MS CSF compartment. Together this indicates the predomination of a more reactive memory phenotype in the CSF space in MS which is consistent with T cell mediated damage associated with the disease. This phenomenon may occur due to either a reversal of the hyporesponsive state within the CNS compartment or be reflective of the preferential migration of activated cells from the blood. Given the potency of PMA/ionomycin stimulation combined with the failure of prior *in vitro* experiments to reverse the non-responsive state the former scenario may be considered less likely. In contrast, there are many reports that document an increased recruitment of activated T cells into the CNS via differential chemokine receptor expression in MS. This is a mechanism by which increased trafficking of relevant (CNS antigen specific) T cell clones to the CNS can occur. An increased expression of the chemokine receptors CXCR3 and CCR5 by $CD4^+$ T cells is highly associated with inflammatory events in MS and coupled with elevated concentrations of chemokine ligand within the inflamed CNS[360,361]. However, expression of CXCR3 is not exclusive to MS as it is reportedly expressed by $CD4^+$ T cells in healthy CSF[288]. Conversely, *Juliá E et al (2006)*

have previously reported *ex vivo* CD69 expression that is exclusive to $CCR5^+$ $CD4^+$ T cells in the blood of MS patients[470]. Therefore, it is possible that preferential migration of $CCR5^+CD69^+$ $CD4^+$ T cells from blood to CSF is responsible for my reported decrease in non-responsive CSF T cells in the MS cohort (such cells would not be gated $CD4^{int}CD69^{lo}$). It is also possible that $CCR5^+$ $CD4^+$ T cells are reactivated by APC within the CSF space and thus physiological CD69 expression is induced intrathecally. These proposals could be substantiated by *ex vivo* examination of CD69 and CCR5 expression by $CD4^+$ T cells in the cohorts investigated in this study. Such work is important as the differential CD69 expression by CSF $CD4^+$ T cells in the OND and MS cohorts may be reflective of alternative homeostatic versus inflammatory recruitment pathways in health and disease.

Due to the low number of $CD4^+$ T cells retrieved from mouse CSF it was not considered appropriate to perform cytokine analysis in this system. IFNγ is a highly expressed Th_1 cytokine both in terms of the number of $CD4^+$ T cells that can produce it and its level of expression on a per cell basis (data shown in Chapter 3 Figure 3.2M). Therefore IFNγ expression by $CD4^+$ T cells was measured in rat spleen, blood, CSF, CP and brain where the cellularity was conducive to a meaningful analysis. In all three CNS compartments the percentage of $IFN\gamma^+$ $CD4^+$ T cells was extremely elevated when compared to the blood and spleen (Figure 5.5). However, it was not possible to perform this analysis in the $CD4^+$ memory T cell compartment specifically. This was because the 'memory' marker (CD45RC) used to define a naïve ($CD45RC^{hi}$) and memory ($CD45RC^{lo}$) T cell phenotype was lost on all PMA/ionomycin stimulated cells. In itself this finding is suggestive that CD45 expression is more representative of activation status than a true memory marker. This was frustrating as it was not possible to precisely quantify how much of the $IFN\gamma^+$ enrichment in CNS, CP and CSF was attributable to an increased representation of memory cells in these compartments. Despite this, what can be drawn from these experiments is that even under the assumption that 100% of CNS-derived $CD4^+$ T cells were a memory phenotype their IFNγ response was

substantial in these assays. This work supports the rejection of the hypothesis that cytokine responses are diminished in the CNS as IFNγ expression by CNS $CD4^+$ T cells was shown to be robust in rat. These results were in line with a study of murine choroid plexus by *Kunis et al (2013)* where approximately 17% of all CP $CD4^+$ T cells were found to express IFNγ in a similar PMA/ionomycin stimulation assay[282]. No data for IFNγ expression by CSF or whole brain $CD4^+$ T cells was presented by the author, but in my investigation the corresponding value for CP derived cells was approximately 22% in rat (Figure 5.5),.

The expression of cytokine in human patient samples was not measured directly as part of this investigation. However, contrary to preliminary studies data here indicates that $CD4^+$ T cells activate readily in the CSF space (Figures 5.3-5.5). With the assumption that $CD69^+$ expression is representative of activation together with findings related to IFNγ expression in rat CSF, this may suggest that homeostatic $CD4^+$ T cells are not significantly influenced by tolerogenic mechanisms that are described in association with the CSF compartment. However, the reactivity and propensity of these CSF cells to undergo apoptosis would need to be measured directly to confirm this. The majority of reports which specifically focus on cytokine expression in the CSF document changes which occur in neuroinflammation. For example, a study by *Ishizu T et al (2005)* reports a moderate increase in free IFNγ in MS patient CSF (by immunoassay) in addition to an increased percentage of IFNγ producing $CD4^+$ T cells in this compartment[471]. This study also reports a significant increase in free TNFα in the CSF of MS patients which is consistent with studies in the 1990's where CSF TNFα levels were shown to positively correlate with the severity of progressive MS disease[472].

An increase in IL-17 expression by CSF $CD4^+$ T cells is also documented in neuroinflammation. A study by *V. Brucklacher-Waldert et al (2009)* reports that in a neurological disease cohort IL-17 expression in the blood is comparable to that in the CSF, but in RR-MS IL-17 expression in the CSF is elevated both in relapse and remission[473]. In a

more recent report *Y. Cao et al (2015)* have used libraries of $CD4^+$ T cell clones from MS patients to show that myelin-specific $CD4^+$ T cells that express CCR6 (a chemokine receptor associated with Th_{17} subset) produce higher amounts of IL-17, IFNγ and GM-CSF than analogous auto-reactive cells from healthy controls[474]. In addition, those $CCR6^+$ clones from healthy controls were more biased towards IL-10 (Tr_1) responses, thus demonstrating a skewing of myelin-specific $CD4^+$ T cell responses towards a more proinflammatory phenotype in MS[474]. Continued investigation into the cytokine potential of intrathecal and peripheral T cells is essential to further understand aberrant behaviour in neuroinflammatory disease and better define current perspectives of CNS immune surveillance and tolerance to CNS antigen.

CHAPTER SUMMARY

This work has demonstrated that in both mouse and human investigations CSF-derived $CD4^+$ T cells activate readily in response to PMA/ionomycin stimulation as indicated by CSF/CNS derived populations express endogenous levels of CD69 which may be evidence of their recent activation or indicative of their residency in CNS tissue. CSF and CNS derived $CD4^+$ T cells in rat exhibit robust IFNγ responses *in vitro*. Although cytokine expression by human CSF $CD4^+$ T cells was not directly measured as part of this investigation, my work suggests that CSF-associated $CD4^+$ T cells have the functional capability to perform immune surveillance, but conversely are capable of evoking a deleterious inflammatory response behind the BCSFB/BBB.

CHAPTER 6

GENERAL DISCUSSION

6 GENERAL DISCUSSION

6.1 What are non-responsive $CD4^+$ T cells?

The inability of $CD4^+$ T cells to elicit robust pro-inflammatory cytokine responses can be associated with a number of deleterious and inter-related immunological states including the inappropriate control of infection, exhaustion and senescence. Conversely, the hyporesponsiveness associated with T cell tolerance and regulatory cell types is essential for preventing autoimmunity through the inhibition of self-reactive T cell clones. Therefore, further defining mechanisms by which T cell responses are negatively regulated *in vivo* is essential for the understanding of optimal T cell function and is highly applicable to vaccine development and strategies supporting tumour immunotherapy.

In this study, the proportion of $CD4^+$ T cells which failed to make any of thirteen cytokines following *in vitro* stimulation was striking (Figure 3.3). Given this test included many of the most abundantly expressed T cell cytokines it could be speculated that there are many cytokines and effector molecules yet to be defined both in the T_{naive} and T_{memory} compartments. Alternatively, there may be heterogeneity in the $CD4^+$ T cell population's response to PMA/ionomycin and so combined PKCΘ and Ca^{2+} signalling may be insufficient to activate the entire population. Findings here have implications for the interpretation of memory $CD4^+$ T cell responses when PMA/ionomycin is used as an *in vitro* stimulus.

This investigation focused on a population of $cytokine^{-ve}$ $CD4^+$ T cells whose hyporesponsive phenotype was revealed through PMA/ionomycin stimulation. The failure of these cells to downregulate CD4 and upregulate CD69 could not be attributed to LCK or PKCΘ deficiency at the mRNA level (Figure 3.31). Therefore, the former may be associated with a dysregulation of CD4 and $p56^{lck}$ interaction (absence of receptor uncoupling) or altered endosomal trafficking of CD4 leading to decreased receptor internalisation. Ignorance to PMA through PKCΘ deficiency may still be related to altered phosphorylation or kinase

activity. This could be revealed through Phosflow™ cytometry techniques given the insufficient cell numbers required for western blotting. It also cannot be discounted that imbalanced as opposed to deficient PKCϴ signalling induces the hyporesponsive phenotype. Published work in cell lines and PKCϴ$^{-/-}$ mice shows that PKCϴ modulates both the NF-κB and AP-1 transcriptional pathways[475,476], with diminished AP-1 activity inextricably associated with T cell anergy[477,478]. Therefore, a skewing away from AP-1 signalling coupled with an increased sensitivity to Ca^{2+} dependent pathways (raised ionomycin input) could force the non-responsive population towards an 'anergic' phenotype. However, the addition of exogenous IL-2 into my stimulation assays may have readdressed such a signalling imbalance but this was shown not to reverse the non-responsive phenotype (Figure 3.24). This suggests that these cells are not truly 'anergic' in the classical sense. It may be informative to test for the elevated expression of anergy associated genes GRAIL, ITCH or Cbl-b in the non-responsive population to further exclude anergy-associated mechanisms from this enquiry.

The importance of further investigating non-responsive cells is highlighted by a significant elevation in their frequency observed in patient blood samples when compared to healthy controls (Figure 5.3B). As the inflammatory nature of the underlying pathology did not influence hyporesponsiveness (when comparing OND and MS cohorts), this is evidence that other factors such as physical or psychological stress markedly influences the functionality of these memory $CD4^+$ T cells. Such a theory is also in keeping with the longitudinal analysis of non-responsive cells in healthy individuals which identified notable intra-donor variability (Figure 3.10). Although the age range of healthy control participants was not conducive to assessing the effect of age-related senescence upon the non-responsive population, anecdotal analysis between the patient and healthy control cohorts is still informative. The median age of healthy control participants (27yrs) was notably lower than the OND and MS groups (44.5 and 47.5yrs respectively) (Table 2.3). Therefore, it remains possible that the non-responsive population is associated with age-related replicative senescence as opposed to disease and the

populations co-association with low CD27 expression supports this (Figure 3.15). Testing for the absence of CD28 expression coupled with the $CD27^{lo}$ definition may further support an association with senescence[225]. In addition, as latent viral infections drive replicative senescence[219,479] testing for a relationship between CMV seropositivity and the frequency of non-responding T cells in both younger adults and aged cohorts may prove informative. Further defining the defective CD69 status of non-responsive $CD4^+$ T cells may complement current literature which describes aberrant cytokine secretion by T cells in replicative senescence[227,233].

Features associated with senescence and exhaustion are more extensively studied in the $CD8^+$ T cell subset as these cells are persistently reactivated through chronic viral infections. Identifying the presence and characteristics of non-responsive $CD8^+$ T cells could provide valuable insight into the biology of this cellular state in future studies. As the CD8 co-receptor is not downregulated in response to PMA stimulation like its CD4 counterpart[480] analysis of the non-responsive population in the $CD8^+$ T cell subset would be restricted to a $CD69^{lo}$ definition. However, this may be sufficient when combined with other characteristics of the $CD4^+$ non-responsive phenotype reported here ($CD45RA^-CCR7^{-/+}CD62L^{lo}CD27^{lo}$). Both virus-specific $CD8^+$ and $CD4^+$ T cell clones are identifiable in seropositive individuals through use of fluorescently labelled MHC I or MHC II-viral peptide tetramer complexes[481,482]. The frequency of these cells (particularly in the $CD8^+$ subset) would permit the analysis of their CD69 status post activation. This would provide a means of assessing the antigen-specificity of the non-responsive population as well as the contribution of persistent antigenic stimulation. It would also be informative to evaluate the PD-1 expression of virus-specific non-responsive $CD8^+$ T cells. In this investigation, PD-1 expression was associated with the memory status of $CD4^+$ non-responsive T cells but was not shown to be specifically elevated within the population (Figure 3.22, Figure 3.23). This observation implies that the non-responsive population do not represent physiologically exhausted $CD4^+$ T cells.

However, the function of the non-responsive population could not be restored with IL-7 or IL-15 which is a feature consistent with exhaustion[483] and suggests that these memory cells may require antigen-specific stimuli to survive (Figure 3.24).

Although PD-1 expression was not specifically elevated on the non-responsive $CD4^+$ T cells it cannot be discounted that these cells have recently engaged PD-1 ligand *in vivo*. PD-L1 engagement by PD-1 is a reported mechanism of tolerising T cells, with constitutive expression of the ligand reported in many non-lymphoid tissues including the heart and lungs[484], brain[315], pancreatic islets[485] and renal tubule epithelium[486]. Therefore, it is possible that some $PD\text{-}1^+$ T cells trafficking through such sites have recently encountered PD-L1 and become non-responsive. As PD-1 signalling is also shown to halt cell cycle progression and increase apoptosis susceptibility[200,201,487], recent PD-L1 engagement may also explain why these traits were identified in the non-responsive population. However, my work does not support such a pathway in the context of T cell trafficking via the CNS, because although PD-L1 is reported to be expressed by perivascular macrophages in the brain[316], I have shown that the non-responsive population was diminished in the CP, CSF and brain compartments (Figure 5.1, Figure 5.2). In addition there is no report of PD-L1 expression by choroid plexus endothelium or epithelium specifically, which are the main barriers to homeostatic T cell migration. Therefore, PD-1/PD-L1 induced hyporesponsiveness may not be applicable to the CNS compartments, but its association with T cell recirculation via other peripheral tissues cannot be ruled out.

The non-responsive phenotype was most prevalent in the $CCR7^-$ effector memory population (Figure 3.13) but was disproportionately over-represented in the $CCR7^+$ population when PBMC were not sorted prior to stimulation (Figure 3.11). Furthermore, purified $CCR7^+CD62L^{lo}$ memory $CD4^+$ T cells demonstrated a high frequency of $CD4^{int}CD69^{lo}$ cells (Figure 3.14). Together this suggests that some non-responsive cells are effector memory cells

that have upregulated CCR7, perhaps for the purpose of returning to the circulation from a peripheral tissue compartment[391]. It is possible that that the non-responsive cells are enriched in a memory population that recirculates between the blood, peripheral tissue and the lymphatics. A report by *S.K Bromley et al (2013)* describes *ex vivo* $CCR7^{+/-}CD62L^{int}CD69^{lo}$ expression by recirculating memory cells that home to the skin[95] and such markers are consistent with the non-responsive subset identified here. However, the authors found that these cells were able to produce IL-2 following stimulation which is not comparable with the $cytokine^{-ve}$ $CD4^{int}CD69^{lo}$ phenotype I describe here. It is unlikely that any recirculating non-responsive memory cells failed to upregulate CD69 through its reciprocal inhibition by increased $S1P_1$ receptor activity. This is because naïve T cells require such interactions to return to the circulation from the lymph nodes and this subset showed minimal non-responsiveness[97,98]. Never-the-less, it cannot be discounted that recirculating memory cells are susceptible to becoming hyporesponsive and thus the non-responsive population represents a tolerised, exhausted or senescent fraction of a recirculating subset.

In addition to what the surface marker expression of the non-responsive population suggests about their migratory behaviour it is important to consider where these cells may fit in line with models of T cell differentiation (as described in Fig1.2A-C). Given their inability to proliferate when cultured *in vitro*, diminished CD27 expression (Figure 3.15) and $CD45RA^{-}$ status (Figure 3.5), it is unlikely these cells represent highly proliferative T_{SCM} which undergo self-renewal[64]. In addition, in light of their propensity to undergo apoptosis following PKCϴ-mediated activation (Figure 3.17) it may be considered improbable that this population is positioned centrally in a linear differentiation model. This would imply that non-responsive cells could maintain sufficient survival and proliferative potential to differentiate into other subsets. However, in line with the linear differentiation model 1 (described in Figure 1.2A) there is some evidence that highly differentiated cells (which are paradoxically shown to be susceptible to exhaustion and senescence) can provide the basis of stable long term

memory[488]. This is exemplified in a study where *ex vivo* expanded tumour antigen-specific memory T cells ($CD8^{+}CD27^{lo}CD28^{lo}CD62L^{-}CCR7^{-}CD127^{lo}$) were transferred into melanoma patients for their therapeutic potential. Here it was shown that a proportion of these transferred cells re-upregulated CD27 and CD28 and formed a persistent tumour-specific memory population[488]. Such results are somewhat conflicting with some studies that show the loss of CD27 and CD28 expression is non-recoverable with the latter associated with permanent transcriptional silencing events[489–491].

Although it can be speculated that the non-responsive population are towards the terminal end of the differentiation spectrum their persistence in the circulation suggests some biological rationale behind their maintenance. With appropriate signals it may be expected that they can elicit some functionality. As T_{reg} ($CD25^{hi}CD127^{lo}$) were shown to contribute to the non-responsive pool (Figure 3.20-3.21) it could be hypothesised that the non-T_{reg} cells which numerically dominate this population also have a suppressive function. It is unclear whether such suppression could be attributed to bystander effects[139] or filling of the memory niche with hyporesponsive cells (as is also described in T cell exhaustion). I am also yet to establish whether these cells represent non-classical T_{reg} subsets such as Tr_1 or Tr_3, although these subsets are typically associated with the ability to secrete anti-inflammatory cytokine[161,492] which is not a characteristic fitting with the non-responsive cell profile.

Although as part of this investigation I have established the co-association of the non-responsive phenotype with a range of phenotypic markers it is imperative that a more comprehensive surface receptor profile be established (by microarray) to move this work forward. An understanding of their biology has been achieved here but the precise mechanisms behind their atypical *in vitro* responses remain elusive. The physiological significance of these cells will be better understood through their identification without the requirement for *in vitro* stimulation, which ultimately drives them into irreversible AICD.

Investigations here were limited by the low retrieval of non-responsive cells in healthy controls which did not permit the more comprehensive gene expression analysis (microarray) required to identify candidate surface makers. cDNA amplification techniques could address this issue and boost the amount of genetic material retrieved from the non-responsive cell purification experiments shown here (Figure 3.27A). Alternatively, as I have shown that the non-responsive cell frequency may increase with age or disease it may be useful to develop experimental systems in these cohorts where a higher percentage of these cells can be retrieved. With a more complete definition of the non-responsive phenotype established processes which restore functionality to these cells may be further investigated. This is particularly relevant if non-responsive cells are also found to be present in the $CD8^+$ T cell compartment or are shown to be enriched in a tumour environment. Such work may be highly relevant to studies aiming to boost the activity of tumour specific T cells. A current example of this is the blockade of the PD-1 pathway with monoclonal antibodies (Lambrolizumab) to increase anti-tumour T cell responses[493]. Conversely, the therapeutic benefit of adoptive cell transfer techniques for tumour immunotherapy could potentially be improved by removing non-responsive cells from *ex vivo* preparations of anti-tumour antigen specific T cell clones. Optimisation strategies in adoptive T cell therapy are important as the differentiation status of engrafted cells is shown to influence ultimate clinical outcomes and the transfer of highly differentiated cells is proven to be less efficacious[494]. In an alternative scenario, tailoring vaccine responses to minimise the expansion of non-responsive cells may be considered highly advantageous, particularly in the elderly where memory T cell responses become compromised[227,495].

6.2 $CD4^+$ T cell responses are not suppressed in the CNS compartments.

Pilot studies preceding this investigation suggested that the cytokine responses of $CD4^+$ T cells in non-inflamed CSF were diminished comparative to the blood (unpublished data, Curnow group, University of Birmingham). Such findings were in keeping with a number of

reports documenting the tolerogenic properties of the CSF milieu[307,308], with some suggesting that the CNS is a hostile microenvironment to infiltrating immune cells to protect neuronal cells from damage[304,306]. However, these proposals are conflicting with the paradigm that homeostatic T cell migration is essential for providing immune surveillance in the CNS as protection against invading pathogens implies a requirement for robust T cell responses[452]. The importance of steady-state CNS T cell recruitment is exemplified when these processes are pharmacologically inhibited by the integrin blocker Natalizumab which can result in fatal JC virus reactivation in the brain[291]. In addition to a role in immunity, work in mice shows that the cytokine profile of choroid plexus T cells has implications for optimal cognitive function and may be dysregulated in age-associated immune senescence[282,447]. In my investigation I show that $CD4^+$ T cells in rat CSF, CP and whole brain preparations have robust IFNγ responses when stimulated *ex vivo* (Figure 5.6). This finding supports the maintenance of $CD4^+$ T cell cytokine responses in the CNS compartments and refutes the original hypothesis of this investigation in showing that cytokine responses in the CSF are not diminished.

The ability of CSF (and brain-derived) T cells to activate in response to *ex vivo* stimulation was also examined as part of my thesis and supported the cytokine data analysis in rat. The activation marker CD69 was readily upregulated by normal murine CSF and brain $CD4^+$ T cells (Figure 5.1-5.2). This trend was reproduced through examination of $CD4^+$ T cells from non-inflamed human CSF (Figure 5.5A). In contrast to the hypothesis of this investigation this work suggests that; 1) $Cytokine^{-ve}$ $CD4^+$ T cells are not preferentially recruited from the blood, 2) $CD4^+$ T cells are not anergised as part of their homeostatic CNS migration and, 3) $CD4^+$ T cells are not functionally suppressed within the CSF space. This data supports the role of $CD4^+$ T cells in immune surveillance and has implications for the current understanding of CNS immunity.

6.3 The representation of non-responsive CD4$^+$ T cells is reduced in the CNS compartments.

At the beginning of this investigation it was questioned whether the CSF CD4$^+$ T cells that failed to make cytokine in preliminary studies were analogous to the non-responsive subtype revealed by PMA/ionomcyin stimulation in the blood. Findings here do not support such a relationship on a number of levels. CNS CD4$^+$ T cells were shown to activate readily and the non-responsive population was not well represented in the CSF (as described in section 6.2). In addition, the phenotype of the non-responsive population as defined by work in Chapter 3 is not consistent with the numerically dominant phenotype in human CSF. The non-responsive population in human blood was skewed towards an effector memory phenotype, whereas the central memory subset dominates the CSF in humans[247,248]. This does not mean that non-responsive cells are excluded from the CNS by means of their memory differentiation as this study demonstrated that CD4$^+$ T cell migration from blood to CSF is permissive to the effector memory subset (Figure 4.10-4.11, Figure 4.13-4.14). However, when the percentage of non-responsive cells was measured within the effector memory population in the CSF a reduction in their frequency was recorded (Figure 5.5A). In addition, the representation of CD69^{lo} CD4$^+$ T cells was reduced in both murine CSF and brain where the effector memory population predominates (Figure 5.1, Figure 5.2). This suggests that non-responsive effector memory CD4$^+$ T cells migrate less readily into the CNS compartments and supports a model where cytokine-competent, functional CD4$^+$ T cells are recruited into the CSF as part of an immune surveillance network.

6.4 A CCR7 and CD69 independent model for homeostatic CD4$^+$ T cell recruitment into the CSF.

In line with the model of CNS immune surveillance described by *B. Engelhardt et al (2011)* findings here support a role for CD4$^+$ T cell mediated immune surveillance that is limited to the brains outer borders[257] as these cells were not found located within the parenchyma of normal mouse brain (Figure 4.5-4.6). The prevalence of CD4$^+$ T cells associated with

unchallenged murine brain was extremely low and in keeping with reports of low level basal recruitment across the choroid plexus into the CSF[282]. However, $CD4^+$ T cells were successfully characterised in association with unchallenged rodent CP and CSF (Figure 4.2-4.10) which fulfilled a primary objective of this investigation. In contrast to human datasets, $CD8^+$ T cells dominated the $CD4^+$ subset in all measured rodent CNS compartments (Figure 4.8-4.9) which may suggest a more dominant role of this subset in rodent CNS immunity. If this $CD8^+$ predominance is reflective of the limited capacity of laboratory animals for T cell memory due to limited antigen exposure this may be indicative that accentuated $CD4^+$ T cell recruitment in humans is driven by exposure to endemic pathogens.

Data from this study suggest that both T_{cm} and T_{eff} memory $CD4^+$ T cells migrate from the blood to CSF by mechanisms that are equally permissive for both subsets, thus refuting the hypothesis that this pathway is T_{cm} specific. In humans, this was identified by a positive correlation between the representation of $CCR7^+$ T_{cm} $CD4^+$ T cells in the blood and CSF (Figure 4.13-4.14). As both $CCR7^+$ and $CCR7^-$ cells are found in human CSF this implies that normal $CD4^+$ T cell recruitment is independent of CCR7 mediated adhesion. The primary site of T cell migration from blood to CSF is across the BSCFB at the CP with the presence of CCR7 ligands at this site often used as evidence supporting a CCR7-dependent pathway[249,286]. However, myeloid DC in the CSF are also shown to express CCR7[249] and the requirement of this receptor for lymph node homing is fitting with a model where CSF DC's migrate to the draining CLN[298,299,303]. Therefore, work here suggests a predominant role of CCR7 in the migration of CSF DC but redundancy in the recruitment pathway of memory $CD4^+$ T cells from the blood.

Consistent with my findings the relationship between blood and CSF memory $CD4^+$ T cell distribution has been previously reported, albeit using an alternative surface marker definition of T_{cm}[249]. Despite this, immune surveillance by CSF T cells is consistently attributed to the

T_{cm} population in current literature with little mention of the T_{eff} population's contribution. It is acknowledged that the frequency of the CSF T_{eff} population in humans is low but my work shows that these homeostatically recruited T_{eff} cells can activate readily and produce cytokine (Chapter 5). Theoretically this implies that if these cells were reactivated intrathecally their potent cytokine-secreting potential may elicit profound effects on the CNS microenvironment. Furthermore, findings here suggest that factors which influence the T_{cm}/T_{eff} balance in the peripheral blood will be reflected in the intrathecal compartment, which may have implications for CNS immune responses. Interestingly, some groups have reported that both T cell deficiency and an imbalance of $CD4^+$ T cell cytokines in the CNS is associated with a decline in cognitive function in mice[447,496]. In addition, cytokine imbalances in the CSF have been associated with human pathologies amongst which psychiatric disorders such as depression and schizophrenia are included[497–499].

Perhaps surprisingly, the consistency of the T_{cm}/T_{eff} ratio between the blood and CSF was not perturbed in MS (Figure 4.14) despite a significant elevation in T cell cellularity associated with inflammatory disease (Figure 4.12). This is consistent with reports that T_{cm} ($CCR7^+CD27^+$) also are the predominating cell type in the CSF of MS patients[249,432], although $CCR7^-$ memory T cells are reportedly associated with MS lesion sites[249,500]. Given the ability of both memory subsets to enter the CSF in the absence of inflammation it is relevant to consider their relative contribution in MS pathogenesis. Induction of EAE is shown to be dependent upon $CCR6^+$ Th_{17} recruitment[338], but as the Th_{17} subset is a mixed $CCR7^{+/-}$ phenotype it may be informative to assess whether CCR7 status influences the encephalitogenic nature of Th_{17} behind the BCSFB. In addition, reactivation of CNS-antigen specific T_{cm} and T_{eff} memory $CD4^+$ T cells in the CSF may have differential consequences in the context of MS relapse events.

The consistency of the T_{cm}/T_{eff} memory $CD4^+$ T cell distribution between the blood and CSF was also observed in murine datasets (Figure 4.10-4.11). However, it is acknowledged that CCR7 was used to separate these phenotypes throughout human datasets but was not applied to mouse experiments. This is because the CD44/CD62L memory definition is more classically used in the literature to define murine $CD4^+$ memory T cell subsets irrespective of CCR7 status[436–438]. However, in murine models of LCMV infection there is some evidence of concurrent $CCR7^+$ and $CCR7^-$ expression in the $CD44^{hi}CD62L^{lo}$ subset within the $CD8^+$ T cell population[501]. Given that my presented findings have implications for the significance of CCR7 expression in CNS migration it may be beneficial to correlate CCR7 and CD62L expression in future experiments where murine CNS T cells are examined.

The high level of positive CD69 staining on murine CSF and brain-derived *ex vivo* $CD4^+$ T cells may be informative regarding the recruitment and residency of these cells within the CNS (Figure 5.1C, Figure 5.2C). With the assumption that the majority of brain-derived $CD4^+$ T cells in these preparations were actually associated with the CP region (Figure 4.6), my work identified that around a third of both CP and CSF $CD4^+$ T cells have physiologically elevated levels of CD69. A model where only recently activated $CD69^+$ memory $CD4^+$ T cells are recruited to the CSF (irrespective of antigen-specificity or CCR7 status) does not account for the two thirds of CP and CSF-derived $CD4^+$ T cells that do not express CD69. It is more probable that recently activated $CD4^+$ T cells have the chemokine receptor repertoire that facilitates BCSFB migration irrespective of whether their CD69 expression is maximal at the time of migration or time of sampling. Therefore, $CD69^+$ $CD4^+$ T cells may appear enriched in the CNS *by proxy*. With consideration to the kinetics of CD69 expression it may be useful to measure other markers of T cell activation in the CSF compartment. Interestingly, the presence of $CD25^{hi}$ and $FOXP3^+$ $CD4^+$ T cells in human MS CSF samples is reported as an enrichment of T_{reg} in some studies[502]. However, given the overlap of CD25 and FOXP3 expression between recently activated and T_{reg} populations it is difficult to discount the

possibility that a proportion of such cells may represent recently activated T_{helper} cells that have transiently upregulated FOXP3[149]. In an alternative scenario it is possible that CD69 expression is lost or acquired by some cells once within the CP or CSF. With reference to the proposed physiological role of CD69 in dampening T cell activation[503] the acquisition of CD69 expression by CP and CSF $CD4^+$ T cells may still serve to negatively regulate their activation *in vivo* irrespective of their proven ability to respond to *ex vivo* stimulation (Figure 5.1-5.2). Interestingly a population of $CD25^-CD4^+CD69^+$ T cells is demonstrated to have a suppressive function and such findings may be relevant to CNS T cell biology[504].

With regard to the association between CD69 expression and the tissue residency of memory T cells it must also be considered whether the $CD69^+$ CP and CSF T cells represent a distinctive, stable population. The pulsatile flow of the CSF fluid and its associated drainage routes suggests this compartment resembles a lymphatics network and is in constant flux[294,348]. Therefore, although 'resident' macrophages and DC are associated with this compartment and some CSF $CD4^+$ T cells express CD69, the likelihood of T cell 'residency' here may seem improbable with acknowledgement to the CSF fluid dynamics. However, it is also shown that CD69 has a role in the retention of activated $CD4^+$ T cells in the secondary lymphoid organs[97,505]. In a theoretical model analogous to that assigned to lymph node egress the CD69 receptor may have a similar role in retaining $CD4^+$ T cell in the CSF. It was also considered whether $CD69^+$ T_{RM} are retained within the CP whilst recirculating $CD69^-$ memory T cells exit into the CSF space. However, I found a similar representation of $CD69^+$ $CD4^+$ T cells in the CSF and whole brain compartments (mainly localised to the CP) which does not favour this theory albeit indirectly (Figure 5.1, Figure 5.2). As no $CD4^+$ T cells were detected in the brain parenchyma it may be assumed that this is not a source of $CD69^+$ T_{RM} in these systems where there is no background infection or inflammation (Figure 4.5-4.6).

In spite of the arguments which may favour the association of CD69 expression with activation as opposed to CNS residency, co-staining of CP and CSF $CD4^+$ T cells with CD103 would be required to identify an absence of T_{RM} in these compartments. The identification of a T_{RM} population behind the BBB or BCSFB in health may have significant implications for therapeutic intervention in neuroinflammatory diseases including MS. It is shown that resident B cell populations are found in the meninges[363], CSF and parenchyma[506] in MS and contribute to disease. Interestingly, the drug Fingolimod acts upon both T and B cell populations but whereas peripheral B cell numbers are reduced with treatment the frequency of resident CNS B cells is unaffected[507]. In addition, peripheral blood $CD4^+$ T cell frequencies are disproportionally reduced comparative to CSF populations. As the CP and CSF present a gateway to the CNS tissue such findings exemplify the importance of further understanding the interaction between blood and CSF T cell compartments in the development of therapeutic targets in MS.

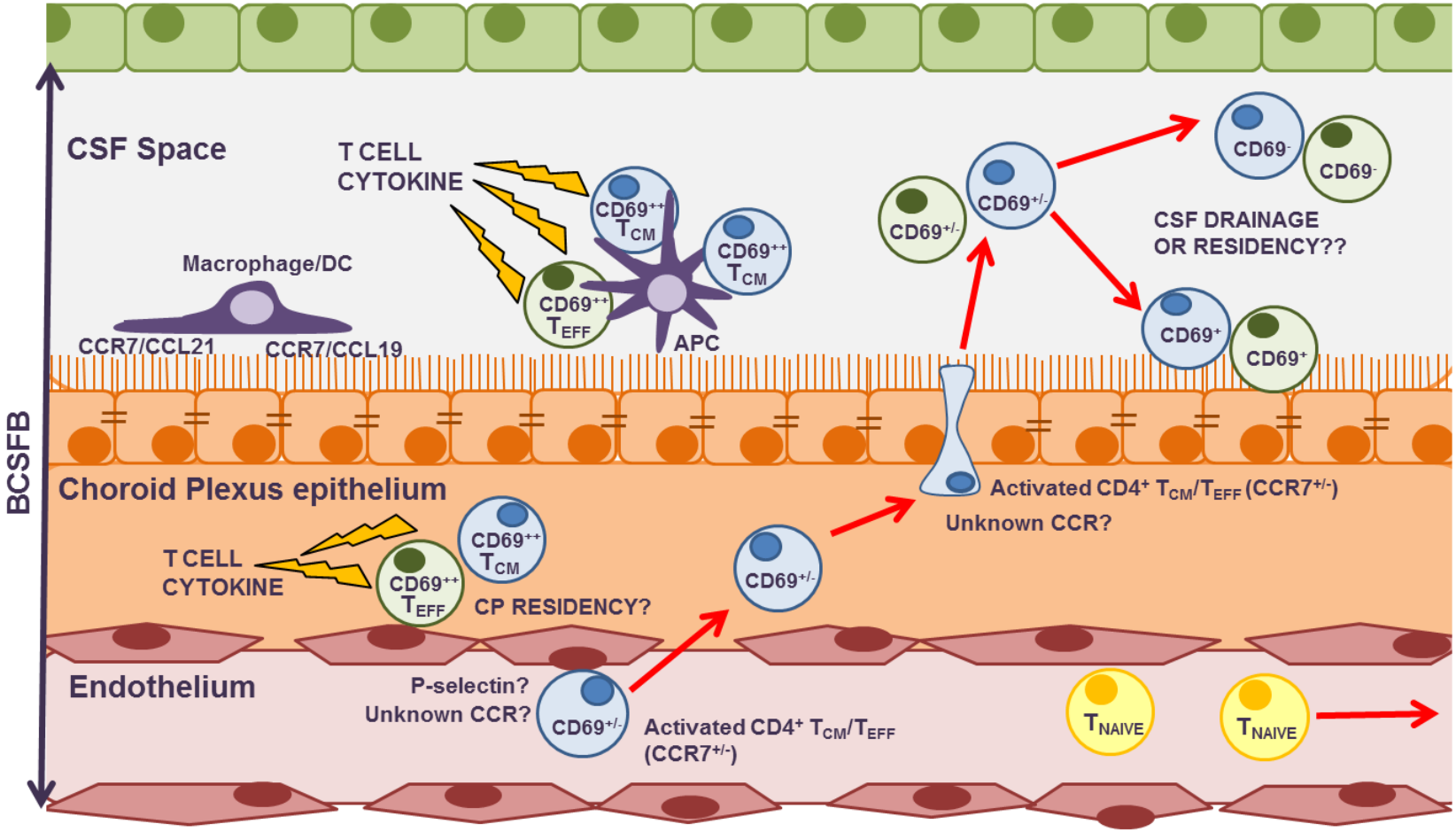

Figure 6.1 Model for the recruitment, residency and functionality of homeostatic CD4$^+$ T cells in the CSF. Recently activated central (T_{cm}) and effector memory (T_{eff}) CD4$^+$ T cells express an unknown chemokine receptor (CCR) repertoire which permits their migration from blood to choroid plexus (CP) in a CCR7 independent manner. CP to CSF migration is also CCR7 independent. T_{cm} and T_{eff} within the CP and CSF have the potential to make cytokine if appropriately reactivated, with potential involvement of antigen presenting cells (APC). CCR7 interaction is important for dendritic cell (DC) migration behind the blood CSF barrier (BCSFB). Expression of CD69 may or may not indicate the residence of a subpopulation of memory CD4$^+$ T cells in the CP and CSF spaces.

REFERENCES

1. Cooper MD, Herrin BR. How did our complex immune system evolve? Nat Rev Immunol. Nature Publishing Group; 2010;10(1):2–3.

2. Belkaid Y, Artis D. Immunity at the Barriers. Eur J Immunol. 2013;43(12):3096–7.

3. Madison KC. Barrier Function of the Skin: "'La Raison d'EOE tre"' of the Epidermis. J Invest Dermatol. 2003;121(2):231–41.

4. Gallo RL, Hooper L V. Epithelial antimicrobial defence of the skin and intestine. Nature Reviews Immunology. 2012. p. 503–16.

5. Grice EA, Segre JA. The skin microbiome. Nat Rev Microbiol. 2011;9(4):244–53.

6. Becker a J, McCulloch E a, Till JE. Cytological demonstration of the clonal nature of spleen colonies derived from transplanted mouse marrow cells. Nature. 1963;197(4866):452–4.

7. Akashi K, Traver D, Miyamoto T, Weissman IL. A clonogenic common myeloid progenitor that gives rise to all myeloid lineages. Nature. 2000;404(6774):193–7.

8. Akira S, Uematsu S, Takeuchi O. Pathogen Recognition and Innate Immunity. Cell. 2006;124(4):783–801.

9. Bordet J, Gengou O. Sur l'existance de substances sensibilisatrices dan la plupart des sérums antimicrobiens. Ann Inst Pasteur. 1901;15:p. 289.

10. Murphy K, Travers P, Walport M. The complement system and innate immunity. Janeway's Immunobiology. Garland Science; 2008. p. 61–81.

11. Litman GW, Rast JP, Fugmann SD. The origins of vertebrate adaptive immunity. Nat Rev Immunol. 2010;10(8):543–53.

12. Ahmed R, Gray D. Immunological memory and protective immunity: understanding their relation. Science. 1996;272(5258):54–60.

13. Zinkernagel RM. On differences between immunity and immunological memory. Current Opinion in Immunology. 2002. p. 523–36.

14. Sakano H, Hüppi K, Heinrich G, Tonegawa S. Sequences at the somatic recombination sites of immunoglobulin light-chain genes. Nature. 1979 Jul 26;280(5720):288–94.

15. Okada T, Cyster JG. B cell migration and interactions in the early phase of antibody responses. Current Opinion in Immunology. 2006. p. 278–85.

16. Boes M. Role of natural and immune IgM antibodies in immune responses. Mol Immunol. 2001;37(18):1141–9.

17. Shinomiya N, Kuratsuji T, Yata J. The role of T cells in immunoglobulin class switching of specific antibody production system in vitro in humans. Cell Immunol. 1989;118(2):239–49.

18. Allen CDC, Okada T, Tang HL, Cyster JG. Imaging of germinal center selection events during affinity maturation. Science. 2007 Jan 26;315(5811):528–31.

19. Arakawa H, Hauschild J, Buerstedde J-M. Requirement of the activation-induced deaminase (AID) gene for immunoglobulin gene conversion. Science. 2002 Feb 15;295(5558):1301–6.

20. Stavnezer J, Guikema JEJ, Schrader CE. Mechanism and regulation of class switch recombination. Annu Rev Immunol. 2008 Jan;26:261–92.

21. Murphy K, Travers P, Walport M. The distribution and functions of immunoglobulins. Janeway's Immunobiology. Garland Science; 2008. p. 400–9.

22. eBiocience. Hematopoiesis from Pluripotent Stem Cell. 2012 [cited 2015 May 14] Available at URL: http://www.ebioscience.com/resources/pathways/hematopoiesis-from-pluripotent-sem-cells.htm.

23. Blom B, Spits H. Development of human lymphoid cells. Annu Rev Immunol. 2006 Jan;24:287–320.

24. Galy A. Precursors of CD3+CD4+CD8+ cells in the human thymus are defined by expression of CD34. Delineation of early events in human thymic development. J Exp Med. 1993 Aug 1;178(2):391–401.

25. Groh V. Human lymphocytes bearing T cell receptor gamma/delta are phenotypically diverse and evenly distributed throughout the lymphoid system. J Exp Med. 1989 Apr 1;169(4):1277–94.

26. Budd RC, Miescher GC, Howe RC, Lees RK, Bron C, MacDonald HR. Developmentally regulated expression of T cell receptor beta chain variable domains in immature thymocytes. J Exp Med. 1987 Aug 1;166(2):577–82.

27. Von Boehmer H, Fehling HJ. Structure and function of the pre-T cell receptor. Annu Rev Immunol. 1997 Jan;15:433–52.

28. Germain RN. T-cell development and the CD4-CD8 lineage decision. Nat Rev Immunol. 2002 May;2(5):309–22.

29. Ueno T, Saito F, Gray DHD, Kuse S, Hieshima K, Nakano H, et al. CCR7 signals are essential for cortex-medulla migration of developing thymocytes. J Exp Med. 2004 Aug 16;200(4):493–505.

30. Anderson MS, Venanzi ES, Klein L, Chen Z, Berzins SP, Turley SJ, et al. Projection of an immunological self shadow within the thymus by the aire protein. Science. 2002 Nov 15;298(5597):1395–401.

31. Björses P, Pelto-Huikko M, Kaukonen J, Aaltonen J, Peltonen L, Ulmanen I. Localization of the APECED protein in distinct nuclear structures. Hum Mol Genet. 1999 Feb;8(2):259–66.

32. Scollay RG, Butcher EC, Weissman IL. Thymus cell migration. Quantitative aspects of cellular traffic from the thymus to the periphery in mice. Eur J Immunol. 1980 Mar;10(3):210–8.

33. Goldrath AW, Bevan MJ. Selecting and maintaining a diverse T-cell repertoire.

34. Gowans JL, Knight EJ. The Route of Re-Circulation of Lymphocytes in the Rat. Proc R Soc B Biol Sci. 1964 Jan;159(975):257–82.

35. Streeter PR, Rouse BT, Butcher EC. Immunohistologic and functional characterization of a vascular addressin involved in lymphocyte homing into peripheral lymph nodes. J Cell Biol. 1988 Nov;107(5):1853–62.

36. Gunn MD, Tangemann K, Tam C, Cyster JG, Rosen SD, Williams LT. A chemokine expressed in lymphoid high endothelial venules promotes the adhesion and chemotaxis of naive T lymphocytes. Proc Natl Acad Sci U S A. 1998 Jan 6;95(1):258–63.

37. Förster R, Schubel A, Breitfeld D, Kremmer E, Renner-Müller I, Wolf E, et al. CCR7 coordinates the primary immune response by establishing functional microenvironments in secondary lymphoid organs. Cell. 1999 Oct 1;99(1):23–33.

38. Ohl L, Mohaupt M, Czeloth N, Hintzen G, Kiafard Z, Zwirner J, et al. CCR7 governs skin dendritic cell migration under inflammatory and steady-state conditions. Immunity. 2004 Aug;21(2):279–88.

39. Weiss S, Bogen B. MHC class II-restricted presentation of intracellular antigen. Cell. 1991 Mar 22;64(4):767–76.

40. Chen L, Flies DB. Molecular mechanisms of T cell co-stimulation and co-inhibition. Nat Rev Immunol. Nature Publishing Group, a division of Macmillan Publishers Limited. All Rights Reserved.; 2013 Apr;13(4):227–42.

41. Linsley PS. CTLA-4 is a second receptor for the B cell activation antigen B7. J Exp Med. 1991 Sep 1;174(3):561–9.

42. Mardiney M, Brown MR, Fleisher TA. Measurement of T-cell CD69 expression: a rapid and efficient means to assess mitogen- or antigen-induced proliferative capacity in normals. Cytometry. 1996 Dec 15;26(4):305–10.

43. Nakamura S, Sung SS, Bjorndahl JM, Fu SM. Human T cell activation. IV. T cell activation and proliferation via the early activation antigen EA 1. J Exp Med. 1989 Mar 1;169(3):677–89.

44. De la Fuente H, Cruz-Adalia A, Martinez Del Hoyo G, Cibrian-Vera D, Bonay P, Pérez-Hernández D, et al. The leukocyte activation receptor CD69 controls T cell differentiation through its interaction with Galectin-1. Mol Cell Biol. 2014;(April).

45. Zajac AJ, Blattman JN, Murali-Krishna K, Sourdive DJ, Suresh M, Altman JD, et al. Viral immune evasion due to persistence of activated T cells without effector function. J Exp Med. 1998 Dec 21;188(12):2205–13.

46. Yi JS, Cox M a., Zajac AJ. T-cell exhaustion: Characteristics, causes and conversion. Immunology. 2010;129(4):474–81.

47. Alari-Pahissa E, Notario L, Lorente E, Vega-Ramos J, Justel A, López D, et al. CD69 Does Not Affect the Extent of T Cell Priming. PLoS One. 2012;7(10).

48. Sancho D, Gómez M, Viedma F, Esplugues E, Gordón-Alonso M, García-López MA, et al. CD69 downregulates autoimmune reactivity through active transforming growth factor-beta production in collagen-induced arthritis. J Clin Invest. 2003 Sep;112(6):872–82.

49. Martín P, Gómez M, Lamana A, Cruz-Adalia A, Ramírez-Huesca M, Ursa MA, et al. CD69 association with Jak3/Stat5 proteins regulates Th17 cell differentiation. Mol Cell Biol. 2010 Oct;30(20):4877–89.

50. Woerly G, Brooks N, Ryffel B. Effect of rapamycin on the expression of the IL-2 receptor (CD25). Clin Exp Immunol. 1996 Feb;103(2):322–7.

51. Caruso A, Licenziati S, Corulli M, Canaris AD, De Francesco MA, Fiorentini S, et al. Flow cytometric analysis of activation markers on stimulated T cells and their correlation with cell proliferation. Cytometry. 1997 Jan 1;27(1):71–6.

52. Watanabe-Fukunaga R, Brannan CI, Copeland NG, Jenkins NA, Nagata S. Lymphoproliferation disorder in mice explained by defects in Fas antigen that mediates apoptosis. Nature. 1992 Mar 26;356(6367):314–7.

53. Adachi M, Suematsu S, Suda T, Watanabe D, Fukuyama H, Ogasawara J, et al. Enhanced and accelerated lymphoproliferation in Fas-null mice. Proc Natl Acad Sci U S A. 1996;93(5):2131–6.

54. Badovinac VP, Porter BB, Harty JT. Programmed contraction of CD8(+) T cells after infection. Nat Immunol. 2002;3(7):619–26.

55. Badovinac VP, Porter BB, Harty JT. CD8+ T cell contraction is controlled by early inflammation. Nat Immunol. 2004;5(8):809–17.

56. Kaech SM, Tan JT, Wherry EJ, Konieczny BT, Surh CD, Ahmed R. Selective expression of the interleukin 7 receptor identifies effector CD8 T cells that give rise to long-lived memory cells. Nat Immunol. 2003 Dec;4(12):1191–8.

57. Sallusto F, Lenig D, Förster R, Lipp M, Lanzavecchia a. Two subsets of memory T lymphocytes with distinct homing potentials and effector functions. Nature. 1999;401(October):708–12.

58. Jacob J, Baltimore D. Modelling T-cell memory by genetic marking of memory T cells in vivo. Nature. 1999 Jun 10;399(6736):593–7.

59. Opferman JT, Ober BT, Ashton-Rickardt PG. Linear differentiation of cytotoxic effectors into memory T lymphocytes. Science. 1999 Mar 12;283(5408):1745–8.

60. Geginat J, Lanzavecchia A, Sallusto F. Proliferation and differentiation potential of human CD8+ memory T-cell subsets in response to antigen or homeostatic cytokines. Blood. American Society of Hematology; 2003 Jun 1;101(11):4260–6.

61. Chang JT, Palanivel VR, Kinjyo I, Schambach F, Intlekofer AM, Banerjee A, et al. Asymmetric T lymphocyte division in the initiation of adaptive immune responses. Science. 2007;315(5819):1687–91.

62. Manjunath N, Shankar P, Wan J, Weninger W, Crowley MA, Hieshima K, et al. Effector differentiation is not prerequisite for generation of memory cytotoxic T lymphocytes. J Clin Invest. 2001;108(6):871–8.

63. Ahmed R, Bevan MJ, Reiner SL, Fearon DT. The precursors of memory: models and controversies. Nat Rev Immunol. Nature Publishing Group; 2009 Sep 14;9(9):662–8.

64. Gattinoni L, Lugli E, Ji Y, Pos Z, Paulos CM, Quigley MF, et al. A human memory T cell subset with stem cell-like properties. Nat Med. 2011;17(10):1290–7.

65. Gattinoni L. Memory T Cells Officially Join the Stem Cell Club. Immunity. Elsevier Inc.; 2014;41(1):7–9.

66. Sallusto F, Geginat J, Lanzavecchia A. Central memory and effector memory T cell subsets: function, generation, and maintenance. Annu Rev Immunol. 2004 Jan;22:745–63.

67. Zaph C, Rook K a, Goldschmidt M, Mohrs M, Scott P, Artis D. Persistence and function of central and effector memory CD4+ T cells following infection with a gastrointestinal helminth. J Immunol. 2006;177:511–8.

68. Ravkov E V., Myrick CM, Altman JD. Immediate Early Effector Functions of Virus-Specific CD8+CCR7+ Memory Cells in Humans Defined by HLA and CC Chemokine Ligand 19 Tetramers. J Immunol. American Association of Immunologists; 2003 Mar 1;170(5):2461–8.

69. Clark R a, Chong B, Mirchandani N, Brinster NK, Yamanaka K-I, Dowgiert RK, et al. The vast majority of CLA+ T cells are resident in normal skin. J Immunol. 2006;176(7):4431–9.

70. Sathaliyawala T, Kubota M, Yudanin N, Turner D, Camp P, Thome JJC, et al. Distribution and compartmentalization of human circulating and tissue-resident memory T cell subsets. Immunity. 2013 Jan 24;38(1):187–97.

71. Mora JR, von Andrian UH. T-cell homing specificity and plasticity: new concepts and future challenges. Trends Immunol. 2006;27(5):235–43.

72. Fuhlbrigge RC, Kieffer JD, Armerding D, Kupper TS. Cutaneous lymphocyte antigen is a specialized form of PSGL-1 expressed on skin-homing T cells. Nature. 1997 Oct 30;389(6654):978–81.

73. Griffith JW, Sokol CL, Luster AD. Chemokines and chemokine receptors: positioning cells for host defense and immunity. Annu Rev Immunol. Annual Reviews; 2014 Jan 21;32:659–702.

74. Kinashi T. Intracellular signalling controlling integrin activation in lymphocytes. Nat Rev Immunol. 2005 Jul;5(7):546–59.

75. Soler D, Humphreys TL, Spinola SM, Campbell JJ. CCR4 versus CCR10 in human cutaneous TH lymphocyte trafficking. Blood. 2003 Mar 1;101(5):1677–82.

76. Hudak S, Hagen M, Liu Y, Catron D, Oldham E, McEvoy LM, et al. Immune surveillance and effector functions of CCR10(+) skin homing T cells. J Immunol. 2002 Aug 1;169(3):1189–96.

77. Ericsson A, Svensson M, Arya A, Agace WW. CCL25/CCR9 promotes the induction and function of CD103 on intestinal intraepithelial lymphocytes. Eur J Immunol. 2004 Oct;34(10):2720–9.

78. Svensson M, Marsal J, Ericsson A, Carramolino L, Brodén T, Márquez G, et al. CCL25 mediates the localization of recently activated CD8alphabeta(+) lymphocytes to the small-intestinal mucosa. J Clin Invest. 2002 Oct;110(8):1113–21.

79. Kalli AC, Campbell ID, Sansom MSP. Conformational changes in talin on binding to anionic phospholipid membranes facilitate signaling by integrin transmembrane helices. PLoS Comput Biol. 2013 Oct 31;9(10):e1003316.

80. Erle DJ, Briskin MJ, Butcher EC, Garcia-Pardo A, Lazarovits AI, Tidswell M. Expression and function of the MAdCAM-1 receptor, integrin alpha 4 beta 7, on human leukocytes. J Immunol. American Association of Immunologists; 1994 Jul 15;153(2):517–28.

81. Johansson-Lindbom B, Agace WW. Generation of gut-homing T cells and their localization to the small intestinal mucosa. Immunol Rev. 2007 Feb;215:226–42.

82. Humphries JD, Byron A, Humphries MJ. Integrin ligands at a glance. J Cell Sci. 2006 Oct 1;119(Pt 19):3901–3.

83. Shulman Z, Shinder V, Klein E, Grabovsky V, Yeger O, Geron E, et al. Lymphocyte crawling and transendothelial migration require chemokine triggering of high-affinity LFA-1 integrin. Immunity. Elsevier; 2009 Mar 20;30(3):384–96.

84. Muller WA. Mechanisms of leukocyte transendothelial migration. Annu Rev Pathol. 2011 Jan;6:323–44.

85. Millán J, Hewlett L, Glyn M, Toomre D, Clark P, Ridley AJ. Lymphocyte transcellular migration occurs through recruitment of endothelial ICAM-1 to caveola- and F-actin-rich domains. Nat Cell Biol. 2006 Feb;8(2):113–23.

86. Ostermann G, Weber KSC, Zernecke A, Schröder A, Weber C. JAM-1 is a ligand of the beta(2) integrin LFA-1 involved in transendothelial migration of leukocytes. Nat Immunol. 2002 Feb;3(2):151–8.

87. Cunningham SA, Rodriguez JM, Arrate MP, Tran TM, Brock TA. JAM2 interacts with alpha4beta1. Facilitation by JAM3. J Biol Chem. 2002 Aug 2;277(31):27589–92.

88. Muller WA, Weigl SA, Deng X, Phillips DM. PECAM-1 is required for transendothelial migration of leukocytes. J Exp Med. 1993 Aug 1;178(2):449–60.

89. Mamdouh Z, Mikhailov A, Muller WA. Transcellular migration of leukocytes is mediated by the endothelial lateral border recycling compartment. J Exp Med. 2009 Nov 23;206(12):2795–808.

90. Dvorak AM, Kohn S, Morgan ES, Fox P, Nagy JA, Dvorak HF. The vesiculo-vacuolar organelle (VVO): a distinct endothelial cell structure that provides a transcellular pathway for macromolecular extravasation. J Leukoc Biol. 1996 Jan;59(1):100–15.

91. Ariotti S, Hogenbirk MA, Dijkgraaf FE, Visser LL, Hoekstra ME, Song J-Y, et al. Skin-resident memory CD8+ T cells trigger a state of tissue-wide pathogen alert. Science (80-). 2014 Aug 28;346(6205):101–5.

92. Shin H, Iwasaki A. A vaccine strategy that protects against genital herpes by establishing local memory T cells. Nature. 2012 Nov 15;491(7424):463–7.

93. Klonowski KD, Williams KJ, Marzo AL, Blair DA, Lingenheld EG, Lefrançois L. Dynamics of Blood-Borne CD8 Memory T Cell Migration In Vivo. Immunity. Elsevier; 2004 May 5;20(5):551–62.

94. Masopust D, Choo D, Vezys V, Wherry EJ, Duraiswamy J, Akondy R, et al. Dynamic T cell migration program provides resident memory within intestinal epithelium. J Exp Med. 2010 Mar 15;207(3):553–64.

95. Bromley SK, Yan S, Tomura M, Kanagawa O, Luster AD. Recirculating memory T cells are a unique subset of CD4+ T cells with a distinct phenotype and migratory pattern. J Immunol. 2013;190(3):970–6.

96. Teijaro JR, Turner D, Pham Q, Wherry EJ, Lefrançois L, Farber DL. Cutting edge: Tissue-retentive lung memory CD4 T cells mediate optimal protection to respiratory virus infection. J Immunol. 2011 Dec 1;187(11):5510–4.

97. Bankovich AJ, Shiow LR, Cyster JG. CD69 suppresses sphingosine 1-phosophate receptor-1 (S1P1) function through interaction with membrane helix 4. J Biol Chem. 2010;285(29):22328–37.

98. Matloubian M, Lo CG, Cinamon G, Lesneski MJ, Xu Y, Brinkmann V, et al. Lymphocyte egress from thymus and peripheral lymphoid organs is dependent on S1P receptor 1. Nature. 2004;427(6972):355–60.

99. Cepek KL, Parker CM, Madara JL, Brenner MB. Integrin alpha E beta 7 mediates adhesion of T lymphocytes to epithelial cells. J Immunol. 1993 Apr 15;150(8 Pt 1):3459–70.

100. Campbell JJ, Murphy KE, Kunkel EJ, Brightling CE, Soler D, Shen Z, et al. CCR7 expression and memory T cell diversity in humans. J Immunol. 2001 Jan 15;166(2):877–84.

101. Carbone FR, Mackay LK, Heath WR, Gebhardt T. Distinct resident and recirculating memory T cell subsets in non-lymphoid tissues. Curr Opin Immunol. Elsevier Ltd; 2013;25(3):329–33.

102. Salter RD, Norment AM, Chen BP, Clayberger C, Krensky AM, Littman DR, et al. Polymorphism in the alpha 3 domain of HLA-A molecules affects binding to CD8. Nature. 1989 Mar 23;338(6213):345–7.

103. Carnaud C, Lee D, Donnars O, Park SH, Beavis A, Koezuka Y, et al. Cutting edge: Cross-talk between cells of the innate immune system: NKT cells rapidly activate NK cells. J Immunol. 1999 Nov 1;163(9):4647–50.

104. Mosser DM. The many faces of macrophage activation. J Leukoc Biol. 2003 Feb 1;73(2):209–12.

105. Mosmann TR, Coffman RL. TH1 and TH2 cells: different patterns of lymphokine secretion lead to different functional properties. Annu Rev Immunol. 1989 Jan;7:145–73.

106. Hughes CC, Male DK, Lantos PL. Adhesion of lymphocytes to cerebral microvascular cells: effects of interferon-gamma, tumour necrosis factor and interleukin-1. Immunology. 1988 Aug;64(4):677–81.

107. Trapani JA, Smyth MJ. Functional significance of the perforin/granzyme cell death pathway. Nat Rev Immunol. 2002 Oct;2(10):735–47.

108. Ju ST, Panka DJ, Cui H, Ettinger R, el-Khatib M, Sherr DH, et al. Fas(CD95)/FasL interactions required for programmed cell death after T-cell activation. Nature. 1995 Feb 2;373(6513):444–8.

109. Carrega P, Ferlazzo G. Natural killer cell distribution and trafficking in human tissues. Front Immunol. Frontiers; 2012 Jan 29;3:347.

110. Vivier E, Ugolini S. NK cells : receptors and functions. Nature. 2010;66(11):2010–2010.

111. Chan WK, Rujkijyanont P, Neale G, Yang J, Bari R, Das Gupta N, et al. Multiplex and genome-wide analyses reveal distinctive properties of KIR+ and CD56+ T cells in human blood. J Immunol. American Association of Immunologists; 2013 Aug 15;191(4):1625–36.

112. Miner KT, Croft M. Generation, persistence, and modulation of Th0 effector cells: role of autocrine IL-4 and IFN-gamma. J Immunol. 1998;160(11):5280–7.

113. Minami Y, Kono T, Miyazaki T, Taniguchi T. The IL-2 receptor complex: its structure, function, and target genes. Annu Rev Immunol. Annual Reviews 4139 El Camino Way, P.O. Box 10139, Palo Alto, CA 94303-0139, USA; 1993 Jan 28;11:245–68.

114. Walsh KP, Mills KHG. Dendritic cells and other innate determinants of T helper cell polarisation. Trends Immunol. 2013 Nov;34(11):521–30.

115. Rochman Y, Spolski R, Leonard WJ. New insights into the regulation of T cells by gamma(c) family cytokines. Nat Rev Immunol. Nature Publishing Group; 2009 Jul;9(7):480–90.

116. Wajant H, Pfizenmaier K, Scheurich P. Tumor necrosis factor signaling. Cell Death Differ. 2003 Jan;10(1):45–65.

117. Mosmann TR, Cherwinski H, Bond MW, Giedlin MA, Coffman RL. Two types of murine helper T cell clone. I. Definition according to profiles of lymphokine activities and secreted proteins. J Immunol. 1986 Apr 1;136(7):2348–57.

118. Szabo SJ, Kim ST, Costa GL, Zhang X, Fathman CG, Glimcher LH. A novel transcription factor, T-bet, directs Th1 lineage commitment. Cell. 2000 Mar 17;100(6):655–69.

119. Zheng W, Flavell RA. The Transcription Factor GATA-3 Is Necessary and Sufficient for Th2 Cytokine Gene Expression in CD4 T Cells. Cell. 1997 May;89(4):587–96.

120. Ouyang W, Ranganath SH, Weindel K, Bhattacharya D, Murphy TL, Sha WC, et al. Inhibition of Th1 Development Mediated by GATA-3 through an IL-4-Independent Mechanism. Immunity. 1998 Nov;9(5):745–55.

121. Zhou L, Chong MMW, Littman DR. Plasticity of CD4+ T cell lineage differentiation. Immunity. 2009 May;30(5):646–55.

122. Hirota K, Duarte JH, Veldhoen M, Hornsby E, Li Y, Cua DJ, et al. Fate mapping of IL-17-producing T cells in inflammatory responses. Nat Immunol. Nature Publishing Group; 2011 Mar 30;12(3):255–63.

123. Ju S-T, Sharma R, Gaskin F, Kung JT, Fu SM. The Biology of Autoimmune Response in the Scurfy Mice that Lack the CD4+Foxp3+ Regulatory T-Cells. Biology (Basel). 2012;1(1):18–42.

124. Bettini ML, Vignali D a a. Development of thymically derived natural regulatory T cells. Ann N Y Acad Sci. 2010 Jan;1183:1–12.

125. Picca CC, Larkin J, Boesteanu A, Lerman MA, Rankin AL, Caton AJ. Role of TCR specificity in CD4+ CD25+ regulatory T-cell selection. Immunol Rev. 2006 Aug;212:74–85.

126. Tai X, Cowan M, Feigenbaum L, Singer A. CD28 costimulation of developing thymocytes induces Foxp3 expression and regulatory T cell differentiation independently of interleukin 2. Nat Immunol. 2005 Feb;6(2):152–62.

127. Sakaguchi S, Miyara M, Costantino CM, Hafler D a. FOXP3+ regulatory T cells in the human immune system. Nat Rev Immunol. Nature Publishing Group; 2010;10(7):490–500.

128. Sansom DM. CD28, CTLA-4 and their ligands: who does what and to whom? Immunology. 2000 Oct;101(2):169–77.

129. Tai X, Van Laethem F, Pobezinsky L, Guinter T, Sharrow SO, Adams A, et al. Basis of CTLA-4 function in regulatory and conventional CD4(+) T cells. Blood. 2012 May 31;119(22):5155–63.

130. Grohmann U, Orabona C, Fallarino F, Vacca C, Calcinaro F, Falorni A, et al. CTLA-4-Ig regulates tryptophan catabolism in vivo. Nat Immunol. 2002 Nov;3(11):1097–101.

131. Fallarino F, Grohmann U, Vacca C, Bianchi R, Orabona C, Spreca A, et al. T cell apoptosis by tryptophan catabolism. Cell Death Differ. Nature Publishing Group; 2002 Oct 1;9(10):1069–77.

132. Huang S, Apasov S, Koshiba M, Sitkovsky M. Role of A2a extracellular adenosine receptor-mediated signaling in adenosine-mediated inhibition of T-cell activation and expansion. Blood. American Society of Hematology; 1997 Aug 15;90(4):1600–10.

133. Sevigny CP, Li L, Awad AS, Huang L, McDuffie M, Linden J, et al. Activation of Adenosine 2A Receptors Attenuates Allograft Rejection and Alloantigen Recognition. J Immunol. American Association of Immunologists; 2007 Mar 19;178(7):4240–9.

134. Zarek PE, Huang C-T, Lutz ER, Kowalski J, Horton MR, Linden J, et al. A2A receptor signaling promotes peripheral tolerance by inducing T-cell anergy and the generation of adaptive regulatory T cells. Blood. 2008 Jan 1;111(1):251–9.

135. Barthlott T, Moncrieffe H, Veldhoen M, Atkins CJ, Christensen J, O'Garra A, et al. CD25+ CD4+ T cells compete with naive CD4+ T cells for IL-2 and exploit it for the induction of IL-10 production. Int Immunol. 2005 Mar 1;17(3):279–88.

136. Grossman WJ, Verbsky JW, Barchet W, Colonna M, Atkinson JP, Ley TJ. Human T regulatory cells can use the perforin pathway to cause autologous target cell death. Immunity. 2004 Oct;21(4):589–601.

137. Gondek DC, Lu L-F, Quezada SA, Sakaguchi S, Noelle RJ. Cutting edge: contact-mediated suppression by CD4+CD25+ regulatory cells involves a granzyme B-dependent, perforin-independent mechanism. J Immunol. 2005 Feb 15;174(4):1783–6.

138. Strauss L, Bergmann C, Whiteside TL. Human circulating CD4+CD25highFoxp3+ regulatory T cells kill autologous CD8+ but not CD4+ responder cells by Fas-mediated apoptosis. J Immunol. 2009 Feb 1;182(3):1469–80.

139. Thornton AM, Shevach EM. Suppressor effector function of CD4+CD25+ immunoregulatory T cells is antigen nonspecific. J Immunol. 2000 Jan 1;164(1):183–90.

140. Wallet MA, Sen P, Tisch R. Immunoregulation of dendritic cells. Clin Med Res. 2005 Aug;3(3):166–75.

141. Fu S, Zhang N, Yopp AC, Chen D, Mao M, Chen D, et al. TGF-beta induces Foxp3 + T-regulatory cells from CD4 + CD25 - precursors. Am J Transplant. 2004 Oct;4(10):1614–27.

142. Shevach EM, Tran DQ, Davidson TS, Andersson J. The critical contribution of TGF-beta to the induction of Foxp3 expression and regulatory T cell function. Eur J Immunol. 2008 Apr;38(4):915–7.

143. Collison LW, Workman CJ, Kuo TT, Boyd K, Wang Y, Vignali KM, et al. The inhibitory cytokine IL-35 contributes to regulatory T-cell function. Nature. 2007 Nov 22;450(7169):566–9.

144. Wang Y, Su MA, Wan YY. An essential role of the transcription factor GATA-3 for the function of regulatory T cells. Immunity. 2011 Sep 23;35(3):337–48.

145. Chaudhry A, Samstein RM, Treuting P, Liang Y, Pils MC, Heinrich J-M, et al. Interleukin-10 signaling in regulatory T cells is required for suppression of Th17 cell-mediated inflammation. Immunity. 2011 Apr 22;34(4):566–78.

146. Huehn J, Siegmund K, Lehmann JCU, Siewert C, Haubold U, Feuerer M, et al. Developmental stage, phenotype, and migration distinguish naive- and effector/memory-like CD4+ regulatory T cells. J Exp Med. 2004 Feb 2;199(3):303–13.

147. Van VQ, Darwiche J, Raymond M, Lesage S, Bouguermouh S, Rubio M, et al. Cutting Edge: CD47 Controls the In Vivo Proliferation and Homeostasis of Peripheral CD4+CD25+Foxp3+ Regulatory T Cells That Express CD103. J Immunol. American Association of Immunologists; 2008 Oct 2;181(8):5204–8.

148. Cretney E, Kallies A, Nutt SL. Differentiation and function of Foxp3+ effector regulatory T cells. Trends Immunol. Elsevier Ltd; 2013;34(2):74–80.

149. Walker MR, Kasprowicz DJ, Gersuk VH, Benard A, Van Landeghen M, Buckner JH, et al. Induction of FoxP3 and acquisition of T regulatory activity by stimulated human CD4+CD25- T cells. J Clin Invest. 2003 Nov;112(9):1437–43.

150. Chen X, Oppenheim JJ, Howard O. BALB/c mice have more CD4+ CD25+ T regulatory cells and show greater susceptibility to suppression of their CD4+ CD25– responder T cells than C57BL/6 mice. J Leukoc Biol. 2005;78(1):114.

151. Wang J, Ioan-Facsinay A, van der Voort EIH, Huizinga TWJ, Toes REM. Transient expression of FOXP3 in human activated nonregulatory CD4+ T cells. Eur J Immunol. 2007 Jan;37(1):129–38.

152. Mantel P-Y, Ouaked N, Rückert B, Karagiannidis C, Welz R, Blaser K, et al. Molecular mechanisms underlying FOXP3 induction in human T cells. J Immunol. 2006 Mar 15;176(6):3593–602.

153. Ziegler SF. FOXP3: Not just for regulatory T cells anymore. Eur J Immunol. 2007;37(1):21–3.

154. Fisson S, Darrasse-Jèze G, Litvinova E, Septier F, Klatzmann D, Liblau R, et al. Continuous activation of autoreactive CD4+ CD25+ regulatory T cells in the steady state. J Exp Med. 2003 Sep 1;198(5):737–46.

155. Attridge K, Walker LSK. Homeostasis and function of regulatory T cells (Tregs) in vivo: Lessons from TCR-transgenic Tregs. Immunol Rev. 2014;259(1):23–39.

156. Shen C-R, Yang W-C, Chen H-W. The fate of regulatory T cells: survival or apoptosis. Cell Mol Immunol. Nature Publishing Group; 2014 Jan 4;11(1):11–3.

157. Tai X, Erman B, Alag A, Mu J, Kimura M, Katz G, et al. Foxp3 transcription factor is proapoptotic and lethal to developing regulatory T cells unless counterbalanced by cytokine survival signals. Immunity. 2013 Jun 27;38(6):1116–28.

158. Pierson W, Cauwe B, Policheni A, Schlenner SM, Franckaert D, Berges J, et al. Antiapoptotic Mcl-1 is critical for the survival and niche-filling capacity of Foxp3^{+} regulatory T cells. Nat Immunol. 2013 Sep;14(9):959–65.

159. Gregori S, Tomasoni D, Pacciani V, Scirpoli M, Battaglia M, Magnani CF, et al. Differentiation of type 1 T regulatory cells (Tr1) by tolerogenic DC-10 requires the IL-10 – dependent ILT4 / HLA-G pathway. Differentiation. 2010;116(6):935–44.

160. Pot C, Apetoh L, Awasthi A, Kuchroo VK. Induction of regulatory Tr1 cells and inhibition of T(H)17 cells by IL-27. Semin Immunol. 2011 Dec;23(6):438–45.

161. Roncarolo MG, Gregori S, Battaglia M, Bacchetta R, Fleischhauer K, Levings MK. Interleukin-10-secreting type 1 regulatory T cells in rodents and humans. Immunol Rev. 2006 Aug;212:28–50.

162. Carrier Y, Yuan J, Kuchroo VK, Weiner HL. Th3 cells in peripheral tolerance. I. Induction of Foxp3-positive regulatory T cells by Th3 cells derived from TGF-beta T cell-transgenic mice. J Immunol. 2007 Jan 1;178(1):179–85.

163. Jenkins MK, Pardoll DM, Mizuguchi J, Quill H, Schwartz RH. T-cell unresponsiveness in vivo and in vitro: fine specificity of induction and molecular characterization of the unresponsive state. Immunol Rev. 1987 Mar;95:113–35.

164. Fathman CG, Lineberry NB. Molecular mechanisms of CD4+ T-cell anergy. Nat Rev Immunol. Nature Publishing Group; 2007 Aug 6;7(August):599–609.

165. Wolf H, Müller Y, Salmen S, Wilmanns W, Jung G. Induction of anergy in resting human T lymphocytes by immobilized anti-CD3 antibodies. Eur J Immunol. 1994 Jun;24(6):1410–7.

166. Sadegh-Nasseri S, Dalai SK, Korb Ferris LC, Mirshahidi S. Suboptimal engagement of the T-cell receptor by a variety of peptide-MHC ligands triggers T-cell anergy. Immunology. 2010 Jan;129(1):1–7.

167. Eynon EE. Small B cells as antigen-presenting cells in the induction of tolerance to soluble protein antigens. J Exp Med. 1992 Jan 1;175(1):131–8.

168. Hayashi RJ, Loh DY, Kanagawa O, Wang F. Differences between responses of naive and activated T cells to anergy induction. J Immunol. American Association of Immunologists; 1998 Jan 1;160(1):33–8.

169. Macián F, López-Rodríguez C, Rao A. Partners in transcription: NFAT and AP-1. Oncogene. Nature Publishing Group; 2001 Apr 30;20(19):2476–89.

170. Fruman DA, Klee CB, Bierer BE, Burakoff SJ. Calcineurin phosphatase activity in T lymphocytes is inhibited by FK 506 and cyclosporin A. Proc Natl Acad Sci. 1992 May 1;89(9):3686–90.

171. Prud'homme GJ, Vanier LE, Bocarro DC, Ste-Croix H. Effects of cyclosporin A, rapamycin, and FK520 on peripheral T-cell deletion and anergy. Cell Immunol. 1995 Aug;164(1):47–56.

172. Mueller DL. E3 ubiquitin ligases as T cell anergy factors. Nat Immunol. 2004 Sep;5(9):883–90.

173. Paolino M, Thien CBF, Gruber T, Hinterleitner R, Baier G, Langdon WY, et al. Essential role of E3 ubiquitin ligase activity in Cbl-b-regulated T cell functions. J Immunol. American Association of Immunologists; 2011 Feb 15;186(4):2138–47.

174. Nurieva RI, Zheng S, Jin W, Chung Y, Zhang Y, Martinez GJ, et al. The E3 ubiquitin ligase GRAIL regulates T cell tolerance and regulatory T cell function by mediating T cell receptor-CD3 degradation. Immunity. 2010 May 28;32(5):670–80.

175. Fang D, Elly C, Gao B, Fang N, Altman Y, Joazeiro C, et al. Dysregulation of T lymphocyte function in itchy mice: a role for Itch in TH2 differentiation. Nat Immunol. 2002 Mar;3(3):281–7.

176. Jeon M-SS, Atfield A, Venuprasad K, Krawczyk C, Sarao R, Elly C, et al. Essential role of the E3 ubiquitin ligase Cbl-b in T cell anergy induction. Immunity. Elsevier; 2004 Aug 8;21(2):167–77.

177. Heissmeyer V, Macián F, Im S-H, Varma R, Feske S, Venuprasad K, et al. Calcineurin imposes T cell unresponsiveness through targeted proteolysis of signaling proteins. Nat Immunol. 2004 Mar;5(3):255–65.

178. Hundt M, Tabata H, Jeon M-S, Hayashi K, Tanaka Y, Krishna R, et al. Impaired activation and localization of LAT in anergic T cells as a consequence of a selective palmitoylation defect. Immunity. 2006 May;24(5):513–22.

179. Fang D, Wang HY, Fang N, Altman Y, Elly C, Liu YC. Cbl-b, a RING-type E3 ubiquitin ligase, targets phosphatidylinositol 3-kinase for ubiquitination in T cells. J Biol Chem. 2001 Feb 16;276(7):4872–8.

180. Krawczyk C, Bachmaier K, Sasaki T, Jones RG, Snapper SB, Bouchard D, et al. Cbl-b Is a Negative Regulator of Receptor Clustering and Raft Aggregation in T Cells. Immunity. Elsevier; 2000 Oct 10;13(4):463–73.

181. Bustelo XR, Crespo P, López-Barahona M, Gutkind JS, Barbacid M. Cbl-b, a member of the Sli-1/c-Cbl protein family, inhibits Vav-mediated c-Jun N-terminal kinase activation. Oncogene. 1997 Nov 20;15(21):2511–20.

182. Su L, Lineberry N, Huh Y, Soares L, Fathman CG. A novel E3 ubiquitin ligase substrate screen identifies Rho guanine dissociation inhibitor as a substrate of gene related to anergy in lymphocytes. J Immunol. 2006 Dec 1;177(11):7559–66.

183. Rellahan BL. In vivo induction of anergy in peripheral V beta 8+ T cells by staphylococcal enterotoxin B. J Exp Med. 1990 Oct 1;172(4):1091–100.

184. Waanders GA, Shakhov AN, Held W, Karapetian O, Acha-Orbea H, MacDonald HR. Peripheral T cell activation and deletion induced by transfer of lymphocyte subsets expressing endogenous or exogenous mouse mammary tumor virus. J Exp Med. 1993 May 1;177(5):1359–66.

185. Pape KA, Merica R, Mondino A, Khoruts A, Jenkins MK. Direct evidence that functionally impaired CD4+ T cells persist in vivo following induction of peripheral tolerance. J Immunol. 1998 May 15;160(10):4719–29.

186. Schwartz RH. Models of T cell anergy: is there a common molecular mechanism? J Exp Med. 1996 Jul 1;184(1):1–8.

187. Schwartz RH. T cell anergy. Annu Rev Immunol. Annual Reviews 4139 El Camino Way, P.O. Box 10139, Palo Alto, CA 94303-0139, USA; 2003 Jan 28;21:305–34.

188. Tanchot C, Barber DL, Chiodetti L, Schwartz RH. Adaptive tolerance of CD4+ T cells in vivo: multiple thresholds in response to a constant level of antigen presentation. J Immunol. 2001 Aug 15;167(4):2030–9.

189. Beverly B, Kang SM, Lenardo MJ, Schwartz RH. Reversal of in vitro T cell clonal anergy by IL-2 stimulation. Int Immunol. 1992 Jun;4(6):661–71.

190. Chiodetti L, Choi S, Barber DL, Schwartz RH. Adaptive tolerance and clonal anergy are distinct biochemical states. J Immunol. 2006 Feb 15;176(4):2279–91.

191. Wherry EJ, Ha S-J, Kaech SM, Haining WN, Sarkar S, Kalia V, et al. Molecular signature of CD8+ T cell exhaustion during chronic viral infection. Immunity. 2007 Oct;27(4):670–84.

192. Migueles SA, Laborico AC, Shupert WL, Sabbaghian MS, Rabin R, Hallahan CW, et al. HIV-specific CD8+ T cell proliferation is coupled to perforin expression and is maintained in nonprogressors. Nat Immunol. 2002 Nov;3(11):1061–8.

193. Andersson J, Kinloch S, Sönnerborg A, Nilsson J, Fehniger TE, Spetz A-L, et al. Low levels of perforin expression in CD8+ T lymphocyte granules in lymphoid tissue during acute human immunodeficiency virus type 1 infection. J Infect Dis. 2002 May 1;185(9):1355–8.

194. Ulsenheimer A, Gerlach JT, Gruener NH, Jung M-C, Schirren C-A, Schraut W, et al. Detection of functionally altered hepatitis C virus-specific CD4 T cells in acute and chronic hepatitis C. Hepatology. 2003 May;37(5):1189–98.

195. Crawford A, Wherry EJ. The diversity of costimulatory and inhibitory receptor pathways and the regulation of antiviral T cell responses. Curr Opin Immunol. 2009 Apr;21(2):179–86.

196. Zhang L, Gajewski TF, Kline J. PD-1/PD-L1 interactions inhibit antitumor immune responses in a murine acute myeloid leukemia model. Blood. 2009 Aug 20;114(8):1545–52.

197. Curiel TJ, Wei S, Dong H, Alvarez X, Cheng P, Mottram P, et al. Blockade of B7-H1 improves myeloid dendritic cell-mediated antitumor immunity. Nat Med. 2003 May;9(5):562–7.

198. Chemnitz JM, Parry R V, Nichols KE, June CH, Riley JL. SHP-1 and SHP-2 associate with immunoreceptor tyrosine-based switch motif of programmed death 1 upon primary human T cell stimulation, but only receptor ligation prevents T cell activation. J Immunol. 2004 Jul 15;173(2):945–54.

199. Yokosuka T, Takamatsu M, Kobayashi-Imanishi W, Hashimoto-Tane A, Azuma M, Saito T. Programmed cell death 1 forms negative costimulatory microclusters that directly inhibit T cell receptor signaling by recruiting phosphatase SHP2. J Exp Med. 2012 Jun 4;209(6):1201–17.

200. Patsoukis N, Sari D, Boussiotis VA. PD-1 inhibits T cell proliferation by upregulating p27 and p15 and suppressing Cdc25A. Cell Cycle. 2012 Dec 1;11(23):4305–9.

201. Parry R V, Chemnitz JM, Frauwirth KA, Lanfranco AR, Braunstein I, Kobayashi S V, et al. CTLA-4 and PD-1 receptors inhibit T-cell activation by distinct mechanisms. Mol Cell Biol. 2005 Nov;25(21):9543–53.

202. Okazaki T, Honjo T. The PD-1-PD-L pathway in immunological tolerance. Trends Immunol. 2006 Apr;27(4):195–201.

203. Jin H-T, Ahmed R, Okazaki T. Role of PD-1 in regulating T-cell immunity. Curr Top Microbiol Immunol. 2011 Jan;350:17–37.

204. Blackburn SD, Shin H, Freeman GJ, Wherry EJ. Selective expansion of a subset of exhausted CD8 T cells by alphaPD-L1 blockade. Proc Natl Acad Sci U S A. 2008 Sep 30;105(39):15016–21.

205. Angelosanto JM, Blackburn SD, Crawford A, Wherry EJ. Progressive loss of memory T cell potential and commitment to exhaustion during chronic viral infection. J Virol. 2012 Aug;86(15):8161–70.

206. Paley MA, Kroy DC, Odorizzi PM, Johnnidis JB, Dolfi D V, Barnett BE, et al. Progenitor and terminal subsets of CD8+ T cells cooperate to contain chronic viral infection. Science. 2012 Nov 30;338(6111):1220–5.

207. Sharpe AH, Wherry EJ, Ahmed R, Freeman GJ. The function of programmed cell death 1 and its ligands in regulating autoimmunity and infection. Nat Immunol. 2007 Mar;8(3):239–45.

208. Ribas A. Tumor immunotherapy directed at PD-1. N Engl J Med. 2012 Jun 28;366(26):2517–9.

209. Sakuishi K, Apetoh L, Sullivan JM, Blazar BR, Kuchroo VK, Anderson AC. Targeting Tim-3 and PD-1 pathways to reverse T cell exhaustion and restore anti-tumor immunity. J Exp Med. 2010 Sep 27;207(10):2187–94.

210. Crawford A, Angelosanto JM, Kao C, Doering TA, Odorizzi PM, Barnett BE, et al. Molecular and transcriptional basis of $CD4^+$ T cell dysfunction during chronic infection. Immunity. 2014 Feb 20;40(2):289–302.

211. Wherry EJ, Ahmed R. Memory CD8 T-cell differentiation during viral infection. J Virol. 2004 Jun 1;78(11):5535–45.

212. Aubert RD, Kamphorst AO, Sarkar S, Vezys V, Ha S-J, Barber DL, et al. Antigen-specific CD4 T-cell help rescues exhausted CD8 T cells during chronic viral infection. Proc Natl Acad Sci U S A. 2011 Dec 27;108(52):21182–7.

213. Penaloza-MacMaster P, Araki K, Kamphorst A, Iyer S, West E, Konieczny B, et al. FoxP3+ CD4+ cells promote CD8 T cell exhaustion during chronic infection. J Immunol. Am Assoc Immnol; 2011 Apr 1;186(Meeting Abstracts 1):105.5.

214. Blackburn SD, Wherry EJ. IL-10, T cell exhaustion and viral persistence. Trends Microbiol. 2007 Apr;15(4):143–6.

215. Tinoco R, Alcalde V, Yang Y, Sauer K, Zuniga EI. Cell-intrinsic transforming growth factor-beta signaling mediates virus-specific CD8+ T cell deletion and viral persistence in vivo. Immunity. 2009 Jul 17;31(1):145–57.

216. Courtois-Cox S, Jones SL, Cichowski K. Many roads lead to oncogene-induced senescence. Oncogene. Nature Publishing Group; 2008 May 1;27(20):2801–9.

217. Kuilman T, Michaloglou C, Mooi WJ, Peeper DS. The essence of senescence. Genes Dev. 2010 Nov 15;24(22):2463–79.

218. Appay V, Rowland-Jones SL. Premature ageing of the immune system: the cause of AIDS? Trends Immunol. Elsevier; 2002 Dec 12;23(12):580–5.

219. Khan N, Shariff N, Cobbold M, Bruton R, Ainsworth JA, Sinclair AJ, et al. Cytomegalovirus Seropositivity Drives the CD8 T Cell Repertoire Toward Greater Clonality in Healthy Elderly Individuals. J Immunol. American Association of Immunologists; 2002 Aug 15;169(4):1984–92.

220. Savva GM, Pachnio A, Kaul B, Morgan K, Huppert F a., Brayne C, et al. Cytomegalovirus infection is associated with increased mortality in the older population. Aging Cell. 2013;12(3):381–7.

221. Maini MK, Soares M V, Zilch CF, Akbar AN, Beverley PC. Virus-induced CD8+ T cell clonal expansion is associated with telomerase up-regulation and telomere length preservation: a mechanism for rescue from replicative senescence. J Immunol. American Association of Immunologists; 1999 Apr 15;162(8):4521–6.

222. Vaziri H, Schächter F, Uchida I, Wei L, Zhu X, Effros R, et al. Loss of telomeric DNA during aging of normal and trisomy 21 human lymphocytes. Am J Hum Genet. 1993 Apr;52(4):661–7.

223. Chou JP, Effros RB. T cell replicative senescence in human aging. Curr Pharm Des. 2013;19(9):1680–98.

224. Effros RB, Boucher N, Porter V, Zhu X, Spaulding C, Walford RL, et al. Decline in CD28+ T cells in centenarians and in long-term T cell cultures: a possible cause for both in vivo and in vitro immunosenescence. Exp Gerontol. Jan;29(6):601–9.

225. Weng N-P, Akbar AN, Goronzy J. CD28(-) T cells: their role in the age-associated decline of immune function. Trends Immunol. 2009 Jul;30(7):306–12.

226. Weng NP, Levine BL, June CH, Hodes RJ. Regulated expression of telomerase activity in human T lymphocyte development and activation. J Exp Med. 1996 Jun 1;183(6):2471–9.

227. Saurwein-Teissl M, Lung TL, Marx F, Gschosser C, Asch E, Blasko I, et al. Lack of Antibody Production Following Immunization in Old Age: Association with CD8+CD28- T Cell Clonal Expansions and an Imbalance in the Production of Th1 and Th2 Cytokines. J Immunol. American Association of Immunologists; 2002 Jun 1;168(11):5893–9.

228. Pieper J, Johansson S, Snir O, Linton L, Rieck M, Buckner JH, et al. Peripheral and site-specific CD4(+) CD28(null) T cells from rheumatoid arthritis patients show distinct characteristics. Scand J Immunol. 2014 Feb;79(2):149–55.

229. Brenchley JM, Brenchley JM, Karandikar NJ, Karandikar NJ, Betts MR, Betts MR, et al. Expression of CD57 de nes replicative senescence and antigen-induced apoptotic death of CD8. 2003;101(7):2711–20.

230. Weyand CM, Brandes JC, Schmidt D, Fulbright JW, Goronzy JJ. Functional properties of CD4+CD28− T cells in the aging immune system. Mech Ageing Dev. 1998 May;102(2-3):131–47.

231. Ibegbu CC, Xu Y-X, Harris W, Maggio D, Miller JD, Kourtis AP. Expression of killer cell lectin-like receptor G1 on antigen-specific human CD8+ T lymphocytes during active, latent, and resolved infection and its relation with CD57. J Immunol. 2005 May 15;174(10):6088–94.

232. Akbar AN, Henson SM. Are senescence and exhaustion intertwined or unrelated processes that compromise immunity? Nat Rev Immunol. Nature Publishing Group; 2011;11(4):289–95.

233. Sakata-Kaneko S, Wakatsuki Y, Matsunaga Y, Usui T, Kita T. Altered Th1/Th2 commitment in human CD4+ T cells with ageing. Clin Exp Immunol. 2000 May;120(2):267–73.

234. Spaulding C, Guo W, Effros RB. Resistance to apoptosis in human CD8+ T cells that reach replicative senescence after multiple rounds of antigen-specific proliferation. Exp Gerontol. 1999;34(5):633–44.

235. Capparelli C, Chiavarina B, Whitaker-Menezes D, Pestell TG, Pestell RG, Hulit J, et al. CDK inhibitors (p16/p19/p21) induce senescence and autophagy in cancer-associated fibroblasts, "fueling" tumor growth via paracrine interactions, without an increase in neo-angiogenesis. Cell Cycle. 2012 Oct 1;11(19):3599–610.

236. Lichterfeld M, Mou D, Cung TDH, Williams KL, Waring MT, Huang J, et al. Telomerase activity of HIV-1 specific CD8+ T cells: Constitutive up-regulation in controllers and selective increase by blockade of PD ligand 1 in progressors. Blood. 2008;112(9):3679–87.

237. Medawar PB. Immunity to homologous grafted skin; the fate of skin homografts transplanted to the brain, to subcutaneous tissue, and to the anterior chamber of the eye. Br J Exp Pathol. 1948 Feb;29(1):58–69.

238. Simpson E. A historical perspective on immunological privilege. Immunol Rev. 2006 Oct;213:12–22.

239. Crane IJ, Liversidge J. Mechanisms of leukocyte migration across the blood-retina barrier. Semin Immunopathol. 2008 Apr;30(2):165–77.

240. Griffith TS, Brunner T, Fletcher SM, Green DR, Ferguson TA. Fas Ligand-Induced Apoptosis as a Mechanism of Immune Privilege. Science (80-). 1995 Nov 17;270(5239):1189–92.

241. Yang W, Li H, Chen PW, Alizadeh H, He Y, Hogan RN, et al. PD-L1 expression on human ocular cells and its possible role in regulating immune-mediated ocular inflammation. Invest Ophthalmol Vis Sci. 2009 Jan;50(1):273–80.

242. Cousins SW, McCabe MM, Danielpour D, Streilein JW. Identification of transforming growth factor-beta as an immunosuppressive factor in aqueous humor. Invest Ophthalmol Vis Sci. 1991 Jul;32(8):2201–11.

243. Taylor AW, Streilein JW, Cousins SW. Immunoreactive vasoactive intestinal peptide contributes to the immunosuppressive activity of normal aqueous humor. J Immunol. 1994 Aug 1;153(3):1080–6.

244. Ryu Y-H, Kim J-C. Expression of indoleamine 2,3-dioxygenase in human corneal cells as a local immunosuppressive factor. Invest Ophthalmol Vis Sci. 2007 Sep;48(9):4148–52.

245. Abi-Hanna D, Wakefield D, Watkins S. HLA antigens in ocular tissues. I. In vivo expression in human eyes. Transplantation. 1988 Mar;45(3):610–3.

246. Galea I, Bechmann I, Perry VH. What is immune privilege (not)? Trends Immunol. 2007;28(1):12–8.

247. De Graaf MT, Sillevis Smitt P a E, Luitwieler RL, Van Velzen C, Van Den Broek PDM, Kraan J, et al. Central memory CD4+ T cells dominate the normal cerebrospinal fluid. Cytom Part B - Clin Cytom. 2011;80 B(November 2009):43–50.

248. Han S, Lin YC, Wu T, Salgado AD, Mexhitaj I, Wuest SC, et al. Comprehensive immunophenotyping of cerebrospinal fluid cells in patients with neuroimmunological diseases. J Immunol. 2014;192:2551–63.

249. Kivisäkk P, Mahad DJ, Callahan MK, Sikora K, Trebst C, Tucky B, et al. Expression of CCR7 in Multiple Sclerosis: Implications for CNS Immunity. Ann Neurol. 2004;55:627–38.

250. Lalor SJ, Segal BM. Lymphoid chemokines in the CNS. J Neuroimmunol. 2010 Jul 27;224(1-2):56–61.

251. Bechmann I, Galea I, Perry VH. What is the blood-brain barrier (not)? Trends Immunol. 2007 Jan;28(1):5–11.

252. Carrithers MD, Visintin I, Kang SJ, Janeway C a. Differential adhesion molecule requirements for immune surveillance and inflammatory recruitment. Brain. 2000 Jun;123 (Pt 6:1092–101.

253. Engelhardt B, Ransohoff RM. Capture, crawl, cross: The T cell code to breach the blood-brain barriers. Trends Immunol. Elsevier Ltd; 2012;33(12):579–89.

254. Obermeier B, Daneman R, Ransohoff RM. Development, maintenance and disruption of the blood-brain barrier. Nat Med. Nature Publishing Group, a division of Macmillan Publishers Limited. All Rights Reserved.; 2013 Dec;19(12):1584–96.

255. Armulik A, Genové G, Mäe M, Nisancioglu MH, Wallgard E, Niaudet C, et al. Pericytes regulate the blood-brain barrier. Nature. Nature Publishing Group, a division of Macmillan Publishers Limited. All Rights Reserved.; 2010 Nov 25;468(7323):557–61.

256. Balabanov R, Dore-Duffy P. Role of the CNS microvascular pericyte in the blood-brain barrier. J Neurosci Res. 1998 Sep 15;53(6):637–44.

257. Engelhardt B, Coisne C. Fluids and barriers of the CNS establish immune privilege by confining immune surveillance to a two-walled castle moat surrounding the CNS castle. Fluids Barriers CNS. BioMed Central Ltd; 2011;8(1):4.

258. McCarty JH. Cell adhesion and signaling networks in brain neurovascular units. Curr Opin Hematol. 2009 May;16(3):209–14.

259. Jones EG. On the mode of entry of blood vessels into the cerebral cortex. J Anat. 1970 May;106(Pt 3):507–20.

260. Cserr HF. Flow of Brain Interstitial Fluid and Drainage into Cerebrospinal Fluid and Lymph. In: Ishii S, Nagai H, Brock M, editors. Intracranial Pressure V. Berlin, Heidelberg: Springer Berlin Heidelberg; 1983. p. 618–21.

261. Szentistványi I, Patlak CS, Ellis RA, Cserr HF. Drainage of interstitial fluid from different regions of rat brain. Am J Physiol. 1984 Jun;246(6 Pt 2):F835–44.

262. Bulloch K, Miller MM, Gal-Toth J, Milner TA, Gottfried-Blackmore A, Waters EM, et al. CD11c/EYFP transgene illuminates a discrete network of dendritic cells within the embryonic, neonatal, adult, and injured mouse brain. J Comp Neurol. 2008 Jun 10;508(5):687–710.

263. Hickey WF, Kimura H. Perivascular microglial cells of the CNS are bone marrow-derived and present antigen in vivo. Science. 1988 Jan 15;239(4837):290–2.

264. Guillemin GJ, Brew BJ. Microglia, macrophages, perivascular macrophages, and pericytes: a review of function and identification. J Leukoc Biol. 2004;75(3):388–97.

265. Ford AL, Goodsall AL, Hickey WF, Sedgwick JD. Normal adult ramified microglia separated from other central nervous system macrophages by flow cytometric sorting. Phenotypic differences defined and direct ex vivo antigen presentation to myelin basic protein-reactive CD4+ T cells compared. J Immunol. 1995 May 1;154(9):4309–21.

266. Zhang GX, Li J, Ventura E, Rostami A. Parenchymal microglia of naïve adult C57BL/6J mice express high levels of B7.1, B7.2, and MHC class II. Exp Mol Pathol. 2002 Aug;73(1):35–45.

267. Steiner O, Coisne C, Cecchelli R, Boscacci R, Deutsch U, Engelhardt B, et al. Differential roles for endothelial ICAM-1, ICAM-2, and VCAM-1 in shear-resistant T cell arrest, polarization, and directed crawling on blood-brain barrier endothelium. J Immunol. American Association of Immunologists; 2010 Oct 15;185(8):4846–55.

268. Alcolado R, Weller RO, Parrish EP, Garrod D. The cranial arachnoid and pia mater in man: anatomical and ultrastructural observations. Neuropathol Appl Neurobiol. Jan;14(1):1–17.

269. McMenamin PG, Wealthall RJ, Deverall M, Cooper SJ, Griffin B. Macrophages and dendritic cells in the rat meninges and choroid plexus: three-dimensional localisation by environmental scanning electron microscopy and confocal microscopy. Cell Tissue Res. 2003 Sep;313(3):259–69.

270. Bartholomäus I, Kawakami N, Odoardi F, Schläger C, Miljkovic D, Ellwart JW, et al. Effector T cell interactions with meningeal vascular structures in nascent autoimmune CNS lesions. Nature. Macmillan Publishers Limited. All rights reserved; 2009 Nov 5;462(7269):94–8.

271. Kivisäkk P, Mahad DJ, Callahan MK, Trebst C, Tucky B, Wei T, et al. Human cerebrospinal fluid central memory CD4+ T cells: evidence for trafficking through choroid plexus and meninges via P-selectin. Proc Natl Acad Sci U S A. 2003;100(14):8389–94.

272. Li Y-SJ, Haga JH, Chien S. Molecular basis of the effects of shear stress on vascular endothelial cells. J Biomech. Elsevier; 2005 Oct 10;38(10):1949–71.

273. Cucullo L, Hossain M, Puvenna V, Marchi N, Janigro D. The role of shear stress in Blood-Brain Barrier endothelial physiology. BMC Neurosci. 2011 Jan;12(1):40.

274. Piccio L, Rossi B, Scarpini E, Laudanna C, Giagulli C, Issekutz AC, et al. Molecular mechanisms involved in lymphocyte recruitment in inflamed brain microvessels: critical roles for P-selectin glycoprotein ligand-1 and heterotrimeric G(i)-linked receptors. J Immunol. 2002 Feb 15;168(4):1940–9.

275. Redzic ZB, Segal MB. The structure of the choroid plexus and the physiology of the choroid plexus epithelium. Adv Drug Deliv Rev. 2004 Oct 14;56(12):1695–716.

276. Maxwell DS, Pease DC. The electron microscopy of the choroid plexus. J Biophys Biochem Cytol. 1956 Jul 25;2(4):467–74.

277. Kamba T, Tam BYY, Hashizume H, Haskell A, Sennino B, Mancuso MR, et al. VEGF-dependent plasticity of fenestrated capillaries in the normal adult microvasculature. Am J Physiol Heart Circ Physiol. 2006 Feb 1;290(2):H560–76.

278. George J. Dohrmann, Paul C. Bucy. Human choroid plexus: a light and electron microscopic study. Journal of Neurosurgery Publishing Group; 2009 May 7;

279. Wolburg H, Lippoldt A. Tight junctions of the blood–brain barrier. Vascul Pharmacol. 2002 Jun;38(6):323–37.

280. Nataf S, Strazielle N, Hatterer E, Mouchiroud G, Belin M-F, Ghersi-Egea J-F. Rat choroid plexuses contain myeloid progenitors capable of differentiation toward macrophage or dendritic cell phenotypes. Glia. 2006 Aug 15;54(3):160–71.

281. Chinnery HR, Ruitenberg MJ, McMenamin PG. Novel characterization of monocyte-derived cell populations in the meninges and choroid plexus and their rates of replenishment in bone marrow chimeric mice. J Neuropathol Exp Neurol. 2010 Sep;69(9):896–909.

282. Kunis G, Baruch K, Rosenzweig N, Kertser A, Miller O, Berkutzki T, et al. IFN-γ-dependent activation of the brain's choroid plexus for CNS immune surveillance and repair. Brain. 2013;136:3427–40.

283. Provencio JJ, Kivisäkk P, Tucky BH, Luciano MG, Ransohoff RM. Comparison of ventricular and lumbar cerebrospinal fluid T cells in non-inflammatory neurological disorder (NIND) patients. J Neuroimmunol. 2005 Jun;163(1-2):179–84.

284. Wolburg K, Gerhardt H, Schulz M, Wolburg H, Engelhardt B. Ultrastructural localization of adhesion molecules in the healthy and inflamed choroid plexus of the mouse. Cell Tissue Res. 1999 May;296(2):259–69.

285. Alt C, Laschinger M, Engelhardt B. Functional expression of the lymphoid chemokines CCL19 (ELC) and CCL 21 (SLC) at the blood-brain barrier suggests their involvement

in G-protein-dependent lymphocyte recruitment into the central nervous system during experimental autoimmune encephalomyeli. Eur J Immunol. 2002 Aug;32(8):2133–44.

286. Krumbholz M, Theil D, Steinmeyer F, Cepok S, Hemmer B, Hofbauer M, et al. CCL19 is constitutively expressed in the CNS, up-regulated in neuroinflammation, active and also inactive multiple sclerosis lesions. J Neuroimmunol. 2007 Oct;190(1-2):72–9.

287. Bahbouhi B, Berthelot L, Pettré S, Michel L, Wiertlewski S, Weksler B, et al. Peripheral blood CD4+ T lymphocytes from multiple sclerosis patients are characterized by higher PSGL-1 expression and transmigration capacity across a human blood-brain barrier-derived endothelial cell line. J Leukoc Biol. 2009 Nov;86(5):1049–63.

288. Kivisäkk P, Trebst C, Liu Z, Tucky BH, Sørensen TL, Rudick RA, et al. T-cells in the cerebrospinal fluid express a similar repertoire of inflammatory chemokine receptors in the absence or presence of CNS inflammation: implications for CNS trafficking. Clin Exp Immunol. 2002 Sep;129(3):510–8.

289. Kivisäkk P, Imitola J, Rasmussen S, Elyaman W, Zhu B, Ransohoff RM, et al. Localizing central nervous system immune surveillance: meningeal antigen-presenting cells activate T cells during experimental autoimmune encephalomyelitis. Ann Neurol. 2009 Apr;65(4):457–69.

290. Flinn IW, Ambinder RF. AIDS primary central nervous system lymphoma. Curr Opin Oncol. 1996 Sep;8(5):373–6.

291. Berger JR, Koralnik IJ. Progressive multifocal leukoencephalopathy and natalizumab--unforeseen consequences. N Engl J Med. 2005 Jul 28;353(4):414–6.

292. Iliff JJ, Wang M, Liao Y, Plogg BA, Peng W, Gundersen GA, et al. A paravascular pathway facilitates CSF flow through the brain parenchyma and the clearance of interstitial solutes, including amyloid β. Sci Transl Med. 2012 Aug 15;4(147):147ra111.

293. Laterra J, Keep R, Betz LA, Goldstein GW. Blood-Brain-Cerebrospinal Fluid Barriers. Basic Neurochemistry: Molecular, Cellular and Medical Aspects. 6th ed. Lippincott-Raven; 1999.

294. Carare RO, Hawkes C a., Weller RO. Afferent and efferent immunological pathways of the brain. Anatomy, Function and Failure. Brain Behav Immun. Elsevier Inc.; 2014;36:9–14.

295. Weller RO, Galea I, Carare RO, Minagar A. Pathophysiology of the lymphatic drainage of the central nervous system: Implications for pathogenesis and therapy of multiple sclerosis. Pathophysiology. 2010;17(4):295–306.

296. Zhang ET, Richards HK, Kida S, Weller RO. Directional and compartmentalised drainage of interstitial fluid and cerebrospinal fluid from the rat brain. Acta Neuropathol. 1992 Feb;83(3):233–9.

297. Cserr HF, Harling-Berg CJ, Knopf PM. Drainage of brain extracellular fluid into blood and deep cervical lymph and its immunological significance. Brain Pathol. 1992 Oct;2(4):269–76.

298. Van Zwam M, Huizinga R, Melief M-JJ, Wierenga-Wolf AF, Van Meurs M, Voerman JS, et al. Brain antigens in functionally distinct antigen-presenting cell populations in cervical lymph nodes in MS and EAE. J Mol Med. 2009 Mar;87(3):273–86.

299. Fabriek BO, Zwemmer JNP, Teunissen CE, Dijkstra CD, Polman CH, Laman JD, et al. In vivo detection of myelin proteins in cervical lymph nodes of MS patients using ultrasound-guided fine-needle aspiration cytology. J Neuroimmunol. 2005 Apr;161(1-2):190–4.

300. Mohammad MG, Tsai VWW, Ruitenberg MJ, Hassanpour M, Li H, Hart PH, et al. Immune cell trafficking fro the brain maintains CNS immune tolerance. J Clin Invest. 2014 Mar;124(3):1228–41.

301. Goldmann J, Kwidzinski E, Brandt C, Mahlo J, Richter D. T cells traffic from brain to cervical lymph nodes via the cribroid plate and the nasal mucosa Abstract : Although drainage pathways of soluble antigens from brain to cervical lymph nodes have. 2006;80(October):797–801.

302. Wolvers DA, Coenen-de Roo CJ, Mebius RE, van der Cammen MJ, Tirion F, Miltenburg AM, et al. Intranasally induced immunological tolerance is determined by characteristics of the draining lymph nodes: studies with OVA and human cartilage gp-39. J Immunol. 1999 Feb 15;162(4):1994–8.

303. Van Zwam M, Huizinga R, Heijmans N, van Meurs M, Wierenga-Wolf AF, Melief M-J, et al. Surgical excision of CNS-draining lymph nodes reduces relapse severity in chronic-relapsing experimental autoimmune encephalomyelitis. J Pathol. 2009 Mar;217(4):543–51.

304. Flügel A, Schwaiger FW, Neumann H, Medana I, Willem M, Wekerle H, et al. Neuronal FasL Induces Cell Death of Encephalitogenic T Lymphocytes. Brain Pathol. 2006 Apr 5;10(3):353–64.

305. Lampson LA, Hickey WF. Monoclonal antibody analysis of MHC expression in human brain biopsies: tissue ranging from “histologically normal” to that showing different levels of glial tumor involvement. J Immunol. 1986 Jun 1;136(11):4054–62.

306. Gimsa U, Mitchison NA, Brunner-Weinzierl MC. Immune privilege as an intrinsic CNS property: Astrocytes protect the CNS against T-cell-mediated neuroinflammation. Mediators Inflamm. 2013;2013.

307. Taylor AW, Streilein JW. Inhibition of antigen-stimulated effector T cells by human cerebrospinal fluid. Neuroimmunomodulation. 1996;3(2-3):112–8.

308. Wilbanks G a, Streilein JW. Fluids from immune privileged sites endow macrophages with the capacity to induce antigen-specific immune deviation via a mechanism involving transforming growth factor-beta. Eur J Immunol. 1992 Apr;22(4):1031–6.

309. Fahrenkrug J, de Muckadell OBS, Fahrenkrug A. Vasoactive intestinal polypeptide (VIP) in human cerebrospinal fluid. Brain Res. 1977 Apr;124(3):581–4.

310. Hammack BN, Fung KYC, Hunsucker SW, Duncan MW, Burgoon MP, Owens GP, et al. Proteomic analysis of multiple sclerosis cerebrospinal fluid. Mult Scler. 2004 Apr 1;10(3):245–60.

311. O'Donohue TL, Charlton CG, Thoa NB, Helke CJ, Moody TW, Pert A, et al. Release of alpha-melanocyte stimulating hormone into rat and human cerebrospinal fluid in vivo and from rat hypothalamus slices in vitro. Peptides. 1981 Mar;2(1):93–100.

312. Shechter R, London A, Schwartz M. Orchestrated leukocyte recruitment to immune-privileged sites: absolute barriers versus educational gates. Nat Rev Immunol. Nature Publishing Group; 2013;13(3):206–18.

313. Sadagopal S, Lorey SL, Barnett L, Sutherland D, Basham R, Erdem H, et al. Enhanced PD-1 expression by T cells in cerebrospinal fluid does not reflect functional exhaustion during chronic human immunodeficiency virus type 1 infection. J Virol. 2010;84(1):131–40.

314. Latchman YE, Liang SC, Wu Y, Chernova T, Sobel RA, Klemm M, et al. PD-L1-deficient mice show that PD-L1 on T cells, antigen-presenting cells, and host tissues negatively regulates T cells. Proc Natl Acad Sci U S A. 2004 Jul 20;101(29):10691–6.

315. Salama AD, Chitnis T, Imitola J, Ansari MJI, Akiba H, Tushima F, et al. Critical role of the programmed death-1 (PD-1) pathway in regulation of experimental autoimmune encephalomyelitis. J Exp Med. 2003 Jul 7;198(1):71–8.

316. Schreiner B, Bailey SL, Shin T, Chen L, Miller SD. PD-1 ligands expressed on myeloid-derived APC in the CNS regulate T-cell responses in EAE. Eur J Immunol. 2008 Oct;38(10):2706–17.

317. Magnus T. Microglial Expression of the B7 Family Member B7 Homolog 1 Confers Strong Immune Inhibition: Implications for Immune Responses and Autoimmunity in the CNS. J Neurosci. 2005 Mar 9;25(10):2537–46.

318. Shechter R, Miller O, Yovel G, Rosenzweig N, London A, Ruckh J, et al. Recruitment of beneficial M2 macrophages to injured spinal cord is orchestrated by remote brain choroid plexus. Immunity. 2013 Mar 21;38(3):555–69.

319. Serot J-M, Béné M-C, Foliguet B, Faure GC. Monocyte-derived IL-10-secreting dendritic cells in choroid plexus epithelium. J Neuroimmunol. 2000 Jun;105(2):115–9.

320. Polman CH, Reingold SC, Banwell B, Clanet M, Cohen JA, Filippi M, et al. Diagnostic criteria for multiple sclerosis: 2010 revisions to the McDonald criteria. Ann Neurol. 2011 Feb;69(2):292–302.

321. Miller DH, Chard DT, Ciccarelli O. Clinically isolated syndromes. Lancet Neurol. 2012 Feb;11(2):157–69.

322. Kremenchutzky M, Rice GPA, Baskerville J, Wingerchuk DM, Ebers GC. The natural history of multiple sclerosis: a geographically based study 9: observations on the progressive phase of the disease. Brain. 2006 Mar;129(Pt 3):584–94.

323. Miller DH, Leary SM. Primary-progressive multiple sclerosis. Lancet Neurol. 2007 Oct;6(10):903–12.

324. Lublin FD, Reingold SC. Defining the clinical course of multiple sclerosis: Results of an international survey. Neurology. 1996 Apr 1;46(4):907–11.

325. Pender MP. The essential role of Epstein-Barr virus in the pathogenesis of multiple sclerosis. Neuroscientist. 2011 Aug;17(4):351–67.

326. Gourraud P-A, Harbo HF, Hauser SL, Baranzini SE. The genetics of multiple sclerosis: an up-to-date review. Immunol Rev. 2012 Jul;248(1):87–103.

327. Correale J, Ysrraelit MC, Gaitán MI. Immunomodulatory effects of Vitamin D in multiple sclerosis. Brain. 2009 May;132(Pt 5):1146–60.

328. Penna G, Amuchastegui S, Giarratana N, Daniel KC, Vulcano M, Sozzani S, et al. 1,25-Dihydroxyvitamin D3 selectively modulates tolerogenic properties in myeloid but not plasmacytoid dendritic cells. J Immunol. 2007 Jan 1;178(1):145–53.

329. De Rosbo NK, Ben-Nun A. T-cell responses to myelin antigens in multiple sclerosis; relevance of the predominant autoimmune reactivity to myelin oligodendrocyte glycoprotein. J Autoimmun. 1998 Aug;11(4):287–99.

330. Hellings N, Barée M, Verhoeven C, D'hooghe MB, Medaer R, Bernard CC, et al. T-cell reactivity to multiple myelin antigens in multiple sclerosis patients and healthy controls. J Neurosci Res. 2001 Feb 1;63(3):290–302.

331. Ota K, Matsui M, Milford EL, Mackin GA, Weiner HL, Hafler DA. T-cell recognition of an immunodominant myelin basic protein epitope in multiple sclerosis. Nature. 1990 Jul 12;346(6280):183–7.

332. Cabbage SE, Huseby ES, Sather BD, Brabb T, Liggitt D, Goverman J. Regulatory T cells maintain long-term tolerance to myelin basic protein by inducing a novel, dynamic state of T cell tolerance. J Immunol. 2007 Jan 15;178(2):887–96.

333. Bettelli E, Carrier Y, Gao W, Korn T, Strom TB, Oukka M, et al. Reciprocal developmental pathways for the generation of pathogenic effector TH17 and regulatory T cells. Nature. 2006 May 11;441(7090):235–8.

334. Goverman JM. Immune tolerance in multiple sclerosis. Immunol Rev. 2011 May;241(1):228–40.

335. Gran B, Zhang G-X, Yu S, Li J, Chen X-H, Ventura ES, et al. IL-12p35-Deficient Mice Are Susceptible to Experimental Autoimmune Encephalomyelitis: Evidence for Redundancy in the IL-12 System in the Induction of Central Nervous System Autoimmune Demyelination. J Immunol. American Association of Immunologists; 2002 Dec 15;169(12):7104–10.

336. Cua DJ, Sherlock J, Chen Y, Murphy CA, Joyce B, Seymour B, et al. Interleukin-23 rather than interleukin-12 is the critical cytokine for autoimmune inflammation of the brain. Nature. 2003 Feb 13;421(6924):744–8.

337. Kroenke MA, Carlson TJ, Andjelkovic A V, Segal BM. IL-12- and IL-23-modulated T cells induce distinct types of EAE based on histology, CNS chemokine profile, and response to cytokine inhibition. J Exp Med. 2008 Jul 7;205(7):1535–41.

338. Reboldi A, Coisne C, Baumjohann D, Benvenuto F, Bottinelli D, Lira S, et al. C-C chemokine receptor 6-regulated entry of TH-17 cells into the CNS through the choroid plexus is required for the initiation of EAE. Nat Immunol. 2009 May;10(5):514–23.

339. Axtell RC, Steinman L. Gaining entry to an uninflamed brain. Nat Immunol. Nature Publishing Group; 2009 May;10(5):453–5.

340. McRae BL, Semnani RT, Hayes MP, van Seventer GA. Type I IFNs inhibit human dendritic cell IL-12 production and Th1 cell development. J Immunol. 1998 May 1;160(9):4298–304.

341. Axtell RC, de Jong BA, Boniface K, van der Voort LF, Bhat R, De Sarno P, et al. T helper type 1 and 17 cells determine efficacy of interferon-beta in multiple sclerosis and experimental encephalomyelitis. Nat Med. Nature Publishing Group; 2010 Apr 28;16(4):406–12.

342. Shi G, Cox CA, Vistica BP, Tan C, Wawrousek EF, Gery I. Phenotype switching by inflammation-inducing polarized Th17 cells, but not by Th1 cells. J Immunol. 2008 Nov 15;181(10):7205–13.

343. Lexberg MH, Taubner A, Albrecht I, Lepenies I, Richter A, Kamradt T, et al. IFN-γ and IL-12 synergize to convert in vivo generated Th17 into Th1/Th17 cells. Eur J Immunol. 2010 Nov;40(11):3017–27.

344. Kebir H, Ifergan I, Alvarez JI, Bernard M, Poirier J, Arbour N, et al. Preferential recruitment of interferon-gamma-expressing TH17 cells in multiple sclerosis. Ann Neurol. 2009 Sep;66(3):390–402.

345. Traugott U, Reinherz E, Raine C. Multiple sclerosis: distribution of T cell subsets within active chronic lesions. Science (80-). 1983 Jan 21;219(4582):308–10.

346. Henderson APD, Barnett MH, Parratt JDE, Prineas JW. Multiple sclerosis: distribution of inflammatory cells in newly forming lesions. Ann Neurol. 2009 Dec;66(6):739–53.

347. Merson TD, Binder MD, Kilpatrick TJ. Role of cytokines as mediators and regulators of microglial activity in inflammatory demyelination of the CNS. Neuromolecular Med. 2010 Jun;12(2):99–132.

348. Romo-González T, Chavarría A, Pérez-H J. Central nervous system: A modified immune surveillance circuit? Brain Behav Immun. 2012;26:823–9.

349. McCandless EE, Wang Q, Woerner BM, Harper JM, Klein RS. CXCL12 Limits Inflammation by Localizing Mononuclear Infiltrates to the Perivascular Space during

Experimental Autoimmune Encephalomyelitis. J Immunol. American Association of Immunologists; 2006 Nov 17;177(11):8053–64.

350. McCandless EE, Piccio L, Woerner BM, Schmidt RE, Rubin JB, Cross AH, et al. Pathological expression of CXCL12 at the blood-brain barrier correlates with severity of multiple sclerosis. Am J Pathol. 2008 Mar;172(3):799–808.

351. Agrawal S, Anderson P, Durbeej M, van Rooijen N, Ivars F, Opdenakker G, et al. Dystroglycan is selectively cleaved at the parenchymal basement membrane at sites of leukocyte extravasation in experimental autoimmune encephalomyelitis. J Exp Med. 2006 Apr 17;203(4):1007–19.

352. Greter M, Heppner FL, Lemos MP, Odermatt BM, Goebels N, Laufer T, et al. Dendritic cells permit immune invasion of the CNS in an animal model of multiple sclerosis. Nat Med. 2005 Mar;11(3):328–34.

353. Tran EH, Hoekstra K, van Rooijen N, Dijkstra CD, Owens T. Immune invasion of the central nervous system parenchyma and experimental allergic encephalomyelitis, but not leukocyte extravasation from blood, are prevented in macrophage-depleted mice. J Immunol. 1998 Oct 1;161(7):3767–75.

354. Cuzner ML, Hayes GM, Newcombe J, Woodroofe MN. The nature of inflammatory components during demyelination in multiple sclerosis. J Neuroimmunol. 1988 Dec;20(2-3):203–9.

355. McCallum K, Esiri MM, Tourtellotte WW, Booss J. T cell subsets in multiple sclerosis. Brain. 1987 Oct;110(5):1297–308.

356. Owens T, Bechmann I, Engelhardt B. Perivascular spaces and the two steps to neuroinflammation. J Neuropathol Exp Neurol. 2008;67(12):1113–21.

357. Simpson JE, Newcombe J, Cuzner ML, Woodroofe MN. Expression of monocyte chemoattractant protein-1 and other beta-chemokines by resident glia and inflammatory cells in multiple sclerosis lesions. J Neuroimmunol. 1998 Apr 15;84(2):238–49.

358. Sørensen TL, Sellebjerg F. Distinct chemokine receptor and cytokine expression profile in secondary progressive MS. Neurology. 2001 Oct 23;57(8):1371–6.

359. Mahad DJ, Ransohoff RM. The role of MCP-1 (CCL2) and CCR2 in multiple sclerosis and experimental autoimmune encephalomyelitis (EAE). Semin Immunol. 2003 Feb;15(1):23–32.

360. Balashov KE, Rottman JB, Weiner HL, Hancock WW. CCR5(+) and CXCR3(+) T cells are increased in multiple sclerosis and their ligands MIP-1alpha and IP-10 are expressed in demyelinating brain lesions. Proc Natl Acad Sci U S A. 1999 Jun 8;96(12):6873–8.

361. Sorensen TL, Trebst C, Kivisäkk P, Klaege KL, Majmudar A, Ravid R, et al. Multiple sclerosis: A study of CXCL10 and CXCR3 co-localization in the inflamed central nervous system. J Neuroimmunol. Elsevier; 2002 Jun 6;127(1-2):59–68.

362. Rosenberg GA. Neurological diseases in relation to the blood-brain barrier. J Cereb Blood Flow Metab. Nature Publishing Group; 2012 Jul 18;32(7):1139–51.

363. Serafini B, Rosicarelli B, Magliozzi R, Stigliano E, Aloisi F. Detection of Ectopic B-cell Follicles with Germinal Centers in the Meninges of Patients with Secondary Progressive Multiple Sclerosis. Brain Pathol. 2004 Apr 5;14(2):164–74.

364. Corcione A, Casazza S, Ferretti E, Giunti D, Zappia E, Pistorio A, et al. Recapitulation of B cell differentiation in the central nervous system of patients with multiple sclerosis. Proc Natl Acad Sci U S A. 2004 Jul 27;101(30):11064–9.

365. Niedel JE, Kuhn LJ, Vandenbark GR. Phorbol diester receptor copurifies with protein kinase C. Proc Natl Acad Sci. 1983 Jan 1;80(1):36–40.

366. Chatila T, Silverman L, Miller R, Geha R. Mechanisms of T cell activation by the calcium ionophore ionomycin. J Immunol. 1989 Aug 15;143(4):1283–9.

367. Jung T, Schauer U, Heusser C, Neumann C, Rieger C. Detection of intracellular cytokines by flow cytometry. J Immunol Methods. 1993 Feb;159(1-2):197–207.

368. Foster B, Prussin C, Liu F, Whitmire JK, Whitton JL. Detection of intracellular cytokines by flow cytometry. Curr Protoc Immunol. 2007 Aug;Chapter 6:Unit 6.24.

369. Beacock-Sharp H, Young JL, Gaston JS. Analysis of T cell subsets present in the peripheral blood and synovial fluid of reactive arthritis patients. Ann Rheum Dis. 1998 Feb;57(2):100–6.

370. Zhou M, Zou R, Gan H, Liang Z, Li F, Lin T, et al. The effect of aging on the frequency, phenotype and cytokine production of human blood CD4 + CXCR5 + T follicular helper cells: comparison of aged and young subjects. Immun Ageing. 2014 Jan;11(1):12.

371. Acres RB, Conlon PJ, Mochizuki DY, Gallis B. Rapid phosphorylation and modulation of the T4 antigen on cloned helper T cells induced by phorbol myristate acetate or antigen. J Biol Chem. 1986 Dec 5;261(34):16210–4.

372. Pelchen-Matthews A. Phorbol ester-induced downregulation of CD4 is a multistep process involving dissociation from p56lck, increased association with clathrin- coated pits, and altered endosomal sorting. J Exp Med. 1993 Oct 1;178(4):1209–22.

373. Olsen I, Sollid LM. Pitfalls in determining the cytokine profile of human T cells. J Immunol Methods. Elsevier B.V.; 2013;390(1-2):106–12.

374. Biolegend. Stimulation guide for intracellular staining of cytokines/chemokines. [cited 2015 May 25] Available at URL: https://www.biolegend.com/media_assets/support_protocol/BioLegend_StimulationGuide_101711.pdf.

375. Kruisbeek A, Shevach EM, Thornton AM. Proliferative Assays for T cell Function. Current protocols in immunology. John Wiley & Sons, Inc; 2004. p. Supplement 60.

376. Smalley DM, Ley K. L-selectin: mechanisms and physiological significance of ectodomain cleavage. J Cell Mol Med. Jan;9(2):255–66.

377. Bennett TA, Lynam EB, Sklar LA, Rogelj S. Hydroxamate-based metalloprotease inhibitor blocks shedding of L-selectin adhesion molecule from leukocytes: functional consequences for neutrophil aggregation. J Immunol. 1996 May 1;156(9):3093–7.

378. Schiött A, Lindstedt M, Johansson-Lindbom B, Roggen E, Borrebaeck CAK. CD27-CD4+ memory T cells define a differentiated memory population at both the functional and transcriptional levels. Immunology. 2004 Nov;113(3):363–70.

379. Fritsch RD, Shen X, Sims GP, Hathcock KS, Hodes RJ, Lipsky PE. Stepwise Differentiation of CD4 Memory T Cells Defined by Expression of CCR7 and CD27. J Immunol. American Association of Immunologists; 2005 Nov 4;175(10):6489–97.

380. Van Genderen H, Kenis H, Lux P, Ungeth L, Maassen C, Deckers N, et al. In vitro measurement of cell death with the annexin A5 affinity assay. Nat Protoc. 2006 Jan;1(1):363–7.

381. Duré M, Macian F. IL-2 signaling prevents T cell anergy by inhibiting the expression of anergy-inducing genes. Mol Immunol. 2009 Feb;46(5):999–1006.

382. Seder RA, Paul WE. Acquisition of lymphokine-producing phenotype by CD4+ T cells. Annu Rev Immunol. Annual Reviews 4139 El Camino Way, P.O. Box 10139, Palo Alto, CA 94303-0139, USA; 1994 Jan 28;12:635–73.

383. Stubbe M, Vanderheyde N, Goldman M, Marchant A. Antigen-Specific Central Memory CD4+ T Lymphocytes Produce Multiple Cytokines and Proliferate In Vivo in Humans. J Immunol. American Association of Immunologists; 2006 Nov 17;177(11):8185–90.

384. Chiang EY, Kolumam GA, Yu X, Francesco M, Ivelja S, Peng I, et al. Targeted depletion of lymphotoxin-alpha-expressing TH1 and TH17 cells inhibits autoimmune disease. Nat Med. Nature Publishing Group; 2009 Jul;15(7):766–73.

385. Mearns H, Forbes-Blom EE, Camberis M, Tang S-C, Kyle R, Harvie M, et al. IL-25 exhibits disparate roles during Th2-cell differentiation versus effector function. Eur J Immunol. 2014 Jul;44(7):1976–80.

386. Ai W, Li H, Song N, Li L, Chen H. Optimal method to stimulate cytokine production and its use in immunotoxicity assessment. Int J Environ Res Public Health. 2013;10:3834–42.

387. Gauchat JF, Walker C, De Weck a L, Stadler BM. Stimulation-dependent lymphokine mRNA levels in human mononuclear cells. Eur J Immunol. 1988;18(9):1441–6.

388. Tsitoura DC, Gelder CM, Kemeny DM, Lamb JR. Regulation of cytokine production by human Th0 cells following stimulation with peptide analogues: differential expression of TGF-beta in activation and anergy. Immunology. 1997 Sep;92(1):10–9.

389. Lee YK, Turner H, Maynard CL, Oliver JR, Chen D, Elson CO, et al. Late developmental plasticity in the T helper 17 lineage. Immunity. 2009 Jan 16;30(1):92–107.

390. Kanno Y, Vahedi G, Hirahara K, Singleton K, O'Shea JJ. Transcriptional and Epigenetic Control of T Helper Cell Specification: Molecular Mechanisms Underlying Commitment and Plasticity *. Annu Rev Immunol. 2012 Apr 23;30(1):707–31.

391. Bromley SK, Thomas SY, Luster AD. Chemokine receptor CCR7 guides T cell exit from peripheral tissues and entry into afferent lymphatics. Nat Immunol. 2005;6(9):895–901.

392. Caccamo N, Meraviglia S, Ferlazzo V, Angelini D, Borsellino G, Poccia F, et al. Differential requirements for antigen or homeostatic cytokines for proliferation and differentiation of human Vgamma9Vdelta2 naive, memory and effector T cell subsets. Eur J Immunol. 2005 Jun;35(6):1764–72.

393. Koch S, Larbi A, Derhovanessian E, Ozcelik D, Naumova E, Pawelec G. Multiparameter flow cytometric analysis of CD4 and CD8 T cell subsets in young and old people. Immun Ageing. 2008 Jan;5(1):6.

394. Testi R, Phillips JH, Lanier LL. T cell activation via Leu-23 (CD69). J Immunol. 1989 Aug 15;143(4):1123–8.

395. Craston R, Koh M, Mc Dermott A, Ray N, Prentice HG, Lowdell MW. Temporal dynamics of CD69 expression on lymphoid cells. J Immunol Methods. 1997 Nov 10;209(1):37–45.

396. Maino VC, Suni MA, Ruitenberg JJ. Rapid flow cytometric method for measuring lymphocyte subset activation. Cytometry. 1995 Jun 1;20(2):127–33.

397. Ziegler SF, Levin SD, Johnson L, Copeland NG, Gilbert DJ, Jenkins NA, et al. The mouse CD69 gene. Structure, expression, and mapping to the NK gene complex. J Immunol. American Association of Immunologists; 1994 Feb 1;152(3):1228–36.

398. López-Cabrera M, Santis AG, Fernández-Ruiz E, Blacher R, Esch F, Sánchez-Mateos P, et al. Molecular cloning, expression, and chromosomal localization of the human earliest lymphocyte activation antigen AIM/CD69, a new member of the C-type animal lectin superfamily of signal-transmitting receptors. J Exp Med. 1993 Aug 1;178(2):537–47.

399. Lai W, Yu M, Huang M-N, Okoye F, Keegan AD, Farber DL. Transcriptional control of rapid recall by memory CD4 T cells. J Immunol. 2011;187(1):133–40.

400. Abdalla AO, Kiaii S, Hansson L, Rossmann ED, Jeddi-Tehrani M, Shokri F, et al. Kinetics of cytokine gene expression in human CD4+ and CD8+ T-lymphocyte subsets using quantitative real-time PCR. Scand J Immunol. 2003 Dec;58(6):601–6.

401. Yu S, Zhang Y, Yang B, Wu C. Human memory, but not naive, CD4+ T cells expressing transcription factor T-bet might drive rapid cytokine production. J Biol Chem. 2014 Dec 19;289(51):35561–9.

402. Steensberg a, Toft AD, Bruunsgaard H, Sandmand M, Halkjaer-Kristensen J, Pedersen BK. Strenuous exercise decreases the percentage of type 1 T cells in the circulation. J Appl Physiol. 2001 Oct;91(4):1708–12.

403. Fan X, Wang Y. β2 Adrenergic receptor on T lymphocytes and its clinical implications. Prog Nat Sci. National Natural Science Foundation of China and Chinese Academy of Sciences; 2009;19(1):17–23.

404. Dimsdale JE. Plasma Catecholamines in Stress and Exercise. JAMA J Am Med Assoc. American Medical Association; 1980 Jan 25;243(4):340.

405. McCarthy DA, Dale MM. The leucocytosis of exercise. A review and model. Sports Med. 1988 Dec;6(6):333–63.

406. Okutsu M, Ishii K, Niu KJ, Nagatomi R. Cortisol-induced CXCR4 augmentation mobilizes T lymphocytes after acute physical stress. Am J Physiol Regul Integr Comp Physiol. 2005 Mar;288(3):R591–9.

407. Dimitrov S, Benedict C, Heutling D, Westermann J, Born J, Lange T. Cortisol and epinephrine control opposing circadian rhythms in T cell subsets Cortisol and epinephrine control opposing circadian rhythms in T cell subsets. 2009;113(21):5134–43.

408. Mannie MD. The post-activation refractory phase: a mechanism to measure antigenic complexity and ensure self-tolerance among mature peripheral T lymphocytes. Med Hypotheses. 1996 Dec;47(6):467–70.

409. Hosking MP, Flynn CT, Botten J, Whitton JL. CD8+ memory T cells appear exhausted within hours of acute virus infection. J Immunol. 2013 Oct 15;191(8):4211–22.

410. Duthoit CT, Nguyen P, Geiger TL. Antigen nonspecific suppression of T cell responses by activated stimulation-refractory CD4+ T cells. J Immunol. 2004;172:2238–46.

411. Reddy M, Eirikis E, Davis C, Davis HM, Prabhakar U. Comparative analysis of lymphocyte activation marker expression and cytokine secretion profile in stimulated human peripheral blood mononuclear cell cultures: an in vitro model to monitor cellular immune function. J Immunol Methods. 2004 Oct;293(1-2):127–42.

412. Barron L, Dooms H, Hoyer KK, Kuswanto W, Hofmann J, O'Gorman WE, et al. Cutting edge: mechanisms of IL-2-dependent maintenance of functional regulatory T cells. J Immunol. 2010 Dec 1;185(11):6426–30.

413. De la Rosa M, Rutz S, Dorninger H, Scheffold A. Interleukin-2 is essential for CD4+CD25+ regulatory T cell function. Eur J Immunol. 2004 Sep;34(9):2480–8.

414. Malek TR, Yu A, Vincek V, Scibelli P, Kong L. CD4 Regulatory T Cells Prevent Lethal Autoimmunity in IL-2Rβ-Deficient Mice. Immunity. Elsevier; 2002 Aug 8;17(2):167–78.

415. Cortés JR, Sánchez-Díaz R, Bovolenta ER, Barreiro O, Lasarte S, Matesanz-Marín A, et al. Maintenance of immune tolerance by Foxp3+ regulatory T cells requires CD69 expression. J Autoimmun. 2014;55:51–62.

416. Gagliani N, Magnani CF, Huber S, Gianolini ME, Pala M, Licona-Limon P, et al. Coexpression of CD49b and LAG-3 identifies human and mouse T regulatory type 1 cells. Nat Med. 2013 Jun;19(6):739–46.

417. Fabre C, Mimura N, Bobb K, Kong S-Y, Gorgun G, Cirstea D, et al. Dual inhibition of canonical and noncanonical NF-κB pathways demonstrates significant antitumor activities in multiple myeloma. Clin Cancer Res. 2012 Sep 1;18(17):4669–81.

418. Barron L, Knoechel B, Lohr J, Abbas AK. Cutting edge: contributions of apoptosis and anergy to systemic T cell tolerance. J Immunol. 2008;180(5):2762–6.

419. Fox CJ, Hammerman PS, Thompson CB. Fuel feeds function: energy metabolism and the T-cell response. Nat Rev Immunol. 2005 Nov;5(11):844–52.

420. Sanli T, Steinberg GR, Singh G, Tsakiridis T. AMP-activated protein kinase (AMPK) beyond metabolism: a novel genomic stress sensor participating in the DNA damage response pathway. Cancer Biol Ther. 2014 Feb;15(2):156–69.

421. Alexander A, Walker CL. The role of LKB1 and AMPK in cellular responses to stress and damage. FEBS Lett. 2011 Apr;585(7):952–7.

422. Lanna A, Henson SM, Escors D, Akbar AN. The kinase p38 activated by the metabolic regulator AMPK and scaffold TAB1 drives the senescence of human T cells. Nat Immunol. 2014;15(10):1–10.

423. Lenz DC, Kurz SK, Lemmens E, Schoenberger SP, Sprent J, Oldstone MBA, et al. IL-7 regulates basal homeostatic proliferation of antiviral CD4+T cell memory. Proc Natl Acad Sci U S A. 2004 Jun 22;101(25):9357–62.

424. Purton JF, Tan JT, Rubinstein MP, Kim DM, Sprent J, Surh CD. Antiviral CD4+ memory T cells are IL-15 dependent. J Exp Med. 2007 Apr 16;204(4):951–61.

425. Sun Z, Arendt CW, Ellmeier W, Schaeffer EM, Sunshine MJ, Gandhi L, et al. PKC-theta is required for TCR-induced NF-kappaB activation in mature but not immature T lymphocytes. Nature. Macmillian Magazines Ltd.; 2000 Mar 23;404(6776):402–7.

426. Manicassamy S, Sun Z. The Critical Role of Protein Kinase C- (theta) in Fas / Fas Ligand-Mediated Apoptosis. J Immunol. 2007;(28).

427. Shin J, Doyle C, Yang Z, Kappes D, Strominger JL. Structural features of the cytoplasmic region of CD4 required for internalization. EMBO J. 1990 Feb;9(2):425–34.

428. Laguette N, Brégnard C, Bouchet J, Benmerah A, Benichou S, Basmaciogullari S. Nef-induced CD4 endocytosis in human immunodeficiency virus type 1 host cells: role of p56lck kinase. J Virol. 2009 Jul;83(14):7117–28.

429. Villalba M, Bi K, Hu J, Altman Y, Bushway P, Reits E, et al. Translocation of PKC[theta] in T cells is mediated by a nonconventional, PI3-K- and Vav-dependent pathway, but does not absolutely require phospholipase C. J Cell Biol. 2002 Apr 15;157(2):253–63.

430. Knyazhitsky M, Moas E, Shaginov E, Luria A, Braiman A. Vav1 oncogenic mutation inhibits T cell receptor-induced calcium mobilization through inhibition of phospholipase Cγ1 activation. J Biol Chem. 2012 Jun 1;287(23):19725–35.

431. Saveliev A, Vanes L, Ksionda O, Rapley J, Smerdon SJ, Rittinger K, et al. Function of the nucleotide exchange activity of vav1 in T cell development and activation. Sci Signal. 2009 Jan 15;2(101):ra83.

432. Giunti D, Borsellino G, Benelli R, Marchese M, Capello E, Valle MT, et al. Phenotypic and functional analysis of T cells homing into the CSF of subjects with inflammatory diseases of the CNS Abstract : The recruitment of lymphocytes across the blood brain barrier (BBB) is mediated by ad- healthy subject , similarly migrated to. J Leukoc Biol. 2003;

433. Meeker RB, Williams K, Killebrew D a., Hudson LC. Cell trafficking through the choroid plexus. Cell Adh Migr. 2012;6(5):390–6.

434. Sparshott SM, Bell EB. Lymphocyte trafficking: CD4 T cells with a “memory” phenotype (CD45RC-) freely cross lymph node high endothelial venules in vivo. Immunology. 1998 Apr;93(November 1997):447–54.

435. Westermann J, Geismar U, Sponholz A, Bode U, Sparshott SM, Bell EB. CD4+ T cells of both the naive and the memory phenotype enter rat lymph nodes and Peyer’s patches via high endothelial venules: within the tissue their migratory behavior differs. Eur J Immunol. 1997 Dec;27(12):3174–81.

436. Swain SL, Bradley LM. Helper T cell memory: more questions than answers. Semin Immunol. 1992 Feb;4(1):59–68.

437. Mackay CR. Homing of naive, memory and effector lymphocytes. Curr Opin Immunol. 1993 Jun;5(3):423–7.

438. Li XY, Matsuzaki G, Yoshikai Y, Muramori K, Nomoto K. T cells expressing both L-selectin and CD44 molecules increase in number in peritoneal exudate cells and in vitro-stimulated spleen cells from mice immunized intraperitoneally with Listeria monocytogenes. Immunology. 1993 Jan;78(1):28–34.

439. Vajkoczy P, Laschinger M, Engelhardt B. Alpha4-integrin-VCAM-1 binding mediates G protein-independent capture of encephalitogenic T cell blasts to CNS white matter microvessels. J Clin Invest. 2001 Aug;108(4):557–65.

440. Poli A, Kmiecik J, Domingues O, Hentges F, Bléry M, Chekenya M, et al. NK cells in central nervous system disorders. J Immunol. 2013 Jun 1;190(11):5355–62.

441. Waschbisch A, Sammet L, Schröder S, Lee D-H, Barrantes-Freer A, Stadelmann C, et al. Analysis of CD4+ CD8+ double-positive T cells in blood, cerebrospinal fluid and multiple sclerosis lesions. Clin Exp Immunol. 2014 Aug;177(2):404–11.

442. Perry VH, Gordon S. Modulation of CD4 antigen on macrophages and microglia in rat brain. J Exp Med. 1987 Oct 1;166(4):1138–43.

443. Almolda B, Costa M, Montoya M, González B, Castellano B. CD4 microglial expression correlates with spontaneous clinical improvement in the acute Lewis rat EAE model. J Neuroimmunol. 2009 Apr 30;209(1-2):65–80.

444. Duvernoy HM, Risold P-Y. The circumventricular organs: an atlas of comparative anatomy and vascularization. Brain Res Rev. 2007 Nov;56(1):119–47.

445. Schulz M, Engelhardt B. The circumventricular organs participate in the immunopathogenesis of experimental autoimmune encephalomyelitis. Cerebrospinal Fluid Res. BioMed Central Ltd; 2005 Sep 30;2(1):8.

446. Stüve O, Marra CM, Bar-Or A, Niino M, Cravens PD, Cepok S, et al. Altered CD4+/CD8+ T-cell ratios in cerebrospinal fluid of natalizumab-treated patients with multiple sclerosis. Archives of neurology. 2006.

447. Baruch K, Ron-harel N, Gal H, Deczkowska A, Shifrut E, Ndifon W. CNS-speci fi c immunity at the choroid plexus shifts toward destructive Th2 in fl ammation in brain aging. 2012;

448. Hawke S, Stevenson PG, Freeman S, Bangham CR. Long-term persistence of activated cytotoxic T lymphocytes after viral infection of the central nervous system. J Exp Med. 1998;187(10):1575–82.

449. Wakim LM, Woodward-Davis A, Bevan MJ. Memory T cells persisting within the brain after local infection show functional adaptations to their tissue of residence. Proc Natl Acad Sci U S A. 2010 Oct 19;107(42):17872–9.

450. Mullen KM, Gocke AR, Allie R, Ntranos A, Grishkan I V., Pardo C, et al. Expression of CCR7 and CD45RA in CD4 + and CD8 + subsets in cerebrospinal fluid of 134 patients with inflammatory and non-inflammatory neurological diseases. J Neuroimmunol. 2012;249(410):86–92.

451. Babbe H, Roers A, Waisman A, Lassmann H, Goebels N, Hohlfeld R, et al. Clonal expansions of CD8(+) T cells dominate the T cell infiltrate in active multiple sclerosis lesions as shown by micromanipulation and single cell polymerase chain reaction. J Exp Med. 2000 Aug 7;192(3):393–404.

452. Ransohoff RM, Engelhardt B. The anatomical and cellular basis of immune surveillance in the central nervous system. Nat Rev Immunol. Nature Publishing Group; 2012;12(9):623–35.

453. Bunce C, Bell EB. CD45RC isoforms define two types of CD4 memory T cells, one of which depends on persisting antigen. J Exp Med. 1997;185(4):767–76.

454. Buonamici S, Trimarchi T, Ruocco MG, Reavie L, Cathelin S, Mar BG, et al. CCR7 signalling as an essential regulator of CNS infiltration in T-cell leukaemia. Nature. Nature Publishing Group; 2009;459(7249):1000–4.

455. Vander Lugt B, Tubo NJ, Nizza ST, Boes M, Malissen B, Fuhlbrigge RC, et al. CCR7 plays no appreciable role in trafficking of central memory CD4 T cells to lymph nodes. J Immunol. 2013;191(6):3119–27.

456. Sporici R, Issekutz TB. CXCR3 blockade inhibits T-cell migration into the CNS during EAE and prevents development of adoptively transferred, but not actively induced, disease. Eur J Immunol. 2010 Oct;40(10):2751–61.

457. Sung JH, Zhang H, Moseman EA, Alvarez D, Iannacone M, Henrickson SE, et al. Chemokine guidance of central memory T cells is critical for antiviral recall responses in lymph nodes. Cell. 2012 Sep 14;150(6):1249–63.

458. Alvermann S, Hennig C, Stüve O, Wiendl H, Stangel M. Immunophenotyping of cerebrospinal fluid cells in multiple sclerosis: in search of biomarkers. JAMA Neurol. American Medical Association; 2014 Jul 1;71(7):905–12.

459. Esplugues E, Sancho D, Vega-Ramos J, Martínez C, Syrbe U, Hamann A, et al. Enhanced antitumor immunity in mice deficient in CD69. J Exp Med. 2003 May 5;197(9):1093–106.

460. Richert JR, Driscoll BF, Kies MW, Alvord EC. Adoptive transfer of experimental allergic encephalomyelitis: incubation of rat spleen cells with specific antigen. J Immunol. 1979 Mar;122(2):494–6.

461. Hickey WF. Migration of hematogenous cells through the blood-brain barrier and the initiation of CNS inflammation. Brain Pathol. 1991 Jan;1(2):97–105.

462. Sancho D, Yáñez-Mó M, Tejedor R, Sánchez-Madrid F. Activation of peripheral blood T cells by interaction and migration through endothelium: role of lymphocyte function antigen-1/intercellular adhesion molecule-1 and interleukin-15. Blood. American Society of Hematology; 1999 Feb 1;93(3):886–96.

463. Gebhardt T, Wakim LM, Eidsmo L, Reading PC, Heath WR, Carbone FR. Memory T cells in nonlymphoid tissue that provide enhanced local immunity during infection with herpes simplex virus. Nat Immunol. Nature Publishing Group; 2009 May;10(5):524–30.

464. Kivisäkk P, Tucky B, Wei T, Campbell JJ, Ransohoff RM. Human cerebrospinal fluid contains CD4+ memory T cells expressing gut- or skin-specific trafficking determinants: relevance for immunotherapy. BMC Immunol. 2006;7:14.

465. Batuman OA, Sajewski D, Ottenweller JE, Pitman DL, Natelson BH. Effects of repeated stress on T cell numbers and function in rats. Brain Behav Immun. 1990 Jun;4(2):105–17.

466. Stefanski V, Engler H. Effects of acute and chronic social stress on blood cellular immunity in rats. Physiol Behav. 1998 Jul;64(5):733–41.

467. Miller GE, Cohen S, Pressman S, Barkin A, Rabin BS, Treanor JJ. Psychological stress and antibody response to influenza vaccination: when is the critical period for stress, and how does it get inside the body? Psychosom Med. Jan;66(2):215–23.

468. Stone AA, Bovbjerg DH, Neale JM, Napoli A, Valdimarsdottir H, Cox D, et al. Development of common cold symptoms following experimental rhinovirus infection is related to prior stressful life events. Behav Med. 1992 Jan;18(3):115–20.

469. Reiche EMV, Nunes SOV, Morimoto HK. Stress, depression, the immune system, and cancer. Lancet Oncol. 2004 Oct;5(10):617–25.

470. Julià E, Montalban X, Al-Zayat H, Issazadeh-Navikas S, Goertsches R, Martin R, et al. Deficient Fas expression by CD4+ CCR5+ T cells in multiple sclerosis. J Neuroimmunol. 2006 Nov;180(1-2):147–58.

471. Ishizu T, Osoegawa M, Mei F-J, Kikuchi H, Tanaka M, Takakura Y, et al. Intrathecal activation of the IL-17/IL-8 axis in opticospinal multiple sclerosis. Brain. 2005 May;128(Pt 5):988–1002.

472. Sharief MK, Hentges R. Association between tumor necrosis factor-alpha and disease progression in patients with multiple sclerosis. N Engl J Med. 1991 Aug 15;325(7):467–72.

473. Brucklacher-Waldert V, Stuerner K, Kolster M, Wolthausen J, Tolosa E. Phenotypical and functional characterization of T helper 17 cells in multiple sclerosis. Brain. 2009;132:3329–41.

474. Cao Y, Goods BA, Raddassi K, Nepom GT, Kwok WW, Love JC, et al. Functional inflammatory profiles distinguish myelin-reactive T cells from patients with multiple sclerosis. Sci Transl Med. 2015 May 13;7(287):287ra74–287ra74.

475. Baier-Bitterlich G, Uberall F, Bauer B, Fresser F, Wachter H, Grunicke H, et al. Protein kinase C-theta isoenzyme selective stimulation of the transcription factor complex AP-1 in T lymphocytes. Mol Cell Biol. 1996 Apr;16(4):1842–50.

476. Pfeifhofer C, Kofler K, Gruber T, Tabrizi NG, Lutz C, Maly K, et al. Protein kinase C theta affects Ca2+ mobilization and NFAT cell activation in primary mouse T cells. J Exp Med. 2003;197(11):1525–35.

477. Kang SM, Beverly B, Tran AC, Brorson K, Schwartz RH, Lenardo MJ. Transactivation by AP-1 is a molecular target of T cell clonal anergy. Science. 1992 Aug 21;257(5073):1134–8.

478. Sundstedt A, Sigvardsson M, Leanderson T, Hedlund G, Kalland T, Dohlsten M. In vivo anergized CD4+ T cells express perturbed AP-1 and NF-kappa B transcription factors. Proc Natl Acad Sci U S A. 1996 Feb 6;93(3):979–84.

479. Weinberger B, Lazuardi L, Weiskirchner I, Keller M, Neuner C, Fischer K-H, et al. Healthy aging and latent infection with CMV lead to distinct changes in CD8+ and CD4+ T-cell subsets in the elderly. Hum Immunol. 2007 Mar;68(2):86–90.

480. Hurley TR, Luo K, Sefton BM. Activators of protein kinase C induce dissociation of CD4, but not CD8, from p56lck. Science. 1989 Jul 28;245(4916):407–9.

481. Altman JD, Moss PAH, Goulder PJR, Barouch DH, McHeyzer-Williams MG, Bell JI, et al. Phenotypic Analysis of Antigen-Specific T Lymphocytes. Science (80-). 1996 Oct 4;274(5284):94–6.

482. Lebowitz MS, O'Herrin SM, Hamad AR, Fahmy T, Marguet D, Barnes NC, et al. Soluble, high-affinity dimers of T-cell receptors and class II major histocompatibility complexes: biochemical probes for analysis and modulation of immune responses. Cell Immunol. 1999 Mar 15;192(2):175–84.

483. Wherry EJ, Barber DL, Kaech SM, Blattman JN, Ahmed R. Antigen-independent memory CD8 T cells do not develop during chronic viral infection. Proc Natl Acad Sci U S A. 2004 Dec 9;101(45):16004–9.

484. Tamura H. B7-H1 costimulation preferentially enhances CD28-independent T-helper cell function. Blood. American Society of Hematology; 2001 Mar 15;97(6):1809–16.

485. Keir ME, Liang SC, Guleria I, Latchman YE, Qipo A, Albacker LA, et al. Tissue expression of PD-L1 mediates peripheral T cell tolerance. J Exp Med. 2006 May 17;203(4):883–95.

486. Ding H, Wu X, Gao W. PD-L1 is expressed by human renal tubular epithelial cells and suppresses T cell cytokine synthesis. Clin Immunol. 2005;115(2):184–91.

487. Shi F, Shi M, Zeng Z, Qi R-Z, Liu Z-W, Zhang J-Y, et al. PD-1 and PD-L1 upregulation promotes CD8(+) T-cell apoptosis and postoperative recurrence in hepatocellular carcinoma patients. Int J Cancer. 2011 Feb 15;128(4):887–96.

488. Powell DJ, Dudley ME, Robbins PF, Rosenberg SA. Transition of late-stage effector T cells to CD27+ CD28+ tumor-reactive effector memory T cells in humans after adoptive cell transfer therapy. Blood. 2005 Jan 1;105(1):241–50.

489. Vallejo AN. CD28 extinction in human T cells: altered functions and the program of T-cell senescence. Immunol Rev. 2005 Jul;205:158–69.

490. De Jong R, Brouwer M, Hooibrink B, Van der Pouw-Kraan T, Miedema F, Van Lier RA. The CD27- subset of peripheral blood memory CD4+ lymphocytes contains functionally differentiated T lymphocytes that develop by persistent antigenic stimulation in vivo. Eur J Immunol. 1992 May;22(4):993–9.

491. Ochsenbein AF, Riddell SR, Brown M, Corey L, Baerlocher GM, Lansdorp PM, et al. CD27 expression promotes long-term survival of functional effector-memory CD8+ cytotoxic T lymphocytes in HIV-infected patients. J Exp Med. 2004 Dec 6;200(11):1407–17.

492. Taylor A, Verhagen J, Blaser K, Akdis M, Akdis CA. Mechanisms of immune suppression by interleukin-10 and transforming growth factor-beta: the role of T regulatory cells. Immunology. 2006 Apr;117(4):433–42.

493. Hamid O, Robert C, Daud A, Hodi FS, Hwu W-J, Kefford R, et al. Safety and tumor responses with lambrolizumab (anti-PD-1) in melanoma. N Engl J Med. 2013 Jul 11;369(2):134–44.

494. Klebanoff C a, Gattinoni L, Restifo NP. Sorting through subsets: which T-cell populations mediate highly effective adoptive immunotherapy? J Immunother. 2012;35(9):651–60.

495. McElhaney JE, Xie D, Hager WD, Barry MB, Wang Y, Kleppinger A, et al. T cell responses are better correlates of vaccine protection in the elderly. J Immunol. 2006 May 15;176(10):6333–9.

496. Kipnis J, Cohen H, Cardon M, Ziv Y, Schwartz M. T cell deficiency leads to cognitive dysfunction: implications for therapeutic vaccination for schizophrenia and other psychiatric conditions. Proc Natl Acad Sci U S A. 2004 May 25;101(21):8180–5.

497. Levine J, Barak Y, Chengappa KN, Rapoport A, Rebey M, Barak V. Cerebrospinal cytokine levels in patients with acute depression. Neuropsychobiology. 1999 Nov;40(4):171–6.

498. Lindqvist D, Janelidze S, Hagell P, Erhardt S, Samuelsson M, Minthon L, et al. Interleukin-6 is elevated in the cerebrospinal fluid of suicide attempters and related to symptom severity. Biol Psychiatry. 2009 Aug 1;66(3):287–92.

499. Miller BJ, Buckley P, Seabolt W, Mellor A, Kirkpatrick B. Meta-analysis of cytokine alterations in schizophrenia: clinical status and antipsychotic effects. Biol Psychiatry. 2011 Oct 1;70(7):663–71.

500. Rus H, Pardo CA, Hu L, Darrah E, Cudrici C, Niculescu T, et al. The voltage-gated potassium channel Kv1.3 is highly expressed on inflammatory infiltrates in multiple sclerosis brain. Proc Natl Acad Sci U S A. 2005 Aug 2;102(31):11094–9.

501. Unsoeld H, Pircher H. Complex memory T-cell phenotypes revealed by coexpression of CD62L and CCR7. J Virol. 2005;79(7):4510–3.

502. Feger U, Luther C, Poeschel S, Melms A, Tolosa E, Wiendl H. Increased frequency of CD4+ CD25+ regulatory T cells in the cerebrospinal fluid but not in the blood of multiple sclerosis patients. Clin Exp Immunol. 2007 Mar;147(3):412–8.

503. Sancho D, Gómez M, Sánchez-Madrid F. CD69 is an immunoregulatory molecule induced following activation. Trends Immunol. Elsevier; 2005 Mar 3;26(3):136–40.

504. Han Y, Guo Q, Zhang M, Chen Z, Cao X. CD69+ CD4+ CD25- T cells, a new subset of regulatory T cells, suppress T cell proliferation through membrane-bound TGF-beta 1. J Immunol. 2009;182(1):111–20.

505. Shiow LR, Rosen DB, Brdicková N, Xu Y, An J, Lanier LL, et al. CD69 acts downstream of interferon-alpha/beta to inhibit S1P1 and lymphocyte egress from lymphoid organs. Nature. 2006;440(March):540–4.

506. Obermeier B, Lovato L, Mentele R, Brück W, Forne I, Imhof A, et al. Related B cell clones that populate the CSF and CNS of patients with multiple sclerosis produce CSF immunoglobulin. J Neuroimmunol. 2011 May;233(1-2):245–8.

507. Kowarik MC, Pellkofer HL, Cepok S, Korn T, Kümpfel T, Buck D, et al. Differential effects of fingolimod (FTY720) on immune cells in the CSF and blood of patients with MS. Neurology. 2011;76(14):1214–21.

508. QIAGEN. TCR Signalling. [cited 2015 May 13] Available at URL: https://www.qiagen.com/gb/products/genes and pathways/pathway details?pwid=427&action=Accept.

509. Gascoigne NRJ. Do T cells need endogenous peptides for activation? Nat Rev Immunol. 2008;8(11):895–900.

510. Gattinoni L, Restifo NP. Moving T memory stem cells to the clinic. Blood. 2013;121(4):567–8.

511. Sethi A, Kulkarni N, Sonar S, Lal G. Role of miRNAs in CD4 T cell plasticity during inflammation and tolerance. Frontiers in Genetics. 2013.

512. Shuai K, Liu B. Regulation of JAK-STAT signalling in the immune system. Nat Rev Immunol. 2003;3(11):900–11.